

## Handbook of Scour and Cable Protection Methods



## Handbook of Scour and Cable Protection Methods



**JIP HASPRO**  
Handbook Scour Protection Methods



# Summary

The Handbook of Scour and Cable Protection methods is the result of a multi-year research programme performed as a Joint Industry Project with the contribution of over 20 industrial partners. This project was initiated from the observation that no good and generically applicable design formulae and guidelines exist to protect offshore structures against scour. Instead, there are various existing methods and concepts that lack a sound basis for design. Different parties apply different solutions against scour around support structures with varying degrees of success. To help decision makers select the most suitable and cost-effective scour protection method for each considered situation the Joint Industry Project Handbook Scour and Cable Protection Methods (JIP HaSPro) was initiated by Deltares. Apart from this research institute, the consortium consists of a certifying body (DNV), utilities (Ørsted, RWE, Vattenfall, Scottish Power, EnBW, Shell, Equinor, Ocean Winds), suppliers (SPT Offshore, Mibau Stema, Airgroup Industries, NoRock, SSCS, Maccaferri), engineering firms (COWI, Kajima) and installation contractors (DEME Group, Boskalis, Van Oord, Jan de Nul, Tideway). The goal of this project is to develop a clear, generic and science-based comparison between different scour protection methods. In this project existing methods (based on loose rock) are optimized and new innovative scour mitigation methods are investigated (proof-of-concept) and made ready for offshore field tests. The resulting findings are presented in this Handbook of Scour and Cable Protections, which is a publicly available document after finalization. All underlying technical reports and experimental data are made publicly available as well to stimulate further development and collaboration on scour protection design within both academia and industry. Developers are actively encouraged to share field data of scour protection performance during the operational phase of wind farms to further validate and improve the present state-of-the-art of scour protection design for offshore support structures.

The Handbook of Scour and Cable Protection methods is aiming to provide guidance on scour protection design. Hence, the main focus of the document is on scour mitigation strategies and scour protection design for various types of offshore support structures. For offshore wind development, monopiles are selected in 60% of the time for their simplicity and adaptability. Although the primary principles discussed in the handbook apply to other foundation types as well, the main emphasis of the material presented in the handbook and the underlying research is on monopile foundations. The handbook is divided into four main parts consisting of eleven technical chapters:

- I. Scour development and mitigation strategies
  1. Scour prediction for offshore foundations
  2. Scour mitigation strategies
- II. Scour protection methods – loose rock
  3. Design of loose rock scour protections
  4. Design of loose rock berms
  5. Offshore rock gradings
  6. Rock scour protection installation
  7. Operation and maintenance of scour protections
- III. Scour protection methods – Alternative
  8. Alternative scour protection systems
  9. Artificial vegetation
  10. Block, gabion and ballast-filled mattresses
- IV. Ecological impact
  11. Nature-inclusive design

A brief description of the contents in each of the chapters is provided.

**Chapter 2: Scour prediction for offshore foundations.** This chapter provides a concise overview of theoretical background on scour and scour prediction methods, ranging from fast, semi-empirical methods like the Dynamic Scour Prediction Model by Deltares to high-resolution numerical modelling making use of CFD.

**Chapter 3: Scour mitigation strategies.** Scour mitigation strategies are introduced, presenting an overview of the various choices that a designer can make when considering the need to mitigate scour development. The various presented options provide a selection framework that can be used to decide upon the optimal protection strategy.

**Chapter 4: Design of loose rock scour protections.** This chapter provides an overview of how to design scour protections to fulfil three performance criteria: external stability (resistance against hydraulic loads), interface stability (sand-tightness) and flexibility (ability to cope with bed level changes at the edge of the protection). The design guidelines are based on an extensive physical model test database consisting of several hundreds of individual test results on different scales (varying between 1:50 and 1:5). The test database was used to develop a scour protection deformation model where for each different scour protection deformation mechanism quantitative formulae are derived that can be used in the design of scour protections.

**Chapter 5: Rock berms.** This chapter deals with the design of loose rock berms at cable crossings by providing guidelines on selecting the appropriate rock grading and berm dimensions from the perspective of external stability, interface stability and flexibility. A rock berm deformation model is presented as well that may be used as an additional aid in the design process.

**Chapter 6: Offshore rock gradings.** Based on various mixed experiences with EN-13383 rock gradings, supplements and alterations to existing loose rock grading specifications will allow optimization and qualification of loose rock production and structure design. These supplements and alterations are given as new loose rock gradings and are named Offshore Sieved Gradings (OSG) and Offshore Weighted Gradings (OWG), with the most important difference that these gradings are closed compared to their EN-13383 counterparts and contain passage criteria. The OSG and OWG gradings align with EN-13383 coarse and light gradings.

**Chapter 7: Rock scour protection installation.** Rock scour protections of offshore wind farm foundations can be installed with different types of vessels. This chapter provides guidance on several types of equipment, the installation sequence, possible interfaces to account for, and an evaluation of the installation and feasible installation accuracy and tolerances.

**Chapter 8: Operation and maintenance of scour protections.** Scour protections are typically designed as passive systems that do not require maintenance over the lifetime of the foundation as long as the design conditions are not exceeded. Thus, operation and maintenance typically relate to surveying and monitoring of the scour protection integrity and functionality. This chapter provides guidelines for scheduling of surveys, survey specification and execution and the evaluation of the surveyed data.

**Chapter 9: Alternative scour protection systems.** This chapter provides a high-level overview of different alternative scour protection systems as opposed to the more conventional loose rock scour protection designs. Generic information on the functioning of these systems, as well as on their installation, operation and maintenance and decommissioning is provided. Several of these concepts are further investigated in more detail.

**Chapter 10: Artificial vegetation.** It is widely acknowledged that densely populated vegetation causes a reduction of near-bed flow velocities due to blockage and can thus also lead to reduced sediment transports and even deposition of sediments. Artificial vegetation attempts to imitate these

properties. An artificial scour protection consists of a large number of individual fronds that are attached to an anchored frame of ballasted mattresses forming a dense vegetation canopy. This chapter presents protection characteristics, potential failure mechanisms and design considerations.

**Chapter 11: Block, gabion and ballast-filled mattresses.** Currently, most alternative scour protection systems consist of weighted mattresses which are placed on the seabed to prevent scour around subsea structures or to protect vital infrastructure like pipelines and cables. This chapter provides an overview of their working principles, characteristics, potential failure mechanisms and design considerations.

**Chapter 12: Nature-inclusive design.** Offshore wind developments inevitably have a significant impact on the environment, especially given the massively accelerated roll-out of offshore wind farms projected in the coming years. Recently, growing interest is shown in possible positive environmental impacts of wind farms, especially related to scour protections around offshore infrastructure foundations. These introduce a hard substrate to the sandy seabed, leading to the formation of new habitats that can affect the composition of marine species occupying this area. The growth of offshore wind through the associated introduction of hard substrates in the sandy seabed areas could, in some cases, lead to an opportunity of partial restoration of lost habitats. This chapter provides an overview of nature-inclusive design principles and concepts of which some have been tested in this Joint Industry Project, providing a basis for further development and field evaluations of ecological performance of scour protections.

# Contents

	<b>List of Abbreviations &amp; Symbols</b>	<b>13</b>
<b>1</b>	<b>Introduction</b>	<b>18</b>
1.1	Background	18
1.2	Considered foundation types	18
1.3	Structure of the handbook	18
	<b>Part I Scour development and mitigation strategies</b>	<b>19</b>
<b>2</b>	<b>Scour prediction for offshore foundations</b>	<b>20</b>
2.1	Introduction	20
2.2	General definitions	20
2.3	General description of the (local) scour process	21
2.4	Scour prediction methodologies	23
2.5	Global bed level lowering	23
<b>3</b>	<b>Scour mitigation strategies</b>	<b>25</b>
3.1	Introduction	25
3.2	Scour mitigation strategies excluding morphodynamics of the seabed	25
3.2.1	Strategy A: Free scour development	26
3.2.2	Strategy B: Immediate scour protection	26
3.2.3	Strategy C: Monitor and React	27
3.3	Scour mitigation strategies including morphodynamics of the seabed	28
3.3.1	Strategy A: Free scour development	28
3.3.2	Strategy B: Immediate scour protection	29
3.3.3	Strategy C: Monitor and React	30
	<b>Part II Scour protection methods – rocks</b>	<b>32</b>
<b>4</b>	<b>Design of loose rock scour protections around monopile foundations</b>	<b>33</b>
4.1	Introduction	33
4.2	Scour protection performance requirements	34
4.2.1	External stability of loose rock scour protections	35
4.2.2	Interface stability of loose rock scour protections	35
4.2.3	Flexibility of loose rock scour protections	37
4.2.4	Scour protection types	39
4.3	Experimental database	40
4.3.1	External stability	40
4.3.2	Interface stability	42
4.3.3	Flexibility	43
4.4	Design approach	44
4.4.1	External stability	44

4.4.1.1	Deformation model	44
4.4.1.2	Layer thickness	50
4.4.1.3	Extent of the scour protection	50
4.4.1.4	Mobility limits	51
4.4.1.5	Rock density	52
4.4.2	Interface stability	53
4.4.2.1	Winnowing scour depth relation	55
4.4.2.2	Design methodology: minimum required thickness to prevent winnowing	56
4.4.2.3	Estimation of equilibrium scour depth	58
4.4.3	Flexibility	59
4.4.3.1	Theoretical background	59
4.4.3.2	Guideline	62
4.5	Design workflow	65
4.5.1	Design parameters	65
4.5.2	Interfaces	66
4.6	Scour protection dimensions	67
<b>5</b>	<b>Loose rock berms at cable crossings</b>	<b>68</b>
5.1	Introduction	68
5.2	Rock berm design	68
5.2.1	External stability	68
5.2.2	Interface stability	71
5.2.3	Flexibility	71
5.2.3.1	Edge scour at rock berms	72
5.2.4	Dimensioning of rock berms	73
5.3	Rock Berm Deformation model	73
5.3.1	Rock berm deformation model application	74
<b>6</b>	<b>Offshore rock gradings</b>	<b>76</b>
6.1	Introduction	76
6.2	Quarry rock	76
6.3	EN 13383: Coarse and Light Gradings	77
6.3.1	Coarse gradings	78
6.3.2	Light gradings	78
6.4	Offshore Sieved and Weighted Gradings	80
6.4.1	Offshore Sieved Gradings	80
6.4.2	Offshore Weighted Gradings	82
6.5	Material properties & testing procedures/methods	85
6.5.1	General	85
6.5.2	Geometrical requirements	85
6.5.3	Physical requirements	86
6.5.4	Durability requirements	86
6.5.5	Additional requirements	87
6.5.6	Conclusion	87
6.6	Quarry operations	87
6.6.1	Production process Offshore Sieved Gradings (OSG)	87
6.6.2	Production process Offshore Weighted Gradings (OWG)	89
6.7	Handling of gradings in installation steps	91



<b>7</b>	<b>Rock scour protection installation</b>	<b>92</b>
7.1	Introduction	92
7.2	Rock Installation Equipment	92
7.2.1	Fallpipe vessel	92
7.2.2	Side Stone Installation Vessel	94
7.2.3	Crane vessel	95
7.2.4	Workability	96
7.3	Installation sequence	96
7.3.1	Preinstalled filter- and armour layer	97
7.3.2	Preinstalled filter layer and post installed armour layer	97
7.3.3	Post installed filter and armour layer	98
7.3.4	Cable crossing rock berms	98
7.3.5	Cable Protection System stabilization	100
7.4	Interfaces	101
7.4.1	Foundation cable entry	101
7.4.2	Impact of falling rocks on the cable	102
7.4.3	Cable burial equipment	103
7.4.4	Pile driving	103
7.4.5	Noise mitigation systems	103
7.4.6	Secondary steel and corrosion protection	104
7.4.7	Pre-mounted cabling and devices	104
7.4.8	Nearby jack-up operations	105
7.4.9	Dredging works for seabed preparation	106
7.4.10	Seabed material and seabed features	106
7.5	Surveys	107
7.5.1	Accuracy requirements & geodetic parameters	107
7.5.2	Monitoring Equipment	108
7.5.3	Survey Platform	108
7.5.4	Survey Specifications	108
7.5.5	Filtering data	108
7.5.6	Calibrations	108
7.5.7	Positioning system	109
7.5.8	Additional notes and considerations	109
7.5.9	Survey activities	110
7.5.9.1	Pre-Subsea Rock Installation Survey	110
7.5.9.2	Progress Surveys	110
7.5.9.3	Post-Subsea Rock Installation Survey	110
7.5.10	Deliverable example	110
7.6	Installation accuracy and tolerances	112
7.6.1	Ensuring constructability of design	113
7.6.2	Tolerance guidance for various rock installations	114
7.6.2.1	Rock Pads defined by thickness	115
7.6.2.2	Rock Pads defined by surface level	117
7.6.2.3	Rock Berms for crossings & cable protection	117
7.6.3	Assessment of as-built conditions and remediation of non-conformances	117
7.7	As-built documentation	118
<b>8</b>	<b>Operation and Maintenance of scour protections</b>	<b>119</b>
8.1	Introduction	119

8.2	Scheduled and event-driven surveys	120
8.3	Survey specification and execution	121
8.4	Survey evaluation and comparison to design	122
8.4.1	Response to seabed change	122
8.4.2	Edge scour	123
8.4.3	Sinkage and monopile installation impact	123
8.4.4	Storm-induced deformation	123
<b>Part III Scour protection methods – alternative</b>		<b>124</b>
<b>9</b>	<b>Alternative scour protection systems</b>	<b>125</b>
9.1	Introduction	125
9.2	Overview of alternative scour protection systems	125
9.3	Installation methods	126
9.3.1	Post-installation of alternative systems	127
9.3.2	Self-installable systems	129
9.3.3	Pre-installation of alternative scour protection systems	130
9.4	Operation and maintenance	130
9.5	Decommissioning	131
<b>10</b>	<b>Artificial vegetation</b>	<b>133</b>
10.1	Introduction	133
10.2	Description and working principle	133
10.3	Protection characteristics	135
10.4	Potential failure mechanisms	135
10.5	Design considerations	137
10.5.1	Introduction	137
10.5.2	Design considerations to prevent scour at the structure	137
10.5.3	Design considerations to prevent stability failure	141
10.5.4	Design considerations to prevent edge scour	141
10.5.5	Design considerations for different foundations	142
10.6	Installation	144
<b>11</b>	<b>Block, gabion and ballast-filled mattresses</b>	<b>146</b>
11.1	Introduction	146
11.2	Description and working principle	146
11.2.1	Block mattresses	146
11.2.2	Gabion mattresses	147
11.2.3	Ballast-filled mattresses	148
11.3	Protection characteristics	149
11.3.1	Block mattresses	149
11.3.2	Gabion mattresses	150
11.3.3	Ballast-filled mattresses	153
11.4	Potential failure mechanisms	154
11.5	Design considerations	156

11.5.1	Introduction	156
11.5.2	Design considerations to prevent scour at the structure	156
11.5.3	Design considerations to prevent stability failure	159
11.5.3.1	Stability formulation: modified Pilarczyk method	161
11.5.3.2	Stability of block mattresses	163
11.5.3.3	Stability of gabion mattresses	166
11.5.3.4	Stability of ballast-filled mattresses	169
11.5.4	Design considerations to deal with edge scour	173
11.5.5	Physical model test considerations	176
11.6	Installation	177
11.6.1	Block mattresses	177
11.6.2	Gabion mattresses	178
11.6.3	Ballast-filled mattresses	179
<b>Part IV Ecological Impact</b>		<b>182</b>
<b>12</b>	<b>Nature Inclusive Design</b>	<b>183</b>
12.1	Introduction	183
12.2	Nature-inclusive design principles	183
12.3	Overview of nature-inclusive design concepts	184
<b>13</b>	<b>Bibliography</b>	<b>195</b>
13.1	Scientific literature	195
13.2	Standards & Guidelines	198
13.3	JIP HaSPro reports and documentation	199
<b>Appendices</b>		<b>201</b>
<b>A</b>	<b>Appendix I– Calculation of mobility number</b>	<b>202</b>
A.1	Introduction	202
A.2	General parameters	203
A.3	Parameters related to rock characteristics	204
A.4	Current-related mobility calculation	205
A.5	Wave-related mobility calculation	206
A.5.1	Near bed wave orbital velocity	206
A.5.2	Wave related shear stress	208
A.6	Combined current- and wave-related mobility calculation	210
A.7	Mobility on a slope	210
<b>B</b>	<b>Appendix II– Calculating total KC number</b>	<b>211</b>
<b>C</b>	<b>Appendix III– Calculation example</b>	<b>213</b>
C.1	Example 1: Calculating hydrodynamic parameters	213
C.2	Example 2: Calculating bed shear stresses	214
C.3	Example 3: Calculating mobility number	215

C.4	Example 4: Estimating depth of deformation	216
C.5	Example 5: Rock berm characteristics	216
<b>D</b>	<b>As-built survey chart scour protection</b>	<b>218</b>
<b>E</b>	<b>Survey examples seabed changes at scour protection</b>	<b>219</b>
E.6	Inline edge scour at featureless seabed	219
E.7	Sand wave migration past a monopile and scour protection	220
E.8	Sand wave migration past a monopile and scour protection	222

# List of Abbreviations & Symbols

## Abbreviations

Abbreviation	Explanation
ADCP	Acoustic Doppler Current Profiler
ASBL	Actual Seabed Level
CAPEX	Capital Expenses
CE	Conformite Europeenne
CFD	Computational Fluid Dynamics
C-O	Configuration and calibration values
CO	Current Only
CP	CE trademarked coarse grading
CPS	Cable Protection System
DGNSS	Differential Global Navigation Satellite System
DOL	Depth of Lowering
DP	Dynamic Positioning
EN	European Norm (Eurocode)
FPROV	Fall pipe ROV
GBS/GBF	Gravity Base Structure / Gravity Base Foundation
GLONASS	Global Navigation Satellite System
GNSS	Global Navigation Satellite System
GPS	Global Positioning System
HaSPro	Handbook of Scour and Cable Protection Methods
HSBL	Highest Seabed Level
HM	CE trademarked heavy armourstone
IWO/IWC	Irregular Waves Without Current / Irregular Waves With Current
LSBL	Lowest Seabed Level
LM	CE trademarked light armourstone
MBES	Multi-Beam Echo Sounding
MSBL	Maximum Seabed Level
MTOC	Minimum Top of Cover
NID	Nature Inclusive Design
OD	Outer Diameter
OPEX	Operational Expenses
OSG	Offshore Sieved Grading (HaSPro Standard Grading)
OWEZ	Offshore Wind Farm Egmond aan Zee
OWF	Offshore Wind Farm
OWG	Offshore Weighted Grading (HaSPro Standard Grading)

Abbreviation	Explanation
O&M	Operation and Maintenance
PAWP	Prinses Amalia Wind Park
PPP	Precise Point Positioning GNSS
ROV	Remotely operated underwater vehicle
ROBED	Rock Berm Deformation Model
RSBL	Reference Seabed Level
RTK	Real-time Kinematic Positioning
RWO	Regular Wave Only
SBJ	Suction Bucket Jacket
SSDV	Side Stone Dumping Vessels
SSS	Side Scan Sonar
SVP	Sound Velocity Profile
TOPC	Top of Product Cover
USBL	Ultra-Short BaseLine
WTG	Wind Turbine Generator
WCROV	Work Class ROV

## Symbols

Symbol	Explanation	Unit
$a$	Dimensionless frontal area plants	[-]
$A_{\text{berm}}$	Cross-sectional area of rock berm	[m <sup>2</sup> ]
$A_{\text{min}}$	Minimal required rock berm cross-sectional area	[m <sup>2</sup> ]
$A_{w,a}$	Amplitude wave orbital	[m]
$A_{w,\text{bed}}$	Amplitude wave orbital motion at the bed	[m]
$A_{w,\text{top}}$	Amplitude wave orbital motion at the bed	[m]
$b$	Width of stem (or frond) as experienced by the flow	[m]
$B$	Buoyancy	[-]
$B_{\text{berm}}$	Bottom-width of rock berm	[m]
$C_1-C_5$	Fitting constants deformation model	[-]
$C_1-C_4$	Fitting constants winnowing scour depth	[-]
$Ca$	Cauchy number	[-]
$C_D$	Drag coefficient	[-]
$d_x$	Base material diameter associated with passing percentage x%	[m]
$d^*$	Dimensionless particle diameter	[-]
$d_{\text{rel}}$	Relative sediment diameter	[-]
$D_{50}$	Median particle diameter	[m]
$D_{50,\text{min}}$	Minimum median particle diameter	[m]
$D_x$	Particle diameter associated with passing percentage x%	[m]

Symbol	Explanation	Unit
$D_x$	Adjusted rock diameter for winnowing	[m]
$D_{cable}$	Cable diameter	[m]
$D_m$	Mattress thickness	[m]
$D_{pile}, D_p$	Pile diameter	[m]
$E$	Elasticity modulus	[Pa]
$E_{additional}$	Additional extent	[m]
$f$	Flexibility coefficient for mattresses	[-]
$f$	Frequency	[Hz]
$Fr(t)$	Froude number based on layer thickness	[-]
$Fr(D_{15})$	Froude number based on $D_{15}$	[-]
$f_w$	Wave friction factor	[-]
$g$	Gravitational acceleration	[m <sup>2</sup> /s]
$h_{bd}$	Bed level drop at edge of protection	[m]
$h_{berm}$	Rock berm height	[m]
$h_{edge;inline}$	Edge scour depth in line with tidal axis	[m]
$h_{edge;transverse}$	Edge scour depth transverse to protection	[m]
$h_{min}$	Minimum required height	[m]
$h_w$	Water depth	[m]
$h_{sill}$	Sill height	[m]
$h_{top}$	Water depth on top of the scour protection	[m]
$h_{tot}$	Total bed level lowering	[m]
$H_s$	Significant wave height	[m]
$I$	Second order moment of vegetation area	[m <sup>4</sup> ]
$k_s$	Equivalent roughness height	[m]
$K_f$	Turbulence factor	[-]
$K_h$	Near-bed current factor	[-]
$K_s$	Slope factor	[-]
$K_{top}$	Factor relating velocity at seabed level to velocity on scour protection	[-]
$KC$	Keulegan Carpenter number	[-]
$KC_{tot}$	Total KC number	[-]
$l$	Length of stem	[m]
$L$	Wave length	[m]
$L(f)$	Wave length as a function of frequency	[m]
$M_{50}$	Median weight of rock grading	[kg]
$M_{em}$	Mean effective mass	[kg]
$MOB$	Relative mobility	[-]
$MOB_c$	Current-related mobility	[-]
$MOB_w$	Wave-related mobility	[-]
$MOB_{top}$	Mobility on top of the scour protection	[-]

Symbol	Explanation	Unit
$MOB_{top;slope}$	Mobility on top of the scour protection slope	[-]
$MOB_{top;flat}$	Mobility on top of the flat scour protection	[-]
$MOB_{bed;slope}$	Mobility at seabed level on the scour protection slope	[-]
$MOB_{thresh}$	Threshold value of mobility	[-]
n	Vegetation population density	[-]
n	Ratio between equivalent roughness height and rock size	[-]
n	Porosity of rock layer	[-]
$N_{D,top}$	Number of rock layers on top of rock berm slope	[-]
$N_{D,bottom}$	Number of rock layers on bottom of rock berm slope	[-]
$N_w$	Number of waves	[-]
$r_{a1}$	Initial radial extent scour protection	[m]
$r_{b1}-r_{b5}$	Radii associated with various protection extents away from the pile	[m]
S	Scour protection deformation	[m]
$S_{x\%}$	Scour protection deformation exceedance percentage x%	[m]
S(f)	Ocean wave spectrum	[m <sup>2</sup> s]
$S_{eq}$	Equilibrium scour depth	[m]
$S_{u,bed}(f)$	Spectrum of near-bed velocity	[m <sup>2</sup> s <sup>-1</sup> ]
$S_{u,top}(f)$	Spectrum of near-bed velocity on top of scour protection	[m <sup>2</sup> s <sup>-1</sup> ]
$t_{armour}$	Armour layer thickness	[m]
$t_{apron,toe}$	Falling apron layer thickness at toe of apron	[m]
$t_{apron,top}$	Falling apron layer thickness at top of apron	[m]
$t_{rock}$	Rock layer thickness	[m]
$t_{single}$	Layer thickness of single-layer scour protection	[m]
$t_{prot}$	Protection thickness	[m]
$t_v$	Vegetation thickness	[m]
T	Temperature	[°C]
$T_p$	Peak wave period	[s]
$T_z$	Zero-crossing wave period	[s]
TOPC	Top of protection cover	[m]
$U_{char}$	Characteristic velocity	[m/s]
$U_{m,a}$	Orbital velocity	[m/s]
$U_{m,bed}$	Orbital velocity near the bed	[m/s]
$U_{m,top}$	Orbital velocity near the bed on top of the scour protection	[m/s]
$u^*,c$	Current-related shear velocity	[m/s]
$u^*,w$	Wave-related shear velocity	[m/s]
$U_c$	Depth-averaged current velocity	[m/s]
$U_{crit}$	Critical velocity for initiation of motion	[m/s]
$U_{crit,KB}$	Critical velocity in filter layer based on Klein Breteler et al. (1992)	[m/s]
$U_{rel}$	Relative velocity	[-]



Symbol	Explanation	Unit
$V_{\text{apron}}$	Falling apron volume	[m <sup>3</sup> ]
$V_{\text{tot}}$	Total volume	[m <sup>3</sup> ]
$V_{\text{unlaunched}}$	Unlaunched apron volume	[m <sup>3</sup> ]
$W_{\text{top}}$	Top-width rock berm	[m]
$X_1 - X_3$	Coefficients for minimum layer thickness to prevent winnowing	[-]
$Z_0$	Roughness length	[m]
$Z_{\text{dol}}$	Depth of lowering	[m]
$Z_{\text{sbl}}$	Seabed level	[m]
$\alpha$	Angle between wave and current direction	[°]
$\alpha$	Initial slope angle of scour protection or rock berm	[°]
$\alpha$	Amplification & reduction function for winnowing	[-]
$\beta$	External slope angle of falling apron	[°]
$\Delta$	Relative density	[-]
$\Delta\rho$	Density difference fluid and vegetation	[kg/m <sup>3</sup> ]
$\Phi$	Stability parameter	[-]
$\varphi$	Angle of repose of rocks	[°]
$\rho_w$	Density of water	[kg/m <sup>3</sup> ]
$\rho_s$	Density of rock/sediment	[kg/m <sup>3</sup> ]
$\theta$	Shields parameter	[-]
$\theta_c$	Current-related Shields parameter	[-]
$\theta_{\text{crit}}$	Critical Shields parameter	[-]
$\theta_w$	Wave-related Shields parameter	[-]
$\nu$	Viscosity of water	[m <sup>2</sup> /s]
$T_c$	Current-related bed shear stress	[N/m <sup>2</sup> ]
$T_m$	Mean wave-current related bed shear stress	[N/m <sup>2</sup> ]
$T_{\text{max}}$	Maximum wave-current related bed shear stress	[N/m <sup>2</sup> ]
$T_w$	Wave-related bed shear stress	[N/m <sup>2</sup> ]

# 1 Introduction

## 1.1 Background

This handbook is the result of a multi-year research programme performed as a Joint Industry Project with the contribution of over 20 industrial partners. This project was initiated from the observation that no good design formulae and guidelines exist to protect offshore support structures against scour. Instead, there are many different methods and concepts that lack a sound basis for design. As a consequence, developers, utilities and contractors have applied very different solutions against scour around support structures with varying degrees of success.

To help decision makers select the most suitable and cost-effective scour protection method for each considered situation the Joint Industry Project Handbook Scour and Cable Protection Methods (JIP HaSPro) was initiated by Deltares. Apart from this research institute, the consortium consists of a certifying body (DNV), utilities (Ørsted, RWE, Vattenfall, Scottish Power, EnBW, Shell, Equinor, Ocean Winds), suppliers (SPT Offshore, Mibau Stema, Airgroup Industries, NoRock, SSCS, Maccaferri), engineering firms (COWI, Kajima) and installation contractors (DEME Group, Boskalis, Van Oord, Jan de Nul). The goal of this project is to develop a clear, generic and science-based comparison between different scour protection methods. In this project existing methods (based on loose rock) are optimized and new innovative scour mitigation methods are investigated (proof-of-concept) and made ready for offshore field tests. The resulting findings are presented in the present Handbook of Scour and Cable Protections.

## 1.2 Considered foundation types

Many different support structures exist for offshore infrastructure. For offshore wind development, in most cases monopiles are selected for their simplicity and adaptability. Although many of the principles discussed in this handbook also apply to other foundation types, the main emphasis is on monopile foundations.

## 1.3 Structure of the handbook

This handbook first provides a brief overview on the background of free scour development (Chapter 2) and possible mitigation strategies (Chapter 3). Then, the handbook focusses on scour protection methods, starting with conventional loose rock protections. Firstly, with the design of loose rock scour protections (Chapter 4), followed by a description of rock gradings to be used in the offshore environment (Chapter 5). Guidelines for scour protection installation are discussed (Chapter 7) before presenting operation and maintenance recommendations (Chapter 8). The next part of the handbook is dedicated to possible alternative scour protection methods (Chapter 9), including artificial vegetation (Chapter 10) and various types of mattress solutions (Chapter 11). Finally, information related to Nature Inclusive Design of scour protections is provided (Chapter 0). The appendices provide background on the calculation methodology and provide some calculation examples.

# Part I

## Scour development and mitigation strategies

## 2 Scour prediction for offshore foundations

### 2.1 Introduction

This chapter provides a concise background on theoretical aspects and terminology related to scour (Sections 2.2 and 2.3) and scour prediction (Section 2.4), as well as global seabed level lowering (Section 2.5). These serve as a basis for the following chapters related to scour mitigation and scour protection design.

### 2.2 General definitions

In order to distinguish between the different types of scour, the following definitions are adopted in this study. Where possible they are closely following the ones used in the offshore standard DNV-RP-0618 (September 2022): Rock scour protection for monopiles.

- *Local scour*: scour around an individual structure, for example around a single monopile or around one leg of a jacket structure (Figure 2.1 and Section 2.3).
- *Global scour*: scour within and closely around the footprint of a multi-legged structure, such as a jacket structure (Figure 2.2)
- *Edge scour*: scour occurring outside the scour protection caused by the interaction of the flow with the structure and protection (Sections 2.3 and 4.2.3 )
- *General (or autonomous) seabed level change*: bathymetric (or topographic) changes which are not influenced by the presence of a structure (as opposed to the above scour types); e.g. caused by migrating sand waves and megaripples, shifting tidal channels or other medium to large scale mobile, degrading or aggravating seabed features.

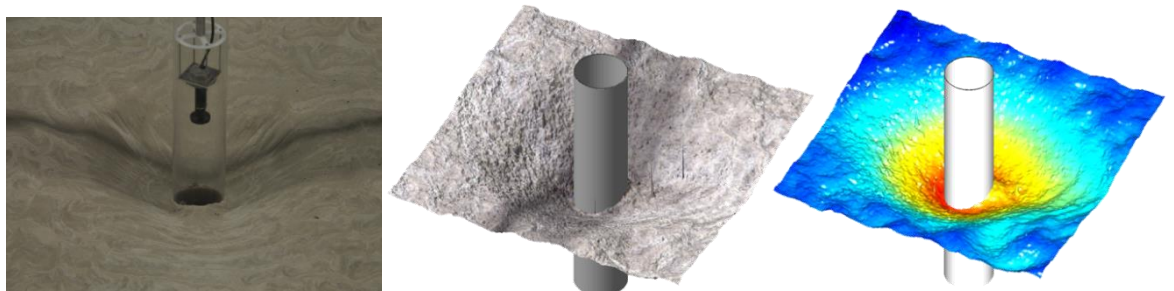


Figure 2.1 (Left) example of a local scour hole around a transparent scale model of a monopile, equipped with a fish eye camera to continuously record scour development during a model test; (middle) 3D-colour image and (right) 3D bathymetry obtained from a measurement.



Figure 2.2 (Left) local scour holes around individual jacket legs and global scour pit around entire footprint (Angus & Moore, 1982); (right) local scour holes around foundation piles and global scour hole around beach house after occurrence of Hurricane Ike.

## 2.3 General description of the (local) scour process

Scour is the local removal of sediment around the base of a structure, resulting from sediment transport gradients that occur due to the impact of the structure on the flow. The structure acts as a local blockage that leads to a local acceleration and subsequent deceleration, often coupled with high turbulence intensities. As a result, a scour hole develops around the structure. The exact scour hole development process depends on the flow phenomena around the structure and thus also the type of structure. Around a single monopile, for example, several hydrodynamic features are present: a pressure gradient related to the presence of the pile causes a downflow at the upstream side and the so-called horseshoe vortex at the base of the pile, whilst at the downstream end of the pile vortices are shed (Figure 2.3). Amplification around a singular pile is typically significant up until a distance of 1.5 times the pile diameter away from the pile. Further away from the pile the amplified flow will generally not induce significant scour.

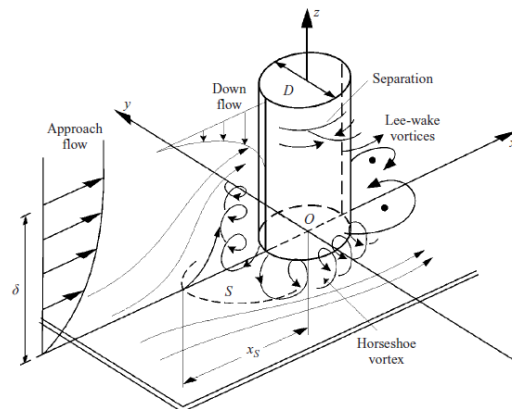


Figure 2.3 Left: characteristic flow features around a pile (Sumer & Fredsøe, 2002).

Around a more complex structure, like a jacket, two different types of scour can be recognized. Even though a jacket is a largely porous structure with limited blockage, such a structure leads to an amplified flow over an area within and around the structure. This leads to the formation of a depression around the entire structure, referred to as a global scour hole. In addition, there is additional amplification around the singular elements of the structure, that lead to larger lowering around them, referred to as local scour. This is illustrated in Figure 2.2 (left). Global and local scour are not mutually exclusive, but in general global scour takes far longer to develop than local scour.

Another mechanism of scour occurs when a scour protection is in place. With the area near the structure protected structure, scour is shifted towards the edge of the protection. These edge scour holes are the result of the disturbance of the flow due to the structure (similar to local and global scour, dependent on the scour protection extent) and the influence of the scour protection itself. Generally, edge scour holes are smaller than local scour holes and take a longer time to fully develop.

The deepest edge scour holes are expected to develop downstream of the structure. However, in offshore conditions the flow direction is constantly reversing because of the tidal current. This results in edge scour development at alternating sides of the structure. Also, during each cycle the scour hole at the upstream will be slightly backfilled by sediment that is transported by the flow and deposited in the existing edge scour hole. This generally limits the average depth of the edge scour. Besides edge scour downstream of the tidal current, edge scour can also occur at the side of the scour protection perpendicular to the main tidal axis due to amplification related to the presence of the scour protection and locally increased turbulence levels. In addition, slight variations in the tidal directions and/or wave action can lead to small differences in the edge scour pattern. It is furthermore noted that elongating the scour protection in the direction of the tidal axis (making an elliptically shaped scour protection) can lead to a significant reduction in edge scour depth (Petersen et al., 2015). This is attributed to covering a larger area of the seabed with erosion resistant material and by weaker forcing on the erodible seabed due to it being further away from the pile.

When there is a (strong) tidal asymmetry (for example when the flood current is stronger than the ebb current) then the pattern shifts. Such a tidal asymmetry causes an asymmetry in sediment transport as well, resulting in a deeper edge scour hole at one side of the structure than at the other side. Figure 2.4 presents field observations of the edge scour development in Egmond aan Zee OWF, averaged over all 36 monopiles. The tidal asymmetry clearly caused asymmetric edge scour development around the scour protection. It can also be observed that edge scour development took years and has reached equilibrium after about 7-8 years. Besides contribution to potential falling apron development, edge scour development (both depth and extent) is highly relevant for the design of the power cables.

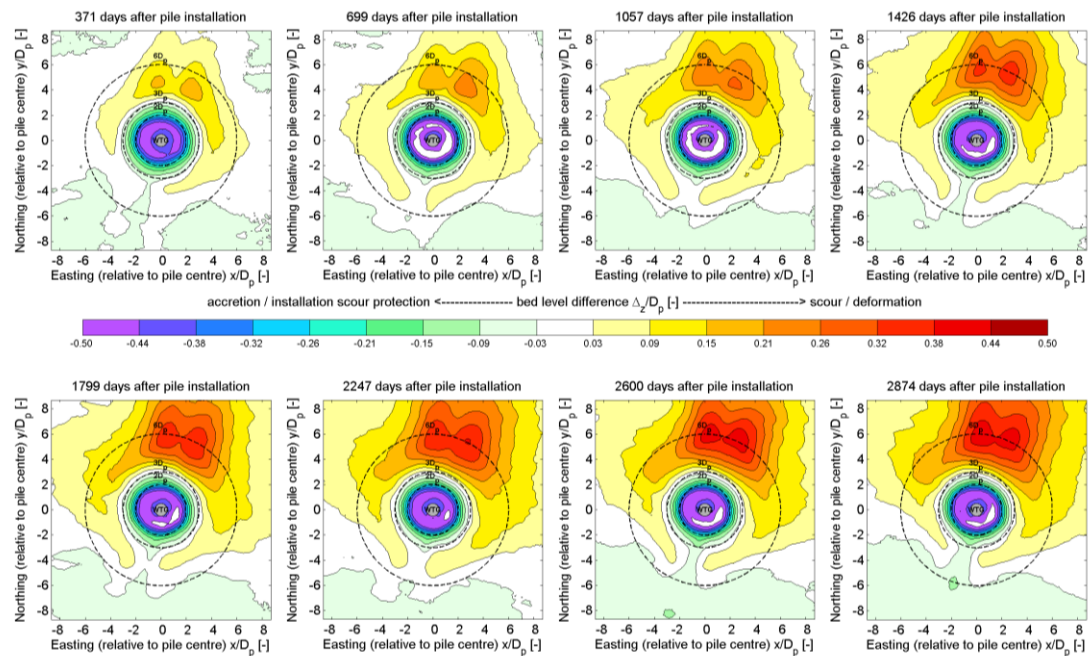


Figure 2.4 Edge scour development in Egmond aan Zee OWF (built in 2006) within 8 years, averaged over all monopiles. All dimensions are normalized by the pile diameter and all coordinates are transposed to the pile center Petersen et al. (2015).

## 2.4 Scour prediction methodologies

Scour prediction methodologies are predominantly (semi-)empirical. A vast amount of experimental research into scour development around various types of structures has been performed, leading to an equally large amount of scour depth prediction formulae with various application ranges, see, for example Sheppard & Miller (2006), Breusers et al. (1977), Hoffmans & Verheij (1997), Melville (2008) and Guan et al. (2022). It is noted that the majority of formulations for scour around cylindrical objects are valid for current-only situations because most of the research for those configurations was performed for scour around bridge piers in rivers. Nevertheless, these formulae are well applicable in offshore environments, although it is noted that typically wave action will lead to a reduction of scour depth.

There are various ways to make a scour prediction using these empirical formulations. Using a time-series of hydrodynamic forcing parameters and assuming a certain shape of time development (for example, hyperbolically converging towards an equilibrium), time development of scour can be predicted using a semi-numerical approach. This is the method followed by the Dynamic Scour Prediction Model developed by Deltares (Raaijmakers & Rudolph, 2008). Alternatively, empirical scour depth formulations may be combined with a numerical model prediction of hydrodynamics. Such a coupling is for example the approach followed in HEC-RAS. It should be noted that typically time-scale relations for scour prediction are based on physical modelling data as well. A direct upscaling of these results is not straightforward due to scaling conflicts, which is good to keep in mind when interpreting laboratory data for field application. Although correcting for the scaling issues is in theory possible, see for example Nagakawa & Suzuki (1976), this is not a straightforward and well-defined task. Recent efforts to improve the definition of time scales of scour may improve this interpretation (Larsen & Fuhrman, 2023).

Recently, the use of Computational Fluid Dynamics (CFD) for scour predictions is also increasing. Although at present this is still a research tool utilized on laboratory scale, the step towards field scale predictions is being made, see for instance Roulund et al. (2005) or De Wit et al. (2023).

## 2.5 Global bed level lowering

Global bed level lowering is typically interpreted as the result of large-scale morphodynamics. It is noted that with global scour, also a general bed level lowering around a structure consisting of multiple foundation elements is meant (right side of Figure 2.3). In addition, a global lowering could also occur around monopiles in areas with significant sediment dynamics. The interruption of the natural dynamics due to the pile (i.e., in the form of a wake) can be observed for a distance of up to 50-60 times the pile diameter. Especially in areas with significant sediment transport presence, this could lead to a global lowering in the wake of the monopile that extends significantly further than a typical (edge) scour hole. Although this lowering can be considered as edge scour as well, it is argued that a better way to define such a scour pattern is to call it global scour.

The remainder of this section is dedicated to global lowering related to large-scale morphodynamics. Typical parameters of geometry and dynamics that distinguish different types of morphological seabed features (wavelength, wave height and mobility) are presented in Figure 2.5. Please note that the dimensions presented are mainly intended to indicate the order of height and length. Individual bedforms can exceed the dimensions presented. The bedforms are classified as either mobile or stationary over the lifetime of the assets. Stationary bedforms however might be mobile over longer periods of time (>100 years). Secondly, a distinction is made between transient and persistent bedforms. Transient bedforms e.g. ripples and megaripples are considered to change shape and appear or disappear as a result of hydrodynamic conditions. Persistent bedforms, on the other hand, are considered to (more or less) retain their shape and mobility throughout the considered period. In the last column, the potential threat to foundations and power cables is indicated per bedform.

	Wavelength	Wave height	Mobility	Threat to foundations and cables
Ripples	0.1 - 5 m	0.01 – 0.1 m	Mobile and transient	Minimal
Megaripples	5- 50 m	0.1 – 1.0 m	Mobile and transient	Minimal
<b>Sand waves</b>	<b>50 - 1000 m</b>	<b>1 - 10 m</b>	<b>Mobile and persistent</b>	<b>Large</b>
Sand banks	1 – 10 km	10 - 100 m	Stationary	Minimal

Figure 2.5 Morphodynamic seabed features and some typical characteristics.

Please note that the presented bedform characterisation is valid for the offshore environment typical for offshore wind farms. In other areas, for example tidal estuaries or coastal zones, bedform mobility and dimensions can differ significantly.



## 3 Scour mitigation strategies

### 3.1 Introduction

A designer of offshore wind turbine foundations must always consider the potential of scour development around the foundation. Scour is the phenomenon that seabed sediments are eroding around the base of the foundation due to the action of hydrodynamics. Scour will, for piled foundations, lower the pile fixation level or, for sit-on-bottom structures, cause undermining of the foundations. The expected scour development depends on many different parameters, such as structural dimensions and shapes, seabed composition and hydrodynamic climate. Predicting scour development for various foundation types was addressed at a high-level in Chapter 2.

Once the predicted scour depth is known, the designer should choose whether scour development can be accepted and how the foundation design can be adjusted to be able to cope with a potential lowering seabed level. This option may be more viable for one foundation type than the other.

If the designer chooses to protect the foundation against scour by installing a scour protection, then multiple strategies can be taken, differentiating between the moment of installation and the type of scour protection applied. The strategies related to timing will be explained in this chapter, whereas the different scour protection methods will be discussed in following chapters. It is noted that all mitigation strategies and scour protection methods are applicable to foundation stability. Nowadays, the industry is facing significant challenges with stability of Cable Protection Systems (CPSs). Mitigation of those issues can be achieved via similar means as achieving foundation stability, but the execution is completely different. The mitigation strategies and scour protection methods presented in this handbook are applicable for foundation stability and were not developed with CPS stability in mind.

This chapter will first introduce the possible scour mitigation strategies to set the framework for the more in-depth chapters that will follow. Several classifications of mitigation strategies will be specified that can then be referred to when discussing the applicability of certain measures later in this handbook. In Section 3.2 the scour mitigation strategies will first be explained for areas with a more or less stable seabed for the entire lifetime of the wind farm; this assumption can both be true for entire wind farms in areas with limited morphodynamic activity or for carefully selected foundation locations in areas with significant morphodynamic activity.

Since many wind farms are (for large parts) characterized by significant, not-to-be-neglected morphodynamic activity, the scour mitigation strategies are extended for areas with a lowering or rising seabed in Section 3.3.

Many different foundation types can be considered for offshore wind turbines. As discussed in Chapter 1, it was chosen to use the monopile foundation for illustration of the different scour mitigation strategies. The reason for this choice is threefold: 1) monopiles are still by far the most commonly applied foundation type for offshore wind turbines; 2) monopiles were used in most physical model tests which form the basis for this handbook and 3) at monopile foundations all the presented mitigation strategies can be applied. However, different mitigation strategies can also be adopted for other foundation types, be it with slight adjustments.

### 3.2 Scour mitigation strategies excluding morphodynamics of the seabed

Before including the full complexity of autonomous morphological processes, first scour mitigation strategies will be developed for (more or less) stationary seabeds. This typically represents sites that are characterized by less than 1 m seabed change during the lifetime of a foundation. Or, in

case the design allows for rising seabeds (see Section 3.3 for more explanation), this criterion can be narrowed down to “less than 1 m seabed lowering during the lifetime of a foundation”. Whether an offshore structure needs to be protected is a matter of cost efficiency and risks.

The following strategies can be adopted:

### 3.2.1 Strategy A: Free scour development

According to this strategy, the foundation is installed into or on top of the unprotected seabed, after which scour is allowed to develop; this strategy is illustrated in Figure 3.1. If a foundation is not protected and a scour hole is predicted to develop, then the structure needs to be designed to be able to cope with a changing fixation level. In most cases this results in increased material consumption; e.g. for a monopile the embedded length is increased.



Figure 3.1 Strategy A: No scour protection and allowing free scour development.

This strategy is often considered when:

- The seabed is not or hardly erodible, e.g. in case of cohesive soils that can be proven to be non-erodible.
- The seabed is only erodible under strongly wave-dominated conditions, which will for many structure shapes not result in severe scour development.
- Non-erodible layers are present at limited depth (e.g. up to a few meters below the seabed).
- The foundation type is not very sensitive to losing the top few meters of seabed sediments.

Apart from adjusting the structure design, it is important to consider the power cables. Special attention to the cable touch down point is recommended: in most construction time schedules the cables are planned to be installed before the scour hole has reached its equilibrium. This means that the cable touchdown point might lower in the months after cable installation. To assess this lowering, both the shape of the predicted scour hole and the orientation of the cables needs to be considered. Please note that in some locations the scour holes will not be perfectly round, but more elliptical in shape.

### 3.2.2 Strategy B: Immediate scour protection

This strategy is based on maintaining the initial seabed level around the foundation. This strategy can typically be used for locations with mobile seabed sediments and strong tidal currents that can cause scour of a few meters in days to weeks. For such a case the position of the seabed needs to be secured before the foundation is installed. An example is illustrated in Figure 3.2 for a monopile with a two-layered scour protection. In this example first a filter layer is installed and then the pile is driven through the filter layer, after which an armour layer is installed on top.

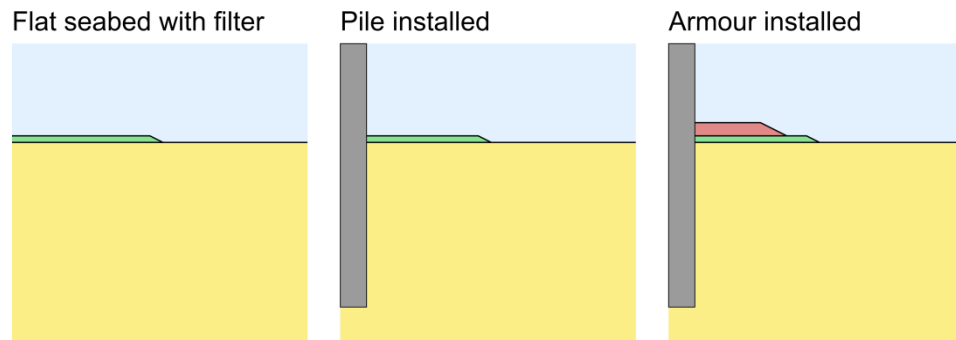


Figure 3.2 Strategy B: Immediate scour protection.

This strategy is often considered when:

- The seabed is well erodible, e.g. in case of sandy, silty or weak clayey soils combined with significant hydrodynamic loads on the seabed.
- The costs related to additional pile length (required when scour would be allowed) are expected to be higher than the costs of a scour protection.
- The foundation type is of the “sit-on-bottom”-type such as a Gravity Base Structure (GBS).
- The foundation type has a limited penetration depth such as a Suction Bucket Jacket (SBJ).

### 3.2.3 Strategy C: Monitor and React

Strategy C is based on first allowing scour development up to a pre-defined level and then install a scour protection inside the scour hole. This strategy is illustrated in Figure 3.3. Due to the sheltered position of the scour protection material close to the pile inside the scour hole, the scour protection will be more stable than in the situation where it is placed on the original seabed. Consequently, lighter materials can be used (than in a protection installed directly on the seabed).

For this strategy it is preferable to apply only one scour protection material, because installation of multiple layers inside an often steeply and irregularly sloping scour hole is rather difficult.

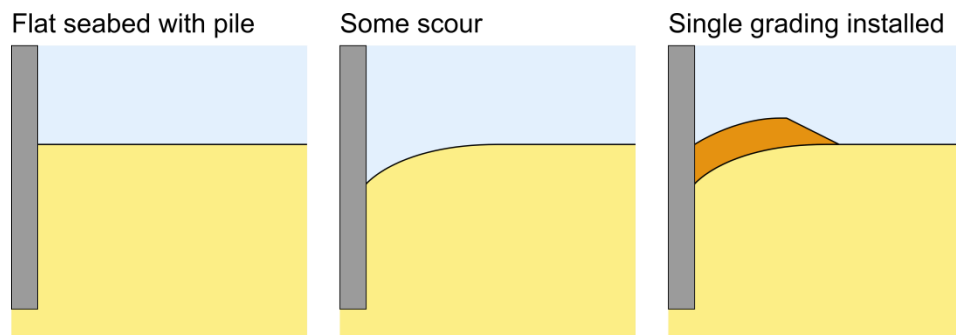


Figure 3.3 Strategy C: No scour protection, allowing some scour development and delayed installation of scour protection.

This strategy requires good predictive capabilities of the scour development. If scour develops much slower than anticipated, the favourable weather windows for installation of the scour protection might be missed. On the other hand, if scour development occurs much faster than anticipated, then the necessary installation equipment might not yet be ready, or the installation schedule is too tight to be able to meet with the equipment at hand.

A variant to this strategy is to wait for the measurements of the structural response of the wind turbine foundation to wind- and wave-loads and then assess the optimum pile fixation level. In situations where Strategy B is adopted, the foundation often behaves stiffer than according to design

due to conservative estimates of the soil stiffness in the design calculations. This can result in fatigue issues. By adopting Strategy C the pile frequency can be tuned (improving the fatigue behaviour), when the scour protection is installed to the optimum level.

### 3.3 Scour mitigation strategies including morphodynamics of the seabed

In the previous section three main scour mitigation strategies were discussed for the situation with a (more or less) stable seabed level. However, for many sites the seabed is not stable. When a wind farm is planned in a morphodynamic area, there are two approaches for dealing with morphodynamics in the scour mitigation strategies:

#### 1. Reactive approach

In the reactive approach morphodynamics are not considered as a design driver when the wind farm layout is determined. This is the case, for instance, when the wind farm layout is only determined based on wind yield calculations, perhaps in combination with geotechnical and geological considerations. In this case, some foundations may be subjected to seabed lowering; others to seabed rising and again others may be located in a more or less stable seabed. Consequently, different scour mitigation strategies may be chosen for three foundation groups (stable/lowering/rising seabed) in a wind farm.

#### 2. Pro-active approach

In the pro-active approach foundations are deliberately planned on locations with selected expected seabed changes. Either the foundation locations are planned on the top of sand wave crests to minimize steel consumption (and accept higher scour mitigation costs) or the foundation locations are planned in the sand wave troughs to minimize risks with lowering seabed levels and free-spanning cables in exchange for higher steel consumption but lower scour mitigation costs.

#### 3.3.1 Strategy A: Free scour development

For Strategy A the consequences of a lowering and rising seabed are depicted in Figure 3.4. Since the timescales of autonomous seabed changes are often much longer (~years to decades) than the timescales of scour development (~days to months), the scour hole will typically be able to follow the changing seabed. A lowering seabed will therefore cause an equally fast lowering of the pile fixation level.

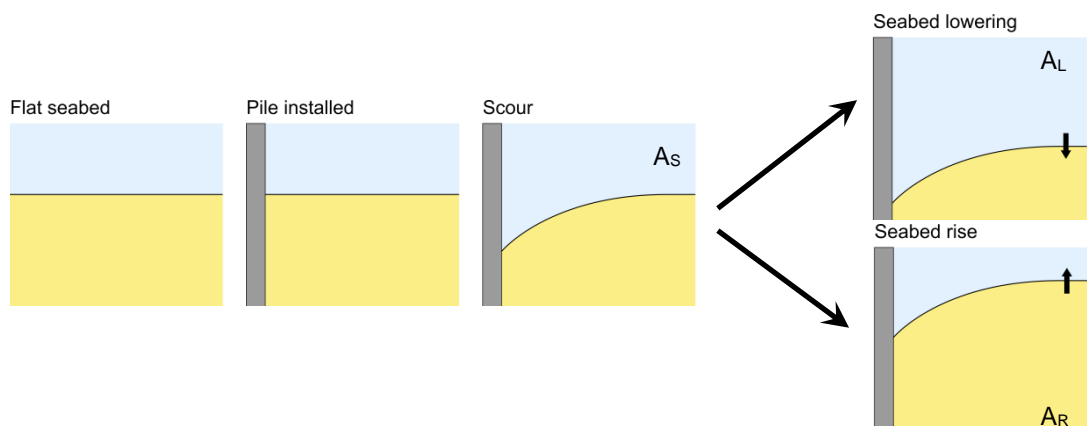


Figure 3.4 Strategy A: No scour protection, allowing free scour development with a lowering seabed (top right) and a rising seabed (bottom right); the abbreviations  $A_S$ ,  $A_L$ ,  $A_R$  represent Strategy A with a stable (S), lowering (L) and rising (R) seabed respectively.

It should be noted, however, that the depth and shape of the scour hole can change, dependent on the type of morphodynamic environment and the related hydrodynamic climate. Morphodynamic

seabed changes can either enhance or dampen out scour effects. In general, we distinguish between these two common types:

- *Sand wave fields:* In offshore environments (at significant distance from the shoreline) largest autonomous seabed changes during the lifetime of a windfarm are typically caused by migrating sand waves (see Section 4.2.3).
- *Tidal flats and channels:* In tidal environments largest seabed changes are typically caused by migrating tidal channels cutting off parts of tidal flats (Riezebos et al., 2016).

In the first case, the current velocities will typically reduce when the current is flowing from a sand wave crest to a trough (related to the perpendicular orientation of the sand waves to the tidal current axis). Since the scour depth is related to the current velocity, scour holes are expected to be shallower when located in sand wave troughs compared to sand wave crests. Also, the rate of scour development is expected to be slower. The opposite is often true for the second case: in tidal channels the flow velocities are typically larger than on the tidal flats. If a tidal channel migrates into a tidal flat, then both the ambient seabed level will drop and the scour hole around the foundation will get deeper due to the increased current velocities; seabed drops at the base of the foundation of ~10-15m have been observed in the past over the lifetime of the windfarm.

### 3.3.2 Strategy B: Immediate scour protection

For Strategy B the two scenarios for a rising and a lowering seabed are illustrated in Figure 3.5 and Figure 3.6 respectively. When the seabed is rising, the scour protection at some distance from the foundation will fill in with seabed sediment. Close to the pile a scour hole will develop in the sand accumulating on top of the scour protection. As a consequence, the pile fixation level will not change too much, resulting in only a moderate increase (or none at all) in horizontal bearing capacity and pile fixity.

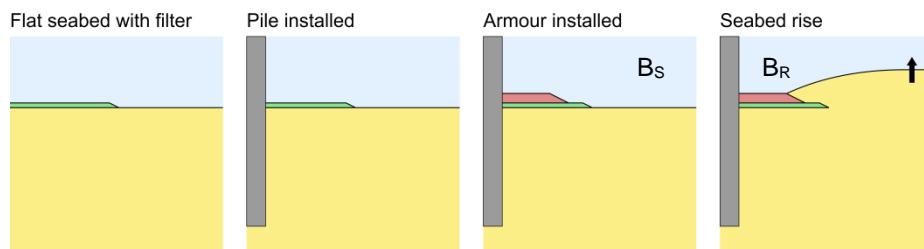


Figure 3.5 Strategy B: Immediate scour protection with **rising** seabed; the abbreviations  $B_S$ ,  $B_R$  represent Strategy B with a stable (S) and rising (R) seabed respectively. In this morphodynamic scenario, the foundation is hardly affected because of local scour development counteracting the rising seabed.

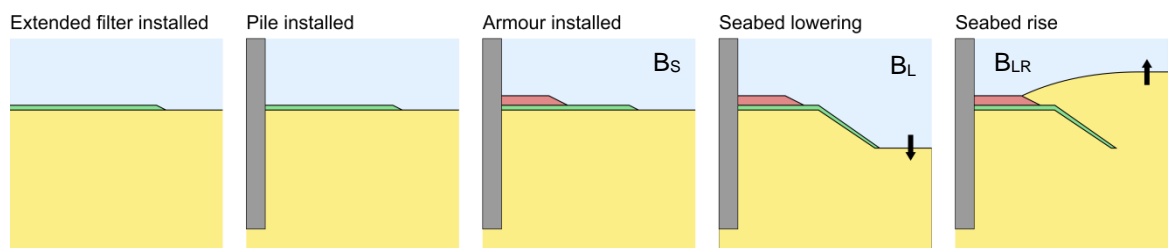


Figure 3.6 Strategy B: Immediate scour protection with **lowering** seabed; the abbreviations  $B_S$ ,  $B_L$ ,  $B_{LR}$  represent Strategy B with a stable (S), lowering (L) and first lowering then rising (LR) seabed respectively. This strategy is relying on flexible behaviour of the protection at the edges in order to maintain the seabed level close to the pile and to ensure the integrity of the scour protection; subsequent rising of the seabed is not expected to harm the protection.

If the seabed is lowering ( $B_L$ ), the situation is more challenging. Then the edge of the scour protection should be sufficiently flexible to follow the seabed to ensure a tight connection between seabed and scour protection. If the extent of the scour protection is sufficiently large, then the amount of soil remaining around the foundation will guarantee only a limited decrease in soil stiffness for the embedded part of the foundation. In case the seabed starts rising again, after a period of lowering ( $B_{LR}$ ), the 'launched' part of the scour protection will get completely buried again. Local scour will limit the effects on soil stiffness.

Dependent on the expected amount of seabed lowering, one additional check should be considered. Due to the more exposed position of the "foundation + scour protection + retained part of seabed" the wave loads on the scour protection can increase. This may be caused by two effects: a) in deeper water depths larger waves can reach the foundation without breaking; b) for larger protected areas waves will refract and shoal on the side slopes causing focused wave action on the scour protection and foundation.

In conclusion, scour protections can be applied in areas with a lowering seabed, as long as the scour protection has good flexible behaviour at the edge and an extent carefully adjusted to the expected seabed drop.

### 3.3.3 Strategy C: Monitor and React

For Strategy C, Figure 3.7 and Figure 3.8 are illustrating the consequences of seabed rising and lowering respectively. For a rising seabed ( $C_R$ ), the edges can become infilled with sediment and the scour protection close to the pile will get an even more sheltered position. For a lowering seabed ( $C_L$ ) the flexibility is again important: in case of loose protection material the volume needs to be sufficiently while for a composite protection the edges need to be sufficiently flexible and strong to allow for a downward movement over the lowered sloping seabed.

An additional design consideration for Strategy  $C_L$  (which also holds for Strategy  $B_L$ ) is edge scour (explained in Section 4.2.3). An increase of the apparent scour protection height will cause an increase in edge scour depth, which also should be considered; see also Section 4.4.3

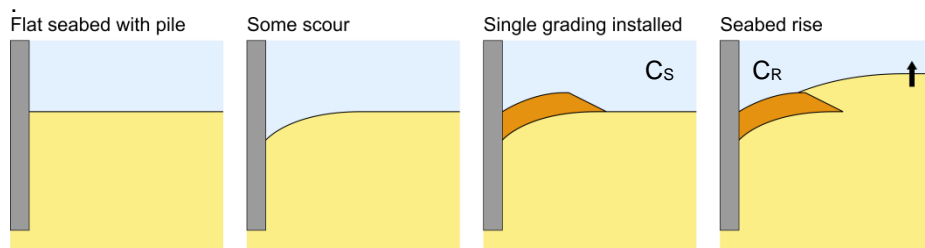


Figure 3.7 Strategy C: Monitor and React with **rising** seabed; the abbreviations  $C_S$ ,  $C_R$  represent Strategy C with a stable (S) and rising (R) seabed respectively. In this morphodynamic scenario, the foundation is hardly affected because of local scour development counteracting the rising seabed.

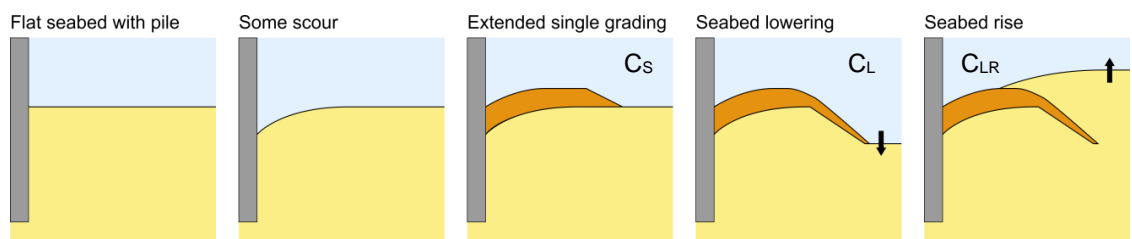


Figure 3.8 Strategy C: Monitor and React with **lowering** seabed; the abbreviations  $C_S$ ,  $C_L$ ,  $C_{LR}$  represent Strategy C with a stable (S), lowering (L) and first lowering then rising (LR) seabed respectively. This Strategy is relying on flexible behaviour of the protection at the edges in order to maintain the seabed level close to the pile and to ensure the integrity of the scour protection; subsequent rising of the seabed is not expected to harm the protection.

Strategy C is typically recommended for situations where large seabed lowering is expected, resulting in an increased hydrodynamic load on the rocks higher up in the water column. In such a case, the scour protection can become very exposed, meaning the rocks are likely more unstable. First allowing scour to develop puts the rocks initially in a more sheltered position, increasing their stability, and leading to less exposure during the lifetime. However, to facilitate that, scour development needs to be predictable and sufficiently fast to be able to install both the foundations and the scour protections (with sufficient time for scour development in between) within the period of favourable weather.

# Part II

## Scour protection methods – rocks



# 4 Design of loose rock scour protections around monopile foundations

## 4.1 Introduction

If the designer has chosen to protect the foundation against scour by installing a scour protection, and has subsequently selected an appropriate strategy, the scour protection layout can be designed. This involves selecting the appropriate rock grading (or gradings, in case a two-layer system is needed). The appropriate rock grading depends on the environmental conditions, but also on what is deemed to be an acceptable performance by the designer. If little to no deformation of the rock is allowed, then this will lead to a different choice of rock grading compared to the situation that (some) reshaping is allowed. In addition to what can be accepted in terms of scour protection behaviour, the scour protection must satisfy various basic performance requirements and more and more often nature-inclusive design considerations are required (see Chapter 0). It is noted that a scour protection, besides being a hydraulic structure in itself also enables other interfaces, like cable stabilization or facilitation of eco-friendly elements.

This chapter will first provide an overview of scour protection performance requirements (Section 4.2). Various methods currently exist to evaluate if a scour protection fulfils these requirements. Within the framework of JIP HaSPRO generic design methods are derived based on an experimental database consisting of a large number of physical model tests. An overview of this experimental database is provided in Section 4.3, including the main outcomes of extensive analysis of the results. Then, for each of the performance criteria described in Section 4.2, a design approach based on the physical model test database is described in Section 4.4. Based on the design approaches, for each of the performance criteria different rock parameters are relevant. An overview of required grading information for each of the performance criteria is listed in Section 4.5. Finally, an overview of the dimensioning of the scour protection is provided in Section 0.

For reasons of conciseness, the handbook does **not** contain an in-depth analysis of the experimental results. The reader is referred to the accompanying analysis report (document ref.: 1230924-002-HYE-0003) for a full elaboration on the analysis that was performed on the physical model test results related to external stability, interface stability and flexibility of loose rock scour protections.

## 4.2 Scour protection performance requirements

The wave and current induced flow is accelerated around a monopile due to the adverse pressure gradient, potential horseshoe vortex and lee-wake vortex, as shown in Figure 4.1. The amplified flow induced bed load is the primary reason for destabilisation of the scour protection layer.

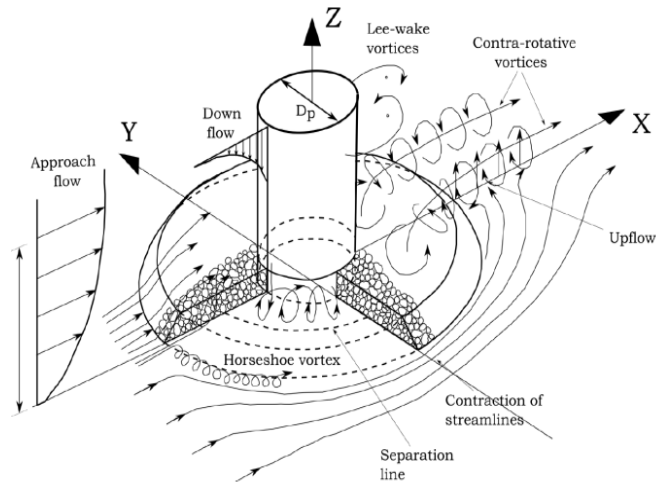


Figure 4.1 Flow patterns around a monopile with a scour protection Petersen et al. (2015).

Three main aspects of stability should be considered in a monopile scour protection design (Figure 4.2):

- External stability: the top layer of rocks should be sufficiently stable under the design load;
- Interface stability: washing out of sediment through the pores of the scour protection should be prevented or mitigated;
- Flexibility: the scour protection should be able to handle edge scour and/or morphological bed level lowering.

Nowadays, especially in the Dutch North Sea wind farms, a fourth criterium becomes more and more important. As a fourth criterium, a scour protection should mitigate the impact of foundation structures on the environment and preferably even enhance biodiversity. Chapter 0 provides a concise overview of Nature Inclusive Design (NID) principles, with the side-note that these developments are in a relatively early stage of knowledge development and application at present.

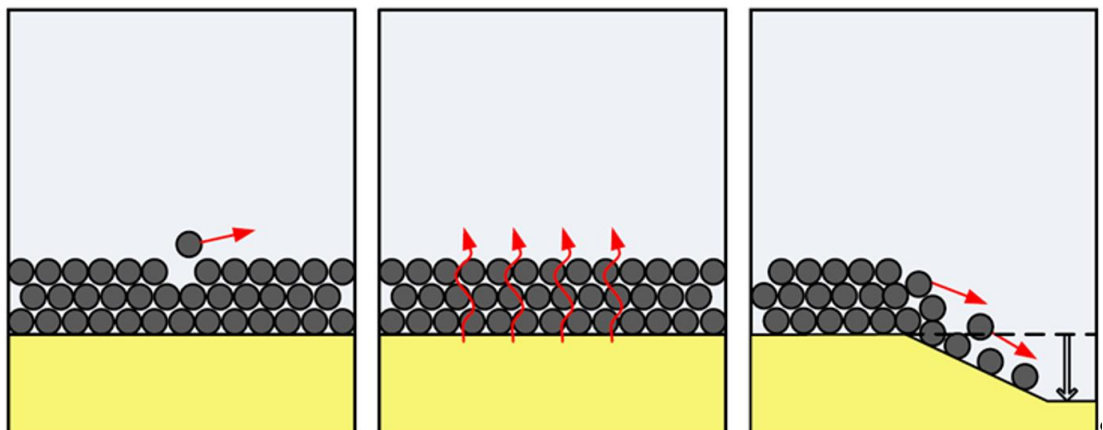


Figure 4.2 Schematisation of external stability (left), interface stability (middle) and flexibility (right).

The performance criteria of loose rock scour protections are separately discussed in Section 4.2.1 to 4.2.3. Subsequently, two different types of loose rock scour protection concepts are presented in Section 4.2.4.

#### 4.2.1 External stability of loose rock scour protections

External stability refers to the resistance of the material against deformation due to hydraulic loads. The external stability criterion can be satisfied by selecting a sufficiently large rock grading. The selected grading can either be statically stable, meaning that no movement occurs under the design hydrodynamic load, or dynamically stable, in which case some movement and reshaping of the top layer is allowed for as long as the required minimum thickness is not exceeded. The difference between a static and dynamic scour protection is illustrated in Figure 4.3. Note that this figure includes deformation at the edge of the protection as well ("falling apron" behaviour due to seabed lowering at the edge) in addition to deformation of the armour layer. This deformation is related to flexibility of the scour protection, which can occur for scour protections that are designed to be completely externally stable as well. This demonstrates that there are many mechanisms that can lead to scour protection deformation, which are quite often interlinked as well.

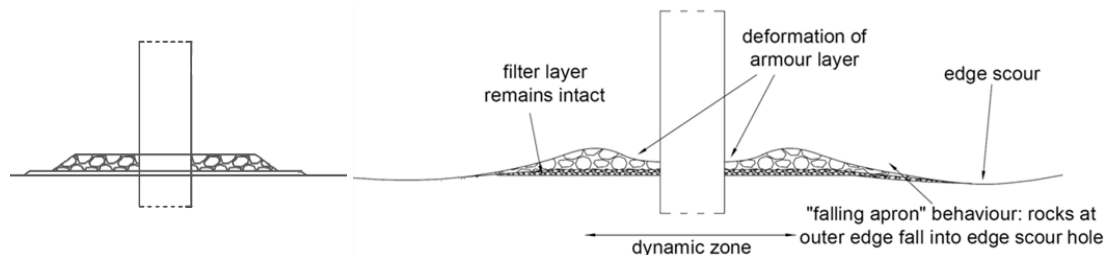


Figure 4.3 Scour protections around a monopile: statically stable (left) and dynamically stable (right).

Various parameters are important to establish the degree of stability of a loose rock scour protection. These are discussed in Section 4.4.1.

#### 4.2.2 Interface stability of loose rock scour protections

A scour protection should be designed taking into account the possibility of suction removal of sediment through the pores of the scour protection (called winnowing). For offshore applications often use is made of geometrically open filters, which means that sediment can escape through the pores of the protection. For such designs winnowing can be controlled by ensuring that sufficient layer thickness is present to reduce the hydrodynamic load at the seabed.

An overview of the applicable theory on the use of open filters around circular structures was given by De Sonnevile et al. (2014). There it was found that existing formulations on the design of open filters either do not take into account the presence of a pile or do not consider the combined effect of waves and currents. Each investigation had its specific focus, and there is no formulation that covers all relevant aspects for the design of geometrically open loose rock scour protection in offshore conditions. Within JIP HaSPRO dedicated tests were performed aimed at filling this knowledge gap.

##### Mechanics of winnowing around a pile

The hydrodynamics around a pile with a scour protection were extensively investigated by Nielsen (2011). From his research, the horseshoe vortex was identified as the main cause of winnowing around the monopile. The horseshoe vortex penetrates into the scour protection and causes a recirculating flow in the rock layer. The recirculation flow gives a return flow at the bed, which is forced out of the rock layer around the separation line (where the return flow meets the approach flow). The separation line generally lies around 0.5 to 1 times the pile diameter from the pile face,

similar to the separation line around an unprotected pile. A sketch of the flow patterns in current-only conditions is shown in Figure 4.4.

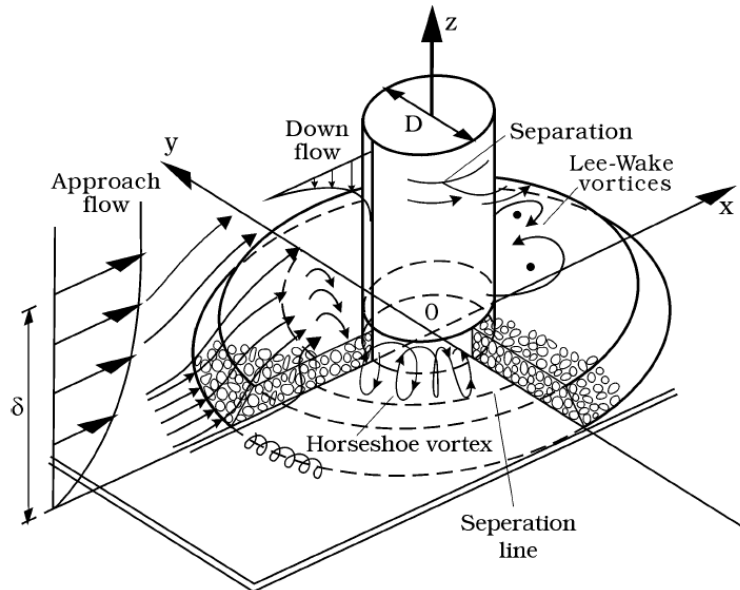


Figure 4.4 Flow patterns around pile with scour protection, from Nielsen (2011).

The size of the horseshoe vortex is typically limited (up to  $D_{pile}/2$ ), which is limiting the penetration depth in the scour protection. For scour protections with a thickness larger than the vertical vortex size, the horseshoe vortex remains in the top layers of the scour protection, and drives a lower, secondary vortex (rotating in opposite direction). This is shown in Figure 4.5. In this case, the bed velocities can increase again due to the presence of the secondary vortex. However, as the turbulent kinetic energy at the bed decreases significantly with larger layer thicknesses, the winnowing potential is in general smaller for larger layer thicknesses.

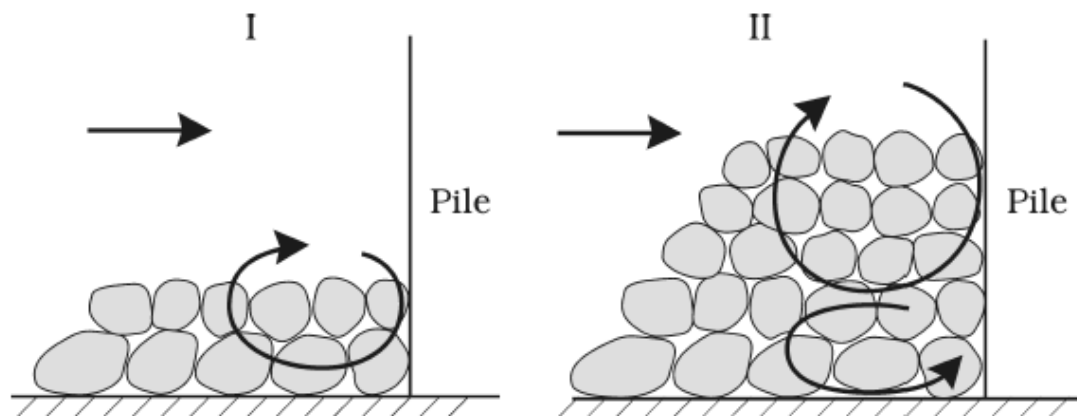


Figure 4.5 Sketch of single (left) or double (right) vortex system, from Nielsen (2011).

Winnowing (transport of base material through the scour protection) occurs by sediment transport either from the return flow (which is swept out of the filter layer at the separation line), or at the pile face if the horseshoe vortex is strong enough. Sediment removal therefore mainly happens adjacent to the upstream sides of the pile, where velocities and turbulence levels are relatively high due to the penetration of the horseshoe vortex through the layer of rock.

### 4.2.3 Flexibility of loose rock scour protections

Undermining of the edges of a scour protection (edge scour) and lowering of the surrounding seabed due to morphological seabed features (see also Section 2.5 and 3.3) could lead to progressive failure of the entire system. To prevent this, a scour protection should be sufficiently flexible. This is typically done by supplying additional material at the outer edge of the protection to serve as a falling apron: the material rolls down the slope of the edge scour hole, stabilising it against further erosion. This behaviour is also visible in Figure 4.2 (right), Figure 4.3 (right) and Figure 4.6. The extent of the scour protection can be increased to handle edge scour effects.

Sand waves form a high threat to offshore foundations and scour protections. The migration of sand waves results in a gradually changing seabed level at the location of an offshore structure over the lifetime. For the design of the scour protections two levels are important:

1. The actual seabed level at the time of installation (ASBL: Actual Seabed Level);
2. The lowest potential seabed level over the lifetime of the structure (RSBL: Reference Seabed Level, sometimes also referred to as LSBL: Lowest Seabed Level).

A third, as of yet undefined, level is shown as well. The Maximum Seabed Level (MSBL), sometimes also referred to as Highest Seabed Level (HSBL), is not directly relevant for the performance of a scour protection when it is higher than the installation level (ASBL), so if seabed rising is expected during the foundation lifetime. For ecological performance of a scour protection the expected amount of seabed rise in relation to armour height is of interest, as clogging of pores with sand limits the habitat space that is created by the protection.

The difference between these two levels is the potential bed level drop ( $h_{bd}$ ), which needs to be accounted for in the design of the scour protection (see Figure 4.6). The design of the extent of the scour protection should be based on the highest possible seabed level drop that can occur during the lifetime, thus taking into account the most unfavourable condition. At locations where the seabed is expected to rise before installation, this could thus mean taking the difference between the highest anticipated seabed level and the lowest anticipated seabed level. This would eliminate the need to validate if the designed extents to account for bed level lowering comply with the actual seabed level at the time of installation.

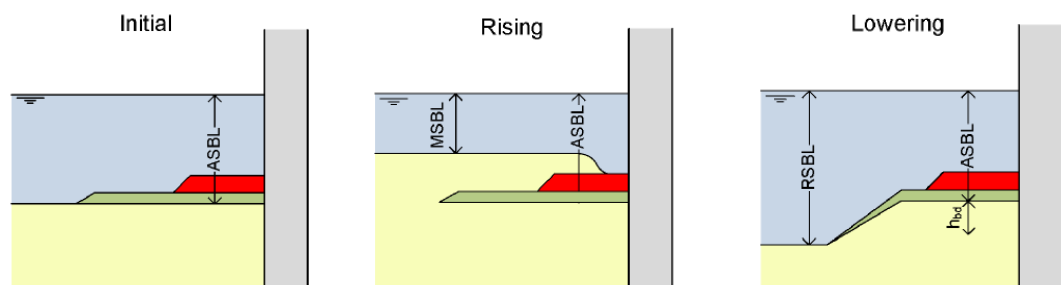


Figure 4.6 Schematic effect of morphodynamic seabed features around a monopile with installed scour protection, dimensions are not proportional. Left to right: initial installation of scour protection, rising of the surrounding seabed and lowering of the surrounding seabed. Note: this schematisation implies a two-layered scour protection, but the principles hold for a single-layer scour protection as well.

#### Edge scour depth estimation

Edge scour development was studied extensively by Petersen et al. (2015), showing there are differences between edge scour development at the scour protection perimeter and edge scour extending downstream of the scour protection. The findings of this study are interpreted as follows:

- Edge scour at scour protection perimeter: this type of edge scour is caused by turbulence from the flow obstruction of the scour protection berm. The edge scour depth generally is in

the range of 0.3 to 0.8 times the scour protection thickness. The edge scour is located adjacent to the scour protection perimeter.

- Edge scour extending downstream of scour protection: this type of edge scour is caused by the vortex shedding originating from current flow around the pile. The edge scour is located approximately 4-10 pile diameters downstream of the pile along the main tidal current direction. The downstream edge scour generally is in the range of 0.3 to 0.6 times the pile diameter. The downstream edge scour is not always observed and is thought primarily to develop in areas with strong asymmetric tidal currents and significant sediment transport. The presence of the pile distorts the flow, leading to transport gradients that can trace back throughout the pile generated wake and lead to a large footprint of bed level changes. This can be interpreted as a 'global' edge scour effect.

In North-Sea conditions, edge scour development is expected to take about 5-10 years to reach its dynamic equilibrium depth. This is based on field measurements of Offshore Wind Farm Egmond aan Zee (OWEZ) in the Netherlands. It is noted that for other locations, with different dynamics, this may be different. As stated above, the expected edge scour depth transverse to the tidal axis shows correlation with the obstruction height of the total protection (including morphology), which makes it a function of  $h_{bd}$  and the thickness of the scour protection, whereas the inline edge scour is related to the pile diameter:

$$h_{edge:inline} = S_d = 0.3 \text{ to } 0.6 \times D_{pile} \quad (1)$$

$$h_{edge:transverse} = S_t = 0.3 \text{ to } 0.8 \times (h_{bd} + t_{prot}) \quad (2)$$

With:  $h_{edge}$  = expected edge scour depth [m]  
 $h_{bd}$  = predicted bed level drop [m]  
 $t_{prot}$  = thickness of the scour protection (including installation tolerances) [m]

The choice for the appropriate factor to use in Equations 1 and 2 to determine edge scour depths is dependent on both the environmental conditions and the scour protection characteristics (Figure 4.8).

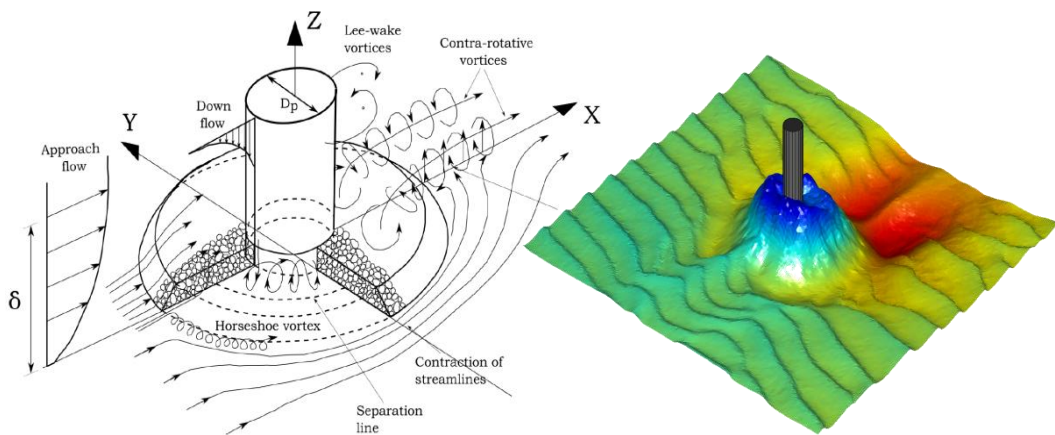


Figure 4.7 Left: Flow patterns around a monopile with a scour protection (Petersen et al., 2015). Right: example of edge scour hole in Egmond aan Zee Offshore Wind Farm (note: vertical scale distorted).

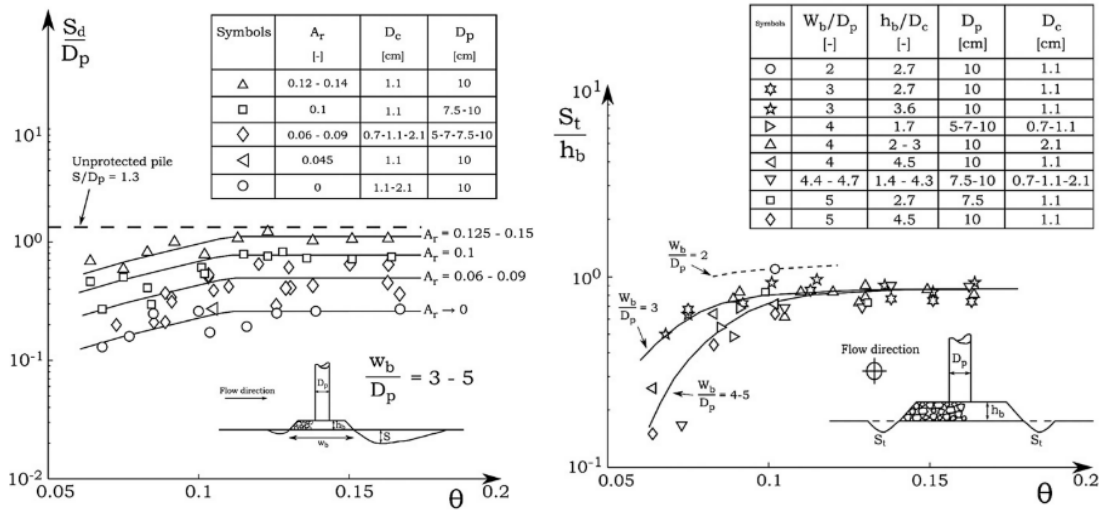


Figure 4.8 Inline edge scour depth  $S_d$  (left) relative to the pile diameter and transverse edge scour depth  $S_t$  (right) relative to the scour protection thickness, both as a function of the Shields parameter (see Appendix A) for current-only conditions. Figures from Petersen et al. (2015).

#### 4.2.4 Scour protection types

Two different scour protection concepts based on loose rock can be distinguished: the double-layer scour protection with armour and filter layer, and the single-layer protection which consists of only one, generally wide-graded, rock grading.

With a double-layer scour protection, the functionality of the protection is divided over two layers. The armour layer should provide external stability (preventing excessive deformation due to hydraulic loads), while the filter layer provides interface stability (preventing winnowing) and ensures sufficient flexibility (ability to follow bed changes and/or edge scour). It is noted that the armour layer can also be designed to extend beyond the filter flayer, in which case the armour layer should provide the flexibility towards seabed lowering.

A single-layer protection consists of a single rock grading, which should fulfil all three functions. Single-layer scour protections typically consist of smaller rock because they need to fulfil the interface stability function (prevent winnowing). The smaller diameter of the material means that it is inherently less stable than a larger armour rock grading. However, because a single-layer scour protection generally consists of many individual rock layers, more deformation can be allowed. Under high hydrodynamic load a single-layer scour protection is therefore expected to reshape into a new equilibrium profile. This is acceptable as long as deformations are within the functional design specifications of the scour protection. An example of both systems (installed around a monopile scale model) is given in Figure 4.9.

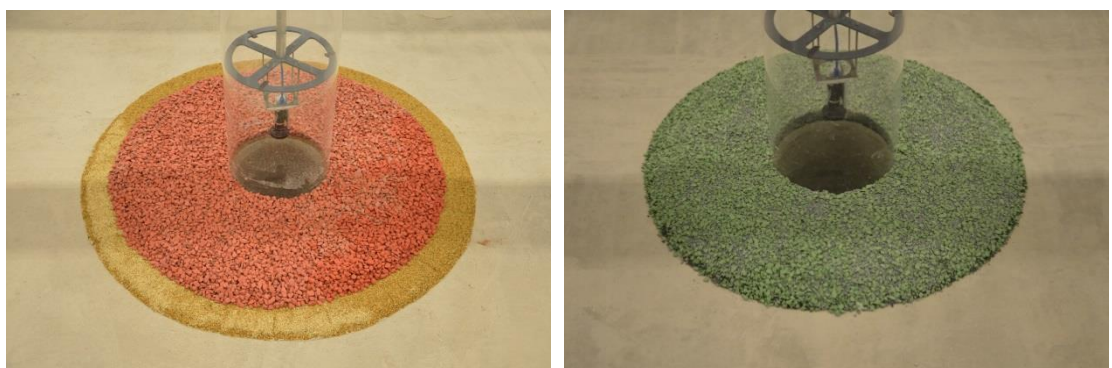


Figure 4.9 Double-layer rock protection (left) and single-layer rock protection (right).

It is noted that alternative geometries than sketched above can be (temporarily) applied. For example, the scour protection can be installed with a doughnut shape, omitting rock in the middle of the protection, so that the monopile can be installed without having to penetrate the rock layers. Other examples may involve leaving out a trench for the cables so that they can be embedded in the scour protection and post-installed berms on top of the cables for their stabilization.

## 4.3 Experimental database

Dedicated tests were performed to study the three scour protection performance requirements (external stability, interface stability and flexibility). For a full elaboration on the set-up, performance and description of the results of the model tests, the reader is referred to the separate model tests reports (external stability: Deltares (2023b), document ref.: 1230924-003-HYE-0001, interface stability: Deltares (2023h), document ref.: 1230924-003-HYE-0003, flexibility: Deltares (2023c), document ref.: 1230924-003-HYE-0002). Here, a brief summary of the experimental database is provided, focussing on the parameter variation of selected (non-dimensional) parameters.

### 4.3.1 External stability

The test database that was used to derive a generic formulation to predict scour protection deformation related to external stability consists of approximately 380 individual test results. Of these 380 test results, 145 datapoints stem from JIP HaSPRO. A total number of 158 tests included an ambient seabed level lowering with respect to the top of the scour protection. In the database, most of the tests consider wave-current loading, with 332 tests having a current direction in alignment with the wave direction, 31 tests having a current direction opposed to the wave direction and 17 tests having no current.

Scour protection deformation depends on a large number of parameters, including hydrodynamic conditions (water depth  $h_w$ , significant wave height  $H_s$ , peak period  $T_p$ , depth-averaged current velocity  $U_c$ , number of waves  $N_w$ , density of the water  $\rho_w$ , viscosity of the water  $\nu$ ), rock properties (rock density  $\rho_s$ , median rock size  $D_{50}$ , grading width  $D_{85}/D_{15}$ ), scour protection layout characteristics (thickness  $t$ , extent  $E$ , single- or double-layer) and foundation properties (for monopiles the pile diameter  $D_{pile}$ ). A large part of these parameters may be grouped together into several dimensionless parameters to perform a more generic (and more broadly applicable) analysis. As such, the analysis aims to find a function describing the deformation,  $S/D_{pile}$ , with the following dependencies:

$$\frac{S}{D_{pile}} = f \left( MOB_{top}, KC_{tot}, \frac{h_w}{D_{pile}}, U_{rel}, N_w, \frac{D_{85}}{D_{15}}, \text{geometric properties}, \dots \right) \quad (3)$$

Naturally, not all parameters are equally important. Based on the analysis performed on the experimental database the observed deformation appears to scale most clearly with the pile diameter, because the occurring deformation is mostly related to the obstruction posed by the foundation. Therefore, the deformation  $S$  is scaled with the pile diameter  $D_{pile}$ . Scour protection deformation was determined using a moving average disk-filter with a diameter of 5 times the  $D_{50}$  to eliminate deformation related to the removal of a single rock.



Figure 4.10 provides an overview of the parameter space present in the physical model test database. This parameter space is expressed in the following non-dimensional parameters:

- Relative mobility on top of the scour protection ( $MOB_{top}$ ): a measure of far field hydraulic stability of rock (evaluated at the top of the scour protection).
- Total KC-number ( $KC_{tot}$ ): A measure of water motion amplitude relative to the pile diameter (evaluated by addition of wave and current velocity contributions).

A third, and often-used, parameter is the relative velocity  $U_{rel}$ , which is a measure of wave or current dominance. The influence of wave or current domination has, in the deformation model, been found to be better represented by the addition of both influences via the total KC-number than by their relative contribution as expressed in  $U_{rel}$ .

Appendix A and Appendix B outline the calculation methodology to determine these parameters. The observed deformation patterns are primarily related to the relative mobility, with a secondary dependence on the total KC-number (Deltares, 2023n, document ref.: 1230924-002-HYE-0003).

There is a weak correlation between increasing mobility and increasing total KC-number as can be seen in Figure 4.10.

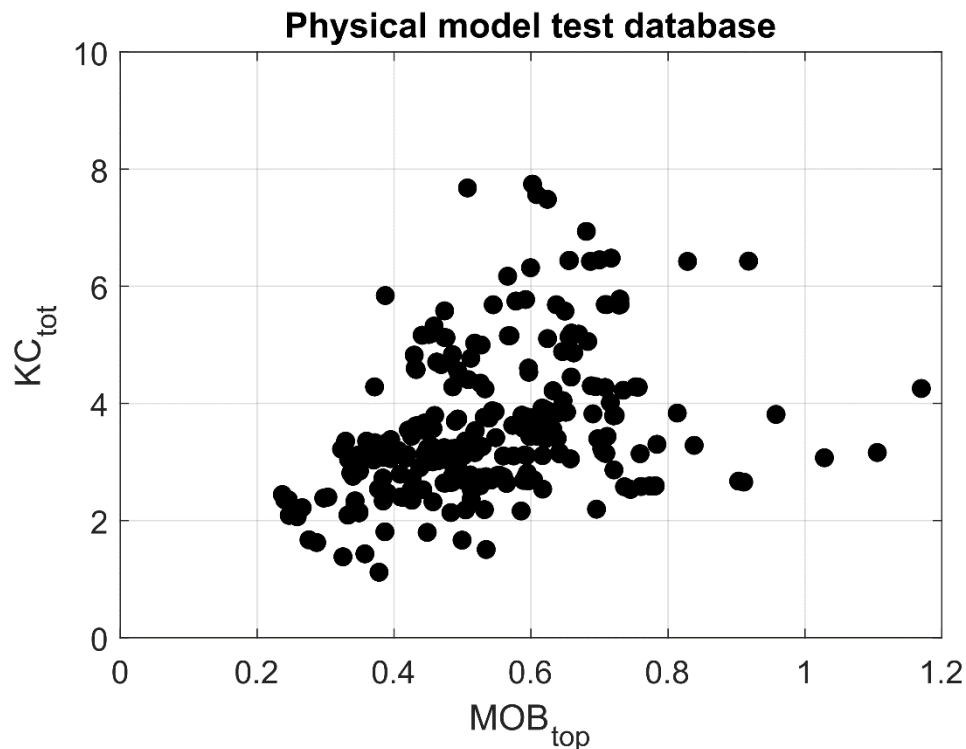


Figure 4.10 Parameter space of the datapoints within the physical model test database. The primary classification parameter is the relative mobility ( $MOB_{top}$ ) and the secondary parameter is the total KC-number ( $KC_{tot}$ ).

An important aspect to mention about the observed deformation in the test database is that typically physical model tests are not singular, separate tests but often performed in a series of consecutive events with increasing severity of conditions. The deformation is always determined based on the same 'before' measurement (zero-measurement); thus, the deformation in the test database represents cumulative deformation. This approach could be considered as (slightly) conservative, yet a valid approach to consider the observed cumulative deformation as deformation related to the specific separate conditions, because the increase in severity of the condition is sufficiently large. It

is implicitly assumed that the deformation occurring for the milder condition would occur rapidly during the more severe conditions as well, therefore limiting the temporal effect of cumulative tests.

Table 4.1 shows the range of relative mobility on top of the scour protection ( $MOB_{top}$ ), total KC-number ( $KC_{tot}$ ) and ratio between the water depth and the pile diameter  $h_w/D_{pile}$  present in the test-database used to derive the generic deformation formula. Deformation relations based on two subsets of the experimental database thought to cover the majority of typical design conditions were derived as well. Naturally, these subsets cover a smaller range of conditions. The following datasets were used to derive a generic deformation formula:

- Complete dataset (Table 4.1, 2<sup>nd</sup> column)
- Truncated dataset omitting deformation larger than 4 rock layers and omitting deformation associated with opposing current conditions (Table 4.1, 3rd column)
- Truncated dataset omitting deformation larger than  $0.075D_{pile}$  and deformation associated with  $KC_{tot}$  numbers larger than 4.2 (Table 4.1, right column)

Table 4.1 Parameter range in used experimental database.

Parameter	Complete dataset	Clipped data set 1	Clipped data set 2
$MOB_{top}$	0.24 – 1.17	0.24 - 0.73	0.24 - 0.96
$KC_{tot}$	1.1 – 7.8	1.1 - 6.4	1.1 – 4.1
$U_{rel}$	-0.56 – 0.63	0.12 - 0.61	0.13 – 0.63

#### 4.3.2 Interface stability

Similar to the external stability analysis, an experimental database with relevant tests for the interface stability is made. This database consists of the results from the JIP HaSPRO tests (Deltares, 2023c), complemented with available data from previous research.

For the JIP HaSPRO tests, it was chosen to use the symmetry axis and distinguish between a ‘left’ and ‘right’ side of the protection. This results in two results per test per pile. The analysis is based on the observed scour at the interface with the pile. As the interface analysis provides a full 180° (upstream to downstream) sediment interface throughout time and the sediment removal is not equal along the pile face, different scour depths (compared to the initial bed level) were considered in the analysis. The best results were obtained with a 90<sup>th</sup> percentile scour depth. As most of the tests were not continued until equilibrium was achieved, the time-varying scour depths were fitted to a scour formula to determine the expected equilibrium scour depth. After fitting of the scour depths, only the tests with logical results and fits have been placed in the database. This selection is based on expert judgment of the fit results, in which evaluation of the fit ( $R^2$ ) and potential unrealistic equilibrium scour depths are included as selection criteria.

Additionally, model test results from previous studies have been added to the database. For consistency, only the results of single-layer scour protections have been taken from these studies. Data from the following sources have been added:

- In-house data: equilibrium scour depths
- Wörman (1989): initiation of scour
- Nielsen et al. (2013): initiation of motion
- De Sonnevile et al. (2014): equilibrium scour depths
- Nielsen et al. (2015): equilibrium scour depths
- Nielsen & Petersen (2018): initiation of scour

In total the database consists of 172 data points with scour due to winnowing, of which 103 data points have been obtained through JIP HaSPRO. It contains 51 wave-only tests, 66 current-only tests and 55 combined waves-and-current tests.

### Relevant parameters

Winnowing depends on a significant number of parameters, including hydrodynamic conditions, rock grading characteristics, foundation dimensions, base material characteristics and the scour protection dimensions. Considering the winnowing mechanics described in Section 4.2.2, the following dimensionless parameters are relevant:

- Relative scour depth:  $S_{eq}/D_{pile}$
- Relative current velocity:  $U_c/U_{crit}$  (or similar)
  - This parameter provides the current velocity relative to the initiation of motion. Please note that this is similar to a mobility number (MOB). Different methods to determine the critical velocity are used in the analysis.
- Froude number based on layer thickness (Wörman, 1989) or based on the rock diameter:

$$Fr(t) = \frac{U}{\sqrt{g \cdot t}} \quad \text{and} \quad Fr(D_{15}) = \frac{U}{\sqrt{g \cdot D_{15}}}$$

- Number of rock layers ( $t/D_{15}$  or  $t/D_{50}$ )
- The relative layer thickness compared to the pile diameter ( $t/D_{pile}$ )
- The relative rock size compared to the pile diameter ( $D_{50}/D_{pile}$ )
- The relative sediment size compared to the rock size ( $d_{85}/D_{15}$  or similar)
- The relative pile diameter ( $h_w/D_{pile}$ )
- The grading width ( $D_{85}/D_{15}$ )

For more information on these parameters, reference is made to the analysis in Deltares (2023n). The parameter space of these variables in the test database (for current-only conditions) is provided in Table 4.2, including an estimation of the parameter range in prototype conditions.

Table 4.2 Parameter range in winnowing experimental database.

Parameter	Database	Prototype	Remarks
$U_c/U_{crit,KB}$	12.5 - 75	12 - 80	The critical velocity is based on the method by Klein Breteler et al. (1992)
$Fr(t)$	0.3 – 1.4	0.1 – 1.0	
$Fr(D_{15})$	0.5 – 3.5	0.5 – 3.0	
$t/D_{15}$	2 – 18	4 – 20	
$t/D_{pile}$	0.2 – 2.0	0.05 – 0.15	
$D_{15}/d_{15}$	82 - 175	60 – 700	
$h_w/D_{pile}$	3.5 – 7.0	2.0 – 5.0	
$D_{50}/D_{pile}$	0.08 – 0.18	0.005 – 0.015	
$D_{85}/D_{15}$	1.2 – 1.8	1.8 – 3.5	

### 4.3.3 Flexibility

Within JIP HaSPro, several dedicated tests related to the launching of a falling apron were performed. For a full elaboration of these tests the reader is referred to the test report (Deltares (2023c), document ref.: 1230924-003-HYE-0002). In the past, several current-only tests were performed by Van Velzen (2012). These were in more recent years supplemented by various wave-current tests (Riezebos et al., 2016). The tests in JIP HaSPro serve as an addition to those tests (see Table 4.3 and Figure 4.11).

Scour protections constructed on top of a sill were subjected to various combinations of tidal currents and wave conditions. The development of the falling apron was continuously monitored using stereophotography in between tests. By doing so, the developing side-slopes can be related to the hydrodynamic conditions the protections are exposed to. An expression is provided that relates the needed additional extent to both the bed level change and side-slopes of the launched apron. This expression is presented in Section 4.4.3.

Table 4.3 Parameter range of the falling apron development tests.

Parameter	Complete dataset
$MOB_{top}$	0.14 – 2.8
$h_{sill}/h_w$	0.04 – 0.55

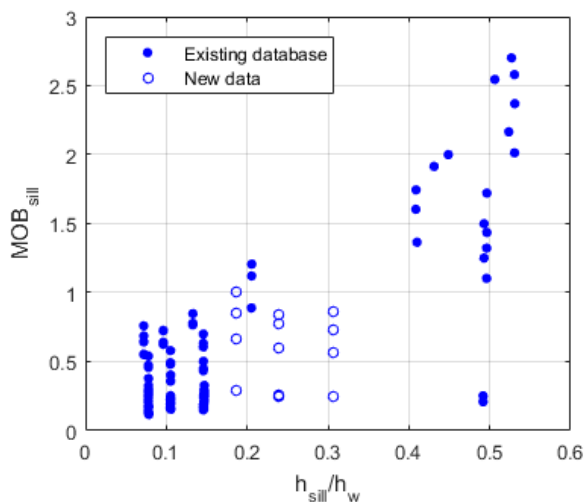


Figure 4.11 Visualization of the test database used for determining flexibility of scour protections. The markers without fill represent the data collected within JIP HaSPro.

## 4.4 Design approach

### 4.4.1 External stability

This section deals with the external stability criterion for loose rock scour protections. Here, a model to compute scour protection deformation for a given (extreme) hydrodynamic condition is presented, including guidance on the use of this model in various forms (Section 4.4.1.1). Then, layer thickness of the armour layer (or in case of single-layer scour protections, the dynamic layer) is discussed in Section 4.4.1.2, followed by the required extent from an external stability point of view in Section 4.4.1.3. Finally, mobility limits as a (not-recommended) alternative to the deformation model are presented that may be used for quick assessments (Section 4.4.1.4).

#### 4.4.1.1 Deformation model

An analysis of scour protection deformation as a function of the forcing conditions based on an extensive physical model test database is provided in Deltares (2023n). The deformation of a scour protection depends primarily on the relative rock mobility on top of the scour protection and secondly on the total KC number related to both wave and current forcing. Other parameters did not show any clear correlation with the deformation after a correction for the KC number was made. This correction for the KC-number involves dividing the observed deformation  $S/D_{pile}$  by a function of the KC-number,  $f(KC_{tot})$ . The deformation model is then dependent on two non-dimensional parameters, being the mobility on top of the scour protection,  $MOB_{top}$ , and the total KC-number,  $KC_{tot}$ . A deformation relation that is a function of the mobility number only was also derived. In this case, the only fitting constants that apply are  $c_1$  and  $c_2$ . This results in a relation that is intuitively easier to understand, but with more spreading in the results compared to explicitly taking along the KC-number in the formula.

The resulting deformation model is presented in Equation 4. The deformation model based on the complete available dataset is able to predict scour protection deformation with an average deviation of 1.5% of the pile diameter. Based on the standard deviation of the fitting constant  $c_1$ , various

levels of non-exceedance values for the fitted data were derived. Values for  $c_1$  for these various confidence bounds are provided. In addition to the complete dataset, an analysis was performed on truncated datasets as well. With the idea that in general scour protections are designed to handle limited deformation, two dataset truncations were applied. Values of the fitting constants are provided assuming a relation including both  $MOB_{top}$  and  $KC_{tot}$  and assuming a relation including only  $MOB_{top}$ . For the truncated dataset where deformation associated with KC-numbers larger than 4.2 was omitted, the result obtained with either of both relations is similar. Performance of the derived deformation model for the complete dataset and truncated datasets, with and without considering the effect of the KC-number is shown in Figure 4.12. Parameter ranges present in the complete dataset and clipped datasets 1 and 2 are provided in Table 4.1.

The total expression for the derived deformation model is:

$$\frac{S}{D_{pile}} = f(KC_{tot}) \cdot c_1 \cdot MOB_{top}^{c_2} \quad (4)$$

$$f(KC_{tot}) = 1 + \frac{c_3}{1 + \exp[-c_4 \cdot (KC_{tot}) + c_5]}$$

The fitting constants are provided in various tables below. The following tables are provided:

- Fitting constants for the deformation model based on a complete dataset (Table 4.3).
- Fitting constants for the deformation model based on a truncated dataset omitting deformation larger than 4 rock layers and omitting deformation associated with opposing current conditions (Table 4.5).
- Fitting constants for the deformation model based on a truncated dataset omitting deformation larger than  $0.075D_{pile}$  and deformation associated with  $KC_{tot}$  numbers larger than 4.2 (Table 4.6),

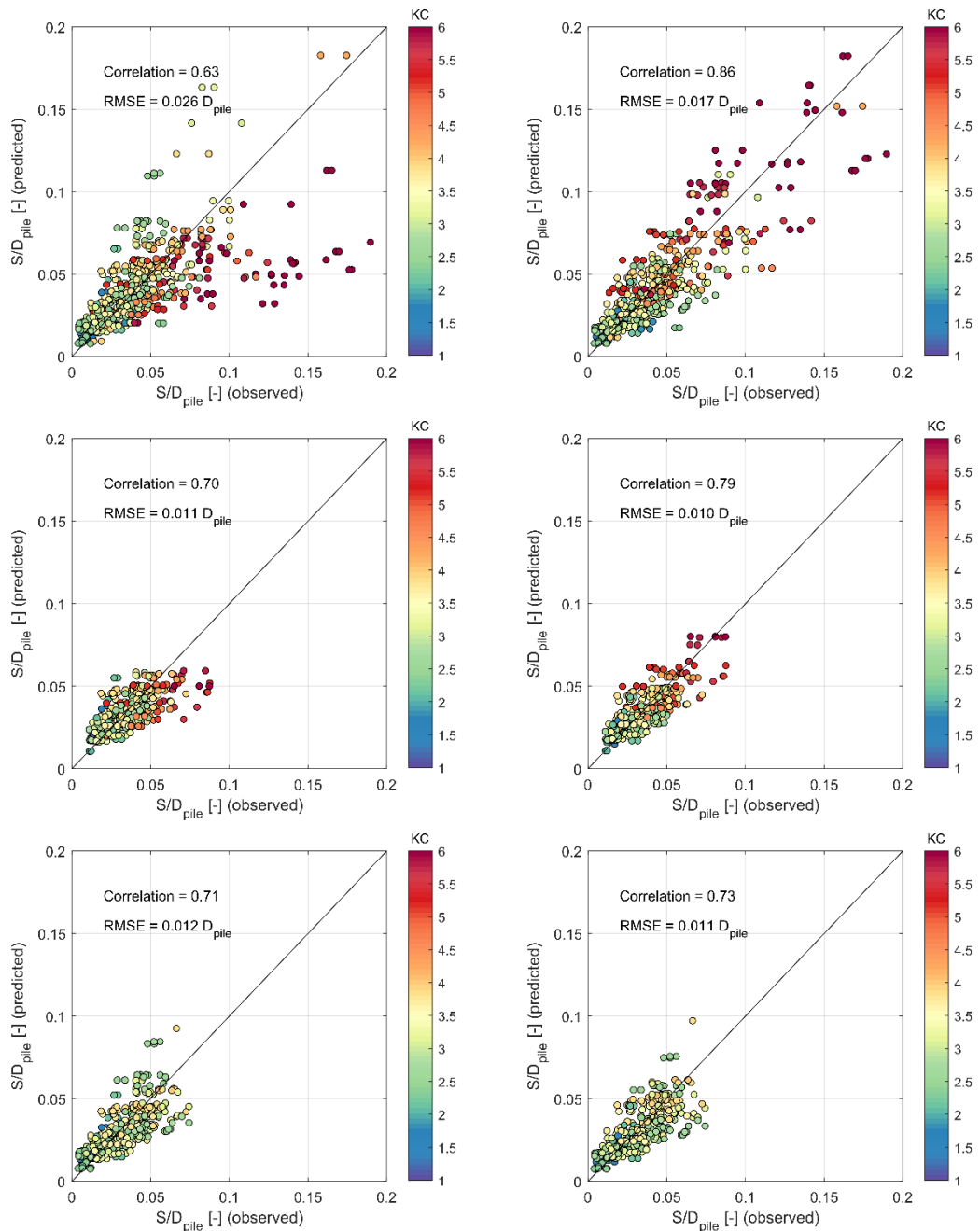


Figure 4.12 Deformation analysis based on truncating the dataset. Performance of the resulting deformation formula. Top left: original data (without correcting for  $KC_{tot}$ ). Top right: original data (with correcting for  $KC_{tot}$ ). Middle left: truncated dataset 1 (without correcting for  $KC_{tot}$ ). Middle right: truncated dataset 1 (with correcting for  $KC_{tot}$ ). Bottom right: truncated dataset 2 (without correcting for  $KC_{tot}$ ). Bottom left: truncated dataset 2 (with correcting for  $KC_{tot}$ ).

Table 4.4 Fitting constants for the deformation model outlined in Equation (4) including KC correction

Prediction	Eq. 21 with KC correction					Eq. 21 without KC correction [f(KC) = 1]	
	C1	C2	C3	C4	C5	C1	C2
S <sub>2.5%</sub>	0.0338	1.6492	3.9274	0.7401	4.7518	0.0543	1.9791
S <sub>10%</sub>	0.0440					0.0751	
S <sub>20%</sub>	0.0518					0.0915	
S <sub>30%</sub>	0.0582					0.1057	
S <sub>40%</sub>	0.0644					0.1194	
S <sub>50%</sub>	0.0707					0.1339	
S <sub>60%</sub>	0.0776					0.1501	
S <sub>70%</sub>	0.0857					0.1696	
S <sub>80%</sub>	0.0964					0.1957	
S <sub>90%</sub>	0.1134					0.2387	
S <sub>97.5%</sub>	0.1478					0.3301	

Table 4.5 Fitting constants for the deformation model outlined in Equation (4) including KC correction for clipped dataset 1 where deformation of the armour layer >4 rock layers is removed.

Prediction	Eq. 21 with KC correction					Eq. 21 without KC correction [f(KC) = 1]	
	C1	C2	C3	C4	C5	C1	C2
S <sub>2.5%</sub>	0.0340	1.3268	5.000	0.5445	4.5000	0.0529	1.5848
S <sub>10%</sub>	0.0416					0.0659	
S <sub>20%</sub>	0.0471					0.0755	
S <sub>30%</sub>	0.0514					0.0832	
S <sub>40%</sub>	0.0555					0.0905	
S <sub>50%</sub>	0.0596					0.0978	
S <sub>60%</sub>	0.0639					0.1057	
S <sub>70%</sub>	0.0690					0.1148	
S <sub>80%</sub>	0.0754					0.1266	
S <sub>90%</sub>	0.0853					0.1450	
S <sub>97.5%</sub>	0.1043					0.1807	

Table 4.6 Fitting constants for the deformation model outlined in Equation (4) including KC correction for clipped dataset 2 where deformation of the armour layer  $> 0.075D_{pile}$  and deformation associated with hydrodynamic conditions with  $KC_{tot} > 4.2$  is removed.

Prediction	Eq. 21 with KC correction					Eq. 21 without KC correction [f(KC) = 1]	
	C1	C2	C3	C4	C5	C1	C2
S <sub>2.5%</sub>	0.0337	1.6976	5.000	0.5918	4.5000	0.0473	1.7878
S <sub>10%</sub>	0.0440					0.0619	
S <sub>20%</sub>	0.0518					0.0730	
S <sub>30%</sub>	0.0582					0.0822	
S <sub>40%</sub>	0.0644					0.0909	
S <sub>50%</sub>	0.0707					0.1000	
S <sub>60%</sub>	0.0776					0.1099	
S <sub>70%</sub>	0.0858					0.1216	
S <sub>80%</sub>	0.0966					0.1370	
S <sub>90%</sub>	0.1136					0.1615	
S <sub>97.5%</sub>	0.1483					0.2113	

### Guidance on the selection of the fitting constants for the deformation model

In Table 4.4, Table 4.5 and Table 4.6 fitting constants for the deformation model are presented, each with their own applicability range as indicated in Table 4.1, to provide a certain freedom to the designer to select the appropriate set of constants as they see fit. Each set has their own benefits and drawbacks, so some guidance is provided here to aid in the design process.

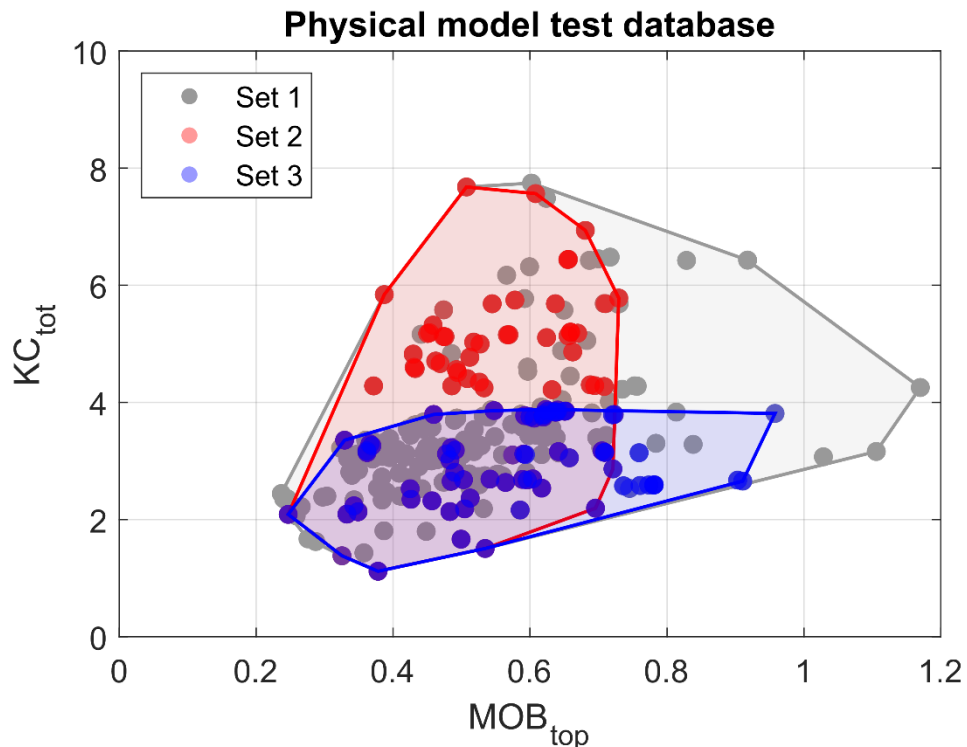


Figure 4.13 Experimental database and datapoints associated with each three sets of fitting constants.



Figure 4.13 shows the datapoints associated with each fitting constant set, and the parameter space they span. The largest set is associated with fitting constant set 1, where it is noted that the data becomes scarce for high mobilities in combination with high KC numbers. Up until roughly a mobility of 0.8 and KC numbers of up to 8 there is a good amount of data available. Both the red (set 2) and blue (set 3) patches show a representation of areas with a good amount of data available, effectively omitting the sparse data region from set 1. However, within these datasets, it is apparent that many of the datapoints from set 1 (grey dots) are simply not represented, as evidenced by the red and blue dots (note that red and blue often overlap). So, by reducing the dataset to represent conditions that are more representative for field conditions, a big amount of data is not taken into consideration for deriving the fitting constants. It is therefore a fair recommendation that the fitting constants from set 1 are a good choice in general.

**Set 1 (Table 4.4):** This set is based on the complete experimental dataset available, including datapoints from JIP HaSPro but also from other experiments performed at Deltares. These constants may always be selected, as they are considered to be derived from a dataset that is as complete as possible. This dataset, however, also contains datapoints from experimental conditions that are not all that likely to occur in reality, and it can be argued that not all processes are captured in a deformation model that is based on only the mobility and the total KC number. Furthermore, the dataset also contains datapoints with deformation that is much larger than what would typically be designed for.

**Set 2 (Table 4.5):** This set is based on a reduced experimental dataset, where datapoints with deformation larger than 4 rock layers are omitted from the dataset. In this way, the deformation model is based on more realistic values for allowable scour protection deformation, with the intention that the scatter in datapoints is reduced and leads to a more straightforward relation between hydrodynamics and deformation. This is indeed supported by Figure 4.12. The downside of reducing the dataset is that the resulting deformation model is based on a less complete collection of data (although the data is more representative for design requirements) and has a smaller applicability range, as indicated in Table 4.1. As an example: for single-layer scour protections, which typically consist of smaller rocks, more deformation may be allowed than 4 rock layers. In that case, it is recommended to use Set 1. If the deformation formula yields an expected deformation larger than 4 rock layers, it is recommended to revert to Set 1 to perform an additional calculation.

**Set 3 (Table 4.6):** This set is based on a further reduced experimental dataset with even stricter values of allowable deformation, and datapoints with total KC numbers of larger than 4.2 are omitted. The argument behind this selection is that, as monopiles keep increasing in diameter, the KC numbers will only get lower. The value of 4.2 is selected, as this was found to be (more or less) the distinction between two deformation regimes: one where deformation increases rapidly with increasing mobility (high KC numbers) and one where this relation is less steep (low KC numbers). In this dataset, the KC effect is almost completely negligible which may be an argument for using an even simpler deformation relation which is only a function of the mobility. An obvious disadvantage of using this drastically reduced dataset is that its applicability is more limited. The use of this fitting constants set is limited to cases with KC numbers lower than 4.2. If the calculated deformation exceeds 0.075 times the pile diameter, it is recommended to revert to Set 1 to perform an additional calculation.

**Fitting constants with or without KC-correction:** Fitting constants are provided with and without taking into account the influence of the KC-number. Without taking the influence of the KC-number into consideration, the deformation model is more straightforwardly interpreted. However, as clearly observed in Figure 4.12, for fitting constants Set 1 and Set 2 this leads to an underprediction of high deformation and overprediction of low deformation. It is therefore strongly recommended **not** to use the deformation formula without considering the effect of the KC-number. For Set 3, where the effect of the KC-number is no longer strongly present in the dataset, using the formula without KC influence may be considered. For the other cases, the values are presented as a reference, but for design purpose it is recommended to not omit the dependency of the result on the KC number.

#### 4.4.1.2 Layer thickness

For designing a loose-rock scour protection, the expected deformation can be used to determine the required layer thickness of armour layer to ensure sufficient coverage of the underlying filter (or, in case of a single-layer scour protection design the dynamic layer thickness to ensure sufficient layer thickness remains for interface stability). Instead of using a fixed mobility limit to determine suitability of a rock grading, now the actual calculated deformation is used as an input parameter in the design. The required layer thickness for a double-layer and a single-layer system are provided in Table 4.7. A rock layer is defined following the rock manual as  $t_{rock} = 0.89D_{n50}$ , where  $D_{n50} = 0.84D_{50}$ . The layer thickness coefficient is based on the single dense highest point survey, as we create a definition for a single layer. The selected value is the most conservative of the options presented in the rock manual. For a double-layer system, the total layer thickness of the armour layer ( $t_{armour}$ ) is the sum of a minimum filter layer coverage of two rock layers ( $t_{rock}$ ) and the expected scour protection deformation  $S_{x\%}$ , with the choice of  $x$  being the responsibility of the designer. For the single-layer system, the same rock grading fulfils both the armour and filter function. The total layer thickness of a single-layer system ( $t_{single}$ ) is the sum of a static layer thickness ( $t_{static}$ ) that should always be satisfied for filter functionality and the expected scour protection deformation  $S_{x\%}$ .

Table 4.7 Required layer thickness for a double-layer and single-layer scour protection system.

Scour protection system	Required layer thickness
Double-layer	$t_{armour} = 2t_{rock} + S_{x\%}$
Single-layer	$t_{single} = t_{static} + S_{x\%}$

The 90% value of the fitting constant  $c_1$  is considered to be a safe upper-limit for the majority of scour protections. If because of other considerations a different choice of the value of  $c_1$  is made this could be acceptable on a case-by-case basis. It is up to the designer to present reasonable argumentation on why a specific choice is made and is acceptable. Reasons for choosing a different value than the 90% non-exceedance value of  $c_1$  could be (but are not limited to):

- Over-conservativeness in the hydrodynamic boundary conditions could be a reason for selecting a lower non-exceedance value.
- Field evidence of scour protection performance in comparable conditions could be a reason for selecting a lower (or higher) non-exceedance value.
- Physical modelling results of comparable conditions could be a reason to select a lower (or higher) non-exceedance value.
- Conditions being outside of the parameter range of the data that was used to derive the deformation formula could be a reason to select a higher non-exceedance value.

An example of the procedure is provided in Appendix C.

#### 4.4.1.3 Extent of the scour protection

As a base extent of the scour protection a radial distance away from the face of the pile of a single pile diameter is recommended. This refers to the extent of the top level of the scour protection. Such an extent amounts to a total diametral extent at the top of the scour protection of 3 times the pile diameter. Typically, for less severe conditions (lower mobility and lower KC number), the footprint of the deformation area is well within the footprint of the scour protection. Conversely, for more severe conditions, especially with higher KC numbers, the deformation area could extend beyond this footprint of 3 times the pile diameter. For large KC numbers (i.e.,  $KC_{tot} > 4.2$ ) a total diametral extent of 3.5 times the pile diameter could be considered. Different choices could be acceptable. Reasons for deviation from the recommendation of this base extent could be:

- Field evidence of scour protection performance in comparable conditions could be a reason for selecting a lower (or higher) extent.

- Physical modelling results of comparable conditions could be a reason to select a lower (or higher) extent.
- Conditions being outside of the parameter range of the data that was used to derive the deformation formula could be a reason to select a higher extent.
- Potential added risks of edge scour could be a reason to select a higher extent.

Reducing the extent of the scour protection to a smaller footprint than 3 times the pile diameter could increase the edge scour depth because an area of exposed seabed is present closer to the pile, being subject to more amplified flow conditions. As argued in Section 4.4.3, this does not necessarily have to lead to additional extent to act as a falling apron, since edge scour is typically associated with mild side-slopes, reducing the risk of material sliding down into the hole. This statement is mostly based on observations of edge scour with scour protections with a diameter of 3 times the pile diameter or larger, thus involving less amplified flow conditions. It can therefore not yet be concluded that this would also hold for scour protections with a smaller extent.

Note that the extent discussed here is a minimum dimension, excluding installation tolerances.

#### 4.4.1.4 Mobility limits

The deformation formula was applied to derive general mobility limits for various deformation classes for a rapid assessment. It is, however, recommended to explicitly calculate the deformation in m using Equation (4) rather than relying on mobility limits. The following tables are provided below:

- Mobility limits for pile diameters of 6 m (Table 4.8)
- Mobility limits for pile diameters of 8 m (Table 4.9)
- Mobility limits for pile diameters of 10 m (Table 4.10)
- Mobility limits for pile diameters of 12 m (Table 4.11)
- Mobility limits for pile diameters of 14 m (Table 4.12)

For pile diameters that fall in between the presented pile diameters, the mobility limits can be linearly interpolated.

Table 4.8 Mobility limits for pile diameter  $D_{pile} = 6$  m.

Deformation category	$S_{50\%}$		$S_{90\%}$	
	$KC_{tot} \leq 4.2$	$KC_{tot} > 4.2$	$KC_{tot} \leq 4.2$	$KC_{tot} > 4.2$
Very limited movement (< 0.25 m)	< 0.60	< 0.45	< 0.42	< 0.30
Limited movement (< 0.50 m)	< 0.89	< 0.67	< 0.62	< 0.45
Significant movement (< 0.75 m)	< 1.12	< 0.85	< 0.78	< 0.56
Extreme movement (> 1.00 m)	> 1.20	> 1.00	> 0.92	> 0.67

Table 4.9 Mobility limits for pile diameter  $D_{pile} = 8$  m.

Deformation category	$S_{50\%}$		$S_{90\%}$	
	$KC_{tot} \leq 4.2$	$KC_{tot} > 4.2$	$KC_{tot} \leq 4.2$	$KC_{tot} > 4.2$
Very limited movement (< 0.25 m)	< 0.51	< 0.38	< 0.36	< 0.25
Limited movement (< 0.50 m)	< 0.76	< 0.57	< 0.53	< 0.38
Significant movement (< 0.75 m)	< 0.95	< 0.72	< 0.67	< 0.48
Extreme movement (> 1.00 m)	> 1.12	> 0.85	> 0.78	> 0.56

Table 4.10 Mobility limits for pile diameter  $D_{pile} = 10$  m.

Deformation category	$S_{50\%}$		$S_{90\%}$	
	$KC_{tot} \leq 4.2$	$KC_{tot} > 4.2$	$KC_{tot} \leq 4.2$	$KC_{tot} > 4.2$
Very limited movement (< 0.25 m)	< 0.45	< 0.34	< 0.32	< 0.22
Limited movement (< 0.50 m)	< 0.67	< 0.50	< 0.47	< 0.33
Significant movement (< 0.75 m)	< 0.84	< 0.63	< 0.59	< 0.42
Extreme movement (> 1.00 m)	> 0.99	> 0.75	> 0.69	> 0.50

Table 4.11 Mobility limits for pile diameter  $D_{pile} = 12$  m.

Deformation category	$S_{50\%}$		$S_{90\%}$	
	$KC_{tot} \leq 4.2$	$KC_{tot} > 4.2$	$KC_{tot} \leq 4.2$	$KC_{tot} > 4.2$
Very limited movement (< 0.25 m)	< 0.41	< 0.30	< 0.28	< 0.20
Limited movement (< 0.50 m)	< 0.60	< 0.45	< 0.42	< 0.30
Significant movement (< 0.75 m)	< 0.76	< 0.57	< 0.53	< 0.38
Extreme movement (> 1.00 m)	> 0.89	> 0.67	> 0.62	> 0.45

Table 4.12 Mobility limits for pile diameter  $D_{pile} = 14$  m.

Deformation category	$S_{50\%}$		$S_{90\%}$	
	$KC_{tot} \leq 4.2$	$KC_{tot} > 4.2$	$KC_{tot} \leq 4.2$	$KC_{tot} > 4.2$
Very limited movement (< 0.25 m)	< 0.37	< 0.28	< 0.26	< 0.18
Limited movement (< 0.50 m)	< 0.55	< 0.41	< 0.39	< 0.27
Significant movement (< 0.75 m)	< 0.69	< 0.52	< 0.49	< 0.35
Extreme movement (> 1.00 m)	> 0.82	> 0.62	> 0.57	> 0.41

#### 4.4.1.5 Rock density

One of the design choices that can be made is related to the density of the rock. High density rock gradings are typically less mobile than normal density rock gradings. The same mass of rock is achieved with smaller rocks (also sometimes schematized with a correction factor), and these smaller rocks experience less loading by the hydrodynamic forces due to a smaller area. High density rocks may thus provide extra stability compared to normal density rock gradings. This is illustrated in Figure 4.14, which shows the deformation of a loose rock scour protection in m as a function of the density of the rock for three different OSG gradings (see Chapter 6) for typical North Sea conditions. The selected conditions are RP50yr storm conditions at Hollandse Kust Noord OWF for a water depth of 23.5 m and a monopile diameter of 8 m. Figure 4.14 clearly shows a decrease in calculated deformation for an increasing rock density. As indicated by the black lines in the figure, a similar degree of deformation is achieved with a normal density OSG<sub>45/180mm</sub> rock grading and the smaller OSG<sub>22/125mm</sub> rock grading if the density is larger than ~3000 kg/m<sup>3</sup>.

Following the guidance provided in Section 4.4.1.2, with less expected deformation a smaller total layer thickness is required, thus reducing the overall rock volume that is needed in the loose rock scour protection. Conversely, high-density rock may allow for selecting smaller rock sizes to achieve a similar expected stability around a foundation. This could be relevant for bedding layers at Gravity Based Foundations, which usually require smaller rocks to provide a more even bedding area for the structure. In addition, smaller rock gradings may have potential installation advantages like, for instance, reduced installation tolerances and easier handling with fall-pipe vessels.

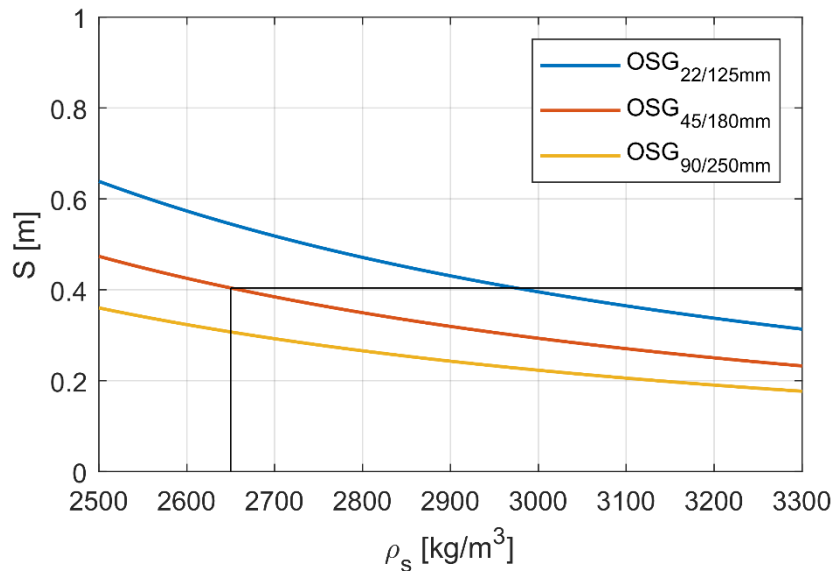


Figure 4.14 Deformation,  $S$ , in m as a function of rock density for three different rock gradings (see Chapter 6) for typical North Sea conditions. The expected deformation decreases as the rock density increases.

The design procedure for high-density rock is the same as for normal-density rock. For example, the experimental database on external stability shows that for similar mobility and  $KC$ -number, the deformation pattern is the same for a scour protection with a normal density rock grading ( $\rho_s = 2650 \text{ kg/m}^3$ ) as for a scour protection with a high-density rock grading ( $\rho_s = 3150 \text{ kg/m}^3$ ). Figure 4.15 illustrates this, showing the observed deformation for two scour protections with a normal and high-density rock grading selected such that the rock mobility for both protections is the same ( $MOB_{top} = 0.56$ ). The normal density rock had a  $D_{50}$  of 5.9 mm, whereas the high-density rock had a  $D_{50}$  of 4.2 mm. The mobility of the material is thus one of the most relevant parameters in determining the amount of deformation. A wider grading could potentially also improve stability of the protection, although the current deformation database shows no significant effect of this parameter.

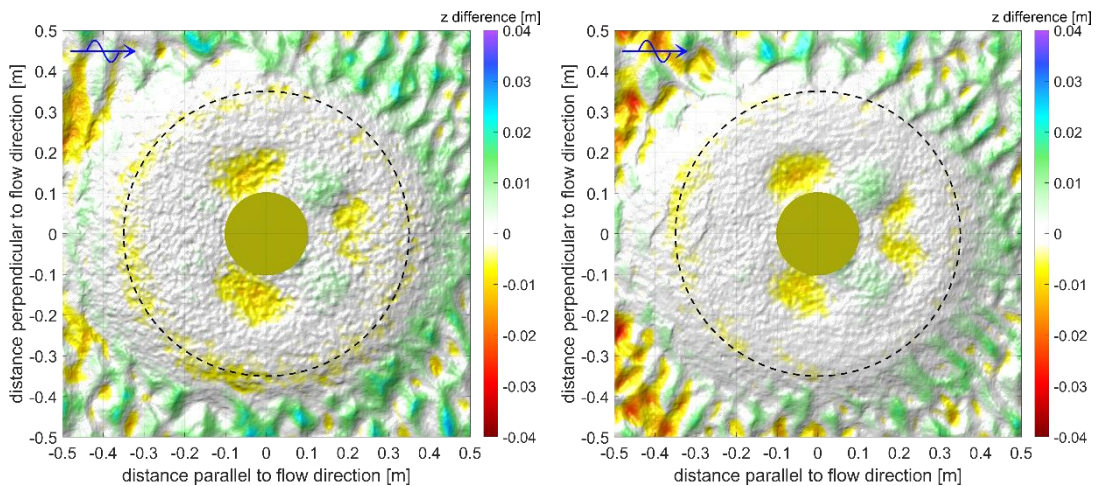


Figure 4.15 Deformation for a scour protection with a normal density rock (left) and a high-density rock (right). The rock was selected in such a way that the mobility on top of the scour protection is the same for both layouts.

#### 4.4.2 Interface stability

This section deals with the interface stability criterion of loose rock scour protection design. Interface stability relates to the sand-tightness of a scour protection, meaning that sand loss through the pores should be prevented (in case of a stable design) or accounted for (in case of a dynamic design). In

the design of offshore scour protections, often use is made of the methods of Hoffmans (2012) and/or Van de Sande et al. (2014) to determine the required layer thickness to control the interface stability. While this is a valid approach, the following should be kept in mind when applying these methods:

- Both methods were developed for horizontal filters and do not explicitly incorporate the presence of a monopile (or other structure).
- Both methods do not explicitly incorporate a representative hydraulic load. Although the hydraulic load is implicitly included as both methods assume an equal stability of filter and bed material (i.e. initiation of motion occurs under the same critical load), it should be noted that the external stability around a structure in offshore conditions is governed by wave conditions or could be provided by a different layer (armour). As a consequence, the filter layer thickness calculated with both methods is only dependent on the bed and rock characteristics (density, diameters) and does not change with a varying current velocity.
- Verheij et al. (2012) have mentioned that indicative tests with a pier, within the same dataset as Van de Sande et al. (2014), showed movement of base material at much lower flow velocities, demonstrating that a monopile has an influence. Therefore, the influence of a structure on the hydraulic loading should be taken into consideration, which may lead to thicker required filter layers.

Despite these limitations, these formulas have been often applied in offshore projects to determine a minimum layer thickness, so far without any (publicly known) failures and/or large sinkage due to winnowing.

Another design method is provided by the formula of Wörman (1989), which takes the presence of the monopile and the representative hydraulic load into account. Based on extrapolation of physical model tests, a simplified formula for initiation of scour at the pile face was derived. It should be noted that, in offshore conditions, this method can lead to significant layer thicknesses, as the layer thickness is linearly related to  $d_{85}/D_{15}$  ratio. As these ratios can be relatively large in offshore conditions, this could require significant layer thicknesses.

Considering the above, a new design methodology was developed in JIP HaSPRO that takes all relevant aspects into account for interface stability around offshore foundations and which is based on a relatively large dataset of physical model test results. This design method can therefore be considered as an addition to the methods mentioned above. In the derivation of this method, a relation is developed for the scour depth underneath a scour protection around a monopile. The aim of this relation is to provide an estimate for the expected scour depth at a pile due to winnowing. More importantly for design purposes is that this relation should provide a method to determine the required layer thickness to prevent winnowing (i.e.  $S_{eq}/D_{pile} = 0$ ) for a certain rock grading. The selected approach therefore includes a threshold of motion, where if the loads at the seabed exceed a certain limit, lowering of the seabed due to winnowing is expected.

#### Governing condition

Based on an analysis of the database results, it was determined that the amount of scour is very similar for both current-only and combined waves-and-current conditions. In general, a bit more scour is observed for the combined wave-and-current under mild currents, which is logical as the effect of the bed orbital velocity will be larger in these conditions. For more severe current conditions, combined waves-and-current generally shows less scour. This can be explained by the continuous breaking up of the strong horseshoe vortex during flow reversal under individual waves.

Therefore, it was chosen to focus the analysis on the current-only conditions. The amount of scour that can occur for both current-only and wave-current conditions is similar, but it should be kept in mind that these extreme wave-and-current conditions occur only sporadically and have a much shorter duration compared to the current-only condition. Therefore, the equilibrium scour depth will generally not be reached during these combined wave-and-current conditions.

#### 4.4.2.1 Winnowing scour depth relation

For determining the loads at the seabed, two separate effects should be considered: 1) the approach depth-averaged current will be amplified by the presence of the structure and the scour protection and 2) the presence of the layer of rock will lead to a reduction of the flow velocity by its dampening effect. These two effects are combined in a single function ( $\alpha$ ), which depends on several of the parameters discussed in the previous section. This function  $\alpha$  is multiplied with the relative current velocity ( $U_c/U_{crit}$ ). The scour depths underneath the scour protection are subsequently based on a relation with this factor and the hydraulic load. This approach captures all the relevant aspects associated with the problem and also provides explicitly the initiation of scour due to winnowing ( $S_{eq}/D_{pile} = 0$ ).

The developed winnowing scour depth function is as follows:

$$\frac{S_{eq}}{D_{pile}} = \tanh\left(\alpha \cdot \frac{U_c}{U_{crit,KB}} - 1\right) \quad (5)$$

$$\alpha = c_1 \cdot \left(\frac{t}{D_{15}}\right)^{c_2} \cdot \left(\frac{U_c}{\sqrt{g \cdot t}}\right)^{c_3} \cdot \left(\frac{d_{15}}{D_{15}}\right)^{c_4}$$

With	$S_{eq}$	=	equilibrium scour depth	[m]
	$D_{pile}$	=	pile diameter	[m]
	$\alpha$	=	amplification & reduction function	[-]
	$U_c$	=	depth-averaged current velocity	[m/s]
	$U_{crit,KB}$	=	critical current velocity based Klein Breteler et al. (1992)	[m/s]
	$t$	=	layer thickness	[m]
	$d_{15}$	=	base material diameter, at 15% of passing by weight	[m]
	$D_{15}$	=	rock material diameter, at 15% of passing by weight	[m]

In this equation,  $c_1$  to  $c_4$  are the fitting constants. The results of the final fit are provided in Figure 4.16.

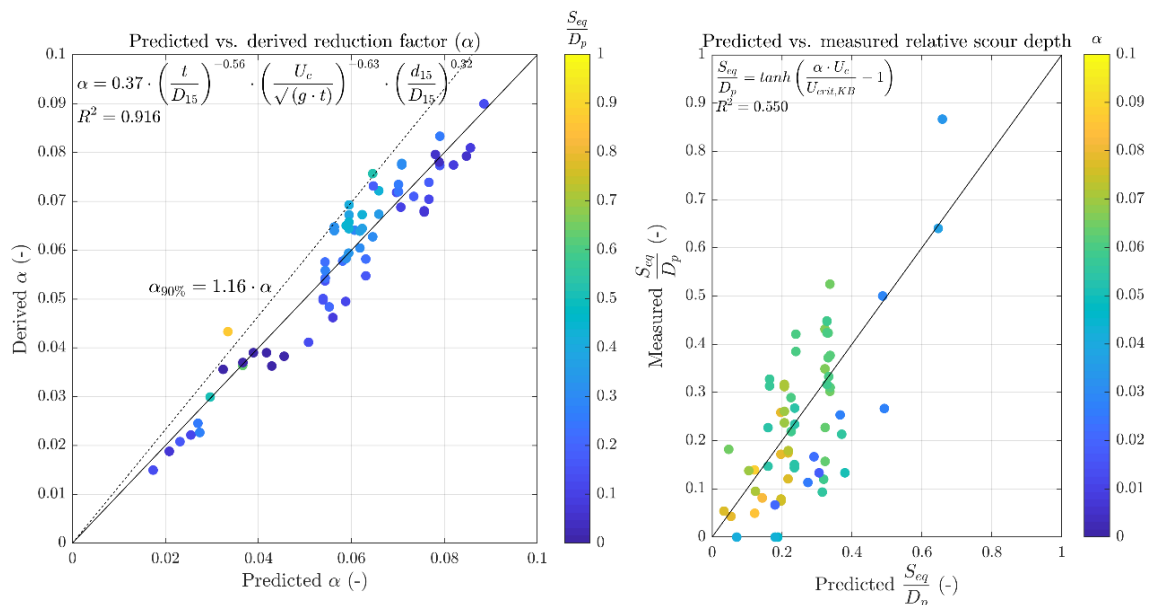


Figure 4.16 Best fit for  $\alpha$ , with the critical velocity based on the method by Klein Breteler et al. (1992). The left plot provides the predicted vs. derived  $\alpha$ -factor, including an upper bound ( $\alpha_{ub}$ ). The effects on the relative scour depth prediction are provided in the right plot.

As visible, the prediction for  $\alpha$  is quite accurate, with a  $R^2$  value of 0.916. However, there is significant more scatter in the prediction of the relative scour depths, which only has a  $R^2$  value of 0.550. The small deviations in the  $\alpha$ -factor result in significant differences for the scour depth prediction. Nevertheless, the general trend is captured quite well.

#### Uncertainty and limitations

It is noted that the available data and analysis have some limitations, which are summarized as follows:

- Significant scatter in the test results, mainly due to the limited amount of rock layers in most tests.
- Scarce or missing data points for larger amount of rock layers due to scaling.
- Lack of data or unusable data at initiation of scour ( $S_{eq}/D_{pile}$ ).
- Lack of public data on interface stability performance on field scale, which makes the translation from model to field difficult.

With the considerations above, it is recognized that the presented formula is not ideal. Nevertheless, it is considered a suitable method with the data that is available. It furthermore provides a calculation method for the required layer thickness to prevent winnowing. Taking the limitations and uncertainties of the data and translation to field scale into account, the following approach is applied in the design methodologies:

- Application of the 90% non-exceedance coefficients.
- Cap the relative sediment diameter ( $d_{15}/D_{15}$ ) at 1/200.
  - This is a conservative approach given the parameter range (see Table 4.2)
- Cap the  $D_{15}$  in the  $t/D_{15}$  ratio at  $D_{50}/1.5$ .
  - This is a conservative approach given the parameter range (see Table 4.2)
- Apply a minimum number of rock layers to cover remaining uncertainties in the translation from model to field scale.

It is noted that this approach contains a good amount of measures to obtain safety/conservatism. This is deemed necessary considering the limitations on the available data and uncertainty in translation from model to field scale. Until additional research, preferably with a focus on initiation of scour and for scour protections with a larger number of rock layers, provides further confirmation of the trends and fits observed here, this conservatism should be upheld. This also holds for the caps, as it is not possible (without additional data) to predict what the effect of wider gradings ( $D_{50}/D_{15} > 1.5$ ) and smaller relative sediment diameters ( $d_{15}/D_{15} < 1/200$ ) is.

#### 4.4.2.2 Design methodology: minimum required thickness to prevent winnowing

Equation (5) can be rewritten to determine the minimum required layer thickness to prevent winnowing ( $S_{eq}/D_{pile} = 0$ ). The minimum required layer thickness to prevent winnowing can be calculated as follows:

$$\frac{t}{D_x} = (d_{rel})^{x_1} \cdot \left( c_1 \cdot \frac{U_c}{U_{crit,KB}} \right)^{x_2} \cdot \left( \frac{U_c}{\sqrt{g \cdot D_{15}}} \right)^{x_3}$$

$$d_{rel} = \max \left( \frac{d_{15}}{D_{15}}, \frac{1}{200} \right)$$

$$D_x = \max \left( D_{15}, \frac{D_{50}}{1.5} \right)$$
(6)



With:	t	= layer thickness	[m]
	D <sub>x</sub>	= Adjusted rock material diameter	[m]
	d <sub>rel</sub>	= Adjusted relative sediment diameter	[-]
	U <sub>c</sub>	= Depth-averaged current velocity	[m/s]
	U <sub>crit,KB</sub>	= Critical velocity in filter, based on Klein Breteler et al. (1992)	[m/s]
	D <sub>15</sub>	= rock material diameter, at 15% of passing by weight	[m]
	d <sub>15</sub>	= base material diameter, at 15% of passing by weight	[m]
	D <sub>50</sub>	= rock material diameter, at 50% of passing by weight	[m]

Please note that this method is applicable for values of  $d_{rel} < 1/200$  or  $D_{15} < D_{50}/1.5$ . In those cases the maximum value should be applied ( $1/200$  for  $d_{rel}$  and  $D_{50}/1.5$  for  $D_x$ ). The design coefficients for Equation (6) are provided in Table 4.13, which is based on the 90% none-exceedance fit. To deal with remaining uncertainties in the translation from model to field scale, it is highly recommended to apply a minimum amount of 7 rock layers:

$$t_{min} = 7 \cdot D_x \quad (7)$$

Table 4.13 Design coefficients in the formula for the minimum required layer thickness.

C <sub>1</sub>	X <sub>1</sub>	X <sub>2</sub>	X <sub>3</sub>
0.4300	1.3082	4.1017	-2.5811

The critical velocity in the filter layer is calculated by the method of Klein Breteler et al. (1992). The method is based on the critical filter velocity, U<sub>crit,KB</sub>, and the Forchheimer equation to convert this critical velocity to a critical hydraulic gradient. The critical velocity in the rock layer can be determined as follows:

$$U_{crit,KB} = \left[ \frac{n}{c} \cdot \left( \frac{D_{15}}{v} \right)^m \cdot \sqrt{\psi \cdot g \cdot \Delta \cdot d_{50}} \right]^{\frac{1}{1-m}} \quad (8)$$

With:	n	= porosity of rock material	[-]
	v	= kinematic viscosity of water	[m <sup>2</sup> /s]
	Δ	= relative density of base material ( $\rho_s/\rho_w - 1$ )	[-]
	d <sub>50</sub>	= base material diameter, at 50% of passing by weight	[m]
	Ψ	= Shields parameter for base material (see Table 4.14)	[-]
	c,m	= coefficients, dependent on d <sub>50</sub> (see Table 4.14)	[-]

The coefficients, including the Shields parameter for base material, are dependent on the diameter of the base material and are provided in Table 4.14. For sediment diameters in between the provided diameters, interpolation may be applied.

Table 4.14 Coefficients in the formula for the critical filter velocity.

d <sub>50</sub> (mm)	0.1	0.15	0.2	0.3	0.4	0.5	0.6	0.7	0.8	≥1.0
Ψ (-)	0.110	0.073	0.055	0.044	0.038	0.036	0.034	0.034	0.034	0.035
c (-)	1.18	0.78	0.71	0.56	0.45	0.35	0.29	0.22	0.22	0.22
m (-)	0.25	0.20	0.18	0.15	0.11	0.07	0.04	0.00	0.00	0.00

Please note that a designer may deviate from the required layer thickness following from Equation (6), for instance if the effectiveness of a different layer thickness in similar conditions can be shown.

#### Maximum required layer thickness

As visible from Equation (6), the required layer thickness can grow rapidly for larger current velocities, which would require a lot of rock layers. Unfortunately, the lack of data at a larger number of rock layers is scarce, while it may be expected that there is a maximum number of rock layers, even for larger current velocities as the load penetration will not grow infinitely. Therefore, often a maximum of  $8 \cdot D_{50}$  is proposed, which is the upper limit proposed by (Hoffmans, 2012). Considering equation (6), this translates to:

$$t_{\max} = 12 \cdot D_x \quad (9)$$

This layer thickness has been applied in layouts for many wind farms, and to the knowledge of the authors, no winnowing has been observed at these locations so far. This can therefore be considered as a safe upper limit for the minimum required layer thickness.

#### Potential effect of an armour layer

It is noted that the influence of a potential armour layer is not taken along. An armour layer will increase the total layer thickness and is expected to reduce the load at the bed even further. However, as not enough data is present to determine the effect of the armour layer, the conservative approach for now is to Klein Breteler et al. (1992) exclude any effect of the armour layer. A potential method to include an armour layer is to then include it in the amount of layers (i.e. make  $t/D_x$  a summation of the filter layers and the armour layers).

#### Selection of input parameters

The input parameters for Equations (6) to (9) should be chosen with care. For the current velocity,  $U_c$ , it is recommended to apply a high, but still frequently occurring current velocity, as sufficient time is necessary to reach the equilibrium scour depth. The spring tidal current velocity or the 90% non-exceedance value of the current velocity are valid choices. If those are not available, the RP1yr current velocity can be considered as a conservative alternative.

For the rock diameters, it is advised to use grading diameters which are higher than the target diameters, as this leads to larger layer thicknesses (or scour depths) to account for variability in the grading diameters. A valid choice would be to select the 75th percentile diameter (75% between the minimum and maximum diameter) of the preferred rock grading for the filter.

For the sediment diameter selection is more difficult, as the method is quite sensitive to small changes in sediment diameters. This is mainly caused by the discontinuous values of the coefficients in the critical filter velocity formula of Klein Breteler et al. (1992). Furthermore, the positive effect of the relative sediment diameter is generally opposing to the decrease of the critical Shields parameter for diameters between 0.1 and 0.6 mm. It is situation-dependent what the dominant factor is. Therefore, it is highly recommended to apply a range of (realistic) local sediment diameters and select an appropriate layer thickness based on the returned range of layer thicknesses.

#### 4.4.2.3 Estimation of equilibrium scour depth

If the minimum required layer thickness is not met, the expected equilibrium scour depth can be estimated as follows:

$$\begin{aligned} \text{if } \alpha \cdot \frac{U_c}{U_{crit,KB}} > 1 &\Rightarrow \frac{S_{eq}}{D_{pile}} = \tanh\left(\alpha \cdot \frac{U_c}{U_{crit,KB}} - 1\right) \\ \text{if } \alpha \cdot \frac{U_c}{U_{crit,KB}} \leq 1 &\Rightarrow \frac{S_{eq}}{D_{pile}} = 0 \\ \alpha &= c_1 \cdot \left(\frac{t}{D_{15}}\right)^{c_2} \cdot \left(\frac{U_c}{\sqrt{g \cdot t}}\right)^{c_3} \cdot (d_{rel})^{c_4} \end{aligned} \quad (10)$$

With:	$S_{eq}$	=	equilibrium scour depth	[m]
	$D_{pile}$	=	pile diameter	[m]
	$\alpha$	=	amplification & reduction factor	[-]
	$c_1 - c_4$	=	coefficients (see Table 4.13)	[-]

Table 4.15 Coefficients in the formula to estimate the equilibrium scour depth.

Prediction	C1	C2	C3	C4
$\alpha - 50\%$	0.3697	-0.5584	-0.6293	0.3189
$\alpha - 90\%$	0.4300	-0.5584	-0.6293	0.3189

Care should be taken when applying Equation (10) to determine the equilibrium scour depth. The fit with the data is not optimal ( $R^2 = 0.55$ ) and there is quite some scatter, especially for smaller  $S_{eq}/D_p$  values (see Figure 4.16, right). This is mainly caused by the fact that most tests consist of a limited number of rock layers, which makes that the positioning and diameter of the rocks becomes quite important for the scour depth. For scour protections with a larger number of rock layers this effect is expected to reduce significantly. Considering this uncertainty, the 90% non-exceedance coefficients for this function should be applied to ensure a sufficiently conservative estimate for the equilibrium scour depth. With the 90% non-exceedance coefficients, almost all predicted scour depths are larger than the measured scour depths (see Deltares, 2023n).

Furthermore, it should be kept in mind, that the maximum predicted scour depth with this formula is equal to the pile diameter. This should not be considered as an upper limit for the amount of scour under a scour protection. As the interest in  $S_{eq}/D_{pile} > 1$  (observations that are not present in the database) is expected to be limited in design, this is considered a valid approach, but it is not advised to use this formula for significant scour depths ( $S_{eq}/D_{pile} > 0.5$ ).

#### 4.4.3 Flexibility

##### 4.4.3.1 Theoretical background

The requirements that determine the extent of the scour protection are twofold. First of all the minimum extent of the scour protection should be sufficiently large to completely cover that part of the seabed, where the hydrodynamic disturbance caused by fluid-structure-interaction is largest. Secondly, the extent of the scour protection is governed by the minimum additional volume that is needed to provide rocks for the falling apron that will develop should the maximum seabed lowering occur. Based on these two requirements, it is common practice to use a minimum diameter of the scour protection extent of the order of  $3D_{pile}$  (see also Section 4.4.1) extended with additional scour protection depending on the predicted seabed lowering. The required volumes and some typical dimensions are illustrated in Figure 4.17 and Figure 4.18. An expression for the required additional volume (and thus, extent) was derived by Van Velzen (2012) for falling aprons with a side-slope of 1:2. The present derivation is a generalization of the approach by Van Velzen (2012).

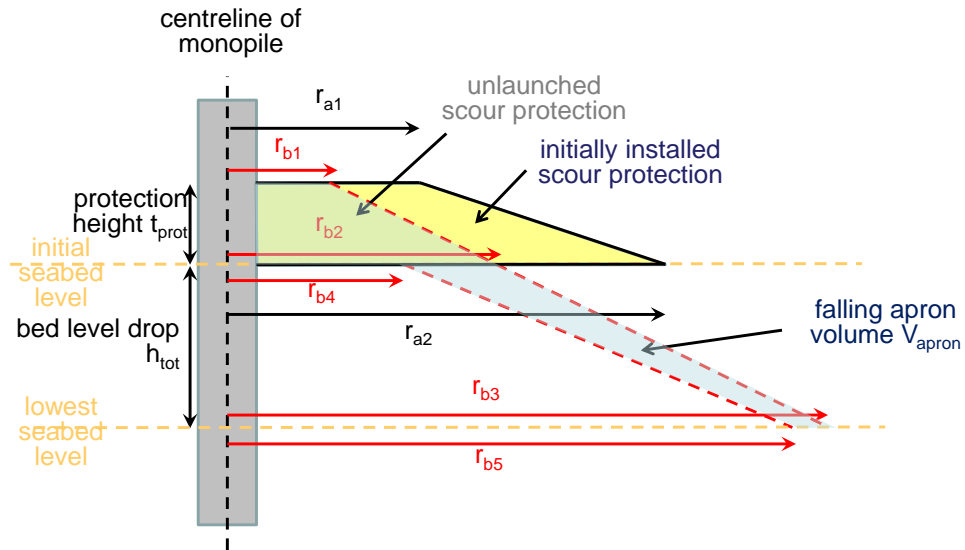


Figure 4.17 Schematisation of different radii describing the falling apron process; “ $r_a$ ” refer to as-built radii, where “ $r_b$ ” refer to radii in the launched state.

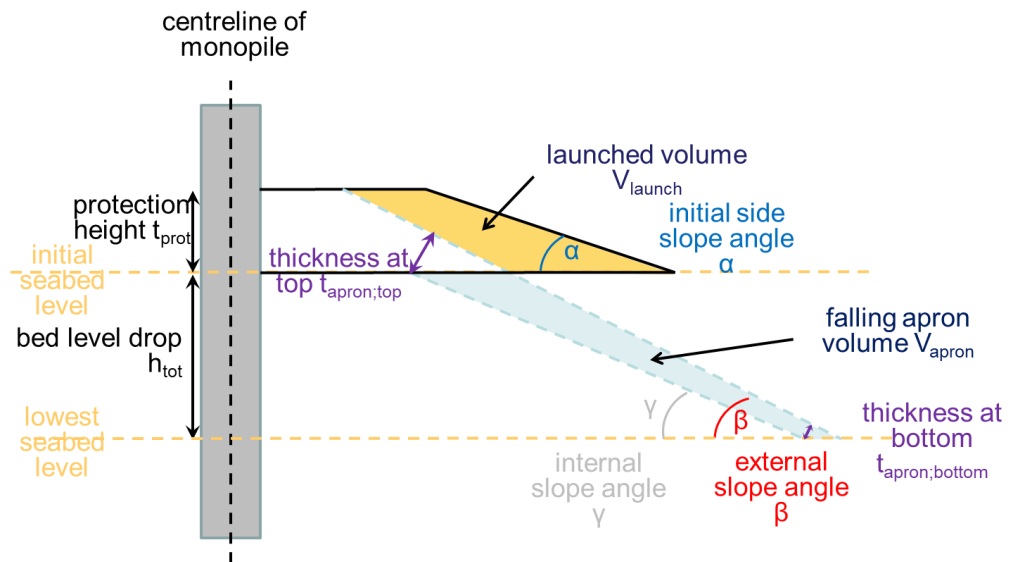


Figure 4.18 Definition of the various used slope angles, layer thicknesses and volumes used in the derivation.

The radii shown in Figure 4.17 are expressed as follows:

$$\begin{aligned}
 r_{b1} &= r_{\min;\text{prot}} + \frac{D_{\text{pile}}}{2}; \\
 r_{b2} &= r_{b1} + \frac{t_{\text{prot}}}{\tan \beta}; \\
 r_{b3} &= r_{b1} + \frac{t_{\text{prot}} + h_{\text{tot}}}{\tan \beta}; \\
 r_{b4} &= r_{b2} - \frac{t_{\text{apron};\text{top}}}{\sin \beta}; \\
 r_{b5} &= r_{b3} - \frac{t_{\text{apron};\text{toe}}}{\sin \beta}
 \end{aligned} \tag{11}$$

With:	$r_{\min;\text{prot}}$	=	the minimum required extent of the scour protection after launching of the apron measured at the top of the protection from the pile face	[m]
	$D_{\text{pile}}$	=	pile diameter	[m]
	$t_{\text{prot}}$	=	as-built thickness of scour protection	[m]
	$\beta$	=	external slope angle of launched protection	[°]
	$\gamma$	=	internal slope angle of launched protection	[°]
	$h_{\text{tot}}$	=	total bed level lowering due to global maximum seabed lowering and edge scour	
	$t_{\text{apron};\text{top}}$	=	layer thickness of launched scour protection, measured at the top of the slope, perpendicular to the external launched slope	[m]
	$t_{\text{apron};\text{toe}}$	=	layer thickness of launched scour protection, measured at the toe of the slope, perpendicular to the external launched slope	[m]

The total required scour protection volume can be computed by adding the volume of the unlaunched part of the scour protection and the launched volume in the falling apron (see Figure 4.17). The volume that is not affected by the launching process ( $V_{\text{unlaunched}}$ ) and remains at its original as-built position can be computed by:

$$V_{\text{unlaunched}} = \pi t_{\text{prot}} \left( \frac{1}{3} (r_{b1}^2 + r_{b1b2} + r_{b2}^2) - \frac{1}{4} D_{\text{pile}}^2 \right) \tag{12}$$

The required (net) falling apron volume can be computed with the following expression:

$$V_{\text{apron}} = \frac{\pi h_{\text{tot}}}{3} (r_{b2}^2 + r_{b2}r_{b3} + r_{b3}^2 - r_{b4}^2 - r_{b4}r_{b5} - r_{b5}^2) \tag{13}$$

The total scour protection volume after launching is then equal to  $V_{\text{tot}} = V_{\text{unlaunched}} + V_{\text{apron}}$ . The initially installed scour protection (indicated by the yellow shading) should be equal to  $V_{\text{tot}}$ , which is expressed as follows:

$$V_{\text{tot}} = \frac{1}{2} \left( \pi r_{a1}^2 + \pi (r_{a1} + t_{\text{prot}} \cot(\alpha))^2 \right) t_{\text{prot}} - \frac{\pi}{4} D_{\text{pile}}^2 t_{\text{prot}} \tag{14}$$

In  $V_{tot}$ , the initial value of the total scour protection extent at top-level,  $r_{a1}$  is then easily extracted by rewriting the expression  $V_{tot} = V_{unlaunched} + V_{apron}$ :

$$r_{a1} = \sqrt{\frac{V_{tot}}{\pi t_{prot}} + \frac{D_{pile}^2}{4} - \frac{t_{prot}^2 \cot^2(\alpha)}{12}} - \frac{t_{prot}}{2} \cot(\alpha) \quad (15)$$

Using the above introduced volume balance, the combination of equations reads:

$$r_{a1} = \sqrt{\frac{V_{apron} - V_{unlaunched}}{\pi t_{prot}} - \frac{D_{pile}^2}{4} - \frac{t_{prot}^2 \cot^2(\alpha)}{12}} - \frac{t_{prot}}{2} \cot(\alpha) \quad (16)$$

This expression relates the required extent to the scour protection volume after launching of the apron. The set of formulae provided above show that the required additional extent becomes larger for:

- Smaller as-built protection thickness  $t_{prot}$ ;
- Larger required thickness of the apron slope  $t_{apron}$ ;
- Smaller external slope angle  $\beta$  (i.e. a milder slope of the falling apron);
- Larger total seabed lowering due to the combination of large-scale morphodynamic processes and edge scour.

It is noted that some of these parameters are coupled. For example, larger scour protection thicknesses are thought to induce larger edge scour depths, which could in turn lead to a larger falling apron length. The list of parameters above are however reflected as being independent. Equation (16) includes the total bed level drop  $h_{tot}$  and the geometric properties of the launched apron. It should be noted that Eq. (16) is a generalization of the equation derived by Van Velzen (2012) to be applicable to any falling apron angle. That expression was simplified in De Sonnevile et al. (2012) into a form where the required additional extent was linearly dependent on the total bed level drop following:

$$r_{a1} - r_{b1} = E_{additional} = c_1 h_{tot} \quad (17)$$

with  $c_1$  having a value of 1.4. This value was derived for a fixed slope of 1:2 and with the assumption that the layer thickness of the falling apron at the toe of the slope equals the layer thickness at the start of the slope. These assumptions lead to a significant simplification of the volume balance, but the parameters that are subject to the assumptions have 1) a significant influence on the required volume and 2) a significant uncertainty in how valid these assumptions are. The relation of Van Velzen (2012) assuming 1.4 times the bed level drop is presently the industry standard, and there is positive experience with using this formula, with all evidence collected so far showing that it leads to safe and sufficient scour protection layouts.

Closing Equation (11) involves finding an expression for:

- The layer thickness on top of the slopes of the falling apron.
- The side-slope steepness of the falling apron.
- Seabed level lowering over which a falling apron will develop.

#### 4.4.3.2 Guideline

In the relation presented by Van Velzen (2012) it was assumed that the layer thickness on top of the falling apron is equal over the length of the apron with a value of the thickness of the scour

protection and that the side-slope steepness is 1:2. The current industry standard is to account for a total lowering equal to the combined effect of morphological lowering and edge scour.

Additional extent

The data collected and analysed within JIP HaSPro is not sufficiently conclusive to derive a different relation for required additional extent than the presently used relation by Van Velzen (2012) of 1.4 times the bed level drop is therefore recommended for use in design. In this relation, the conservativeness in assuming an equal layer thickness of rocks over the entire falling apron slope is, on average, compensated for with the optimistic assumption of a side-slope steepness of 1:2 (with HaSPro data showing that milder side-slopes than 1:4 can develop, see for example Figure 4.19 which shows a variation of slopes between 30 and 15 degrees). Note that based on the HaSPro data no clear relation was found between external forcing and the side-slope of the apron, with significant scatter being present in a simple power-fit as shown in Figure 4.19.

Overall, it is therefore concluded that the relation by Van Velzen (2012) is a reasonable and sufficient choice, which can potentially be optimized if 1) a more explicit relation between side-slope steepness and forcing and 2) an explicit relation between layer thickness of the falling apron and forcing is derived. For now, the recommended additional extent is expressed as follows:

$$E_{additional} = 1.4 \cdot h_{tot} \tag{18}$$

Where  $E_{additional}$  is the required additional extent and  $h_{tot}$  is the bed level lowering at the edge of the scour protection.

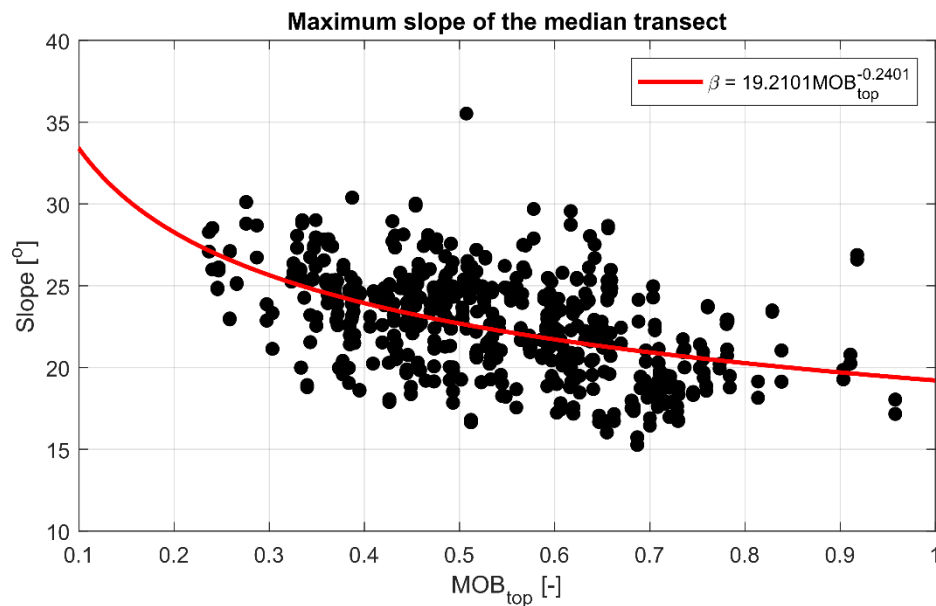


Figure 4.19 Relation between mobility on top of the scour protection ( $MOB_{top}$ ) and slope angle (in degrees) of the launched falling apron showing the best estimate trend (red).

Bed level drop

Although there are not many public sources of field data of edge scour available, the general consensus is that side-slopes of edge-scour holes are relatively gentle (milder than 1:4-1:5). Field data from Offshore Windfarm Egmond aan Zee (Petersen et al., 2015) shows edge scour slope steepness of 1:5 (see, for example, Figure 4.20). Field data at Gemini Offshore Windfarm (made available by project partner Van Oord) shows both significantly milder edge scour depths and milder slopes (as mild as 1:20, see Figure 4.21). The difference between Egmond aan Zee and Gemini is the flow conditions: these are significantly milder at Gemini than at Egmond aan Zee.

These observations, although sparingly available, support the notion that edge scour development is likely associated with relatively mild side-slopes. The slope steepness of the side-slopes of the scour protection and falling apron vary between roughly 1:2 and 1:4. Given that the side-slopes of edge scour holes are milder, it can be argued that the amount of scour protection material sliding down into the edge scour hole is limited. This argument is corroborated by field experience of the project partners.

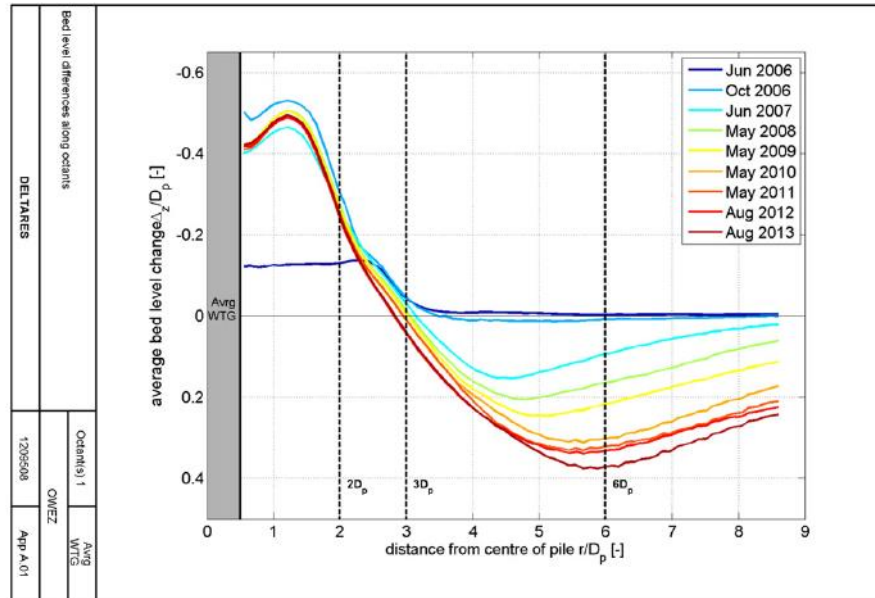


Figure 4.20 Edge scour development in Offshore Windfarm Egmond aan Zee in time, averaged over all monopiles, radially averaged in downstream direction and made non-dimensional with the pile diameter (Petersen et al., 2015).

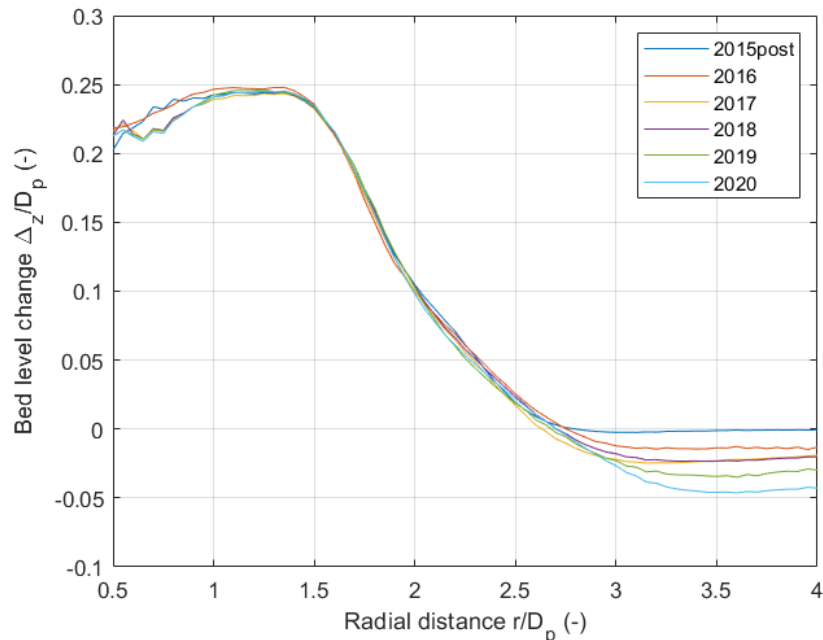


Figure 4.21 Edge scour development in Offshore Windfarm Gemini in time, averaged over all monopiles, radially averaged in downstream direction and made non-dimensional with the pile diameter.



For morphological lowering the situation is different; seabed lowering due to large-scale morphodynamics, like passing sand waves or even sand bank dynamics, could be interpreted as a uniform lowering of the seabed. Due to sediment transport being interrupted by the scour protection and foundation, the seabed level at the location of the scour protection is unaffected. Physical model test observations where a uniform seabed level lowering is mimicked in extremis (i.e., a scour protection constructed on top of a sill) demonstrate that in this case there is clear falling apron development. Although in reality such a configuration with a scour protection on top of a sandy island with a height of several meters will not occur, this schematization shows that in the case of a uniform lowering of the seabed flexibility deformation of the scour protection will occur. Thus, morphological lowering should be accounted for in selecting additional extent of the scour protection.

There are limited publicly available datasets on edge scour around scour protections available, making it not straightforward to make conclusive statements about the total seabed level lowering at the edge of the scour protection that should be accounted for when determining additional extent of the protection. It is the general experience of the consortium that edge scour holes are associated with relatively mild side-slopes, milder than the side-slopes that can develop along the apron under extreme conditions. The likelihood of material sliding into the edge scour hole is therefore limited, but at this stage it cannot be fully excluded that steeper slopes could develop for more extreme conditions. However, based on all available evidence, selecting a total bed level lowering  $h_{tot}$  of twice the morphological lowering plus the possible associated edge scour depth is overconservative. At minimum, the morphological lowering shall be considered as the expected bed level lowering at the edge of the scour protection. It may be a designer's choice to include edge scour depth in this quantity, for example, if limited morphodynamic activity is expected. As general guidance, the following rule-of-thumb is suggested for determining the total height of the falling apron:

$$h_{tot} = h_{bd} \quad (19)$$

where  $h_{bd}$  is the expected bed level drop due to large-scale morphodynamics. It is recommended to at least consider adding the scour protection thickness,  $t_{prot}$ , to the expected bed level drop to account for uncertainties. The scour protection thickness is then considered as a reasonable value for edge scour depth around the entire perimeter of the scour protection. The value of  $h_{tot}$  may be reduced to  $h_{bd}$  if field data of, for example, wind farms in comparable conditions show that indeed there is no rock sliding down into the edge scour hole. Conversely, if a designer feels there are significant uncertainties associated with the site, a larger value of  $h_{tot}$  could be selected upon the designers' discretion. It is noted that, in general, edge scour development is a relatively slow process, thus providing good opportunity for monitoring and, if needed, performance of repairs in case more material is sliding down into the edge scour hole than anticipated.

## 4.5 Design workflow

This section provides an overview of the most relevant parameters required for the design of loose rock scour protections based on Section 4.4. In addition, an overview of the calculation process is provided.

### 4.5.1 Design parameters

For each of the scour protection performance criteria the most relevant parameters to assess its functioning are provided in Table 4.16.

Table 4.16 Design parameters for the loose rock scour protection performance criteria.

Function	Most relevant input parameters	Output
<b>External stability</b>	Minimum $D_{50}$ , i.e., $D_{50/\min}$ . Mobility on top of the scour protection, $MOB_{top}$ (Appendix A) Total KC number, $KC_{tot}$ (Appendix B)	Required rock grading Required layer thickness (armour) rock Base extent
<b>Interface stability</b>	Depth-averaged current velocity, $U_c$ Range of base material diameters ( $d_{15}$ ) Filter rock diameters ( $D_{15}$ , $D_{50}$ )	Filter rock grading Layer thickness
<b>Flexibility</b>	Layer thicknesses armour + filter layers Base extent Morphological lowering	Required additional extent

#### 4.5.2 Interfaces

Scour protection design may be influenced by other aspects than just external stability, interface stability and flexibility. That is to say, these criteria should always be met, but various other constraints may limit the freedom of choice the design parameters. These may include:

- Pile driveability; in case a fully pre-installed scour protection is desired then the (armour) rock choice is limited by the possibility to drive the foundation pile(s) through the rock layer(s). This would lead to either accepting more deformation, the use of high-density rocks or post-installation of armour being needed.
- CPS stability; to prevent excessive motion of the CPS sometimes integration of the CPS into either the scour protection or a rock berm is required. It is noted that the impact of a rock berm on scour protection deformation is not yet completely understood. Furthermore, impact energy of falling rocks on top of the CPS should be considered as well.
- Cable installation; sufficient distance between the top of the scour protection (including installation tolerance) and cable entry holes needs to be present to allow cable pull-in without compromising cable bending radius.
- Jack-up operation; the need for a jack-up vessel for installation may limit the possible (initial) extent of the scour protection .
- Nature-inclusive design; for ecological enhancement of the protection, larger crevices and holes may be desirable, which could influence the choice of rock (and possibly, installability).

## 4.6 Scour protection dimensions

The basic, **minimal** dimensions of a scour protection are as follows:

- Armour layer thickness: for a double-layer system two armour rock layers plus the anticipated deformation; for a single-layer system the static layer thickness (based on filter criteria) plus the anticipated deformation. See also Table 4.7.
- Filter layer thickness: for a double-layer system the minimum required layer thickness to prevent winnowing following from Equation (6); for a single-layer system the minimum required layer thickness (based on Equation (6)) plus the anticipated deformation. See also Table 4.7.
- Armour layer extent: as a base recommendation, a top extent of the armour layer of a radial distance of 1 times the pile diameter is recommended (total diametral extent is then 3 times the pile diameter). Deviating from this extent is possible as long as it can be reasonably justified.
- Filter layer extent: a base filter layer extent constitutes the extent of the armour layer at the bottom (top extent + side-slope steepness multiplied by the thickness) plus at least 1 m to stabilize the armour layer. Deviation of the extent is possible, e.g. for designs where the armour layer extends beyond the filter layer.
- Additional extent: additional extent is calculated as  $E_{additional} = 1.4h_{tot}$ , where  $h_{tot}$  is the total lowering due to at least the large-scale morphological action. In case of uncertainties the scour protection thickness added. This is a designer's choice. Deviating from lowering is possible as long as it can be reasonably justified. It is strictly recommended to always consider as a minimum the lowering due to large-scale morphodynamics. Additional extent is typically applied in the filter layer, but it can also be applied in the armour layer if needed based on the expected dynamics of the rocks.

# 5 Loose rock berms at cable crossings

## 5.1 Introduction

This chapter deals with loose rock berms installed on the seabed to protect, for example, cable crossings. It is noted that this chapter does not deal with rock berms on top of a scour protection, which could be the case for stabilizing a Cable Protection System (CPS). For loose rock berms, the same performance criteria as for scour protections around monopile foundations apply (see Section 4.2). Additionally, rock berms should ensure sufficient cable coverage to protect against external influences (for example, fishing gear) whilst at the same time not cause any overheating of the cables. The work performed in JIP HaSPRO focusses on hydraulic performance of rock berms under extreme conditions only (i.e., external stability). Some remarks on interface stability and flexibility are provided in this chapter.

Within JIP HaSPRO several physical model test programmes were performed to study deformation of rock berms (see also Deltares (2023d), document ref.: 1230924-033-HYE-0001 (Delta Flume tests) and Deltares (2023e), document ref.: 1230924-033-HYE-0002 (Atlantic Basin tests)). An elaborate analysis of these tests is provided in the JIP HaSPRO analysis report (Deltares (2023n), document ref.: 1230924-002-HYE-0003).

The physical model tests were used to validate design relations derived by Roulund et al. (2018b). Furthermore, a theoretical model was derived to predict rock berm deformation as an additional method to verify rock berm performance. This rock berm deformation model could be used within the design cycle of a berm to assess possible reshaping of the berm given the selected material. This model may be used as an additional check within the complete design cycle to verify if, for example, a cable or pipeline is at risk of becoming exposed during extreme conditions given a specific design. The reshaped profile can be evaluated against the performance criteria that are established in the design phase.

This chapter first details the rock berm design methodology, after which the rock berm deformation model is discussed.

## 5.2 Rock berm design

### 5.2.1 External stability

It was found by Roulund et al. (2017) and Roulund et al. (2018b) that rock berms reshape under severe wave and current conditions to a parabolic shaped cross-section with berm bottom width to height ratio ( $B_{berm}/h_{berm}$ ) being a function of the Shields parameter. This observation forms the basis for determination of the rock berm geometry for installation. A functional relation between  $B_{berm}/h_{berm}$  was derived by Roulund et al. (2018b) as:

$$\frac{B_{berm}}{h_{berm}} = 6000\theta^2 + 50\theta + 2.4 \quad (20)$$

where  $\theta$  is the Shields parameter at the ambient seabed level (calculated following the method described in Appendix A, see also Eq. A.33),  $B_{berm}$  is the reshaped bottom width of the berm and  $h_{berm}$  is the reshaped berm height. Figure 5.1 shows how this relationship compares to physical model test observations in the Delta Flume and Atlantic Basin (data obtained in JIP HaSPRO) and to data from Roulund et al. (2018b). It is noted that from the data collected in JIP HaSPRO, only datapoints with significant deformation were considered as the 'final' stable reshaped rock berm

profile to avoid the data being influenced by the additional rock berm geometry. It was attempted to update the fit from Eq. 14 with the data from HaSPro, but this led to minimal differences. From comparing the fit it appeared that Eq. 14 shows a more rapid increase of  $B_{berm}/h_{berm}$  for larger values of  $\theta$ , which is considered a more realistic representation of complete rock berm washout for higher Shields numbers. Caution with Shields numbers larger than roughly 0.06 is advised; these Shields numbers coincide with a mobility that is roughly 1 or larger, which represents a complete flattening of the berm due to environmental conditions. This is further demonstrated with the rock berm deformation model.

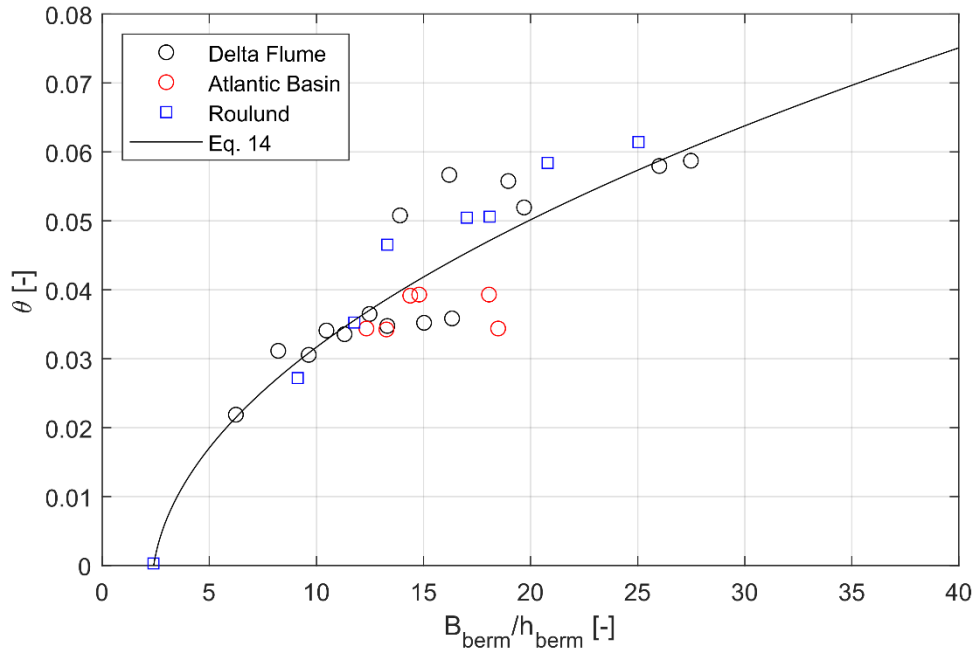


Figure 5.1 Stable reshaped rock berm bottom width to height ratio, including observations from HaSPro physical model tests performed in the Delta Flume (black dots) and the Atlantic Basin (red dots), as well as the original data from Roulund et al. (2018b) in blue squares.

Rock berm geometry for installation is illustrated in Figure 5.2 as a trapezoidal cross section defined by minimum dimensions and intersection with as-found seabed:

- Top width,  $W_{TOP}$
- Side slope,  $1:\alpha$
- Top of product cover,  $TOPC$ .

For the same  $TOPC$ , the berm height and hence rock volume and seabed footprint will vary depending on whether the cable is surface laid, buried or free spanning. An extreme event may cause the rock berm height to lower due to reshaping. The  $TOPC$  is determined such that the coverage after reshaping remains above or equal to the required Minimum top of cable cover,  $MTOC$ . Target and minimum berm heights are defined vertically along the cable centre line:

$$\begin{aligned} h_{berm} &= TOPC + \Delta \\ h_{min} &= MTOC + \Delta \end{aligned} \quad (21)$$

Here,  $\Delta$  is introduced as an offset which depends on whether the cable is surface laid, buried or free spanning. For engineering design,  $\Delta$  can be taken as:

- Surface laid cable:  $\Delta = D_{cable}$ .
- Burial depth of free spanning cable:  $\Delta = Z_{DOL} - Z_{SBL}$ .

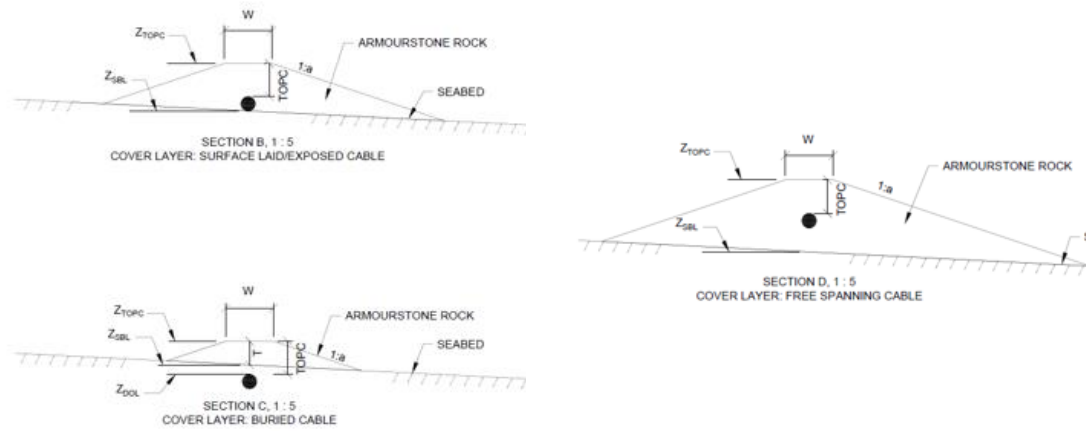


Figure 5.2 Generic rock berm cross section for installation.

A definition sketch showing the installed rock berm profile and the reshaped rock berm profile is provided in Figure 5.3.

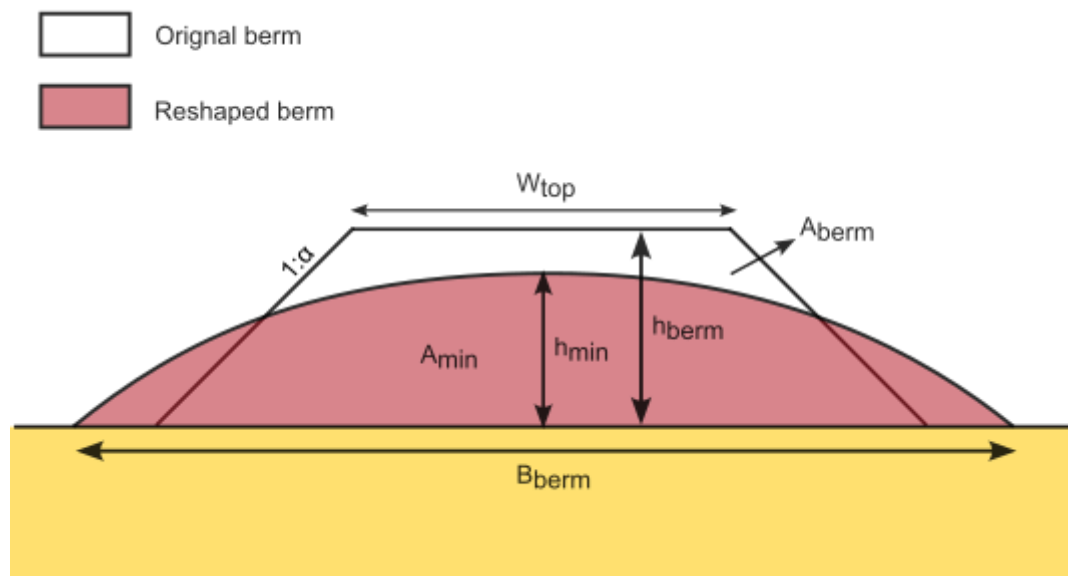


Figure 5.3 Definition sketch showing the installed rock berm profile and the reshaped rock berm profile.

The top of product cover,  $TOPC$ , is now determined for a given hydraulic exposure defined by the Shields parameter and Eq. 14 for given values of  $W_{TOP}$ ,  $MTOC$  and  $D_{cable}$  as follows:

1. The cross-sectional berm area,  $A_{berm}$ , of the installed berm is:

$$A_{berm} = h_{berm} \cdot W_{TOP} + h_{berm}^2 \alpha \quad (22)$$

2. The cross-sectional berm area of a reshaped parabolic berm with height  $h_{min}$  and bottom width  $B_{berm}$  is given by:

$$A_{min} = \frac{2}{3} B_{berm} \cdot h_{min} \quad (23)$$

3. The installed berm cross section area is set equal to the minimum reshaped area. This leads to a quadratic equation for variable  $h_{berm}$ :

$$h_{berm}^2 + \frac{W_{TOP}}{\alpha} \cdot h_{berm} - \frac{A_{min}}{\alpha} = 0 \quad (24)$$

4. Seeking the maximum root of Eq. 24 and inserting Eq. 21 and Eq. 23 yields:

$$h_{berm} = 0.5 \left[ \sqrt{\left( \frac{W_{TOP}}{\alpha} \right)^2 + \frac{4}{\alpha} \frac{2}{3} (6000\theta^2 + 50\theta + 2.4) h_{min}^2} - \frac{W_{TOP}}{\alpha} \right] \quad (25)$$

5. Then, finally, inserting Eq. 15 yields the required  $TOPC$ .

$$TOPC = 0.5 \left[ \sqrt{\left( \frac{W_{TOP}}{\alpha} \right)^2 + \frac{4}{\alpha} \frac{2}{3} f(\theta) (MTOC + \Delta)^2} - \frac{W_{TOP}}{\alpha} \right] - \Delta \quad (26)$$

$$f(\theta) = 6000\theta^2 + 50\theta + 2.4$$

### 5.2.2 Interface stability

Due to the absence of a monopile that induces significant flow amplification, winnowing is less of an issue for rock berms used as cable coverage. As a rule-of-thumb, from data by Verheij et al. (2012) it can be derived that a filter layer thickness of 4-5 rock layers is sufficient to prevent winnowing. Field experience with performance of rock berms is needed to verify this. It is noted that some sinking of the berm (including the asset) may be beneficial for the hydraulic performance of the berm.

### 5.2.3 Flexibility

A method that can be used to calculate the volume for the falling apron has similarities to the method of Van Velzen (2012), which was derived for a falling apron around a circular pile in current-only conditions. The calculation method is based on a volume balance of the *waiting apron* and the actually *launched apron*. The falling apron volume (per m rock berm length for one side of the rock berm) is computed with the following fairly simple relationship, which is valid for two-dimensional rock berms:

$$V_{apron} = \gamma_s \frac{D_{50} \cdot (n_{D,top} + n_D)}{2 \sin \alpha} h_{tot} \quad (27)$$

where  $V_{apron}$  is the needed volume,  $D_{50}$  is the diameter of the protection material,  $n$  denotes the layer thickness (amount of rock layers, red.) of the falling apron on and at the bottom of the slope,  $\alpha$  the developed falling apron slope,  $\gamma_s$  a safety factor to account for both rock loss due to imperfect launching and three-dimensional effects, and  $h_{tot}$  the total amount of bed lowering. For the values of the side-slope and layer thickness on the falling apron the same considerations as discussed in Section 4.4.3 are valid. As a rule-of-thumb, a layer thickness of 5 rock layers at the top of the berm slope and 1 rock layer at the toe of the berm slope may be applied.

#### 5.2.3.1 Edge scour at rock berms

Although much work has been done on the topic of interaction between a rock berm and the seabed, there are still uncertainties (Sumer, 2014), and quantitative guidelines are lacking. Edge scour development around rock berms and the potential sliding of the rock into the edge scour (falling apron behaviour) are important to consider in the design. A number of different edge scour inducing mechanisms around rock berms are mentioned by Roulund et al. (2018a), by considering the analogy with similar configurations:

- Local blockage of sediment transport (as is, for instance, the case at river/coastal groynes) which leads to transport gradients, and thus morphological changes: erosion is expected in the lee-side of the rock berm.
- Scour due to locally changed hydrodynamics like flow contraction and turbulence (as is, for instance, the case at the tip of breakwaters).
- Flow separation in case of sharp geometry (as is, for instance, the case at backward facing steps or rock berms with sharp cross-sections). At the reattachment point, turbulence intensities are high, which are an important driver for potential scour. For obliquely located rock berms, helical flow patterns are often observed to be the major driver of edge scour.
- Due to increased roughness at the berm the flow may not separate at the steep slopes and remain attached. As a result, there are downward directed vertical velocities that may impinge on the bed and lead to relatively high bed shear stresses (Broekema et al., 2018).
- Edge scour due to local secondary flows and increased turbulence intensities resulting from a roughness transition (as is, for instance, the case at protections around offshore structures, see Petersen et al. (2015)). The expected edge scour is found to scale with the protection height and with the change in roughness.
- In the case of a more wave-dominated situation, waves may stabilize the rock berm due to backfill effects both of the developed edge scour holes and within the pores of the rocks, thus limiting the extent of edge scour.

Given the uncertainty in both the current knowledge on rock berm induced edge scour, as well as in the exact protrusion of the rock berm above the seabed and the local composition of the soil, edge scour estimates are rather uncertain. Potential for edge scour can be minimised by making the rock berm wider and the side-slopes relatively gentle. Large-scale morphological changes are expected to have a larger impact than the rock berm itself.



#### 5.2.4 Dimensioning of rock berms

The following steps may be taken to dimension a rock berm that can be used as a cable cover:

- Calculation of the minimum dimensions for stability using Eq. 20-26. It is noted that for the use of these equations, the required  $D_{50}$  of the berm must be selected a-priori. The rock grading may be varied to optimize the required rock berm volume. The rock berm deformation model (Section 5.3) may be used as well. As a starting point, it is recommended to select a rock grading with a relative mobility smaller than 1 at the top of the berm. The provided calculation method is independent of the orientation of the rock berm w.r.t. the direction of the waves and currents. The method was derived for the (normative) case of perpendicular waves and currents. It is noted that the method described in Eq. 20-26 is valid for rock berms that show reshaping, so for relatively high Shields numbers. For lower Shields numbers the deformation model described in Section 5.3 may provide additional insight in rock berm performance.
- Check winnowing potential of the designed berm. If the minimum berm height is lower than 4 rock layers, additional measures may be required. These may include increasing berm height or an appropriate monitoring strategy.
- Check ability of the designed berm to follow seabed level changes at the edge. Additional volume/width may be supplied if it is expected that there is not sufficient material present to act as a falling apron.

### 5.3 Rock Berm Deformation model

A full elaboration of the theoretical background behind the Rock Berm Deformation (RoBeD) model is provided in the loose rock physical model tests analysis report (Deltares (2023n), document ref.: 1230924-002-HYE-0003). The basic principle behind the Rock Berm Deformation (RoBeD) model is that reshaping of the rock berm will occur until the mobility for each rock in the berm is lower than a threshold value where motion can occur. In other words: if any of the rocks within the berm are mobile then reshaping of the berm will occur, either local or global, depending on the degree of instability. This is illustrated in Figure 5.4, where 4 different deformation classes are defined:

- Deformation class 0:  $MOB_{top;slope} \leq MOB_{thresh}$ . The mobility on top of the slope is lower than the selected threshold value, so reshaping of the berm is not necessary. No deformation is expected in this case.
- Deformation class 1:  $MOB_{top;slope} > MOB_{thresh}$  &  $MOB_{top;flat} \leq MOB_{thresh}$ . The mobility on top of the slope is larger than the selected threshold value but the mobility on top of the flat part of the berm is smaller than the selected threshold value. No lowering on top of the berm is needed but reshaping of the profile will occur. Reshaping could lead to regression and, depending on the width of the berm, this could as a consequence lead to lowering of the top of the berm.
- Deformation class 2:  $MOB_{top;slope} > MOB_{thresh}$  &  $MOB_{top;flat} > MOB_{thresh}$ . Both the mobility on top of the slope and on top of the flat part of the berm is larger than the selected threshold value. Besides reshaping of the side-slopes, a lowering of the top is required to reach a stable berm profile.
- Deformation class 3:  $MOB_{bed;flat} > MOB_{thresh}$ . Even the mobility on the seabed is larger than the selected threshold value, so the profile will eventually erode away. It is likely that before complete wash-away of the profile there will be a flat profile that is somewhat stable. This regime coincides with the earlier mentioned Shields numbers larger than  $\sim 0.06$ .

For lower Shields numbers, the method as described in Section 5.2 could be supplemented with the above schematization to check the expected deformation class. For deformation class 0 and 1, no lowering of the berm is expected. A mobility threshold of 0.95 is recommended.

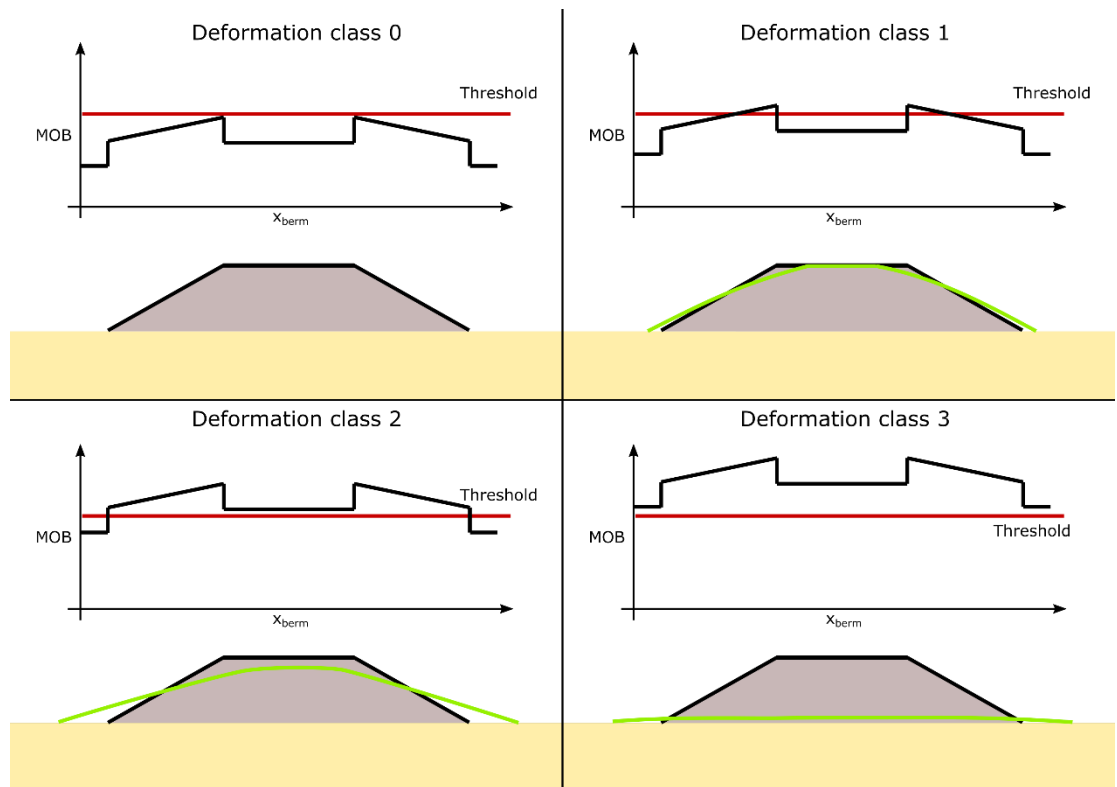


Figure 5.4 Visualization of different deformation classes and resulting rock berm deformation depending on the relative mobility along the berm profile. The jump in mobility is related to the destabilizing effect of the slope on the mobility.

### 5.3.1 Rock berm deformation model application

An example of the application of the RoBeD model is provided in Figure 5.5. Here, the model is applied to reproduce observed deformation patterns during delta flume experiments (Deltares (2023d), document ref.: 1230924-033-HYE-0001). The model was also applied to physical model tests in the Atlantic Basin, on a much smaller scale. In both cases, agreement between model calculation and observations are reasonable. The following notes are made with regards to model application:

- A mobility threshold of 0.95 is a limit that leads to best results for all considered cases.
- A slope angle of internal friction of the rocks of 40 degrees was assumed. This is mostly valid for limited infill of sand, and not for the falling apron slopes.
- The RoBeD model is only applicable for external stability, not for interface stability or flexibility.

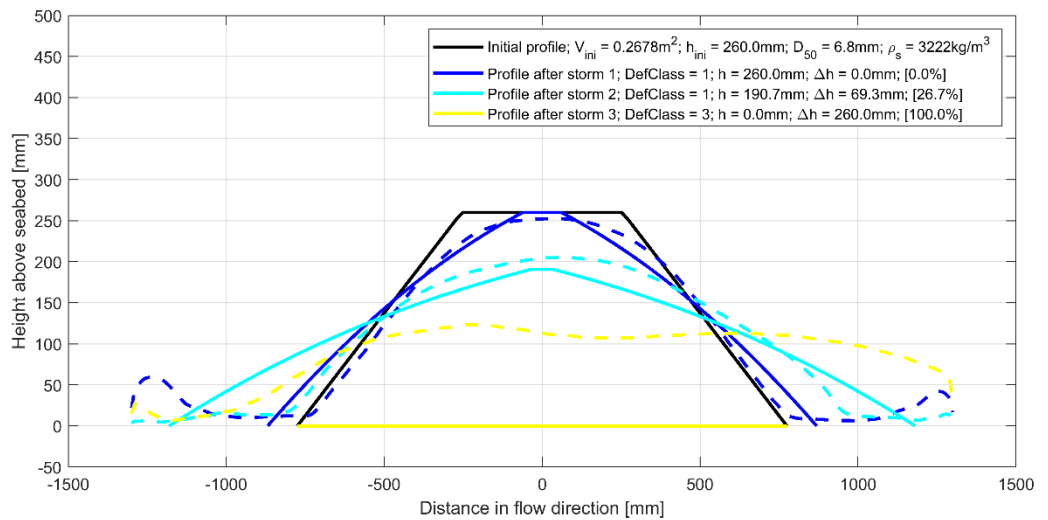
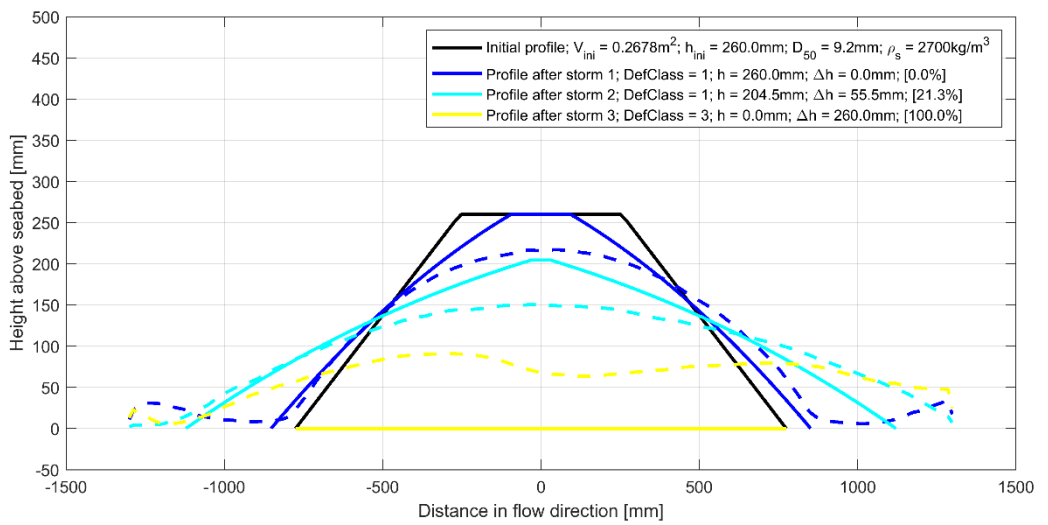
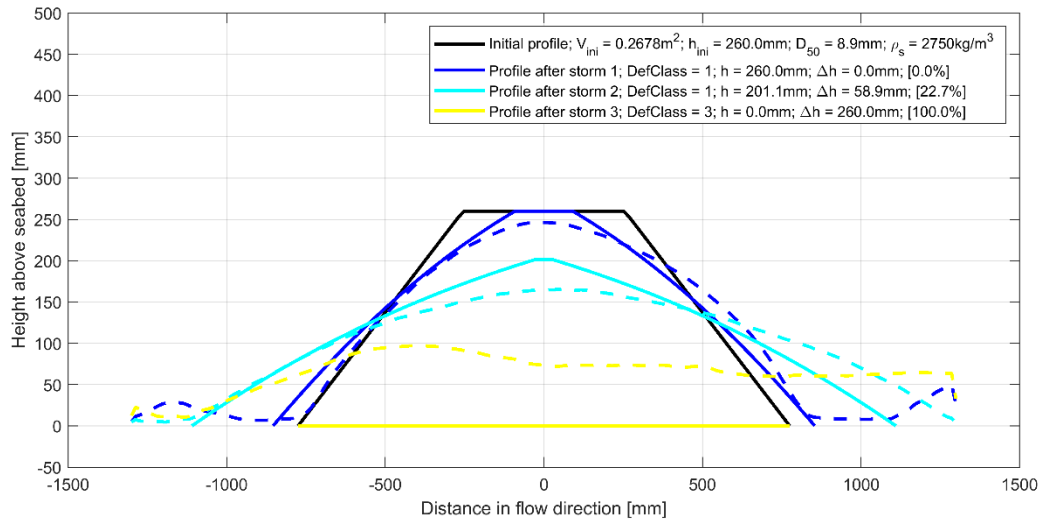


Figure 5.5 Predicted (solid lines) and observed (dashed lines) rock berm deformation for Test Series A in the Delta Flume.

# 6 Offshore rock gradings

## 6.1 Introduction

This chapter deals with specifications and characteristics of offshore rock gradings to be used in loose rock scour protection designs. A concise background of quarry rock is provided in Section 6.2. Standard rock gradings as defined in the Eurocode are presented in Section 6.3, followed by a renewed definition as developed within this handbook in Section 0. Information on material properties and testing procedures is given in Section 6.5, followed by a description of quarry operations in Section 6.6. Finally, Section 6.7 provides guidance on the handling of rock gradings during the various installation steps.

## 6.2 Quarry rock

In Aggregate Quarries, the rock aggregates are produced by blasting of rock faces and subsequent sorting, crushing and sieving of the blast dump. Rock products may also origin from Dimension Stone Quarries or from Glacial-, River- or Marine deposits or from recycled or re-handled rock. For efficient usage of the materials, the rock quarries will often seek to cover a range of rock products. Rock products for construction- and civil works are termed Aggregates. Aggregates for the concrete and asphalt industry are finely crushed rock materials applied bound into a matrix of other materials. The term Armourstone is used for coarse aggregates. It is primarily used for river- and coastal training works, breakwater structures and for offshore works used as cable- and pipeline cover, scour protection works or bedding layers for gravity structures. Armourstone will normally be applied as unbound material without mixing in of other materials.

The classification of a rock product as armourstone, does not relate to its use or application. E.g., both filter- and armour layers of a double-layer rock scour protection will consist of armourstone. Armourstone products are classified in gradings. A large step forward in harmonising grading specification was made with the European Standard EN-13383:2002 part 1&2 providing basis for the CE trademarked Coarse (CP)-, Light (LM)- and Heavy (HM) armourstone gradings. In-depth elaboration on armourstone rock materials is provided in the Rock Manual (CUR/CIRIA/CETMEF, 2007), Chapter 3, providing both background and derived properties of the EN-13383 Coarse, Light and Heavy gradings.

The grading limits of the EN 13383 are open (only either an upper or a lower bound limit). The open limits implicitly assume that the rock grading is a primary product from blasted rock faces following a smooth distribution of rock sizes. Re-handled or mixed rock products may contain gaps in the grading curve while still complying to the open boundaries of the EN 13383 specifications.

The EN 13383 light and heavy gradings do not include requirements to the  $M_{50}$  (50 % passage rock weight), used by designers to calculate rock stability. Instead, the EN 13383 light and heavy gradings contain subdivision into class A and B gradings. The difference between A and B gradings is that Effective Mean Mass ( $M_{em}$ ) criteria are applied to type A gradings. The  $M_{em}$  criteria form an easy control of the mean rock weight (sample weight divided by number of rocks in the sample). Even so, the  $M_{em}$  remains unsuitable as a design parameter. The  $M_{em}$  criteria do not apply to type B gradings such that for type B gradings there is no mean rock weight control in the grading specifications.

It has been observed that designers have added values of  $M_{50}$  as additional grading requirement to the EN 13383 light and heavy gradings. Apart from conflicting with the CE-marked grading specification, the values requested for  $M_{50}$  have often been seen to conflict with what is readily

obtainable within the given rock grading, thus adding significant cost, delays and disputes on non-conformance to rock production.

In response to above listed experience with the EN 13383 gradings, The JIP HaSPro participants have found that supplements and alterations to existing armourstone grading specifications will allow optimisation and qualification of armourstone production and rock works design. These supplements and alterations are given as a guideline for new additional armourstone rock gradings and named Offshore Sieved Gradings (OSG) and Offshore Weighted Gradings (OWG), so as not to be mistaken for the CE-marked CP-, LM- and HM gradings of EN 13383.

The proposed offshore gradings follow the same terminology as the EN 13383 gradings having nominal and extreme lower and upper limits (ELL, NLL, NUL and EUL). Offshore Sieved Gradings (OSG<sub>NLL/NULmm</sub>) are defined by sieve size (in mm) like the EN13383 coarse gradings. Similarly, the Offshore Weighted Gradings (OWG<sub>NLL/NULkg</sub>) are defined by weight (in kg) like the EN13383 light gradings.

The Offshore Sieved and Weighted grading limits are closed (both upper and lower bound limits) and the weighted gradings are supplemented with the  $M_{50}$  percentage passage criteria, while the  $M_{em}$  criteria are not maintained.

The Offshore Sieved and Weighted gradings are defined to align with EN 13883 coarse and light gradings, while including above mentioned considerations. A higher fines content allowance is included in the sieved gradings to make the production suitable for high volume production. It is noted that although more fines may be more efficient for quarry production, this leads to more loss of fines during offshore installation. This may result in more volume being needed for purchase and thus possibly more trips required during installation. Finally, three new gradings have been included for flexibility of design.

Grading limits for EN 13383 coarse and light gradings are reproduced in section 6.3. Grading limits for Offshore Sieved and Weighted gradings are given in section 0.

In addition to the OSG, OSW or EN 13383 gradings a new non-standard grading can be defined, as outlined in the Rock Manual, section 3.4.3.9. These non-standard gradings can also be safely applied as scour protection as long as grading requirements are satisfied. An example of this is the (tested in JIP HaSPro) 2-180 mm grading. It is advised that the number of requirements is kept to the minimum possible, such that rock acquisition and production is not unnecessarily complicated.

## 6.3 EN 13383: Coarse and Light Gradings

The European Standard 'EN 13383-1:2013 Armourstone – Part 1: Specifications' and 'EN 13383-2:2019 Armourstone – Part 2: Test methods' provides the basis for the CE trademarked Coarse, Light and Heavy armourstone rock gradings. Reference is made to these standards for more details.

For offshore application the coarse and light gradings are relevant, which are defined as follows:

- Coarse grading: designation of grading with a nominal upper limit defined by a sieve size between and including 125mm and 250 mm.
- Light grading: designation of grading with a nominal upper limit defined by a mass between and including 25 kg and 500 kg.

### 6.3.1 Coarse gradings

The standard Coarse Gradings defined in the EN 13383 are:

- CP<sub>45/125</sub>
- CP<sub>63/180</sub>
- CP<sub>90/250</sub>
- CP<sub>45/180</sub> (wide grading)
- CP<sub>90/180</sub> (narrow grading designated for special applications such as gabions)

Coarse gradings are defined by the percentage passing (by mass) a certain sieve size. The grading designation is based on the 15% and 90% passing limits. Other gradings can be declared by the producer (CP<sub>declared</sub>). The requirements of the particle size distribution of standard Coarse gradings are defined in “Table 1” of EN 13383, which is reproduced in amended form in Table 6.1.

Table 6.1 Coarse grading armourstone limits. Amended from EN 13382-1:2013.

EN 13383 Coarse Gradings	CP <sub>45/125</sub>	CP <sub>45/180</sub> *	CP <sub>63/180</sub>	CP <sub>90/180</sub> **	CP <sub>90/250</sub>
D <sub>50min</sub> [mm]	63	63	90	-	125
Sieve size [mm]	Percentage passing (by mass)				
360	-	-	-	-	98 to 100
250	-	98 to 100	98 to 100	98 to 100	90 to 100
180	98 to 100	90 to 100	90 to 100	80 to 100	-
125	90 to 100	-	-	-	0 to 50
90	-	-	0 to 50	0 to 20	0 to 15
63	0 to 50	0 to 50	0 to 15	-	-
45	0 to 15	0 to 15	-	0 to 5	0 to 5
31.5	-	-	0 to 5	-	-
22.4	0 to 5	0 to 5	-	-	-
* Wide grading					
** Gabion grading					

### 6.3.2 Light gradings

The standard Light Gradings defined in the EN 13383 are:

- LMA<sub>5/40</sub> and LMB<sub>5/40</sub>
- LMA<sub>10/60</sub> and LMB<sub>10/60</sub>
- LMA<sub>40/200</sub> and LMB<sub>40/200</sub>
- LMA<sub>60/300</sub> and LMB<sub>60/300</sub>
- LMA<sub>15/300</sub> and LMB<sub>15/300</sub>

Notable difference with coarse gradings is that the light gradings are not defined by particle size, but by particle mass. Another difference is that the grading designation is based on the 10% and 70% limits. Other light gradings can be declared by the producer (LM<sub>declared</sub>).

A distinction is made between LMA and LMB category light gradings. For LMA gradings additional requirements are imposed on the average individual stone mass (effective mean mass, M<sub>em</sub>). For LMB gradings no requirements are imposed on M<sub>em</sub>. The grading requirements of standard light gradings (LMA and LMB) are given in ‘Table 2’ and ‘Table 3’ of EN 13383. These tables are reproduced in amended form in Table 6.2.

The EN 13383 does not specify minimum values for the 50% percentage passage rock weight ( $M_{50min}$ ) for light and heavy gradings. For design guidance, the Rock Manual (CUR/CIRIA/CETMEF, 2007) presents a methodology for non-standard gradings to assess min and max values of  $M_{50}$  based on the grading designation nominal lower and -upper limits,  $M_{NLL}$  and  $M_{NUL}$ . For the standard gradings of EN 13383, the Rock Manual provides tabulated values of  $M_{50min}$  and  $M_{50max}$  reproduced in Table 6.3. The methodology to derive  $M_{50}$ -values from the  $M_{em}$ -value is indicative only and not part of the CE marked grading specifications.

Table 6.2 Light grading armourstone limits. Amended from EN 13382-1:2013.

EN 13383 Light Gradings	LMA <sub>5/40kg</sub>	LMA <sub>10/60kg</sub>	LMA <sub>40/200kg</sub>	LMA <sub>15/300kg</sub>	LMA <sub>60/300kg</sub>
	LMB <sub>5/40kg</sub>	LMB <sub>10/60kg</sub>	LMB <sub>40/200kg</sub>	LMB <sub>15/300kg</sub>	LMB <sub>60/300kg</sub>
$M_{em}$ [kg] (only for LMA)	10 to 20	20 to 35	80 to 120	45 to 135	120 to 190
Rock weight [kg]	Percentage passing (by mass)				
450	-	-	-	97 to 100	97 to 100
300	-	-	97 to 100	70 to 100	70 to 100
200	-	-	70 to 100	-	-
120	-	97 to 100	-	-	-
80	97 to 100	-	-	-	-
60	-	70 to 100	-	-	0 to 10
40	70 to 100	-	0 to 10	-	-
30	-	-	-	-	0 to 2
15	-	-	0 to 2	0 to 10	-
10	-	0 to 10	-	-	-
5	0 to 10	-	-	-	-
3	-	-	-	0 to 2	-
2	-	0 to 2	-	-	-
1.5	0 to 2	-	-	-	-

Table 6.3 Light grading armourstone. Expected minimum and maximum 50 percent passage. Amended from Rock Manual (CUR/CIRIA/CETMEF, 2007).

Rock Manual Light Gradings	LMA <sub>5/40kg</sub>	LMA <sub>10/60kg</sub>	LMA <sub>40/200kg</sub>	LMA <sub>15/300kg</sub>	LMA <sub>60/300kg</sub>
$M_{50min}$ [kg]	14	27	101	70	149*
$M_{50max}$ [kg]	28	47	152	211	236

\* Value from errata to Rock Manual.

## 6.4 Offshore Sieved and Weighted Gradings

Supplements and alterations to the EN 13383 armourstone gradings are given as new armourstone rock gradings and named Offshore Sieved Gradings (OSG) and Offshore Weighted Gradings (OWG) so as not to be mistaken for the CE-marked CP-, LM- and HM-gradings of EN 13383.

### 6.4.1 Offshore Sieved Gradings

The standard Offshore Sieved Gradings defined within the framework of the JIP HaSPro are:

- OSG<sub>22/90mm</sub>
- OSG<sub>22/125mm</sub>
- OSG<sub>22/180mm</sub>
- OSG<sub>45/180mm</sub>
- OSG<sub>90/250mm</sub>

Offshore Sieved Gradings are defined by the percentage passing (by mass) a certain sieve size. The grading designation is based on the 15% and 90% passing limits. Other gradings can be declared by the producer (OSG<sub>declared</sub>). The requirements of the particle size distribution of standard offshore sieved gradings are defined in Table 6.4, the gradings are visualized in Figure 6.1 to Figure 6.5. With these grading definitions, the use of ‘inch’ gradings may be avoided. For completeness, inch-equivalent names are provided as an alternative naming reference. In addition to the gradings below, alternative gradings may be specified as well (like the 2-180 mm grading that was also investigated in JIP HaSPro).

For the sieved gradings a maximum diameter  $D_{max}$  is not specified, however a maximum sieve size may be added in case of project specific installation and operational constraints (contractor-specific requirement due to fall pipe dimensions/conveyor belts), see also Section 7.2.

Table 6.4 Offshore Sieved Grading armourstone limits. By percentage passage of sieve size.

Offshore Sieved Gradings	OSG <sub>22/90mm</sub>	OSG <sub>22/125mm</sub>	OSG <sub>22/180mm</sub> *	OSG <sub>45/180mm</sub>	OSG <sub>90/250mm</sub>
Inch equivalent	1-3"	1-5"	1-8"	2-8"	4-10"
D <sub>50min</sub> [mm]	45	63	80	90	125
Sieve size [mm]	Percentage passing (by mass)				
360	-	-	-	-	98 to 100
250	-	-	98 to 100	98 to 100	90 to 100
180	-	98 to 100	90 to 100	90 to 100	50 to 90
125	98 to 100	90 to 100	50 to 90	50 to 90	15 to 50
90	90 to 100	50 to 90	35 to 60	15 to 50	0 to 15
63	50 to 90	15 to 50	15 to 35	-	-
45	15 to 50	-	-	0 to 15	0 to 5
22.4	0 to 15	0 to 15	2 to 15	0 to 5	-
16	0 to 5	0 to 5	0 to 5	-	-
2	-	-	-	-	-

\* For the OSG<sub>22/180mm</sub> grading D<sub>50,min</sub> is indirectly defined by linear interpolation between the sieves closest to the D<sub>50,min</sub> value. Since the two nearest sieves are used, the possibility that D<sub>50,min</sub> is in practice smaller than the value obtained through linear interpolation is considered to be negligible.



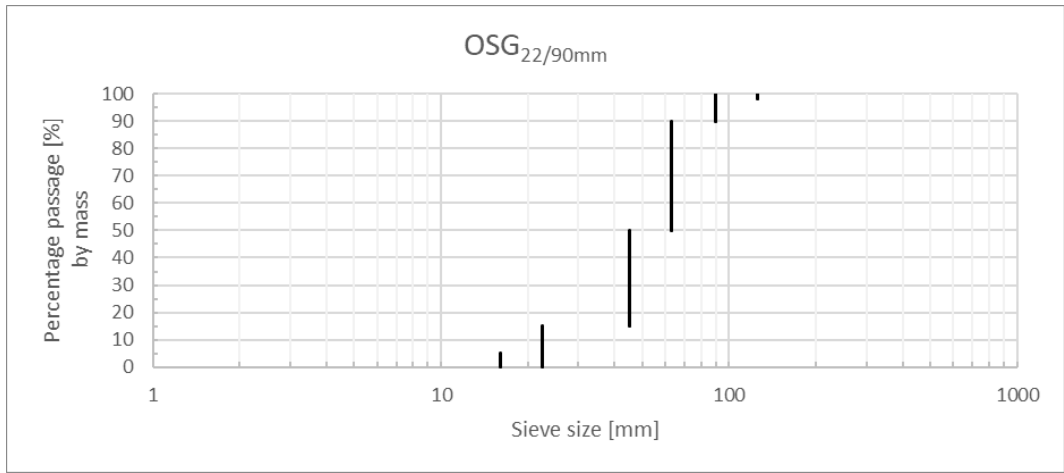


Figure 6.1 OSG<sub>22/90mm</sub> offshore sieved grading limits.

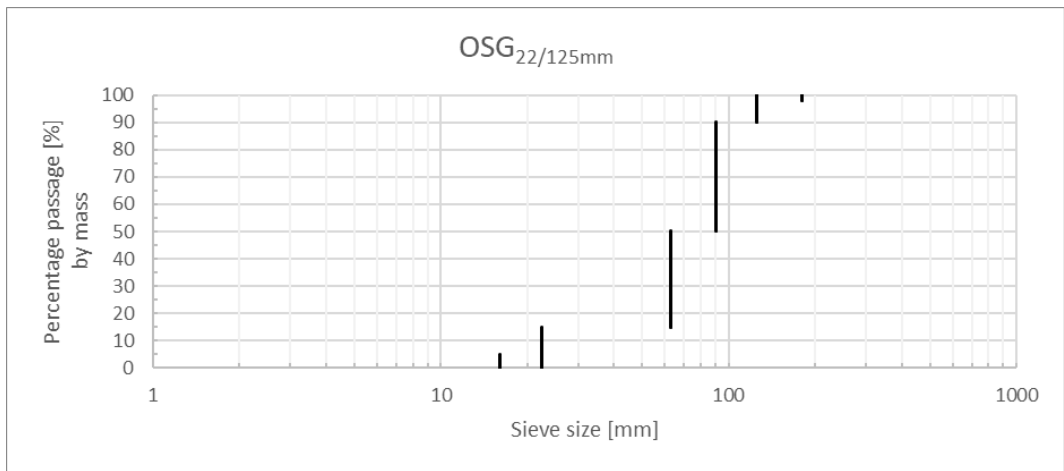


Figure 6.2 OSG<sub>22/125mm</sub> offshore sieved grading limits.

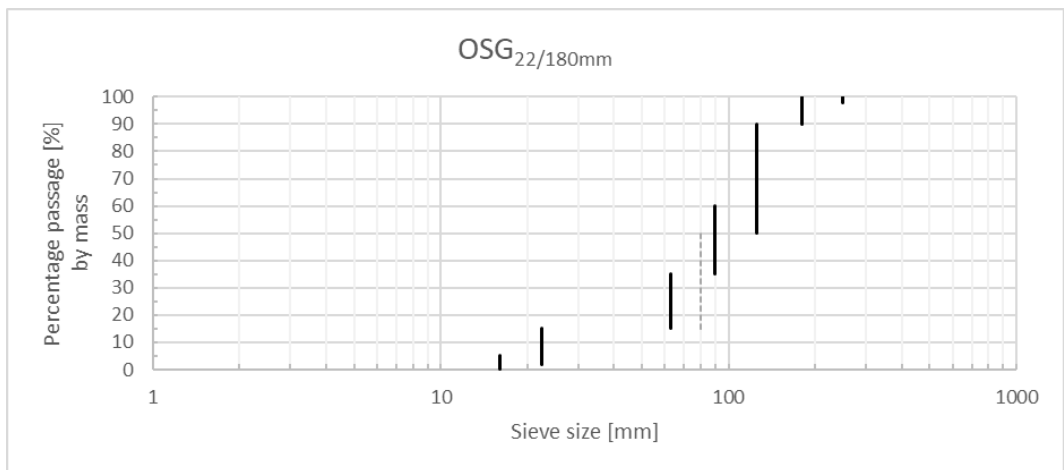


Figure 6.3 OSG<sub>22/180mm</sub> offshore sieved grading limits. The dashed line represents the 15-50 passing percentage line as presented in the other gradings. For the OSG<sub>22/180mm</sub> grading the sieve definition deviates, the dashed line is included to reflect on this difference.

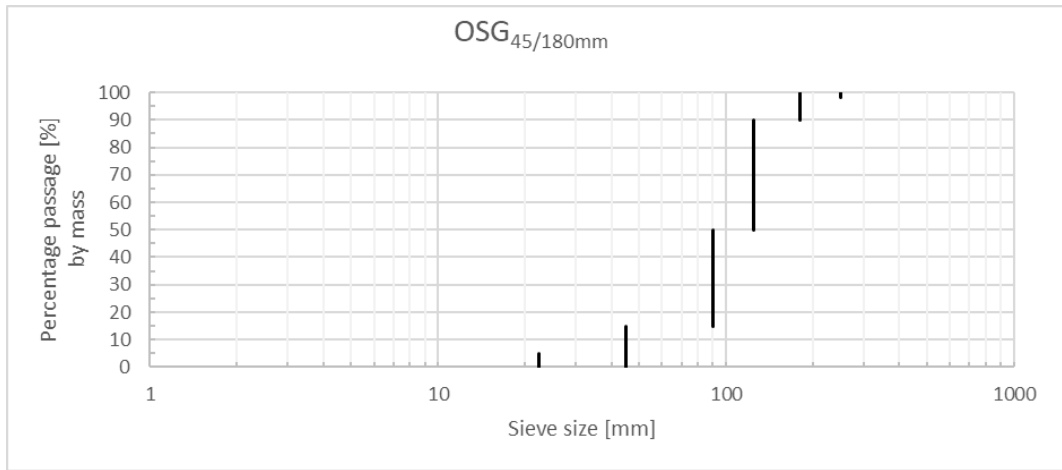


Figure 6.4 OSG<sub>45/180mm</sub> offshore sieved grading limits.

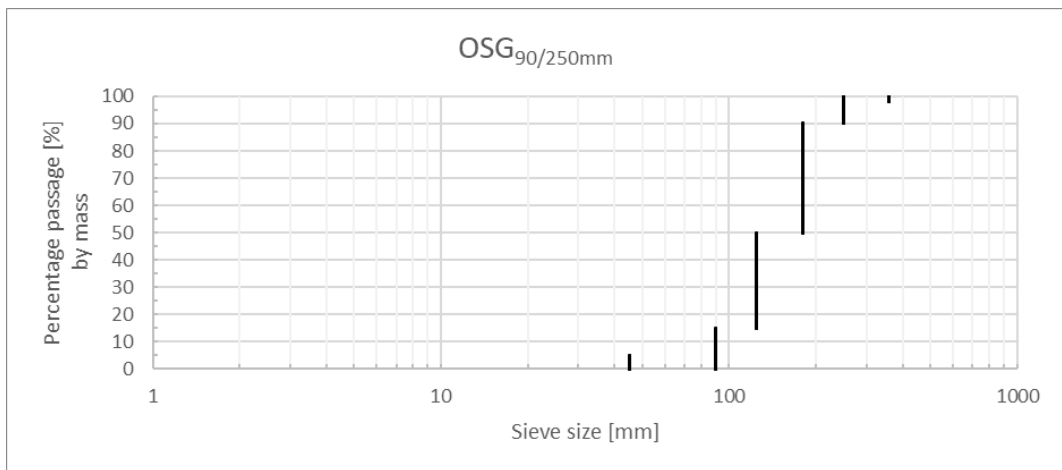


Figure 6.5 OSG<sub>90/250mm</sub> offshore sieved grading limits.

#### 6.4.2 Offshore Weighted Gradings

The standard Offshore Weighted Gradings defined in framework of the JIP HaSPro are:

- OWG<sub>2/20kg</sub>
- OWG<sub>5/40kg</sub>
- OWG<sub>10/60kg</sub>
- OWG<sub>15/120kg</sub>
- OWG<sub>40/200kg</sub>
- OWG<sub>60/300kg</sub>

Offshore Weighted Gradings are defined by the percentage passing (by mass) a particle weight. Sizes may thus vary depending on the rock density. The grading designation is based on the 10% and 70% passing limits. Other gradings can be declared by the producer (OSW<sub>declared</sub>). The requirements of the weight distribution of standard Offshore Weighted Gradings are defined in Table 6.5. The gradings are visualized in Figure 6.6 to Figure 6.11. In addition to the gradings below, alternative gradings may be specified as well.

Table 6.5 Offshore weighted grading armourstone limits. By percentage passage of particle weight.

Offshore Weighted Gradings	OWG <sub>2/20kg</sub>	OWG <sub>5/40kg</sub>	OWG <sub>10/60kg</sub>	OWG <sub>15/120kg</sub>	OWG <sub>40/200kg</sub>	OWG <sub>60/300kg</sub>
M <sub>50min</sub> [kg]	7	14	27	53	101	149
Rock weight [kg]	Percentage passing (by mass)					
450	-	-	-	-	-	97 to 100
300	-	-	-	-	97 to 100	70 to 100
236	-	-	-	-	-	50 to 90
200	-	-	-	97 to 100	70 to 100	-
152	-	-	-	-	50 to 90	-
149	-	-	-	-	-	10 to 50
120	-	-	97 to 100	70 to 100	-	-
101	-	-	-	-	10 to 50	-
86	-	-	-	50 to 90	-	-
80	-	97 to 100	-	-	-	-
60	-	-	70 to 100	-	-	0 to 10
53	-	-	-	10 to 50	-	-
47	-	-	50 to 90	-	-	-
40	-	70 to 100	-	-	0 to 10	-
38	97 to 100	-	-	-	-	-
30	-	-	-	-	-	0 to 2
28	-	50 to 90	-	-	-	-
27	-	-	10 to 50	-	-	-
20	70 to 100	-	-	-	-	-
15	-	-	-	0 to 10	0 to 2	-
14	50 to 90	10 to 50	-	-	-	-
10	-	-	0 to 10	-	-	-
7	10 to 50	-	-	-	-	-
5	-	0 to 10	-	0 to 2	-	-
2	0 to 10	-	0 to 2	-	-	-
1.5	-	0 to 2	-	-	-	-

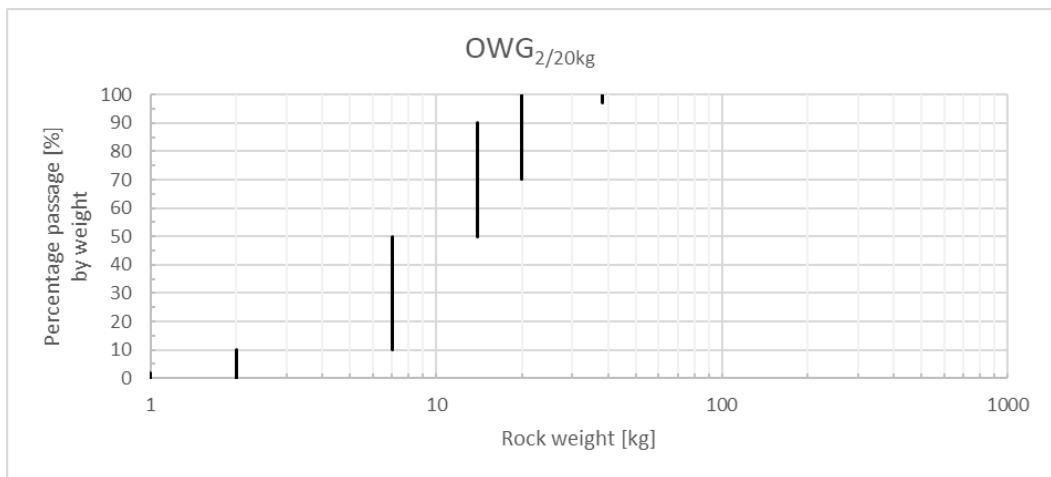


Figure 6.6 OWG<sub>2/20kg</sub> offshore weighted grading limits.

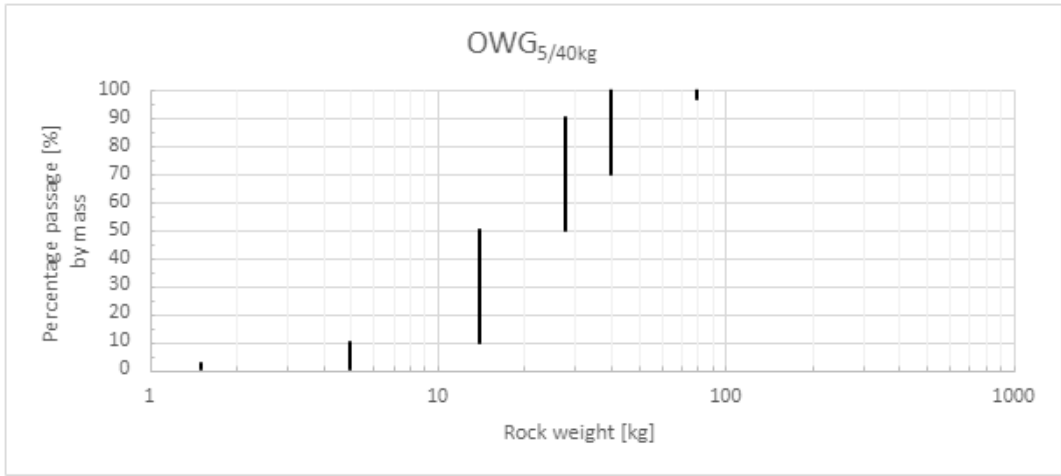


Figure 6.7 *OWG<sub>5/40kg</sub> offshore weighted grading limits.*

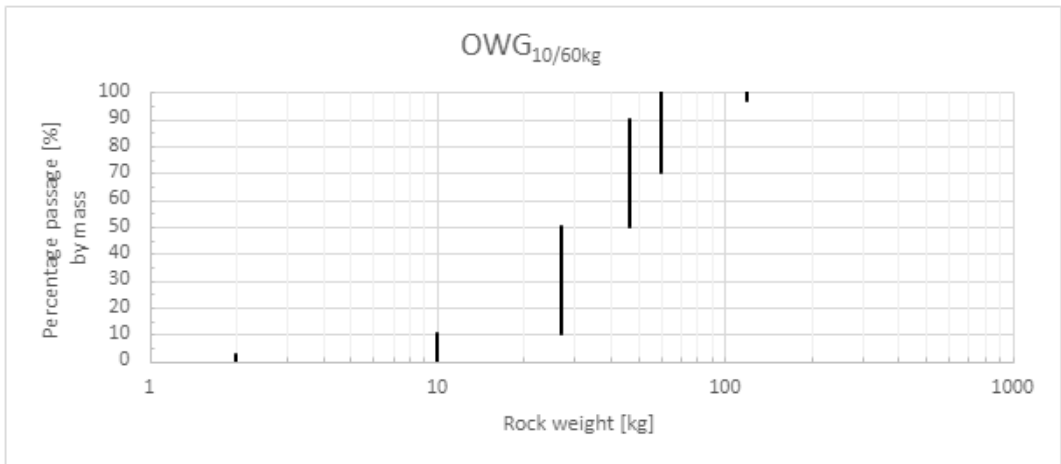


Figure 6.8 *OWG<sub>10/60kg</sub> offshore weighted grading limits.*

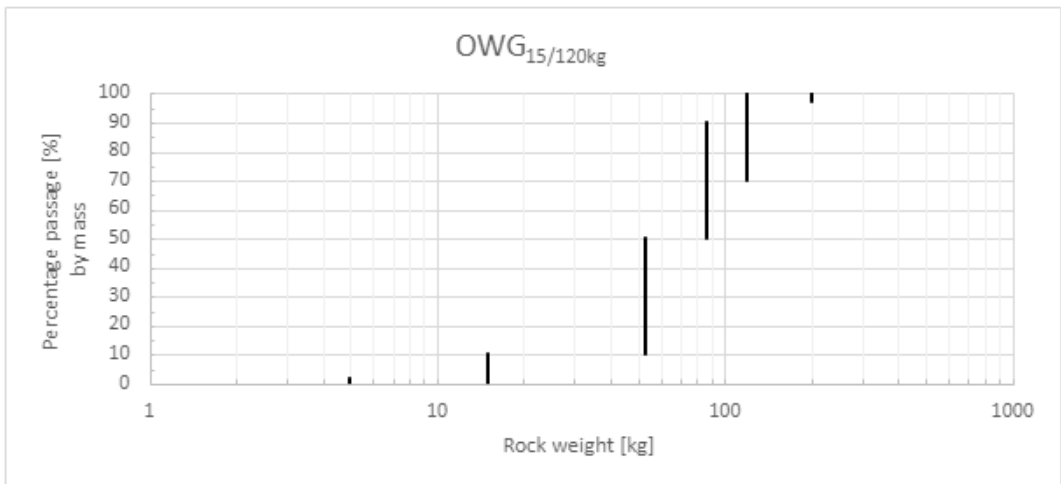


Figure 6.9 *OWG<sub>15/120kg</sub> offshore weighted grading limits.*

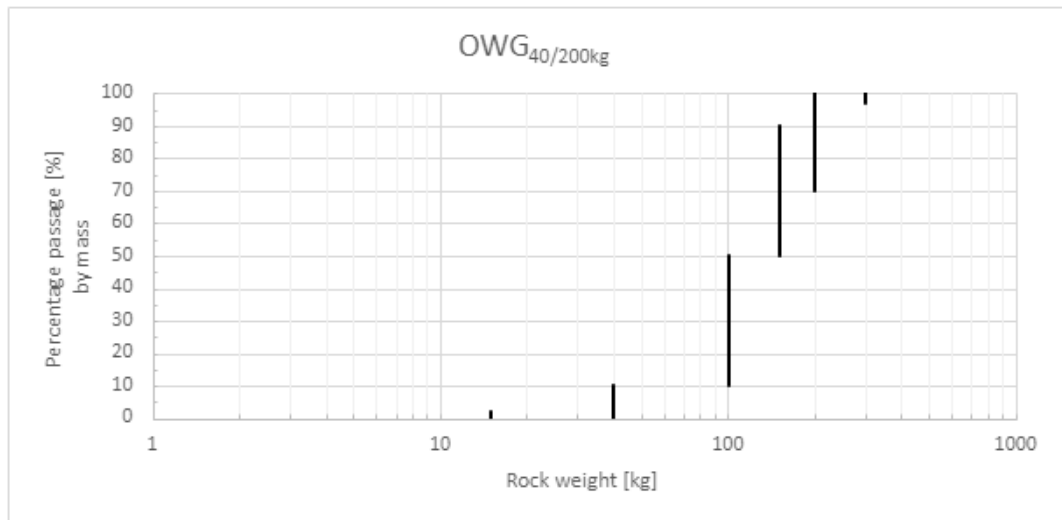


Figure 6.10 OWG<sub>40/200kg</sub> offshore weighted grading limits.

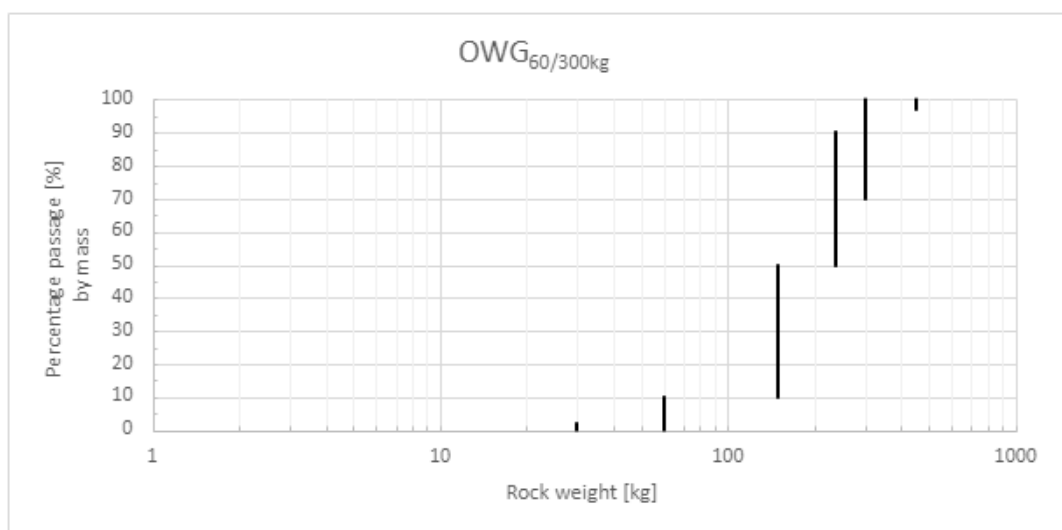


Figure 6.11 OWG<sub>60/300kg</sub> offshore weighted grading limits.

## 6.5 Material properties & testing procedures/methods

### 6.5.1 General

Rock material properties and associated test procedure and methods form an integral part of scour protection design. The description of the required rock material properties and the methods and procedures to verify these are included in the European standard for armourstone 'EN 13383-1:2013' and 'EN 13383-2:2019'.

The European standard for armourstone 'EN 13383-2:2019 Armourstone – Part 2: Test methods' provides guidance for rock material properties and test method specifications. The EN 13383 considers rock for many different applications (civil works, coastal structures, offshore). Only the properties/requirements mentioned in EN13383 considered relevant for offshore scour protections and rock berms (cable protection) are addressed in subsections below.

### 6.5.2 Geometrical requirements

The *particle size distribution* is an important parameter of the produced rock. The EN13383 provides the requirements for standard gradings (also summarized in Section 6.3). Section 0 provides additional Offshore Gradings applicable for scour protection/cable berm protection. A rock grading

can also be a mix of different gradings, engineered specifically for the project. It is important for any grading that the requirements reflect the design parameters properly and that testing of the grading can be done at the quarry in a practical manner.

For testing the size distribution, reference is made to the EN standards. A summary of the samples and test specimen is given in Table 3.19 of the Rock Manual.

To have a proper set of rocks to perform the test, the sample needs to be taken at the most representative moment. Preferably the sample should be taken directly from production (e.g. from the conveyor belt) to have the most representative sample. However, if rehandling of rock will take place once or several times within the quarry, samples will need to also be taken from the stockpile. Should segregation have occurred within the stockpile, rock shall be mixed again in order to obtain the correct grading. Procedures for testing and taking samples are described in the EN 13383-2 and will not be discussed further.

The *shape of the particles* is relevant for installation considerations. Odd-sized particles may block conveyor belts or chutes during loading or get stuck in fall pipes during installation by vessels. Tests need to be carried out simultaneously to the grading tests to identify the amount of flat/odd shaped rocks. Category  $LT_A$  of EN13383 is usually applied.

The *proportion of crushed or broken surfaces* is relevant for design considerations if the rock fulfils a stability requirement, which is the case for scour protection designs. According to EN 13383, category  $RO_5$  is then required, but the Rock Manual suggests specifying this only when naturally rounded boulders of riverine or glacial origin are used. Where rock is produced by crushing a solid rock face, the entire amount of rock will consist of crushed or broken surfaces thus the requirement for broken or crushed surfaces does not need to be checked.

### 6.5.3 Physical requirements

The *particle density* is an intrinsic property of the rock. Low density rock is less durable. The EN 13383 provides a minimum density of  $2300 \text{ kg/m}^3$  while the Rock Manual considers such rock as poor in terms of quality and durability. It is recommended that rock density is at least  $2500 \text{ kg/m}^3$  and that the effects of density are considered by the designer during the design stage (see Section 0).

For density tests, the EN13383-1 describes that 10 rocks shall be tested and if the average density of these rocks is equal to or larger than the specified density, the rock meets the requirement. If not, an extra 30 rocks shall be tested to come to a total of 40 rocks. 36 of the 40 rocks need to be equal or larger than the 'specified density –  $100 \text{ kg/m}^3$ '. If this criterion is passed, the rocks meet the requirement for the density. If this requirement is not fulfilled, the density is considered too low.

*Resistance to breakage* is a parameter that is important for handling and installation, as breaking of rocks may lead to different (and deteriorated) gradings. Resistance to breaking is validated by compressive strength tests with tests being done in the planar direction of the most pronounced layering should there be one visible. Category  $CS_{60}$  is considered the minimum in order to have rock that has a good resistance to breakage.

*Resistance to wear* is required as the armourstone is exposed to an abrasive environment. The Micro Deval  $M_{DE20}$  is used as standard value.

### 6.5.4 Durability requirements

A low *water absorption value* generally means good durability, and good resistance to freeze and thaw. This value is not relevant for rock that always stays underwater (refer to Annex C of EN 13383), but possible deterioration during transport and logistics must be considered as well. Typically, a value of 2% is given. According to the EN standards, if the absorption is less than 0.5%

( $WA_{0.5}$ ), then the rock is assumed to be resistant to freezing and thawing and salt crystallization. Rock with high water-absorption rates may possibly be used as well, but the scour protection must never be exposed to air (which can only happen at very shallow locations).

### 6.5.5 Additional requirements

Bulk density is not a parameter that is related to the quality of the rock and thus not required as design input value. However, a value for the bulk density may be important for procurement and commercial discussions as a volume of rock needs to be installed and in general rock will be purchased in tons. Often transport is limited by the weight of the rock as well. Therefore, it is important to know the bulk density to estimate the amount of sailing trips. It is therefore recommended to perform bulk density tests specifically for a project.

### 6.5.6 Conclusion

The most relevant properties for offshore scour protections rocks are summarized in the Table 6.6 below. For reference, the commonly applied values for these properties are also given. These values should not be mistaken for minimum requirements (thus seen as “standards”) as these should always be determined based on the specific project circumstances.

Table 6.6 Relevant properties for offshore scour protections.

Property	Test standard	Commonly applied value
Grading (mass distribution)	EN 13383-2: 2019	Refer to section 6.3 and 6.4 Ad hoc gradings can also be applied by the designer if these are validated
Type of rock	-	Crushed rock produced with crusher (should river rock be used, designer to validate the design)
Shape	EN 13383-2: 2019	$LT_A \leq 20\%$ of stones with $l/d > 3$
Density	EN 13383-2: 2019, Clause 8	$\geq 2500 \text{ kg/m}^3$
Water absorption	EN 13383-2: 2019, Clause 8	$\leq 2 \%$
Compressive strength	EN 1926: 2006 (Annex A)	CS60 $> 60 \text{ N/mm}^2$
Micro Deval (abrasion)	EN 1097-1:2011	$M_{DE20}$ $< 20\%$ Loss of Material

## 6.6 Quarry operations

For production of the scour protection materials different production processes are possible. The process depends on the production setup of each quarry, the geology, blasting method and the rock grading(s) to be produced. The following describes the production processes for Offshore Sieved Gradings (OSG) and Offshore Weighted Gradings (OWG).

### 6.6.1 Production process Offshore Sieved Gradings (OSG)

The main production process method for Offshore Sieved Gradings is shown in Figure 6.12. The process starts with drilling and blasting of the rock. The blasted material is processed through a primary crusher, feeding a screen where the Offshore Sieved Gradings are sieved out. After stockpiling the various gradings will be tested and loaded on installation vessels.

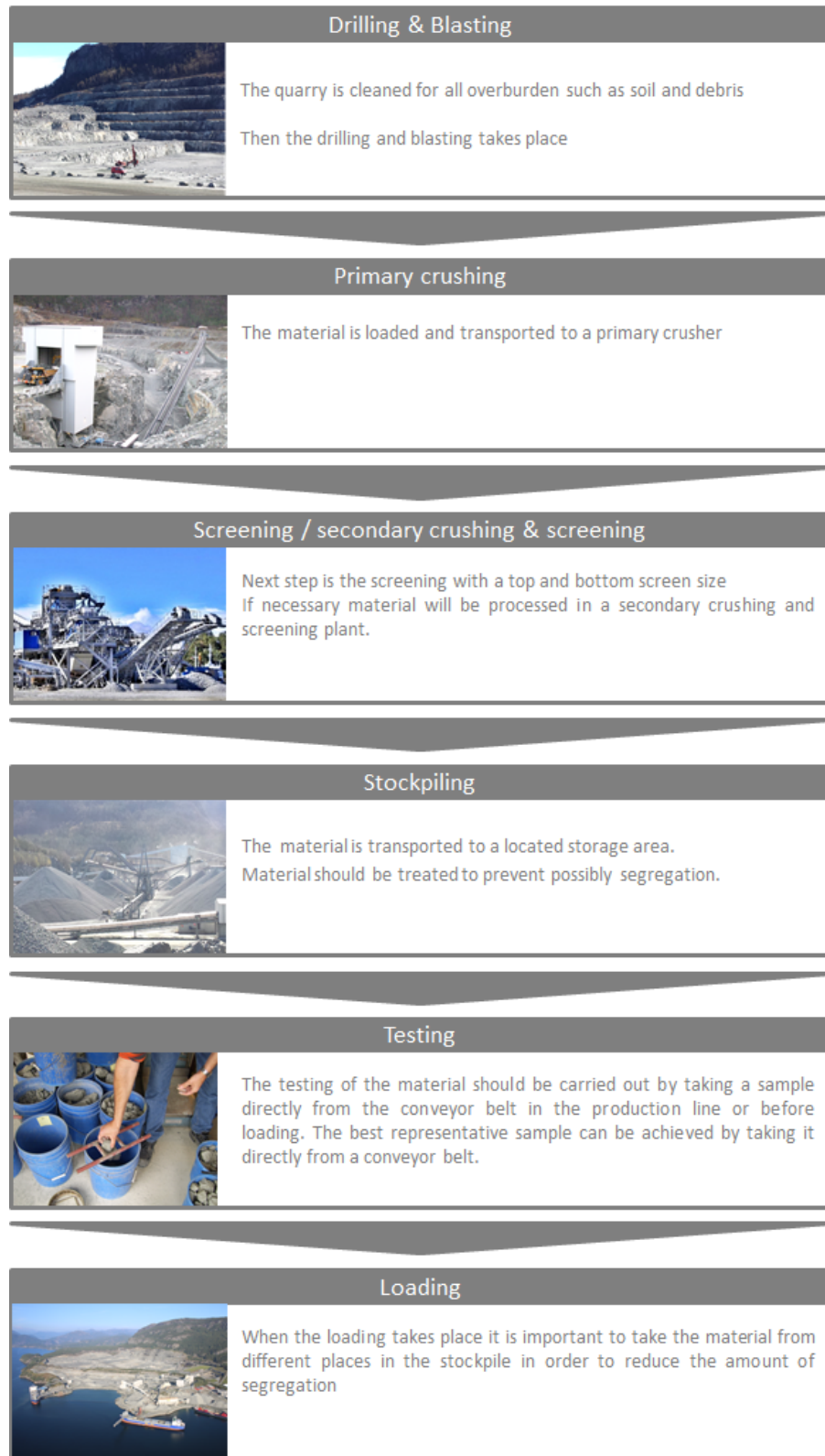


Figure 6.12 Production process of Offshore Sieved Gradings (OSG).

Depending on quarry size and crusher output, OSG gradings can be produced with a variable capacity and volume, depending on grading, size, production, setup and sales situation in the quarries.



### 6.6.2 Production process Offshore Weighted Gradings (OWG)

The production process for Offshore Weighted Gradings will depend on the rock sizes, geology, blasting method and the quarry processes. Two different methods are shown in Figure 6.13.

Production process OWG – 1, starts with drilling and blasting, similar to the OSG grading process. The material goes through a crusher and the materials are screened using a mechanically operated screen. After stockpiling the material will be tested prior to loading, after which it will be loaded. This process is mainly used for the smaller 2-20 kg, 5-40 kg and 10-60 kg rock armour gradings.

Production process OWG – 2, starts either with selection of rocks from the blast face (in an aggregates quarry) or selection of larger rocks (dimension stone quarry). At an aggregates quarry, the rocks will be selected by an excavator or other mechanical machine and taken to a static (Grizzly) or mechanical (drum) screen for processing.

In a dimension stone quarry, the selected material will be crushed down with a hydraulic hammer. The rocks will then be taken to a static (Grizzly) or mechanical (drum) screen for processing. For the heavy rock armour (rock armour larger ~1000 kg or larger) the material will be sorted out by weighing each stone. The smaller (LMA) grades will be stockpiled and tested before loading. Materials like 15-120 kg, 40-200 kg, 60-300 kg and 300-1000 kg will be sieved out.

The sieve diameter of the grizzly/drum needs to be carefully made depending on the density of the material and the permissible l/t parameters.

OWG gradings can be produced with a variable capacity and volume up to 10,000 tons per week, depending on: grading, number of gradings ordered (i.e., can the quarry get 'full production'), production, setup and sales situation in the quarries.

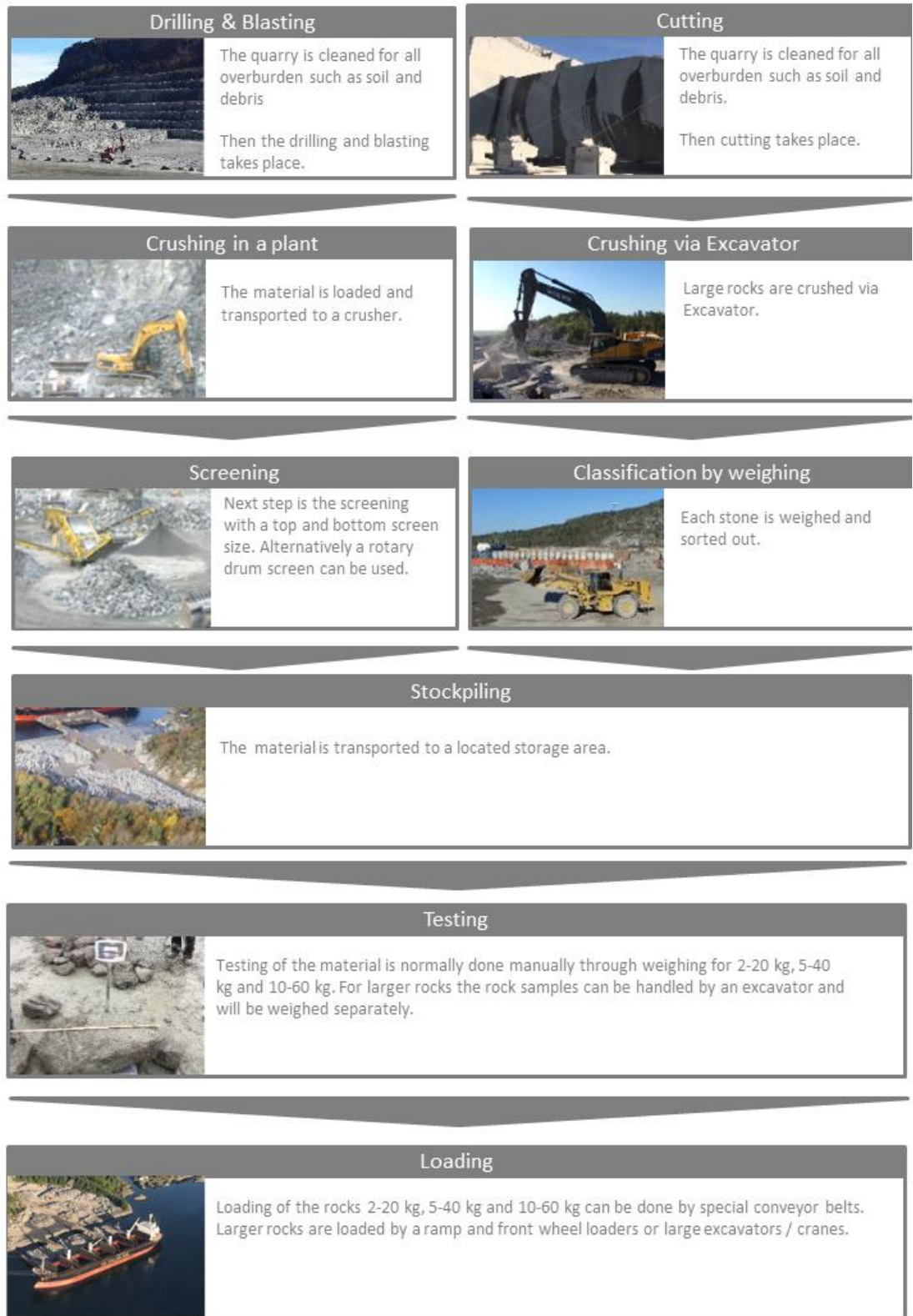


Figure 6.13 Production process OWG.

## 6.7 Handling of gradings in installation steps

Since a rock grading consists of rocks with different sizes, it will always have the tendency to segregate. It is important to minimize the segregation and keep the grading of the material as constant as possible, to fulfil after installation the design requirements as specified in Chapter 4. Attention must be paid to the handling process in the quarry and during the transportation and installation process.

When the material is produced and placed in a stockpile at the production site, the material is preferably stored in layers of limited height. Likewise, when the material is loaded onto a vessel the front wheel loader (excavator) feeding the conveyor belt should take the material from random areas of the stockpile. During loading of the vessel, the rocks need to be evenly distributed over the holds. This can be done by continuously moving the loading belt transversely across the holds, whereas the vessel moves in the longitudinal direction. Simultaneously, the vessel excavators (if any) can actively distribute and level the material in the holds. When discharging the material at location, the operator of the excavator should randomly pick up the material in the vessels hold in order to get a uniform material flow.

# 7 Rock scour protection installation

## 7.1 Introduction

Rock scour protection of wind farm foundations can be installed with different types of vessels. These vessels and their specific capabilities are described in Section 7.2. The type of equipment to be used is dependent on the rock size and the installation sequence. The required (armour) rock grading of the scour protection determines whether the scour protection can be pre-installed before the foundation installation i.e., whether the monopile foundation can be driven through the scour protection or whether the (armour) rock grading should be installed afterwards. It therefore determines whether a vessel can move freely for rock installation or whether it should manoeuvre around the foundation. Section 7.3 describes the possible installation sequences and the preferred types of equipment for each sequence or part of the installation.

The installation of the foundation and the inter array cables influences the rock installation and vice versa. In Section 7.4 the interfaces between foundation and cable installation and rock installation are described. The interfaces which influence the design of the scour protection have been described in Chapter 4.

The installation of the scour protection has to be verified against the design requirements; this verification is performed with offshore surveys by means of a multibeam echo sounder. A detailed description of the survey equipment, calibration and execution is described in Section 7.5. The results of these surveys are generally provided in a 0.2 m grid. For the evaluation of the rock installation by means of the survey data, tolerances will need to be defined. The accuracy of rock installation will depend on the rock grading and method of installation. The tolerances will need to be defined based on what is practically achievable without compromising the design requirements. Guidance on how to define tolerances for scour protection and cable crossing rock berms is described in Section 7.6.

## 7.2 Rock Installation Equipment

Different types of vessels can be used for subsea rock installation. The size of the rock, the installation requirements and the sequence of installation determine which type of equipment can be applied.

### 7.2.1 Fallpipe vessel

A fallpipe vessel is a self-propelled dynamically positioned vessel that is used to install rock on the seabed. The fall pipe can be lowered below or on the side of the vessel. A remotely operated vehicle (ROV) is positioned at the bottom of the fallpipe and is used to accurately position the fallpipe (at a height of approximately 5 m) above the seabed. Moreover, it serves as a platform for survey sensors. Examples of a ROV are shown in Figure 7.1 and Figure 7.2.

The rock size is limited by the diameter of the fallpipe and the rock transport system on the vessel. In general, various coarse gradings consisting of crushed rock can be installed with a fallpipe. The minimum operational water depth depends on several factors that have to be assessed prior to the start of the rock installation activities. An indicative lower limit for the operational water depth is approximately 15 m.

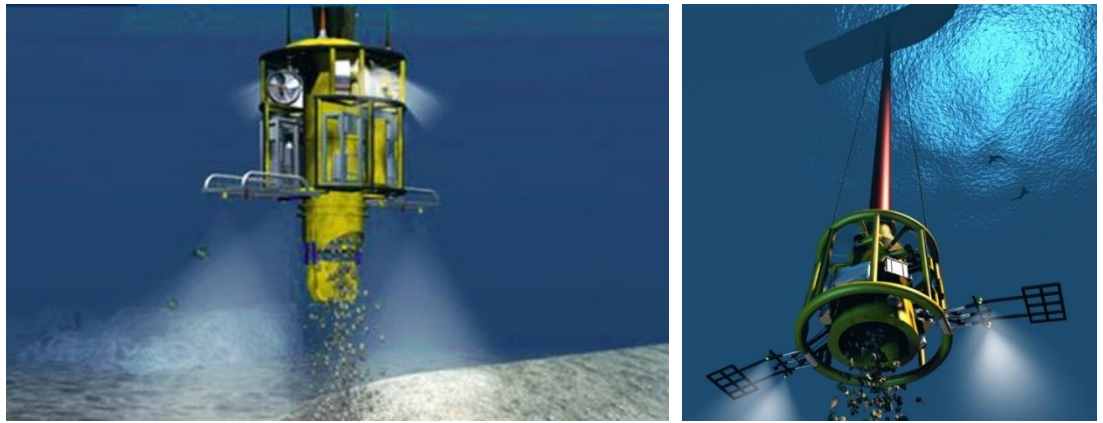


Figure 7.1 Fallpipe ROV (courtesy of Van Oord (left) and DEME Offshore (right)).



Figure 7.2 Fallpipe ROV (courtesy of Jan De Nul).

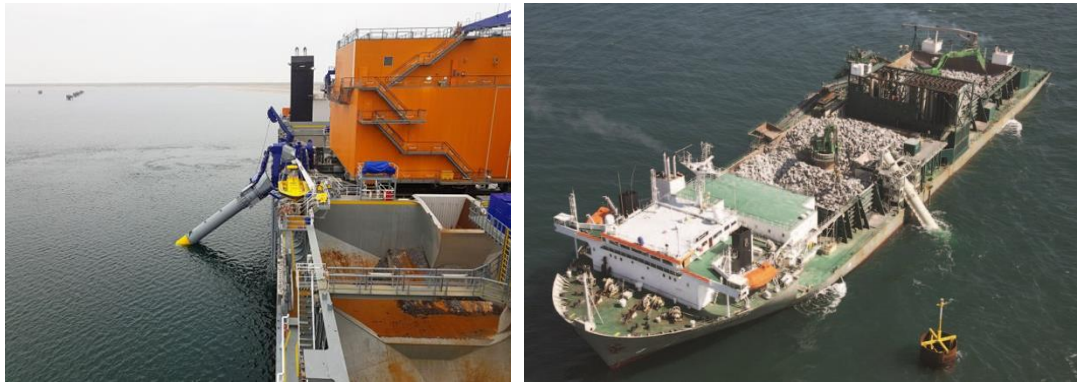


Figure 7.3 Vessel with inclined fallpipe (courtesy of Van Oord (left) and Boskalis / DEME Offshore (right)).

An inclined fallpipe or tremie pipe can be used in case of close-proximity operations and for rock gradings exceeding the operational limits of conventional fallpipes. The inclined fallpipe is deployed over the side of the vessel and various configurations are possible with regards to its length and angle. Accurate rock installation is possible by movement of the pipe and pre-set rock output within the working envelope, i.e., the required rock volume within the designed footprint. Examples of vessels equipped with inclined fallpipes are shown in Figure 7.3 and Figure 7.4.



Figure 7.4 Vessel with inclined fallpipe (courtesy of Jan de Nul).

Typically, the rock material is loaded into the cargo-holds of the fallpipe vessel at a quarry by means of conveyor belts (Figure 7.5). Most fallpipe vessels have multiple cargo-holds and provide the capability to carry several different rock gradings in one trip.



Figure 7.5 Typical loading site (courtesy of DEME offshore).

Upon arrival of the vessel at the site, a pre-installation survey can be executed. This is typically done with the hull or ROV mounted survey sensors. The pre-installation survey will provide the profile of the installation area. This survey is used as the basis for the rock installation plan and the acceptance of the rock installation results.

The build-up of the rock profile depends on the actual material flow (tons per hour) in combination with the tracking speed of the vessel (meters per second). The installed quantities are controlled and monitored on board of the vessel. After the completion of the rock installation operations a post-installation survey is performed.

### 7.2.2 Side Stone Installation Vessel

Side Stone Dumping Vessels (SSDV, Figure 7.6) are sea going and self-propelled with a strong reinforced deck divided in bays. Rock can be loaded onto the deck and dozer blades are used to gradually push the rock over the side(s) of the vessel. The SSDVs can handle many different rock types and sizes from small diameter crushed rock or gravel to large boulders weighing several tons each. A SSDV can be used in shallow water conditions and for close proximity operations. The SSDV is also equipped with a multibeam echosounder which is used for the pre and post installation surveys.



Figure 7.6 Side Stone Installation Vessel (courtesy of Van Oord).

The vessel's position can be accurately controlled either by means of a dynamic positioning system or manually. The heading and position for the rock installation depends on the prevailing environmental conditions (wind, waves and current). ADCP monitoring instrumentation, which is mounted in the hull, can be used to indicate the current velocity and direction. The vessel position is adjusted based on the actual current profile.

Ideally, the rock is installed with low currents to reduce the deflection and segregation of rock material. Installation with an SSDV has a risk that rock will be carried by the current and deflected away from the intended rock profile, especially when a rock grading consists of a high amount of finer rock. The minimum possible installation profile depends on the width of the bays, the orientation angle of the vessel in relation to the intended rock berm, and the position of the rock material inside the cargo holds.

The output quantity depends on the shoveling speed of the cargo bays. Furthermore, the installed volume along the profile depends on this shoveling speed combined with the tracking speeds of the vessel. An excavator can be positioned in one of the cargo bays and can be used for accurate spot installation or levelling activities in case high precision is required. SSDVs are typically shallow draft vessels.

### 7.2.3 Crane vessel

Another option is to install rock with a crane vessel (Figure 7.7). Ideally, a DP vessel is used for operations around foundations. Moored barges are however also an option if the foundation is not yet installed or for the installation of a rock berm. Spud barges can also be considered but can be unfavorable because of the seabed disturbance by the spuds. Rock installation with a barge is typically preferred in the following situations:

- at very shallow locations, often requiring a large armour rock grading
- at locations that are difficult to reach
- in case accurate spot installation is required.



Figure 7.7 Crane Vessel (courtesy of Van Oord)

#### 7.2.4 Workability

Limiting wave heights for rock installation equipment are shown in Table 7.1 below. These values are generally applicable, but the workability also depends on the wave period (short crested wind waves or swell), current velocity and the scope of work. If rock is installed close to a foundation, working in a so-called “blow on situation<sup>1</sup>” poses a higher risk and hence reduces the workability. For fallpipe equipment that uses wires, a limiting factor is the launch and recovery through the splash zone. This results in the highest loads on the wires which increase with the length of the fallpipe. For a tremie pipe or inclined fallpipe the installation water depth will be limited by the length of the fallpipe.

The ultimate limiting significant wave height is to be under the discretion of the captain.

Table 7.1 Indicative limiting wave heights for rock installation

Type of vessel	Operational mode	Limiting wave height, $H_s$ [m]
Fallpipe vessel	Fallpipe	3.5-6.0
Fallpipe vessel	Inclined / tremie pipe	1.5-3.5
Side stone installation vessel	Dumping	1.5
Crane barge	Placing	0.5

### 7.3 Installation sequence

For the installation of the scour protection different sequences are possible in relation to the foundation installation. The preferred sequence depends on the possibilities related to the required rock grading and the type of foundations. The installation sequence of a cable crossing rock berm is described in the last paragraph of this section.

A pre-installation and post-installation survey are performed before and after the installation of rock. The difference between the two surveys shows the installed layer thickness and rock volume and is used to verify whether the design criteria are met. Intermediate surveys can be performed between installation of rock layers to monitor progress.

<sup>1</sup> The so-called “blow on” is the situation where the direction of current and wind results in a net force towards the structure.



In the following sections, several rock installation sequences are described relative to the foundation installation.

### 7.3.1 Preinstalled filter- and armour layer

The first option is to install a filter layer and armour layer and install the foundation afterwards (Figure 7.8). It ensures that the scour protection provides full protection immediately after pile installation. Secondly, the rock installation and pile installation scopes can be executed independently. The concept however is only feasible in case the armour grading and thickness are small enough to drive through the foundation. For certain armour gradings, the complete rock installation can be executed by fallpipe. This method is also applicable for single grading scour protection designs.

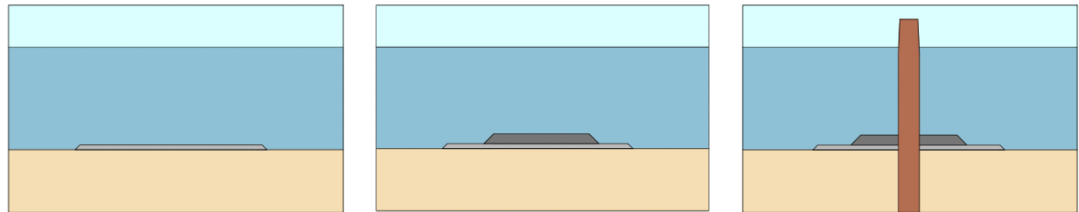


Figure 7.8 Installation sequence pre-installing filter (left), followed by armour (middle) after which the pile is installed (right).

### 7.3.2 Preinstalled filter layer and post installed armour layer

A second possibility is to first install the filter layer, then the foundation and finally install the armour at a later stage (Figure 7.9). This concept requires a split of the scour protection installation sequence: the filter layer will be preinstalled and needs to survive the wave and current actions occurring during the period between the filter installation and the installation of the armour layer. After pile installation the load on the filter layer is increased due to the flow amplification around the foundation. An additional survey of the filter layer just before the armour layer installation is required to verify the condition of the filter layer and to serve as reference for the thickness of the installed armour layer

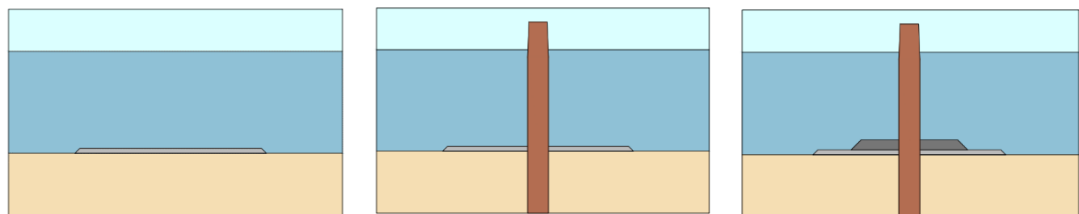


Figure 7.9 Installation sequence pre-installing filter (left), installation of the pile (middle) followed by post-installation of armour rock.

An advantage is that the cable can be installed before armour installation and therewith the cable can be covered and protected by the armour rock. This installation sequence can also be applied for suction bucket and gravity-based foundations. For the latter, the filter layer may also serve as a bedding layer for the foundation. A disadvantage is that during armour installation, due to the close-proximity operations next to the foundation, the maneuverability and therewith the workability and production of the vessel are reduced. This means that this installation sequence is at a higher risk of enduring weather delays and will affect the accuracy and duration of the armour rock placement. Depending on the project requirements, vessels with DP capabilities may be required for close proximity operations. For jacket foundations another disadvantage is that it is difficult or not feasible to install armour rock below/inside the structure.

### 7.3.3 Post installed filter and armour layer

The final possibility is to first install the foundation and at a later stage the scour protection rock layers (Figure 7.10). With this installation sequence, it is likely that some scouring will occur to the seabed around the foundation between the time of foundation installation and the scour protection installation. This installation sequence is especially used in situations with extreme hydrodynamic conditions: Rocks are installed in a pre-developed scour hole, lower in the water column in a sheltered position. This improves the rock stability in storm conditions. Figure 7.10 shows a double-layer scour protection installed in the scour hole; as discussed in Section 3.2.3 it is usually preferred to install a single-layer design in an already developed scour hole, as installing multiple layers can be challenging due to the presence of steep slopes.

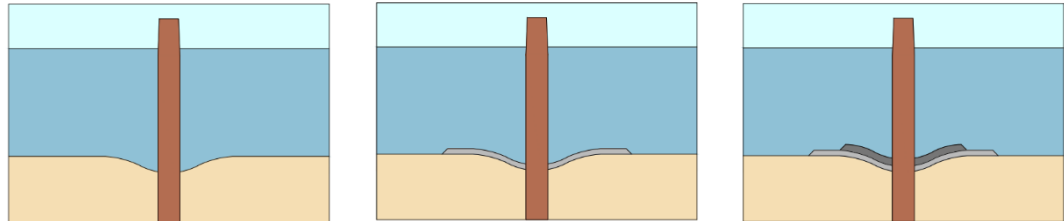


Figure 7.10 Installation sequence first installing the pile and allow scour development (left), followed by installation of the filter (middle) and armour rock (right).

Predictions of the scour development are required to estimate the moment of rock installation and the required rock volume in case a certain rock level must be guaranteed. At the time of the scour protection installation, a survey of the scour hole needs to be performed to determine the exact amount of rock to be installed as it is difficult to estimate the required amount of rock beforehand. In case the seabed design level of the foundation is close to the anticipated scour depth, the design rock layer thickness can be applied, and this uncertainty can be mitigated.

For this installation sequence, the rock is usually installed either by inclined fallpipe (tremie pipe), a side stone installation vessel or grab vessel with DP capabilities, because a safe distance between the vessel and the foundation is required. Again, for jacket foundations rock installation underneath/inside the structure will be difficult or impossible.

### 7.3.4 Cable crossing rock berms

The sequence of installation of a cable crossing rock berm is dependent on the burial depth of the existing pipeline or cable and the required separation between the latter and the new cable. In case the burial depth of the existing line is less than the required separation distance, then a separation rock layer is required before cable installation. This layer should be stable during the period in between the cable installation and the installation of its cover layer. The cable cover can consist of just armour rock if the impact remains within the limits of the cable. Otherwise, a cushion layer needs to be installed first to reduce the impact from installing the armour rock on the cable.

Figure 7.11 includes several cross sections for a rock berm design with a cable at different heights relative to the seabed level ( $z_{sbl}$ ). In this figure “TOPC” stands for Top of product cover, the width at the top of the berm is defined with “w” and the depth of lowering of the cable into the seabed is defined as “ $z_{dol}$ ”.

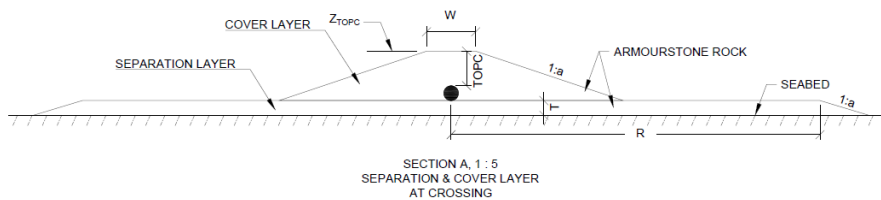
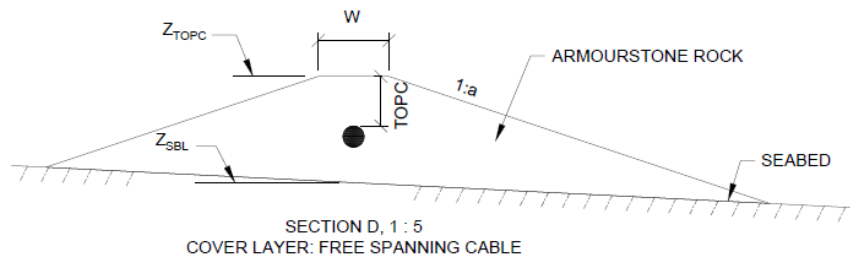
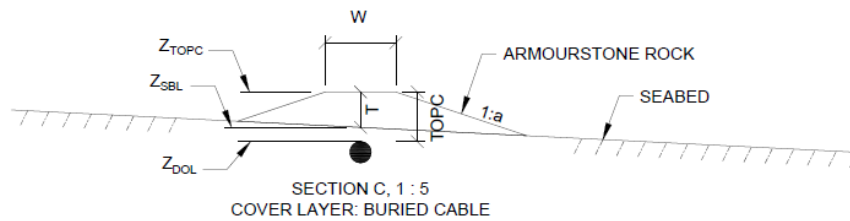
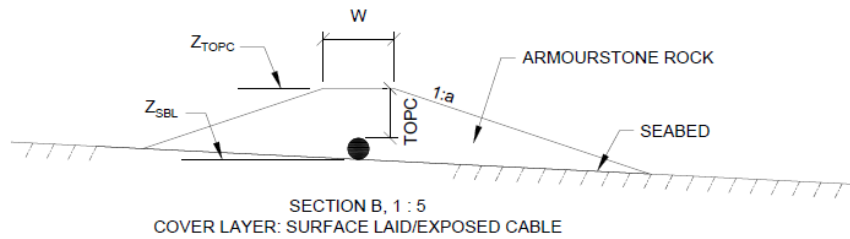


Figure 7.11 Crossing designs for various situations.

If the water depth is sufficiently large, all different types of installation equipment can be applied for cable crossing rock berms. However, the maximum allowable impact of the rock on the subsea assets needs to be verified for the type of equipment used.

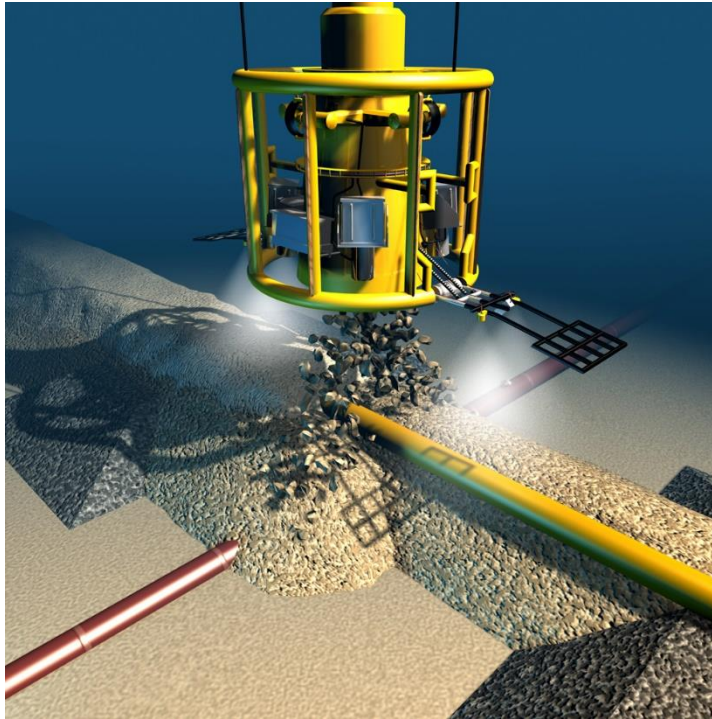


Figure 7.12 Example of cable crossing rock berm installation (Courtesy of DEME Offshore).

### 7.3.5 Cable Protection System stabilization

Depending on the CPS and cable properties and the maximal possible cable elevation, a certain free span is established between the structure and the touchdown point. In the CPS design, a fatigue and abrasion analysis are recommended to determine whether further stabilization of the CPS or cable is required. There are multiple options to offer stabilization visualized in the sketches of Figure 7.13.

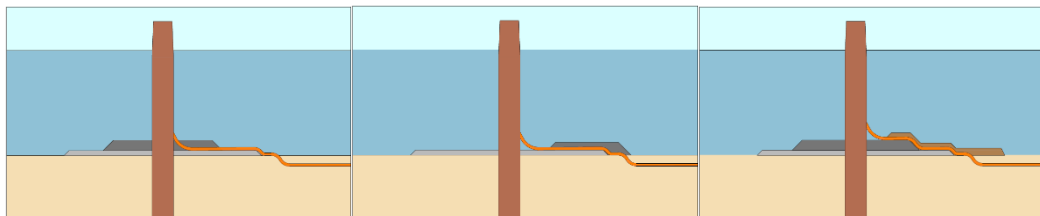


Figure 7.13 Left: Armour Layer to stabilize CPS / cable, middle and right: Separate rock berm to stabilize CPS / cable.

In case a double-layer scour protection strategy is opted, by means of a pre-installed filter and post-installed armour, the armour layer is often used to stabilize the CPS.

For pre-installed scour protections, the CPS / cable is placed on top of the scour protection and there might be a requirement to install additional rock to stabilize the CPS. Since this CPS rock berm will be in the vicinity of the monopile, additional loading due to flow enhancement around the foundation might be accounted for in the design of the rock cover. This depends on the distance of the touch-down point from the face of the monopile. In general, additional rock placed near the monopile will experience high flow amplification and is therefore less stable compared to rock placed further away. As edge scour increases with height of the scour protection, then the installation of a CPS berm on top of the scour protection may lead to increased edge scour. The CPS and cable can also be designed to be able to withstand the possible fatigue and abrasion over the operational lifetime. This topic is not part of the scope of this handbook.

## 7.4 Interfaces

In this paragraph several interfaces between scour protection installation and other wind farm installation/maintenance works are discussed. Nearly all rock installations have an interface with cables, either being a scour protection nearby a structure requiring rocks or a crossing between one or more cables.

### 7.4.1 Foundation cable entry

Cable installation commences typically after installation of the scour protection and foundation. There are several interfaces between the cable installation and the scour protection.

The connection of the cable with a structure such as a monopile or jacket typically consists of one of these solutions:

- A tubeless hang-off.
- A J-tube.

A tubeless hang-off, where the cable is entering the structure through a cable entry hole in the face of the structure (Figure 7.14). This solution requires suitable cable protection systems to reduce dynamic stress during service life of the cable. Common solutions are installation of a cable bend restrictor and a Cable Protection System (CPS).

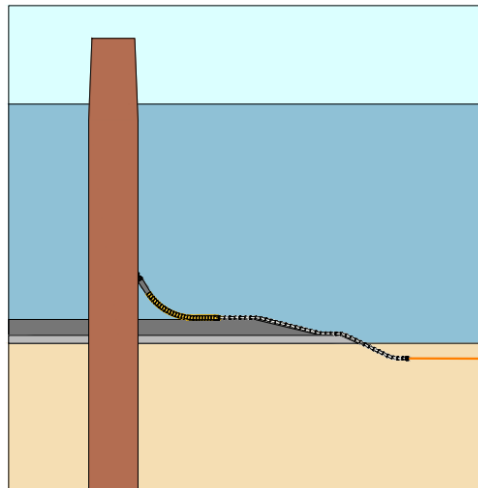


Figure 7.14 Tubeless cable hang-off system where the cable is entering the structure through a cable-entry hole.

Offshore structures such as jackets or monopiles can be equipped with J-tubes (Figure 7.15). A J-tube is made of steel or polymeric materials, reaching from the seabed up to the platform deck. The tube is open at the top and has a bell-mouth at the bottom end in order to guide the cable from the seabed into the tube. Depending on the design of the connection, a Cable Protection System (CPS) might be required to protect the cable until full burial into the seabed has been achieved.

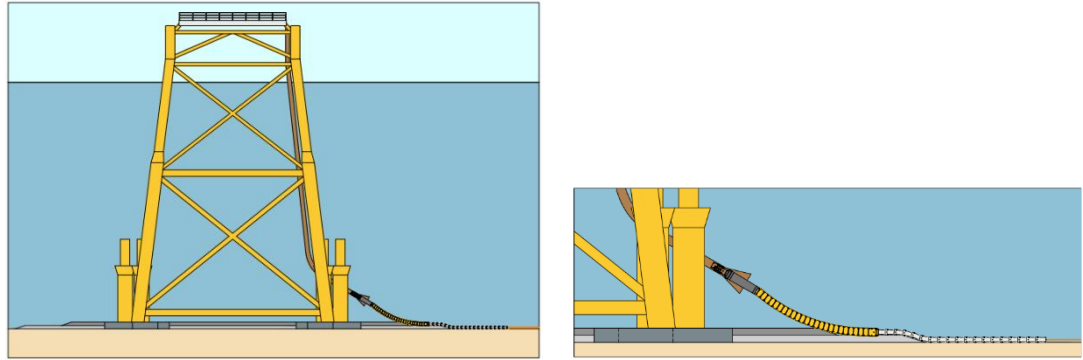


Figure 7.15 J-tube connection of the cable with the structure.

Both systems guide the cable to a certain height above the seabed or scour protection. Important in this interface is to establish the correct cable entry height or J-tube height above the scour protection. If the entry height is too low, then risk arises that the Minimal Bending Radius (MBR) might be violated during the pull-in operation. A too high entry height gives a risk for increased movement of the CPS / Cable which can cause fatigue, see also Section 7.3.5.

There are several parameters which can influence the cable height during installation (Figure 7.16):

- Vertical tolerance of the scour protection.
- Vertical installation tolerance of the foundation (typically +/- 0.1 m).
- Changes in seabed level due to morphological processes given that there is an uncertainty in the prediction of the seabed level at the time of installation.
- Maximum and minimum height of J-tube or cable entry. Typical this ranges in the order of 2 m to 4 m above the scour protection.

It is recommended to account for the vertical installation tolerances of the scour protection, see also Section 7.6, in the design of the cable interface. This is only applicable in the cable corridor.

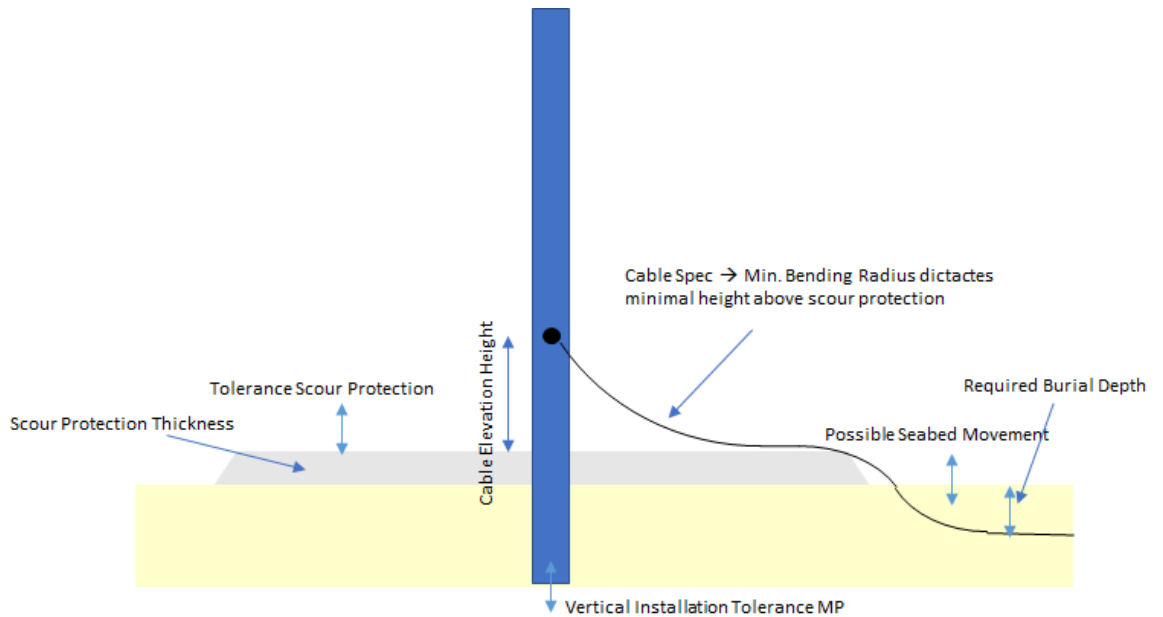


Figure 7.16 Definition sketch of the parameters influencing cable height during installation.

#### 7.4.2 Impact of falling rocks on the cable

When rock is installed directly on a cable, it is required to check the allowable amount of impact energy on the cable. The integrity of the cable during rock installation can be verified by ensuring that the impact of the largest rocks in a rock grading is below the allowable amount of impact on the

cable. This property can be derived during type testing according to CIGRE TB623. Preferably the cable should be designed to allow for rock impact. Guidance is available in the Rock Manual and DNVGL-RP-F107.

#### 7.4.3 Cable burial equipment

In order to reach the required burial depth of the cable, various specialized cable burial tools are deployed depending on the local seabed conditions and the burial depth. All solutions can be categorized with regards to the moment of burial as follows:

- Pre-trenching: dredging a sleeve before installation of a monopile or scour protection. Pre-trenching within the footprint of the scour protection should be avoided since it might lead to a disturbed distribution of rock material during the scour protection installation.
- Post-trenching. After installation of a monopile or jacket and after installation of a scour protection, a cable burial tool will bury the cable at the required burial depth. It is important to acknowledge the required distance of the burial tool with respect to the edge of the scour protection.

#### 7.4.4 Pile driving

In case a monopile is installed by means of pile driving, after the scour protection has been installed, there is an interface between the pile driving and scour protection. Firstly, it needs to be checked that the driving shoe (or lowest can) of the monopile is strong enough to prevent buckling when piled on the rocks. When the top layer of the pre-installed scour protection consists of large rocks (e.g. armour layer) this risk may be significant. Conversely, when the top layer consists of finer-grained material (e.g. filter layer) this risk is often minimal. If the scour protection material is finer than the regular boulders considered for the driving process, or if the self-weight penetration of the monopile will make it sink through the scour protection material before pile-driving commences, the risk of buckling is minimal. The pile drivability through the scour protection depends on several factors like pile wall thickness, pile diameter, local soil conditions, rock sizes and layer thickness of scour protection and hence an assessment is required on a project-by-project basis.

Another risk is the so-called “punch through”. This is when the monopile stands on the scour protection and then suddenly drops through a soft seabed layer underneath. This poses a risk for the controlled installation of the foundation and might affect the integrity of the piling process.

Furthermore, it has been observed that due to the vibrations and friction with the monopile during driving, a depression of the scour protection might occur near the monopile face. This means that the top of the scour protection could be lowered, without reducing the number of installed rock layers. One can question if this a problem for the functioning of the scour protection, because the rocks are still in place, covering the seabed close to the foundation.

#### 7.4.5 Noise mitigation systems

To limit noise during monopile driving, several noise mitigation systems can be used. Figure 7.17 shows some common methods, including:

- Noise-insulating sleeve or system around the pile during piling.
- Bubble curtain around the pile during installation.
- Installation with reduced piling energy.

The sleeves or systems that can be placed around the pile during piling, often are standing on the seabed or -when the scour protection is pre-installed- on the scour protection. These systems therefore do have an interface with the scour protection when the scour protection is installed before the monopile. When the noise mitigation system has a large weight, its footprint can cause an indent

in the scour protection when lifted onto it, see Figure 7.18. This imprint depends on the sleeve footprint, sleeve weight, landing impact and grain size of the scour protection.

Bubble curtains and installation with reduced piling energy have minimal interfaces with the scour protection and hence are more favourable noise mitigation measures when the scour protection is installed prior to the foundation.

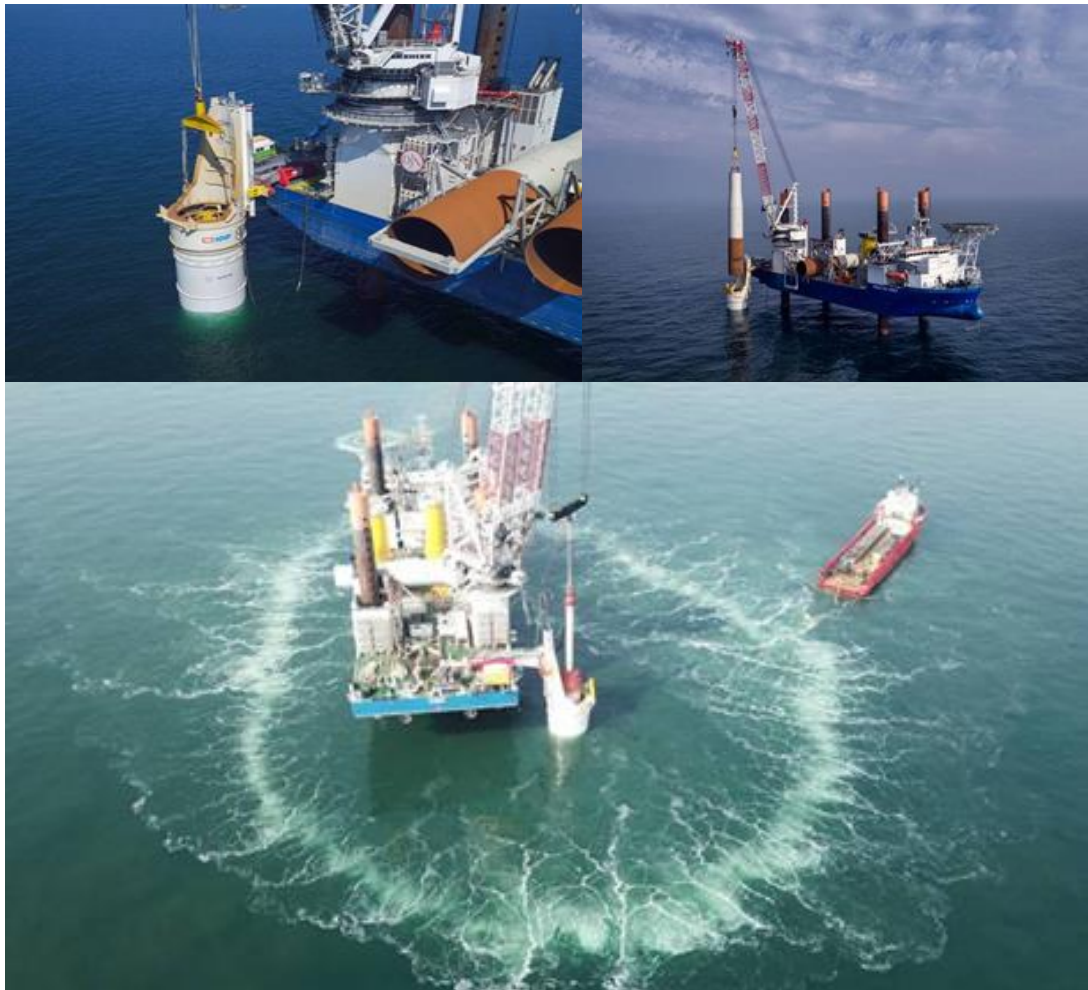


Figure 7.17 Example of Noise Mitigation Sleeve (top panels) and bubble curtain (bottom panel, courtesy by Jan de Nul).

#### 7.4.6 Secondary steel and corrosion protection

Items protruding outside of the monopile circumference like corrosion protection systems, such as anodes, or any other secondary steel near the seabed can be subject to rock impact in case scour protection rock is installed after pile installation. There is a risk of damaging these items which requires mitigation. This can be achieved by applying protection to these systems and/or mitigating measures in the rock installation procedures.

#### 7.4.7 Pre-mounted cabling and devices

Pre-mounted cabling for sub-seabed measurements or other devices mounted in- or -outside piles below scour protection level, will be exposed to severe abrasion when installed through the scour protection rock material. Due consideration for this interface should be made, either in the scour protection design, installation method or -scheduling, or in the design of cabling- and device housings.



#### 7.4.8 Nearby jack-up operations

Since the installation works for wind turbines are often done by means of heavy lift jack-up vessels, it is likely that jack-up footprints are made in the vicinity of the foundation. Several footprints could result from the different jack-up legs of the various vessels involved in the installation sequence, or due to multiple jack-up positions of one vessel (Figure 7.18).

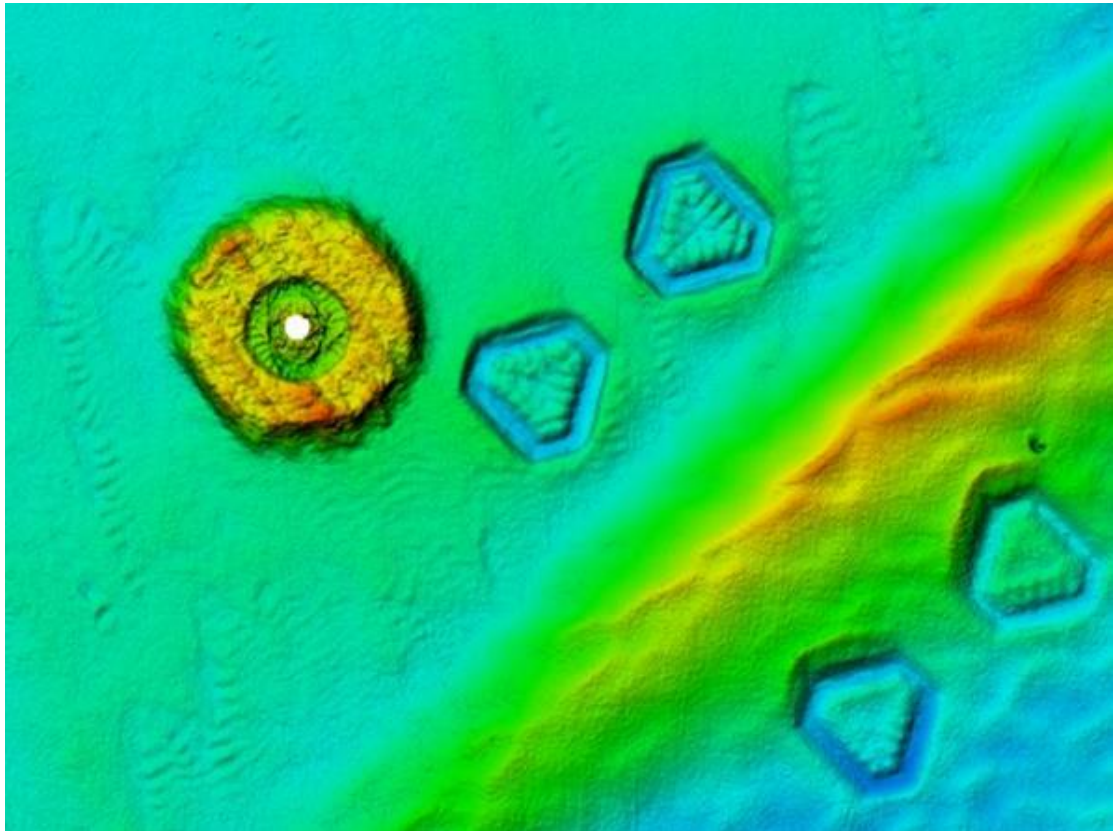


Figure 7.18 Example of scour protection depression caused by usage of noise reduction sleeve. Jack-up vessel spudcan footprints and mobile sand wave visible to east of scour protection.

When the jack-up footprint is made before the scour protection is installed, the risks are the following:

- A local deepening of seabed inside the considered footprint of the scour protection. This depression needs to be filled up with extra protection material or else it results in a similar trough at the top of the scour protection.
- Local depression of the seabed at the edge or immediately outside the considered scour protection footprint. First, this may cause the edge of the scour protection once installed to become unstable. For example, rock material might roll into the trough left by the jack-up operation. However, if the predicted imprint is smaller than the predicted seabed lowering due to morphological reasons this might not be a problem, because the filter is installed to serve as a falling apron.

When a jack-up vessel operates after the scour protection is installed, the risks are the following:

- If the scour protection extends further than planned or the jack-up position is closer to the foundation than planned then there is a risk of jacking on top of the scour protection. Consequences might involve damage to the scour protection and inability to finish jacking operations due to unexpected soil resistance or large slopes in case jacking is attempted on the edge of the protection (see also Figure 7.19);

- In soft soils the jack-up spud-can leg penetration may become so large that upon retrieval of the leg, a large depression is left in the seabed potentially undermining the scour protection.

The impact of jack-up operations needs to be assessed beforehand by analysing the possible footprint depths and slopes which are largely determined by the local soil conditions. Based on the outcome of the analyses, a recommended safety zone can be applied around the scour protection. Spudcan holes will backfill in time, but scarcity of mobile sediments as in the case of clayey seabed might prolong or prevent this process. As a remediation measure, protection material can be used to fill jack-up footprints if deemed needed.

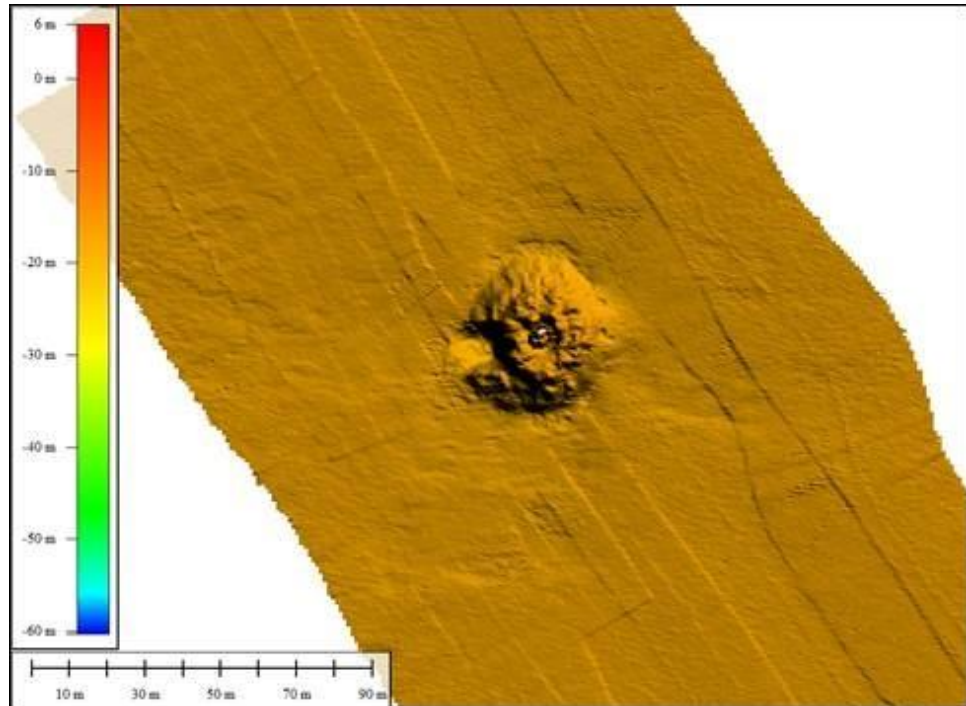


Figure 7.19 Jack-up footprint on scour protection (only filter layer affected).

#### 7.4.9 Dredging works for seabed preparation

Dredging works might be required in case of a seabed characterized by high mobility and steep slopes to ensure cable burial, jack-up operations or to mitigate future seabed lowering. For dredging works in the vicinity of an already installed scour protection it is important to consider the interface with the falling apron design of the scour protection. In case the dredging level exceeds the amount of bed lowering accounted for in the scour protection design, additional rock placement might be required to stabilize the falling apron. The time between dredging and rock installation needs to be considered as seabed features might re-occur if this takes too long.

#### 7.4.10 Seabed material and seabed features

In some cases, the seabed morphology can be overprinted by the rock installation. For instance, short crested sand ripples consisting of very soft material may collapse, or wash away, under the influence of the rock installation. In that case, a pre installation survey will show these features, but they will not appear in the post installation survey. Eventually, it could mean that it is difficult to prove that the installed layer thickness is in accordance with the design if this is solely based on the comparison of both surveys. It is therefore of great importance that the installed rock is properly documented, for instance by vessel output of rock tonnage to confirm installed layer thickness. Alternatively, the seabed features could be removed before rock installation with seabed preparation. As this is a costly operation, this is not needed as standard practice but rather if there are serious concerns about the evenness of the to be installed scour protection. If all features are

explicitly known before installation they could be accounted for within the required rock volumes. However, this is practically not feasible and thus not preferred.

The survey plots in Figure 7.20 show the bathymetry before rock installation and a difference plot after installation. Typically, the difference between the pre and post installation survey is used to prove the installed rock layer thickness. In this case, the difference plots show a reduced layer thickness at the footprint of the ripples. However, in reality this is not the case as can be concluded from the continuous rock output of the vessel.

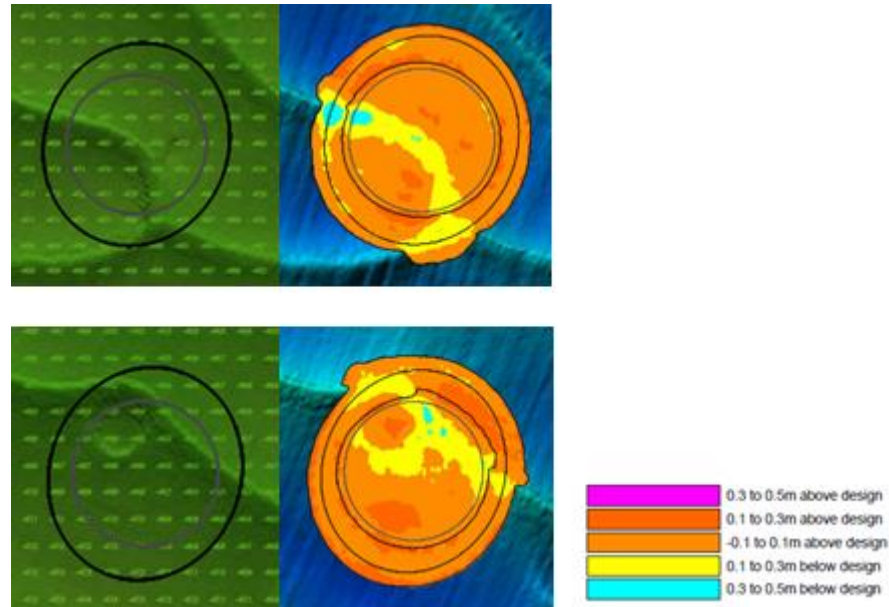


Figure 7.20 Pre-installation survey on the left and post installation difference chart on the right showing a reduced layer thickness at the location of sand ripples.

## 7.5 Surveys

The key tasks of surveys in the domain of scour protection is to prove the scour protection is in the correct position, has the required layer thickness and (if applicable) is at the required absolute height. A number of tools are at the surveyor's disposal to assist in the operations and to prove the result to the Client.

### 7.5.1 Accuracy requirements & geodetic parameters

Scour protection is often the first construction activity in the field. It is crucial that at first, the geodetic parameters and vertical reference system are unambiguously defined.

The horizontal reference system should be fixed to the continental plate on which the project takes place. All continents are notorious to move over the earth's asthenosphere, as the Himalaya mountains make clear. The movement is slow, though in the same order of magnitude as accuracies required by the developers. To this effect, the parameters between for instance WGS84 (the system in which the GNSS antenna makes its observations) and the local datum (e.g., ETRS89 in Europe) need to be established with time-dependent parameters. All this can be referenced by industry standard EPSG codes to avoid ambiguities.

Moreover, the vertical reference system, should be agreed on upfront by defining the geoid that needs to be used. All contractors on a given project should use the same geoid to avoid differences in height.

With the abovementioned agreed between contractor and developer, it will be possible to compare datasets throughout the construction period and throughout the lifetime of the wind farm.

### 7.5.2 **Monitoring Equipment**

A Multi-Beam Echo Sounder (MBES) is typically used as the primary method to monitor the scour protection installation works. The remainder of this section will refer to this measurement technique.

### 7.5.3 **Survey Platform**

To perform survey activities a suitable survey platform is selected considering the offshore location, weather conditions and regulations. Preferably, the suitable survey platform is equipped with a hull mounted MBES or a moonpool. Generally, the hull mounted MBES will give the most accurate survey data and should be preferred. Nevertheless, depending on the water depth and the possible approach of the vessel in the vicinity of the structure, it might be required to use a Work Class ROV (WCROV) or a Fall Pipe ROV (FPROV) to perform the multibeam survey and achieve the necessary measurement accuracy. The absolute accuracy will be largely influenced by the accuracy of the pressure sensor and the Ultra-short baseline (USBL) positioning system.

### 7.5.4 **Survey Specifications**

A survey is performed by sailing in parallel tracks. A minimum overlap of 25% between adjacent swathes is recommended for satisfactory integration of successive swath data to ensure a full coverage of the survey area. It is recommended to have sufficient data density for all survey passes i.e., sufficient observations per gridded bin. Gridding is subsequently done by averaging all depth observations in each bin. The speed of the survey vessel is adjusted to guarantee this requirement.

With multibeam, as with any echosounder, a main concern is sound in water. Once the projector transmits acoustic energy into the water, many factors influence that energy's velocity and coherence. The major influence on the propagation of acoustic energy is the sound velocity of the water column. As the acoustic pulse passes through the water column, the velocity of the wave front will vary based on the sound velocity; this is called refraction. If the sound velocity through the water column is not accounted for in the data collection software an error will be introduced in the measured water depths. For this reason, sound velocity casts (Sound Velocity Profiles, SVP) are an often-repeated routine during multibeam surveys.

The velocity of sound in water varies both horizontally and vertically. It cannot be assumed that the velocity of sound in the water column remains constant over large areas or throughout the day in a more local area. The main influences on sound velocity are conductivity (due to salinity), temperature and water depth (pressure).

### 7.5.5 **Filtering data**

After a survey is performed, the data is processed to remove outliers and unrealistic features. Care should be taken when using automatic filters to process the data. To prevent unwanted changes, one can choose to manually clean the data.

### 7.5.6 **Calibrations**

The quality of MBES data is exposed to several potential error sources, which are identified and resolved by calibrations. Such error sources are summarized in the following:

- Instrumental errors ('electronic' errors embedded in the instrumentation)
- Offsets (static relative positions between MBES and positioning systems)
- Transducer depth (depth of the transducer below the water line)
- Transducer head alignment(s)
- Sound Velocity, calibrated by fabricator on a regular time interval
- Vessel/ROV attitude biases (i.e., heading, pitch, roll biases)

- Latency biases (asynchronous time tagging of data)
- Vessel/ROV positioning calibration accuracy of the USBL system
- Tidal data, accuracy of predications and/or real-time measurements

The calibration of the survey setup consists of:

- the dimensional control (establishing the physical positions of the different sensors with respect to each other) and;
- the misalignment checks (establishing the Calculated – Observed values that will be used either in the sensor or in the survey software to compensate for the small misalignments when mounting the survey sensors on a vehicle)

Additionally, each instrument will have a valid factory calibration certificate, if applicable.

At the start of a project, the surveyor ensures all valid factory calibration certificates, dimensional control and misalignment checks are in place. Best practice is to repeat the calibration at least every 6 (e.g., multibeam) to 12 months (e.g., USBL system). A recalibration of affected sensors is required after a change in the setup on the vessel or when doubts occur on the data quality. The Calibration Plan will define the calibration interval and which sensors in the setup need to be recalibrated when a sensor is replaced, as replacing a sensor may have a knock-on effect on other observations.

On vessels with permanent hull-mounted subsea positioning and multi-beam sonar systems, the documentation history of equipment configuration and calibration values (C-O's) established during the installation of these systems and regular checks can be considered as valid for the project if they are well documented.

On vessels with temporary MBES mountings, including ROV's, full system calibrations are typically done prior to data acquisition to determine the C-O's. When all system biases have been identified and documented, the C-O values are used in performance verifications at the work area for confirmation.

### 7.5.7 Positioning system

The required positioning accuracy is typically determined from a case-by-case decision. This depends on several factors including the kind of work, the type of vessel, the survey method. Furthermore, this is agreed upon between the different parties involved such as the Contractor, Client and Certifier. There are several positioning systems available in the market which provide different accuracy levels:

- DGNSS – Differential GNSS technique
  - GPS, GLONASS, Galileo, Beidou
  - RTK base station
  - Accurate Elevation  $\pm 5$  cm, Position Accuracy  $\pm 10$  cm
- PPP – Precise Point Positioning GNSS technique
  - GPS, GLONASS, Galileo, Beidou
  - No base station
  - Elevation Accuracy  $\pm 30$  cm, Position Accuracy  $\pm 10$  cm

### 7.5.8 Additional notes and considerations

The possible underestimation of the installed layer thickness of a scour protection based on MBES and the vertical referencing between in- and out-surveys are typical considerations regarding the measurement campaigns.

A multibeam survey always underestimates the layer thickness of a rock layer; this phenomenon has been described in the Rock Manual and in the MV2 CUR document. As a result of the interaction between the survey system (typically MBES) and the rock bed the returned observation can also penetrate the cavities between the rocks leading to an average measured level below the reference level.

The MV2 CUR document describes some tests that were performed to measure the difference between the MBES survey measurements and the actual result of the installation. This document can be used as a guideline to calculate the influence of MBES measurements on the installation of large armour rock.

## **7.5.9 Survey activities**

### **7.5.9.1 Pre-Subsea Rock Installation Survey**

Before the commencement of the rock installation works, the contractor usually conducts a multibeam in-survey of the seabed level at the foundation location. This survey covers the footprint of the rock installation design and typically an additional radius of approximately 50 m. The survey is conducted within a certain agreed period in the order of days prior to any rock installation works. The determination of this period will be based on an engineering study that accounts for seabed mobility and weather impact as well as on possible simultaneous operations. The pre-subsea rock installation survey is conducted to establish the seabed topography as a baseline for subsequent surveys and to confirm that no unexpected objects are located inside the work area.

### **7.5.9.2 Progress Surveys**

Progress surveys are used for controlling the work and will be carried out on a regular basis or as required to accurately monitoring the installation process. These surveys are compared to the pre-subsea rock installation survey.

### **7.5.9.3 Post-Subsea Rock Installation Survey**

After completion of rock installation operations, a post-rock installation survey is performed for each installed rock layer. The survey covers, as a minimum, the area affected by the scour protection works and some undisturbed seabed to facilitate the vertical referencing. Finally, post-intervention surveys are conducted with the following objectives in mind:

- to confirm compliance with the Contractual and Project Requirements
- to establish the as-built documentation demonstrating compliance
- to provide reliable assessment of rock volume installed per location

## **7.5.10 Deliverable example**

Typical deliverables after rock installation operations can be the following:

- Gridded multibeam data in XYZ format
- Cross profiles of the rock berm
- Seabed intervention outline
- As-built chart

The as-built charts can include the following information:

- Legend with following info
  - Used equipment.
  - Used vessel.
  - Geodetic Info.
  - Scale bar.

- Legend of the symbols used in the chart.
- Colour scale.
- Pre rock installation planview with indication of the cross-section location, design and MBE data contours with depth labels.
- Post Rock dumping planview with indication of the cross-section location, design and multi-beam data depth labels with contours.
- Difference chart with indication of the cross-section location, design and mb data depth labels with contours.
- Cross or fan shaped sections with design, mb data and tolerance.
- Keyplan with overview of OWF layout and location of the drawing.

An example of an as-built chart is shown in Appendix D.

Figure 7.21 presents several examples of images in the survey deliverables. Figure 7.22 provides examples of pre-survey and post-survey data of a rock berm design, including the minimum and maximum design envelopes to verify compliance of the as-built situation with the design values.

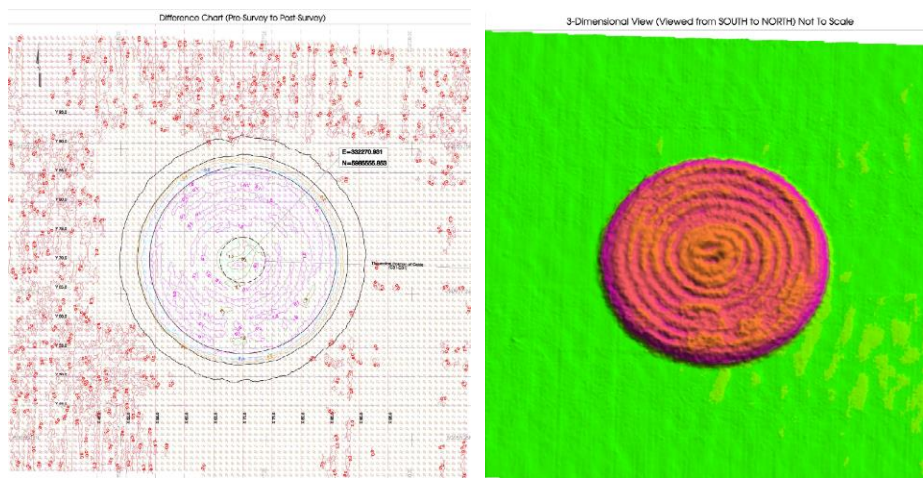


Figure 7.21 Example of survey deliverable, Diff chart pre- to post-survey (left) and 3D view (right).

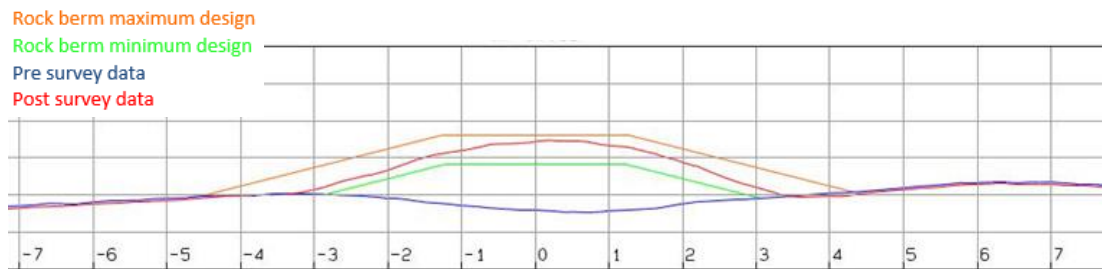


Figure 7.22 Example of cross section of a berm including tolerances.

## 7.6 Installation accuracy and tolerances

The achievable installation accuracy is influenced by workmanship, repetition, installation speed, equipment, installation method, metocean conditions, rock grading, presence of any seabed bedforms and of dredging or other seabed preparation works. The selection of appropriate tolerances at the design stage is based on a balance of what can practically be achieved, what is required for the rock structure and cost.

Installation tolerances are evaluated at time of installation, but it should be noted that long term settlements of the installed rock structure may take place as a result of consolidation of the underlying seabed or as a result of winnowing out of sediment from below the rock.

In every design, it is required to consider and ensure constructability. This can partly be achieved by the Developer specifying relevant and achievable installation tolerances in consultation with the Contractor. Specifying too strict tolerances may inevitably lead to extensive non-conformities and an increase in time spent on installation, whereas too loose tolerances risk installation of unnecessary rock volume and/or increases in any adverse effects related to the volume of rock installed.

The following sections provides guidance on selecting tolerances for the installation of various offshore rock structures by recommending magnitudes that are realistic to accommodate. Guidance on how to evaluate the installed accuracy of a rock structure and how to assess non-conformities, are also provided. Preferably, a framework addressing accuracy and tolerances should be agreed upon between involved stakeholders before the initiation of installation works.

To ensure that sufficient rock is carried for the installation, it is important to consider that during installation an additional amount of rock is needed to compensate for material washed away when the rock falls through the water columns and for an immediate rock penetration into the seabed. The immediate penetration depends on the local soil conditions and can be in the order of 5 - 10 cm (Beemsterboer, 2013). For extreme soft clay higher values can be reached. These rocks are still present and functional as scour protection, although they cannot be observed in the MBES post-installation survey. For short berms so-called run-in and run-out will also need to be accounted for in the quantity estimate. Finally, for any rock structure for which compaction is applied, the volume loss due to compaction must be accounted for. An illustration of tolerance and losses is given in Figure 7.23 and Figure 7.24.

The quantity of rock by weight needed for the installation works can be assessed by multiplying the theoretical berm volume with an installation factor. The installation factor is based on the bulk density of the material and an estimate of different installation losses discussed above and listed in Table 7.2.

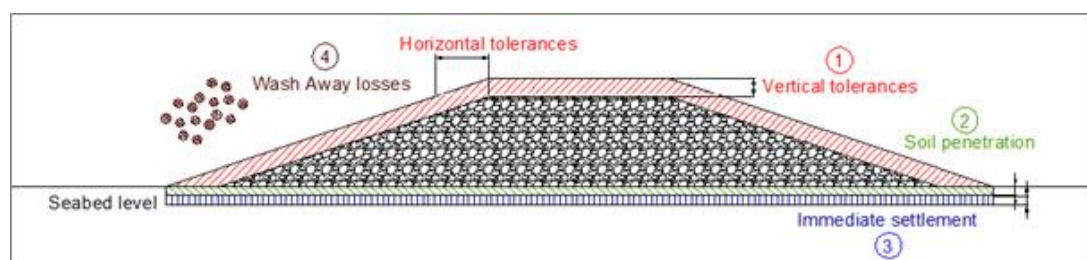


Figure 7.23 Illustration of tolerances and losses.



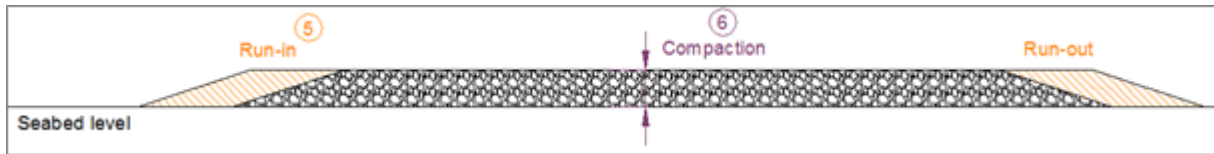


Figure 7.24 Run-in and run-out volume at start and end of rock berm.

Table 7.2 Installation losses to be accounted for when estimating total carried rock quantity.

Item	Description
1	Vertical and horizontal tolerances: depending on rock grading, berm dimensions, installation method, weather conditions on site
2	Soil penetration: depending on rock grading and soil parameters
3	Immediate settlement: depending on rock and soil parameters and height of the berm
4	Wash away losses: depending on rock grading and current on site
5	Run-in and run-out: depending on water depth and berm dimensions
6	Compaction: depending on height of berm

### 7.6.1 Ensuring constructability of design

There are many factors which influence the achieved installation result. The type of equipment, the water depth, the manoeuvrability of the vessel, the weather during installation, the rock grading and the currents during installation all influence the end result as well as the installation speed.

The type of equipment is important as a fallpipe vessel equipped with dynamic positioning can reach a different accuracy than a side stone dumping vessel or a hydraulic crane barge. The advantage of a fallpipe vessel is that the accuracy is independent of water depth, while a side stone dumping vessel will face increased inaccuracy with increasing water depth due to the larger fall height (see Figure 7.25). Crane barges have a discontinuous installation process which increases the inaccuracy and speed. For a more detailed description of the different types of equipment see Section 7.2.

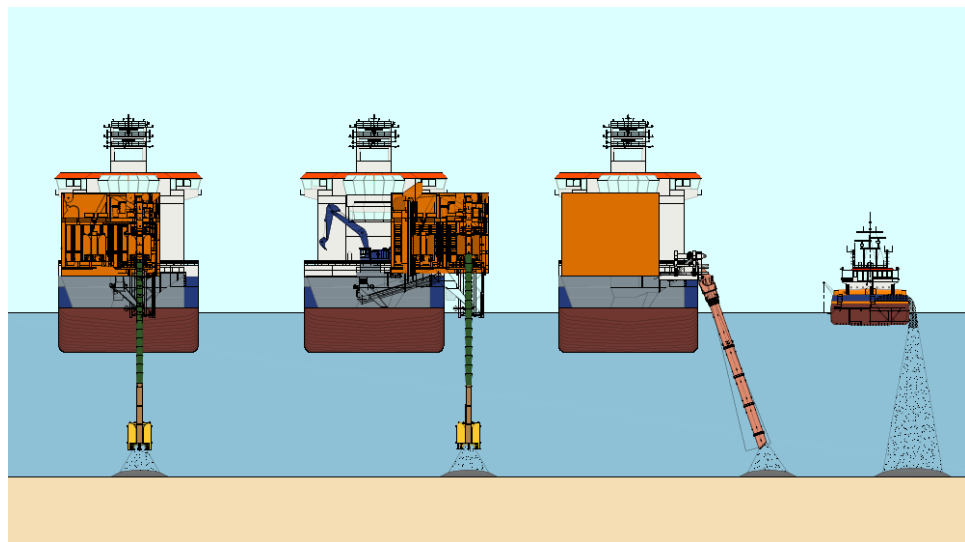


Figure 7.25 Placement of rocks using different types of equipment, showing fallpipe vessels with the pipe below, at the side, or inclined (from left to right) and a side stone dumping vessel.

The weather conditions (wind, waves and currents) during installation determine the motions of the installation vessel and thus influence the installation accuracy. Therefore, the manoeuvrability of the vessel is important as a vessel with freedom in manoeuvrability will position in a favourable orientation with respect to wind, waves and currents. In case of the presence of a structure such as a jacket or monopile the manoeuvrability is limited, and an unfavourable orientation of the vessel might be used during installation which increases the inaccuracy. Currents are important as they are a driving force for the horizontal movement of the rocks below the water line. During strong currents the rocks will displace further than during mild currents. Furthermore, the rock grading is also influencing the accuracy as the rocks are a natural product and, independent of the installation methodology, the end result is bound by the properties of the rock. Tolerances should therefore account for the largest possible rock size within a rock grading. As all these factors contribute to the installability, it is advised to assess the installability prior to specifying tolerances. The tolerances specified in this chapter are expected to be generally achievable by means of a fallpipe vessel.

For the contractor to be able to assess the installability, all tolerances should be specified in combination with a grid size to average over. Larger grid sizes mean stricter tolerances can be obtained while smaller grid sizes will force the requirement of more relaxed tolerances. For larger rocks, looking at too small grid sizes will result in a distorted image of the overall performance of the scour protection, as it might show large variations when one is zooming in into the cavities in between large rocks.

In case of very strict tolerances, it is sometimes feasible for smaller rock gradings to level the surface up to a certain extent and improve the installation result. It should be kept in mind that this is a time consuming and costly process which should be avoided if not strictly necessary.

### **7.6.2 Tolerance guidance for various rock installations**

This section provides tolerance guidance for different type of rock structures. Tolerances are grouped for (a) Rock Pads defined by thickness, (b) Rock Pads defined by surface level and finally (c) Rock Berms defined by width and so-called top-of-product cover thickness.

Tolerance will typically be related to a certain MBES survey gridding size for averaging. The tolerances and associated evaluation grid size will normally be selected as to address low and high spots, installed rock volume, cover thickness and surface level and -inclination as needed. The evaluation may be performed in predefined grids as illustrated in Figure 7.27, or alternatively by a moving average approach.

The tolerances are normally specified as an acceptable vertical and horizontal allowance  $\Delta_{ZTOL}$  and  $\Delta_{XTOL}$  relative to a given design geometry as illustrated in Figure 7.26 and related to a given evaluation grid size defined in subsections below.

The horizontal tolerance can be used to define the maximum seabed footprint on uneven seabed by offsetting of the rock slope if defined. A maximum seabed footprint can be assessed by assuming a rock slope of about 1:3 plus a horizontal tolerance.

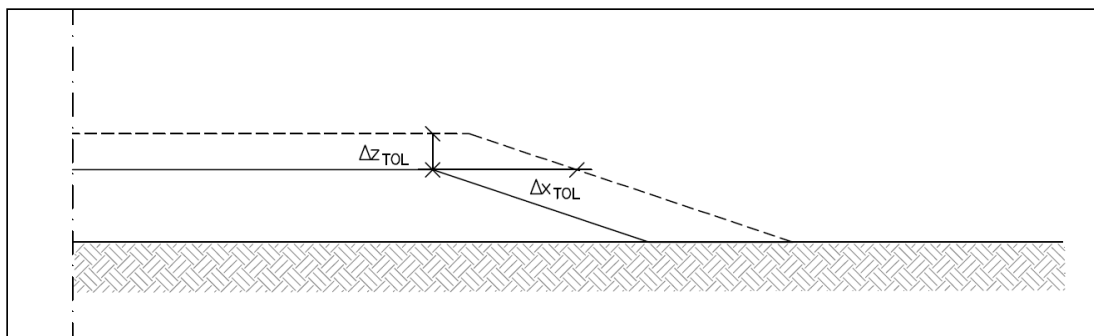


Figure 7.26 Schematic illustration of vertical and horizontal tolerances.

#### 7.6.2.1 Rock Pads defined by thickness

Scour protections around foundations can in most cases be classified as Rock Pads defined by thickness and horizontal extent. Tolerances are applied to the layer thickness (relative to the seabed or previous layer) and to the horizontal extent of the scour protection, listed in Table 7.3. Two evaluation grid sizes are proposed: a smaller grid size to allow for local underdumps and a stricter larger grid size without under-dump allowance to ensure the designed volume is installed (Figure 7.27). Other grid sizes or shapes (see Figure 7.28) may be selected. It is furthermore noted that the tolerances provided in the table serve as a guideline and should always be carefully considered with respect to the functionality of the scour protection. Depending on the scour protection functionality alternative tolerances can be defined for (part of) the scour protection without compromising any of its functions. This may lead to shorter installation time or lower costs.

Table 7.3 Tolerance guidance for rock pads defined by thickness. The  $D_{n50}$  is the average nominal rock size, typically defined as  $0.84 \cdot D_{50}$ .

Rock pad defined by thickness			
Grading	Evaluation grid [m]	Vertical tolerance $\Delta z_{TOL}$ [m]	Horizontal tolerance $\Delta x_{TOL}$ [m]
Coarse Gradings (OSG)	1.0 x 1.0 or 1 m <sup>2</sup>	-0.2 to +0.5	-0.0 to +2 m
	3.0 x 3.0 or 9 m <sup>2</sup>	-0.0 to +0.4	
Light Gradings (OWG)	1.0 x 1.0 or 1 m <sup>2</sup>	-0.2 to +3x $D_{n50}$	-0.0 to +2 m
	3.0 x 3.0 or 9 m <sup>2</sup>	-0.0 to +2x $D_{n50}$	

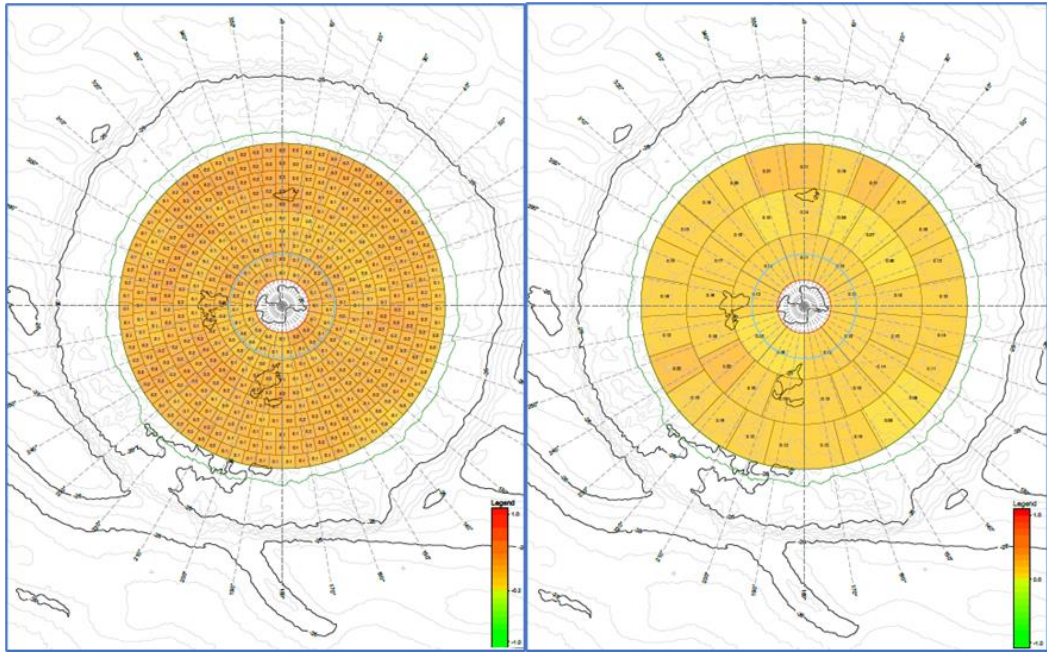


Figure 7.27 Example of evaluation grids of 1 m<sup>2</sup> (left) and 9 m<sup>2</sup> (right)

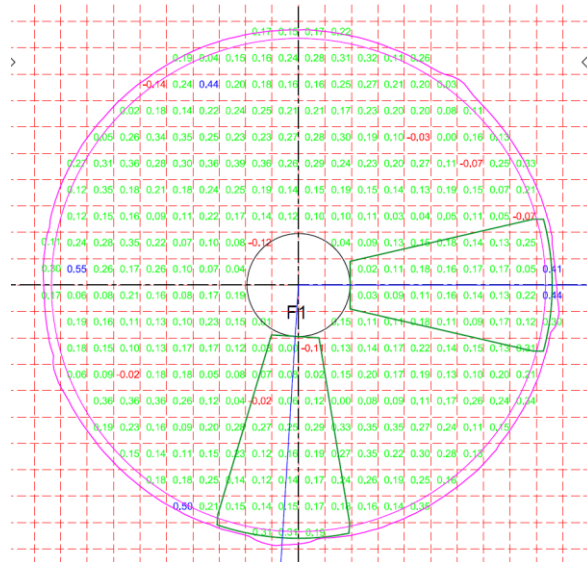


Figure 7.28 Rectangular grid example 4 m<sup>2</sup>.

It should be noted that in case of double-layer systems the tolerances for the different layers can add up.

When cables are being pulled into foundations across already installed rock, sufficient aperture height between the cable touch down point and cable entry hole is needed. To ensure that this aperture height is met, the thickness requirement of the scour protection may need to be caveated with a level requirement within the cable touch down zone. In event of conflict between thickness and level requirement, the level requirement will most often need to have priority in order to allow cable installation.

Other limitations to the thickness tolerances might be related to remaining water depth at the boat landing and allowable installation volumes from permit requirements.

### 7.6.2.2 Rock Pads defined by surface level

A specific surface level will typically be specified for Rock Pads serving as bedding layer for direct foundation, e.g., Gravity Based Foundations (GBFs), Piling Templates or Jackets with Mudmat/Pile-sleeve arrangements. The design requirement for the vertical tolerance around the specified level will often relate to structure inclination and high spots. The achievable tolerance will be highly depending on the size of the rock material and the time spent on the installation and leveling.

Local high spots can have significant impact on the design of some structure types like for the base plate of GBFs, while other structures may be less sensitive.

No recommendation for tolerance are given for rock pads defined by levels, but it is noted that to achieve tolerances less than those provided in Table 7.3, longer time for installation must be anticipated and post installation treatment such as leveling and/or compaction may be required.

Vertical tolerance less than the rock size of the applied grading cannot be expected to be achievable, just as validation of achieved tolerance will also depend on accuracy of applied MBES survey equipment.

### 7.6.2.3 Rock Berms for crossings & cable protection

Rock berms are often installed as protection for a product (e.g., cables and/or pipelines) in case of crossings, jointing's or in case burial is not feasible or sufficiently achieved. The installation of a rock berm is typically assessed by a longitudinal section along the product covered by the rock berm. Depending on the function of the berm minor underdumps could be accepted. It is advised to use an evaluation grid. Tolerance guidance for the evaluation of the cover on top of the product is given in Table 7.4. Secondly, the berm is typically assessed by either a minimum geometry or a minimum rock volume depending on the purpose of the berm and the applicable design requirements. Evaluation can be performed based on top view difference charts or cross sections.

Table 7.4 Tolerance guidance for rock berms for cable protection. Note 1: it is advised to determine an evaluation grid which fits project specific requirements.

Rock berms				
Gradings	Location	Evaluation grid [m]	Vertical tolerance $\Delta z_{TOL}$ [m]	Horizontal tolerance $\Delta x_{TOL}$ [m]
Coarse Gradings (OSG)	Longitudinal section - top of product	note 1	-0.0 / +0.7	N/A
Light Gradings (OWG)	Longitudinal section - top of product	note 1	-0.0 / +3xD <sub>n50</sub>	N/A

### 7.6.3 Assessment of as-built conditions and remediation of non-conformances

This section discusses the possible presence of post-construction non-conformances. It focuses on two main aspects: (i) what can be considered in a non-conformance assessment, and (ii) what remediation options are available.

To evaluate the scour protection the installed rock tolerances will need to be agreed in advance as described in 6.6.1. To evaluate the installation accuracy, every tolerance specification should be evaluated on a specified grid resolution. The original high resolution measurement data will be averaged over this grid size before evaluation, or alternatively applied directly as input for moving average evaluation. If the installed rock layers are positively evaluated, the scour protection can be accepted as is. If this is not the case the non-conformity should be evaluated. The purpose and

boundaries of the structure should always be kept in mind. In that case possible deviations/non-conformities are addressed with the necessary level of attention, without compromising the design or affecting interfaces. If a local under-dump is either not very deep, or very far from the monopile, it might not pose an integrity hazard and could possibly be neglected. For example, a local over-dump on the edge of a scour protection that is expected to act as a falling apron might not be of concern.

If the minimal requirements are not fulfilled, a remediation strategy is necessary. If there are local spots that are installed below the minimum required thickness, and in the overall cross section the volume balance of installed material compared to the theoretical design is positive, levelling of the cross section can be considered. Conversely, if the installed rock volume in the overall cross section is less than the design volume, additional rock can be installed. However, in practice, small repairs should be avoided as much as possible because of the risk of over-dump. In certain cases, the preferable action might be to monitor the behavior of the rock structure and assess its behavior during certain events (e.g., a storm). Such a decision obviously depends on how severely the tolerances are violated, and the position of the non-conformance.

It may be necessary to recertify the design if the as-built situation deviates from the initial design and it is not preferred or feasible to take any corrective measures.

## 7.7 As-built documentation

After scour protection installation, it is essential to deliver a clear as-built documentation. During the operation and maintenance phase, the wind farm owner can use this information to compare the actual state of the protection with the design. The as-built documentation should include:

- Rock grading specifications of the installed scour protection material
- All pre- and post-installation MBES surveys of the individual installed rock layers (see Section 7.5.10)
- 3D cable trajectories in the near vicinity of the foundations
- Design drawings
- Design philosophy
  - Expected deformation in relation to storm occurrence
  - Expected and acceptable response of the scour protection to seabed dynamics
- Monitoring plan

# 8 Operation and Maintenance of scour protections

## 8.1 Introduction

Scour protections are passive systems, typically designed not to require maintenance over the lifetime of the wind farm, as long as the design conditions are not exceeded. As such, the primary operation and maintenance work in relation to scour protections relates to survey and monitoring of the scour protection integrity and functionality.

The scour protection integrity is best monitored by Multi Beam Echo Sounding (MBES) surveys of the scour protection and surrounding seabed. The MBES survey provides a digital terrain model of the seabed and scour protection surface. This surface can then be compared to design specifications and previous surveys for assessment of scour protection and seabed change compliance.

The functionality of the scour protection can be indirectly assessed by monitoring the frequency response of the wind turbine. This is because changes in seabed and scour protection levels will impact the frequency response of the wind turbine. Changes in the frequency response of the wind turbine can therefore be indicative of scour protection damage or seabed lowering.

Free spanning cables, cable protection systems (CPSs), J-tubes, anodes and similar structural elements will often not be captured well in the MBES survey digital terrain models. To capture such features the MBES data must be high resolution and processed as point cloud data. Supplementary survey techniques such as Side Scan Sonar (SSS), MBES Backscatter or stereo-photography analysis or equivalent may be useful in assessment of cable free spans across the scour protection, at the edges of a scour protection or across a scour hole if no scour protection is installed. It is however outside the scope of the present handbook to provide guidance on such survey application.

In Figure 8.1 a schematic overview is presented for the monitoring procedure in the Operation & Maintenance (O&M) phase. It is assumed that preceding this phase an as-built survey of the scour protection has been carried out (see Section 7.7).

In this chapter, the required surveys, techniques for execution and evaluation of the surveys are discussed. Section 8.2 discusses the difference between scheduled and event-driven surveys and provides frequency recommendations for both. Section 8.3 further details survey specification and execution, whilst Section 8.4 concerns survey evaluation.

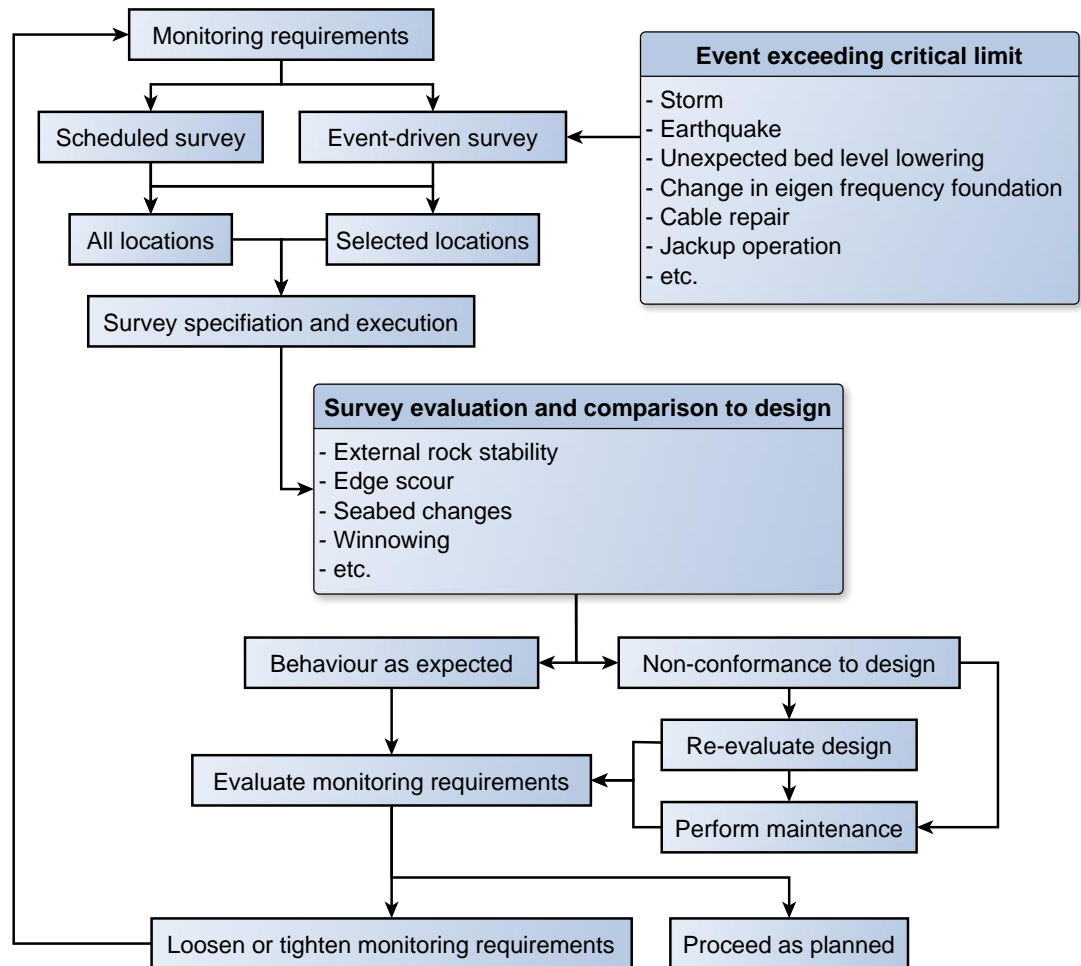


Figure 8.1 Flow chart illustrating example of monitoring procedure of offshore scour protections

## 8.2 Scheduled and event-driven surveys

O&M surveys are typically carried out a number of times over the lifetime of the wind farm. The surveys are used to demonstrate that the integrity of the scour protection and seabed levels at the foundation remains within design specifications of the foundation design. The surveys may also be applied for other uses such to update design specifications in relation to design validation, turbine control updates or turbine and foundation lifetime expansions or other. The survey may or may not be bundled together with cable route surveys or clustered together with surveys of neighboring wind farms for cost reduction.

The requirement for Operation and Maintenance (O&M) surveys of the seabed and scour protection at offshore wind farm foundations can be driven by authority-, certification- and commercial requirements. Apart from such obligations, a prudent and risk-based operation of the wind farm may also add to the scope and schedule of O&M surveys.

Field experience over the last decade has demonstrated a high robustness of installed scour protections. This goes both for double- and single-layer type of scour protections and for scour protection located in areas of high or low seabed bed mobility. Severe edge scour has primarily been observed on relative shallow areas with strong currents and has been seen to develop over time span of several years. The observed robustness of scour protections has gradually led the industry to reduce the number of surveys of scour protections. Particularly the number of surveys in the first years of operation have reduced, compared to early guidelines.



### 8.3 Survey specification and execution

The selected survey methodology must enable the establishment of a digital terrain model of scour protection and seabed surface within an area relevant for specifications of the foundation design. This will typically be a MBES type of survey with a square or rectangular seabed coverage with side lengths in the order of 100 m to 200 m. At locations where excessive edge scour is observed or expected or in areas of significant seabed lowering, the footprint may need to be extended to fully cover the scour protection and seabed dynamics of the location.

The spatial resolution of the terrain model should be enough to detail change in scour protection and seabed levels. As guidance a grid size of 0.2 to 0.5 m within the scour protection footprint and 0.5 to 1.0 m outside the scour protection footprint will normally provide enough detail.

An O&M seabed and scour protection survey schedule will normally be site specific and adaptive and must adhere to local legislation and regulation. The adaptiveness of a survey schedule relates to allowance for combining surveys of different scopes or neighboring wind farms for optimized execution, e.g. by shifting the survey year of a particular scope. Shifting of survey years can also be relevant or required due to lack of vessel availability, survey permit issues or other.

A generic survey plan is presented below in Table 8.1 for guidance, in which practicality, cost and gain of seabed surveys are in balance.

Scour protections are designed for extreme events with a low likelihood of having occurred within the first years of operation. Still, it is considered prudent to survey the scour protection for any unexpected damage to or response of the scour protection. This verification of the scour protection integrity is the primary objective of the two first surveys of the survey plan. These surveys will also demonstrate if all or individual positions are likely to experience severe edge scour.

Table 8.1 Generic survey plan. Scheduled O&M MBES seabed survey scope.

O&M Survey No.	Survey year counting from time of wind farm inauguration	Seabed coverage	Main observation purpose
1	2 (Before second storm season)	100x100 m	Unexpected damage to or response of scour protection
2	3 to 4 (After second and before fourth storm season)	100x100 m	Unexpected damage to or response of scour protection
3	5 to 8 (After fourth and before eighth storm season)	100x100 m  For this survey it can be relevant to increase survey area to say 200x200m if the foundation is in an area of moving sand waves or equivalent or there has been made observations of extensive scour/edge scour	Long term seabed changes
...	5 to 10 years after last survey	100x100 m	Long term seabed changes

Wind farm sizes vary significantly, from a few to more than hundreds of turbines. For larger wind farms the seabed survey may not need to cover all turbine positions but can rely on fewer positions, representatively selected based on difference in water depth, seabed geology, scour protection design etc. Even so, it can be advantageous for the wind farm operation that some of the surveys cover all positions to form a new baseline of the condition of the installed scour protection and the overall seabed conditions. The post storm survey is suggested to cover a minimum 10 WTG positions or 10 percent of all WTG positions, whichever is largest.

An event driven post storm bathymetric survey is recommended within a year from passage of a severe storm event. A 10-year return period storm condition has often been considered appropriate as trigger for a post storm survey. Depending on the risk profile of the foundation and scour protection design, different return periods can be used for the definition of the threshold for post storm initiated scour protection and seabed surveys.

The return period of the storm can be defined based on a combination of wave height, -period, current speed and water level. Alternatively, the significant wave height can be used for the return period assessment.

## 8.4 Survey evaluation and comparison to design

The survey evaluation addresses the scour protection integrity and seabed level conditions in respect to scour protection and foundation design specifications.

Observation of scour protection conditions can be included and may address response to seabed lowering and edge scour, local sinking or depression near the monopile, damage due to wave and current action and impact from construction/operation work such as cable repair and/or cable stabilization and jack-up footprints. When interpreting the survey, the various mechanisms that could lead to deformation of the scour protection should be considered. These are extensively described in Section 4.2. For completeness, these are repeated here briefly, with additional remarks on how to consider these in the evaluation of the performance of the scour protection.

### 8.4.1 Response to seabed change

General seabed lowering can undermine the scour protection whereby the edge of the scour protection will adapt to the seabed changes by launching into a so-called falling apron as illustrated in Figure 8.2. The slope of a falling apron is typically varying between 1:2 and 1:4 (Section 4.3.3). As the falling apron develops, loose rock will slide down along the slopes. A minimum required footprint where the scour protection maintains its original height may be defined a-priori to serve as a baseline comparison for the surveys. In general, the time scales of migrating features that can affect the scour protection, like sand waves, is relatively long. These long timescales allow ample time for monitoring and potential maintenance if so required. An example of field surveys of a sand wave passing a scour protection is provided by Ørsted and shown in Appendix E.



Figure 8.2 Falling apron - illustration of scour protection adaption to seabed lowering. Physical model test from De Sonnevile et al. (2012).

#### 8.4.2 Edge scour

The scour protection may by its own presence cause so-called edge scour at the scour protection perimeter and downstream of the scour protection. Edge scour normally develops to equilibrium depth over a time span of several years. Edge scour may undergo backfilling during storm events and expand during spring tide conditions. Field experience and model tests of edge scour for scour protected monopiles are described in Petersen et al. (2015). Section 4.2 discusses edge scour mechanisms and consequences in more detail. Edge scour is, in general, a relatively slow process, thus allowing ample time for monitoring and potential maintenance. As discussed in Section 4.4.3, edge scour may not always be relevant for falling apron performance of the scour protection, but it is relevant for the cables. An example of an edge scour survey is provided by Ørsted and shown in Appendix E. On this survey, the cable can be clearly recognized in the footprint of the edge scour hole.

#### 8.4.3 Sinkage and monopile installation impact

During or after monopile installation the scour protection may experience local sinking near the monopile due to initial mobilisation of the sediment below the rock close to the monopile. This mobilisation stops as the rocks of the scour protection sink into the seabed. Field experience indicates that sinking is in the order of 0.5 m.

Scour protection depression close to the monopile can sometimes be observed, possibly as a result of impact from monopile installation works, and from use of noise mitigation sleeves in the monopile installation. At the sleeve footprint, the weight of the sleeve can cause the scour protection material to be pressed partly into the underlying seabed. Hence, a post-monopile installation survey could form the basis for any further O&M surveys.

#### 8.4.4 Storm-induced deformation

Most scour protections are designed to allow for storm-induced deformation (by the combined action of waves and current). This deformation resembles so-called clear water scour in unprotected seabed conditions. Basically, damage occurs when rock is relocated by waves and current, but it becomes increasingly difficult for waves and currents to remove rocks located within depressions of the scour protection. Thus, damage, sinkage and monopile installation impact add stability to the remaining rock. Sinking and installation impact of the scour protection and the damage to the scour protection from waves and currents should therefore not be superimposed when evaluating scour protection performance under hydraulic loads. However, for foundation stability total lowering along the pile might be relevant. Thus, for different evaluations, different comparisons may be required. These should be specified a-priori.

# Part III

## Scour protection methods – alternative

# 9 Alternative scour protection systems

## 9.1 Introduction

Next to the conventional loose rock scour protection designs alternative concepts are possible. These alternatives make use of different materials and can offer advantages in terms of cost-effectiveness and ease of procurement and installation. These concepts are new for the offshore wind market and few guidelines exist as to how to design and deploy them. Within JIP HaSPro several alternative concepts were investigated by means of physical model tests in order to improve the understanding of their behaviour and potential failure mechanisms under various conditions and with various foundations.

In order to develop solid guidelines for the design of these alternative scour protections a combination of physical scale model research and field validation is necessary. By testing the concepts in a controlled laboratory environment JIP HaSPro sets the first steps in this iterative process.

The mechanisms of scour prevention that are used in these alternative scour protections are not new in the wider hydraulic engineering industry; the offshore concepts are drawing on existing experience in other fields of hydraulic engineering, for example in bridge scour or coastal protection. In JIP HaSPro the focus is in particular on the offshore conditions and foundations common to offshore wind. As with the loose rock scour protections, the focus of the presently described research is on hydraulic performance of these systems in the prevention of scour.

In this chapter a general overview of the alternative concepts is given, including the installation and operation and maintenance aspects common to the considered alternative systems. The specific concepts are discussed in more detail in Chapters 10 and 11. Section 9.2 gives a high-level overview of alternative scour protection concepts, Section 9.3 discusses different installation methods for these alternatives, Section 9.4 deals with operation and maintenance requirements and in Section 9.5 decommissioning of the solutions is discussed.

## 9.2 Overview of alternative scour protection systems

An overview of the alternative scour protection systems that were considered in JIP HaSPro is given in Table 9.1, together with a brief description and the type of tests that were performed. Medium-scale tests refer to basin tests performed at a scale of approximately 1:30, and large-scale tests refer to the wave tests performed in the Delta Flume at a scale of approximately 1:6.

The four concepts are: artificial vegetation (frond mats), concrete block mattress, gabion mattress and ballast-filled mattress. These concepts differ in terms of the manufacturing process, materials, weight and flexibility. One common property of these systems is that they all consist of units (mats, mattresses) that can be manufactured in different shapes and are used as building blocks of a scour protection.

These scour protection types can offer advantages such as:



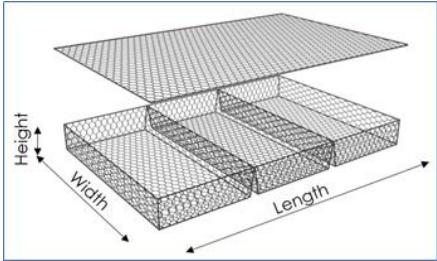
- Procurement and manufacturing: can be manufactured on site or pre-fabricated elsewhere and ballasted with locally available material - versatility in procurement (note that quality control needs be taken into account);
- Installation: the units (mattresses) that make up a scour protection can be installed with an offshore crane (whereas accurate installation of loose rock scour protections often requires a

fall pipe vessel). The units can be designed to be lighter than a loose rock protection of equivalent effect, and thus require less operations or less heavy-duty equipment;

- The potential for designing pre-installed and self-deployable systems that may simplify the installation procedures.

The alternative concepts, however, present their own unique challenges as well. These are related to accurate positioning to avoid gaps between units, as well as potentially more complex maintenance strategies. But most importantly to the designer, the behaviour of the scour protection system must be well understood in order to design a system with appropriate parameters that withstand the design loads (i.e. weight, flexibility, thickness etc.).

Table 9.1 An overview of the alternative scour protection concepts tested in JIP HaSPro.

Scour protection concept	Description of mechanism	Tests performed in JIP HaSPro
Artificial vegetation	<p>Ballasted or anchored frond mats. Imitates natural vegetation to slow down near-bed velocities to prevent scour.</p> 	<p>Medium and large-scale around monopiles; Medium scale around suction bucket jackets.</p>
Concrete block mattress	<p>Concrete blocks closely joined with a flexible connection to form a mattress.</p> 	<p>Medium scale around monopiles.</p>
Gabion mattress	<p>Mesh baskets filled with rock.</p> 	<p>Medium and large scale around monopiles;</p>
Ballast-filled mattress	<p>Impermeable mattresses filled with ballast material.</p>	<p>Medium and large scale around monopiles; Medium scale around suction bucket jackets.</p>

### 9.3 Installation methods

Installation of the alternative scour protection systems at the seabed is generally a controlled process requiring relatively light and simple equipment. These scour protection systems would

mostly be installed after the foundation, although for some systems methods for installing them simultaneously with the structure are under development. Pre-installation of alternative systems is not commonly considered, as very specific designs are necessary to prevent/mitigate damage to the scour protection during foundation installation.

A generic description of these installation methods and the related equipment is presented in the sections below. Please note that system-specific installation considerations are discussed in more detail in the separate chapters per system (Chapters 10 and 11).

### 9.3.1 Post-installation of alternative systems

Post-installation of alternative scour protection systems can be used for applications including monopiles, jackets, cables and pipelines. The risk of scour developing in the time window between the foundation installation and scour protection installation should be assessed and mitigated, if necessary.

#### Generic installation method

The alternative scour protections, considered in this project, consist of multiple individual mattresses, which need to be installed separately. After construction and transport to the pre-installed foundation, the general installation procedure for alternative systems is as follows:

1. Final assembly of mattresses and attachment to lifting frame;
2. Lifting and lowering by crane of lifting frame with mattress attached;
3. Positioning on seabed using vessel crane in conjunction with diver, GPS (on lifting frame) or ROV to ensure accurate placement;
4. Release of mattress on the seabed.

This installation procedure requires the following (minimal) main equipment:

- Scour protection system units;
- Lifting frame;
- Crane with sufficient lifting capacity;
- ROV, diver or another tool for accurate positioning of mattresses on seabed;

A DP2-vessel is generally sufficient to install a (light) alternative scour protection. Some systems may require additional operations before installation, such as filling, wiring, etc. These can either be performed on shore (requiring sufficient deck space to store the finished mattresses) or at sea (requiring additional equipment and time). Which option is preferred depends on the system and other factors such as available deck space or special equipment requirements.

#### Lifting and handling devices

Equipment designs and specifications may differ between various methods, installation contractors, clients and geographic regions. However, all lifting components should be designed with adequate factors of safety to account for:

- the load being lifted in air and in water and the possible lifting of the mattresses in pairs;
- the added mass effects during in-water lift;
- passage through the splash zone;
- multiple use in a harsh environment;
- unequal loading of the slings linking the mattress to the lifting frame because of the rigidity in the mattress.

Different types of lifting frames can be used to install the mattresses, such as spreader beams, mechanical lifting frames or multi-deployment frames (i.e. can install multiple mattresses simultaneously). Release of the mattresses at the seabed is generally achieved through a

mechanical release (often requires an ROV) or by hydraulic release, both of which release all hooks/straps in one operation.



Figure 9.3 Examples of lifting arrangements with different alternative systems. Top left: automatic lifting frame for gabion mattresses. Bottom left: lifting of frond mat. Right: concrete mattress suspended by 16x 6 m webbing slings.

#### Rigging of mattresses on the lifting frame

The scour protection mattresses must be attached to the handling frame with sufficient rigging that will provide a safe and simple operational state. The rigging should be inspected, tested and certified according to industry standards (e.g. DNV GL) and designed with good and reliable work practices. The rigging tasks need to be executed by trained, skilful and experienced riggers according to the rigging design study.

An adequate vertical clearance should be maintained between the handling tool and the mattress, especially for mechanical handling devices where ROVs may work beneath it. The heave motion of the vessel and the type of crane used (either with heave compensation or not) should be considered and also determine the appropriate length of the webbing slings.

During the rigging design procedure adequate safety factors should be incorporated, such as dynamic factors for weight in air and water, added mass coefficients and effects, dynamic factors including splash zone effect and unequal loading of the slings linking the mattress to the lifting device due to flexibility in the mattress.

#### Placement of mattresses on the seabed

Accurate placement of the individual mattresses on the seabed with respect to each other and the structure is important. Gaps between the mattresses (i.e. exposed seabed) or excessive overlapping of mattresses should be prevented. This should already be considered in the design phase, as the mattresses have a certain horizontal installation accuracy. This horizontal installation accuracy depends amongst others on the system, installation method and conditions. Based on model scale tests, gaps between individual mattresses in the order of 0.10 m can already lead to significant wash-out of sediment. Combined with the extent of any overlapping area (for instance extended geotextile), this provides a first estimation of the maximum horizontal installation tolerance (overlap



extent + maximum gap size). Please note that this might be different for the artificial vegetation due to the flexible fronds.

Accurate placement of the mattresses on the seabed is generally achieved by using the vessel crane, in combination with a diver, ROV or special equipment on the lifting frame (GPS, cameras). After installation of the scour protection visual inspection is recommended.

Special attention needs to be given to the placement of the mattresses close to the structure to ensure a tight transition between the scour protection and the structure. Especially around foundation structures (monopiles, jackets, etc.) it is generally difficult to install mattresses adjacent to the foundation due to lifting frame or crane excursion limitations. For some scour protection systems, self-installable systems or pre-installation of the scour protection might be a better solution to ensure a tight transition.

### 9.3.2 Self-installable systems

The alternative scour protections generally consist of large separate elements, but innovative installation methods can be considered to optimize the installation process. One such method is the use of a self-installable frame, where the scour protection elements are attached to a structure that can be lowered to the seabed as a whole and deployed by unfolding once it reaches the seabed. This method presupposes that the structure (monopile) is installed first, and then the frame is lowered around it. An example of such a system is illustrated in Figure 9.1. Other installation methods are considered for suction piles, where the installation of the scour protection can be coupled with the installation of the structure.

When using the self-installable system, the connections between the mattresses lead to a different stability behaviour than in the case of separate unconnected mattresses. The stability of such a scour protection should be assessed taking into account the design of the self-installable frame.

In JIP HaSPro large-scale tests were performed to improve understanding of the dynamics of the self-installable system. It is apparent that the process of lowering and unfolding of the self-installable frame is best done in calm conditions, since, especially a strong tidal current can influence the unfolding process (see Deltares, 2023a, document ref.: 1230924-004-HYE-0011).

The self-installable system is especially favourable for use with the lighter scour protection concepts, such as frond mats. The system has not yet been demonstrated in the field at the time of writing this handbook, therefore field trials are expected to provide extra information on the installation method.

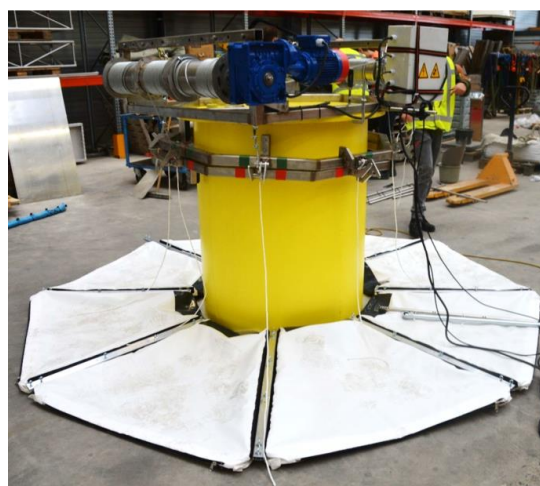


Figure 9.1 Self-installable system scale model that was used in the large-scale Delta Flume tests in JIP HaSPro.

### 9.3.3 Pre-installation of alternative scour protection systems

In some cases, it may be favourable to pre-install an alternative scour protection before installing the structure. This may be necessary for logistical reasons or when the structure is complex, restricting access to some of the areas that should be covered by a scour protection (e.g. in case of jacket structures).

It is particularly important to consider the tolerances between the scour protection and the structure installation. The mattress units of the alternative scour protections should maintain physical integrity after the structure installation, i.e. it may not be desirable, or even possible, to penetrate the scour protection with the foundation pile. On the other hand, gaps between the mattresses and the structure should be minimized to prevent wash-out of sand close to the pile. Extra measures may be required to mitigate the risk of winnowing in case of pre-installed systems.

## 9.4 Operation and maintenance

A project-specific operation and maintenance (O&M) manual for the scour protection system needs to be developed and agreed with the structural designer. In this manual, it can be defined in advance when (state/condition of protection) the scour protection system is considered stable (i.e. protects the structure against scour) or requires inspection and/or maintenance (i.e. needs remedial measures to remain stable or prevent scour around the structure). Furthermore, the manual should at least include a monitoring plan and pre-defined remedial actions in case of developing failure.

### Failure models of alternative scour protection systems

Scour protection is functioning properly as long as it is able to prevent scour development beyond acceptable levels. Failure models of the scour protections are discussed in detail in the dedicated chapters per alternative system and are briefly summarised below.

The following can lead to a failure of alternative scour protection:

- Excessive scour development at the structure;
- Winnowing through the scour protection;
- Sliding (displacement) of mattresses;
- Uplift of mattresses;
- Excessive edge scour / undermining of mattresses.

The failure modes above either directly lead to excessive scour development or result in exposure of the seabed and reduction in scour protection effectiveness, leading to progressive scour development.

### Monitoring

A major part of the O&M manual would be the monitoring strategy to observe the integrity and functioning of the scour protection. In general, the recommendations described in Chapter 8 can be followed for the alternative systems as well. However, standard MBES surveys might not be able to cover all failure mechanisms for these alternative systems, especially with regard to integrity of the scour protection (i.e. gaps between mattresses or material failures). Therefore, the alternative systems may need additional ROV surveys to investigate the integrity of the mattresses and scour protection. These ROV surveys, similar to rock scour protection surveys, can be performed periodically and after significant storm events.

Table 9.2 is an example of a non-exhaustive list of aspects to be considered in periodic surveys, including potential survey methods and examples of recommended frequency of survey.

Table 9.2 Non-exhaustive list of survey aspects for alternative systems.

Aspect	Potential survey method	Frequency (example)	Comments
Stability and positioning of mattresses	Sonar / MBES / ROV visual	E.g. 1 year after installation, periodically afterwards and after significant storm events. If stability is proven under certain conditions, the survey frequency can be decreased.	If moved mattresses (or the system itself) block the ability of the survey to determine the mattress positions, then it may be necessary to have more than one angle of survey or use close-up ROV visual inspections. It is also important to check the distance between individual mattresses and at the interface with the structure, as gaps may induce localized scour.
Integrity of the alternative scour protection	ROV visual	E.g. 1 year after installation, periodically afterwards and after significant storm events.	Although the materials of alternative scour protections are generally sufficiently durable for offshore applications, severe events (storms/extreme currents) may affect the integrity of the alternative systems due to wear/tear. Also, shallow waters can have more exposure to sunlight, which could alter the durability of certain materials.
Global and/or edge scour	Sonar / MBES	E.g. 1 year after installation, and periodically afterwards.	Edge scour development, flexibility of mattresses (i.e. no undermining of scour protection) and fixation of bed level.
Scour adjacent to the structure	Sonar / MBES / ROV visual	E.g. 1 year after installation, periodically afterwards and after significant storm events.	Gaps between the structure and mattresses could potentially induce localized scour.
Other damages to the system	Sonar / MBES / ROV visual	E.g. 1 year after installation, periodically afterwards and after significant storm events.	E.g. dropped objects, abrasion due to friction between mattresses, etc.

### Remedial measures

The O&M manual should also include pre-defined remedial actions in case incipient or developing failure is observed. Examples of remedial measures are backfilling, replacing mats, additional mats, etc. These remedial actions should preferably be determined up-front, such that a remedial measure is prepared for all expected possible failure mechanisms of the alternative scour protection. Ideally such actions should be time bounded (e.g. time allowances for the structure to cope with design deviations such as lost support soil). This is an aspect that, when considered at the design stage, can optimize planning and logistics of the remedial actions, and therefore OPEX.

## 9.5 Decommissioning

For the end of life of the structure a decommissioning plan would depend on the requirements from the relevant authorities. Some authorities may not have defined a clear position with regard to alternative or artificial materials as they may have for rock protections. In those cases, it is

recommended to make clear agreements with the authority to prevent surprises at the end of life of the structure. The decommissioning method of an alternative scour protection is dependent on the chosen scour protection method and the condition of the scour protection at the end of life.

As there might be stricter requirements to the decommissioning of alternative scour protections compared to rock protections, it is recommended to already consider the decommissioning approach in the design phase of the scour protection.

Factors to consider in the decommissioning of the alternative systems:

- Sedimentation within or on top of the scour protection (e.g. in case of artificial vegetation and gabion mattresses);
- Possibility of reduced material durability over the lifetime;
- Possibility of pre-installing slings or leaving lifting attachments in place to facilitate recovery of the mattresses at the end of the lifetime.

In some cases, a scour protection may be allowed to remain on the seabed (not be decommissioned), if the relevant local authorities permitted this. For example, this may happen when the scour protection has a clear ecological benefit.

# 10 Artificial vegetation

## 10.1 Introduction

This chapter discusses artificial vegetation as an alternative scour protection solution. An artificial vegetation scour protection consists of a large number of individual fronds that are attached to an anchored frame or a ballasted mattress forming a dense vegetation canopy that is permeable to the flow and sediment. In this chapter, the main working principles of this alternative scour protection solution are discussed in Section 10.2. Then, main characteristics of this protection type are described in Section 10.3. Section 10.4 concerns potential failure mechanisms, whilst Section 10.5 provides some design considerations. Finally, Section 10.6 deals with installation of artificial vegetation.

## 10.2 Description and working principle

Flow through submerged vegetation has been a subject of many theoretical and experimental studies, primarily focusing on vegetation in open-channel flows and coastal areas. It is widely acknowledged that densely populated vegetation causes reduction of near-bed flow velocities due to the flow inhibition and reduces bed shear stresses and sediment transport. In densely vegetated open-channel flows raised riverbeds have been observed and significant amount of sediment can be deposited within the vegetation. In nature this property is not only protecting vegetation from uprooting but promotes retention of nutrients necessary for plant growth.

Above-mentioned properties of vegetation can be utilized in the design of an offshore scour protection; artificial vegetation can be deployed as scour protection that imitates the hydraulic behaviour of natural vegetation. The use of artificial vegetation as scour protection was described by Pilarczyk & Zeidler (1996).

An example of an artificial vegetation scour protection is the frond mat system supplied by Seabed Scour Control Systems Ltd. (SSCS), illustrated in Figure 10.1. An SSCS frond mat has a rectangular shape with flexible edges and rows of buoyant fronds (long flexible strips of polypropylene) attached to these edges. Depending on the fixation method, the edges are either equipped with bed anchors or with flexible ballast tubes filled with shingle. Bed anchors require installation by divers, while the ballasted mattresses can be installed by lowering them in the water by a crane while attached to an installation frame. Several standard sizes of frond mats are available. Quantitative characteristics of the SSCS frond mats are further discussed in Section 8.2.

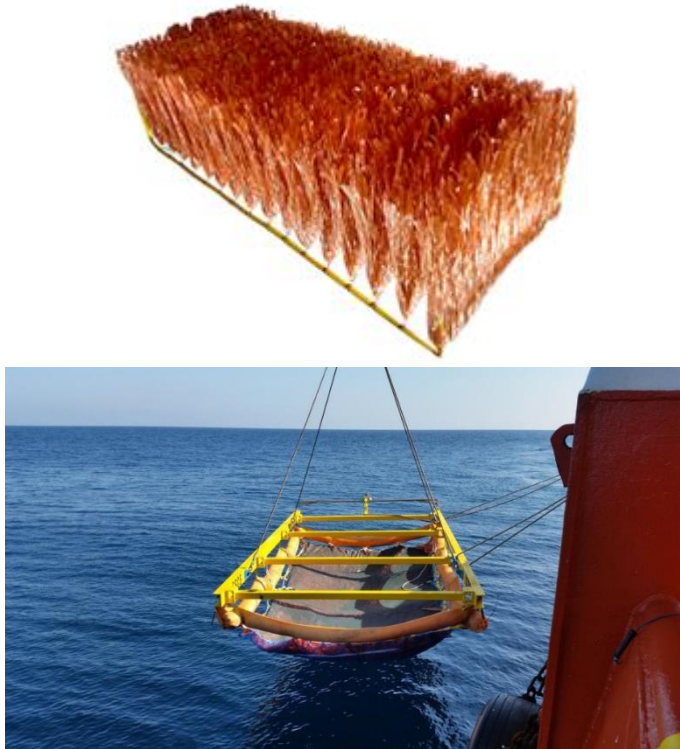


Figure 10.1 Top: SSCS frond mat without ballast tubes. Bottom: SSCS frond mat attached to an installation frame.

FronD mats of SSCS have been deployed as scour and erosion protection in many different applications: as pipeline scour protection in rivers and offshore, as scour protection around jack-up vessel legs, suction pile foundations, monopile wind turbine foundations and met masts, as well as to prevent erosion of river banks. They were also deployed as a scour protection measure in the Arklow Bank offshore wind farm around a met mast and two monopile foundations. According to SSCS, qualitative observations have confirmed that the frond mats were able to stop scour development and promote the formation of sediment banks in these cases. Besides the frond mat of SSCS, Pipeshield has developed a system with fronds on top of a concrete mattress. This system has not been tested within the framework of JIP HaSPro.

Apart from the two examples of the SSCS frond mat and the Pipeshield frond mattress, no other designs are available on the market (to the knowledge of the authors of this Handbook at the moment of writing) and there are no solid guidelines available for the design of this system. The design characteristics of the SSCS frond mat have been applied in multiple projects globally and, according to SSCS, have proven to be effective in combating scour. In order to generate design guidelines and to apply this system more widely around offshore wind monopile foundations and other structures, it is necessary to determine what characteristics of artificial vegetation are most favourable for its scour protection properties. The terms “artificial vegetation” and “frond mats” will both be used in this Handbook chapter almost interchangeably and are not restricted to the description of the SSCS frond mat.

A considerable challenge for the application of the frond mats in the field is the use of artificial materials in the manufacturing of the fronds. If the frond mats are made of plastic materials, consenting authorities may require extra measures to make sure the project is done in an ecologically responsible way. For example, stricter decommissioning guidelines may be applied, and integrity of the scour protection needs to be ensured. However, the material design of the artificial vegetation is beyond the (hydraulic) scope of this project.

## 10.3 Protection characteristics

Parameters of a frond mat scour protection can be subdivided into several groups, namely: system-scale parameters related to the number of frond mats and their positioning around the structure, mat-scale parameters (size, shape, ballast/anchoring parameters, number of fronds and their attachment) and frond-scale parameters (frond length, width, thickness, material density). All of these parameters can have an impact on the performance of the overall frond mat scour protection.

The parameters of the existing SSCS frond mat design can be used as a representative example of an artificial vegetation scour protection system. A summary of relevant parameters for an SSCS frond mat (model T12) is presented in Table 10.1. Other sizes are available from SSCS, i.e. 2.5 x 5 m<sup>2</sup> or 7.5 x 5 m<sup>2</sup> (only the overall size of the mat and the number of frond rows are different between the different mat sizes, with all other parameters remaining the same).

The prototype frond mats of SSCS have a rectangular shape and a full scour protection layout would normally consist of multiple separate mats arranged around the structure to cover the required area. For some applications it may be more favorable to design mats of a different shape (e.g. trapezoidal) in order to cover the area around a structure more effectively with minimal gaps.

SSCS frond mats can be either equipped with seabed anchors or ballast tubes on the perimeter of the mat to ensure its stability. Ballast tubes of SSCS are made of flexible polyester webbing and are filled with shingle.

Table 10.1 Parameters of an SSCS frond mat (model T12).

Parameter	Value
Size	5 x 2.5 m <sup>2</sup>
Frond length	1.25 m
Frond width	50-80 mm
Frond thickness	±60 µm
Number of fronds	~500 per m <sup>2</sup>
Number of rows	17
Distance between rows	0.30 m
Frond material	Low-density polypropylene (LDPP)
Density of frond material	905-915 kg/m <sup>3</sup>
Elasticity modulus of frond material	1.5-2 GPa

## 10.4 Potential failure mechanisms

A frond mat scour protection system is a soft countermeasure against scour that is permeable to the flow. As for any scour protection, its function is to prevent excessive scour development beyond acceptable levels. Failure to fulfil this function constitutes failure of the scour protection.

Failure of the scour protection may be linked to its interaction with the hydrodynamics and sediment erosion processes (hydraulic failure mechanisms), but (especially for alternative systems), there are also failure mechanisms related to the material strength and durability of the scour protection in offshore conditions. The durability of a material component or system is defined as its ability to continue performing adequately in a specific working environment and is therefore a balance between the intrinsic resistance of the material and the aggressiveness of the forces acting in service. According to the frond mat supplier, SSCS, previous offshore experiences have shown that the frond mats are able to withstand degrading forces such as abrasion by sand and ultraviolet exposure. However, project conditions should be assessed with respect to their possible effects on the materials of the frond mats.

In this Handbook we mainly focus on the hydraulic failure mechanisms, but the other failure mechanisms are also important to be considered in the final design.

Potential hydraulic failure mechanisms of an artificial vegetation scour protection (illustrated in Figure 10.2):

- 1 Scour at the structure (pile/cable scour)  
Minimal scour development at the structure may still be acceptable if it is successfully limited by the scour protection and does not exceed the acceptable scour levels. However, if deep scour develops at the structure bed interface or directly in the vicinity of the structure (in the area covered by the frond mats) this constitutes failure of the scour protection. The reason for such failure can be incorrect vegetation parameters (e.g. too low population density or incorrect flexibility of the fronds), but also gaps between the mat and other mats or the structure can lead to scour.
- 2 Stability-related failure (uplift or sliding)  
Uplift of (a part of) a frond mat due to the hydrodynamic action results in an exposed bed, and is therefore regarded as failure. When the lift forces are greater than the gravity force, (a part of) the frond mat will be lifted up. Similarly, sliding or moving of the frond mat will directly result in an exposed bed, which is considered as failure.
- 3 Edge scour  
Edge scour is bound to occur around the protected area and it only constitutes failure if it reaches unacceptable levels. Edge scour is stronger around larger, more rigid and impermeable obstacles, and it is dependent on the ballast tube size and on how densely populated and rigid the frond field is. A too small outer extent of the scour protection may also cause extensive edge scour.

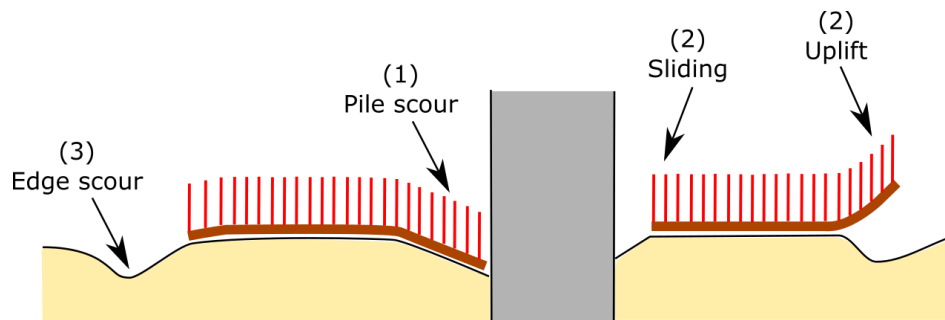


Figure 10.2 Schematic representation of failure mechanisms for an artificial vegetation scour protection

It is important to realize that some parameters of the frond mats may be linked to multiple failure mechanisms. For instance, the size of the ballast tubes can be linked to both stability-related failure mechanism and the edge scour failure mechanism.

Artificial vegetation scour protection can be applied under a wide range of conditions and on different types of bed material. The potential of artificial vegetation is especially high for application on sandy seabed, because of its ability to capture mobile sediment transported from upstream and acquire extra stability by becoming embedded in the seabed.

Fron mats could potentially be applied in areas with seabed morphological changes (sand waves), if they are flexible enough to follow the lowering of the bed at the edges of the protection, although no practical experience with frond mats in areas with active morphology is known to date. Seabed lowering around frond mats increases the risk of sliding or undermining of the mattresses at the edges and may reduce the effectiveness of the protection if the mattress is undermined significantly.



## 10.5 Design considerations

### 10.5.1 Introduction

There is limited experience in applying frond mats with different parameters around offshore structures. Moreover, there are no design guidelines to support the design choices of a frond mat. Model tests performed within JIP HaSPro were therefore aimed at exploring what design choices would be optimal in a frond mat and providing a first estimate and proof-of-concept for frond mats. The resulting considerations should not be viewed as all-conclusive and definitive, but as an indication for the design. Validation by physical model tests will still be needed where the available results of JIP HaSPro are not sufficiently conclusive.

In the sections below the design considerations are discussed per failure mechanism (for hydraulic mechanisms), which are illustrated with an example for monopiles. Subsequently special considerations are given for other types of structures.

### 10.5.2 Design considerations to prevent scour at the structure

A functional scour protection should prevent scour at the structure (e.g. at monopile face or suction pile). In case of the artificial vegetation scour protection this means that the vegetation should prevent washing away of sand around the foundation, which is (in theory) achieved if the near-bed flow in the vicinity of the structure is sufficiently reduced by the vegetation.

#### Key design parameters

Several key parameters of the artificial vegetation scour protection are identified for the effectiveness of the protection in preventing scour. Assuming the protection is stable (e.g. remains in place in all hydrodynamic conditions), the correct vegetation parameters (frond length, width, thickness, material and population density) are important for an effective scour protection. In addition, mat placement is important. For example, according to SSCS, any gaps between the mats should be no greater than 0.5 m to avoid scouring.

#### Design considerations for key parameters

Vegetation parameters define the reconfiguration of the vegetation under hydrodynamic loading and the reduction of near-bed velocity within the frond field. For example, a dense field of very flexible fronds will behave differently in the flow than a field of very stiff (or very buoyant) fronds. All of these parameters can be considered in terms of flexibility (degree of bending, as a result of material stiffness and buoyancy) of fronds in the flow and in terms of the frontal area of the fronds (which is linked to the drag and friction exerted by the fronds on the flow). The vegetation of the frond mats can therefore be designed for a certain degree of flexibility and a total frontal area of fronds.

**FronD length** is an important parameter that affects both the degree of bending of the fronds and the frontal area. Frond length in relation to the structural dimensions (i.e. monopile diameter or stick-up height for piles with limited stick-up height) is also important for the behaviour of the fronds in the direct vicinity of the pile face. The ratio between the frond length and the monopile diameter employed in the medium-scale physical model tests in JIP HaSPro was 1:4, based on field examples of SSCS and scaling considerations. Much shorter fronds in relation to pile diameter may prove to be less effective against scour, in which case it would be recommended to verify the effect of significantly decreased relative frond length by means of model tests.

**FronD flexibility** (degree of bending) of fronds is defined by the frond length, cross-section, material (elasticity modulus and density) and the hydrodynamic conditions. One way to estimate the degree of bending of a frond under the given flow conditions is to use the method proposed by Luhar & Nepf (2011) where the effective blade length (bent height of a frond relative to the original frond length) is defined by the dimensionless Cauchy and buoyancy numbers. Essentially the Cauchy number is the ratio between the inertial force and the elastic force, and the buoyancy number is the

ratio between the buoyancy force and the elastic force. For a frond with rectangular cross-section these dimensionless numbers can be calculated as follows:

$$Ca = \frac{1}{2} \frac{\rho_w \cdot C_D \cdot b \cdot U_c^2 \cdot l^3}{EI} \quad (28)$$

$$B = \frac{\Delta\rho \cdot g \cdot b \cdot t_v \cdot l^3}{EI}$$

where:	Ca	=	Cauchy number	[-]
	B	=	Buoyancy number	[-]
	$\rho_w$	=	density of fluid	[kg/m <sup>3</sup> ]
	$C_D$	=	drag coefficient of the stems	[-]
	b	=	width of the stem as seen by the flow	[m]
	U	=	flow velocity	[m/s]
	l	=	length of the stem	[m]
	E	=	elasticity modulus of the vegetation material	[Pa]
	I	=	second moment of area of the vegetation cross-section	[m <sup>4</sup> ]
	$\Delta\rho$	=	difference in density between fluid and the vegetation material	[kg/m <sup>3</sup> ]
	g	=	gravitational acceleration	[m/s <sup>2</sup> ]
	t	=	thickness of the vegetation stem	[m]

It is noted that the considerations by Luhar & Nepf (2011) are limited to steady currents. Subsequent studies by Luhar & Nepf (2016) and Jacobsen et al. (2019) have analysed relevant non-dimensional parameters in wave-dominated environments. These have not been considered within the scope of JIP HaSPro. Figure 10.3 shows the influence of the Cauchy number and Buoyancy number on the effective blade length for a single frond under steady flow. The blade remains upright in the flow for Ca lower than 1 and is fully bent for large Ca numbers in the order of 10<sup>3</sup>. For intermediate Ca numbers the buoyancy effect (increasing B value) leads to reduced degree of bending. Estimating the bending degree of fronds that are arranged in a dense vegetation field is more complex, because the ambient flow parameters for each single frond depend not only on the oncoming hydrodynamics in front of the vegetation, but also on the population density of surrounding fronds. Also, in oscillatory flow (waves) the bending degree of fronds has a more complex dependency on the hydrodynamics. However, the Ca and B numbers can be used as an indication of the frond flexibility.

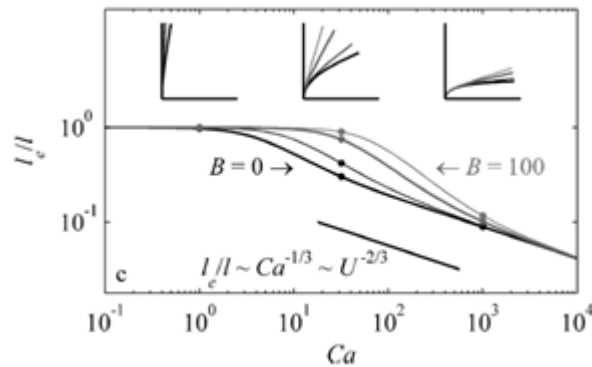


Figure 10.3 Effective blade length as a function of Cauchy and buoyancy numbers for a single frond (Luhar & Nepf, 2011).

In the JIP HaSPro model tests the effectiveness of frond mats with different degrees of flexibility of vegetation was compared. Three types of fronds were defined according to their flexibility: stiff, medium and flexible. Stiff fronds were characterized by Ca numbers between 10 and 60, medium -

by  $Ca$  in the range 100 – 700, and flexible – by  $Ca$  in the range 1000 – 6000. The upper  $Ca$  values were calculated based on the total near-bed velocity in wave-current conditions (sum of wave- and current-induced velocities).

Indicative tests on scour development for different types of fronds were performed in JIP HaSPro. Some qualitative results are illustrated in Figure 10.4. In the model tests it was found that medium fronds performed most optimally in the vicinity of the monopile face. In very stiff fronds scour can develop upstream of the pile due to the downflow at the pile face that can relatively easily penetrate the frond field and cause scouring. In very flexible fronds, on the other hand, the fronds can bend around the pile by the amplified flow and the downflow at the pile face, and part of the pile face may become exposed, leading to scour. This scour, however, does not extend far from the pile and remains within  $D/4$  from the pile face, and is expected to have a much smaller equilibrium scour depth than if no scour protection was installed. In other words, the maximum depth of scour in very flexible vegetation may still be acceptable to the designer.

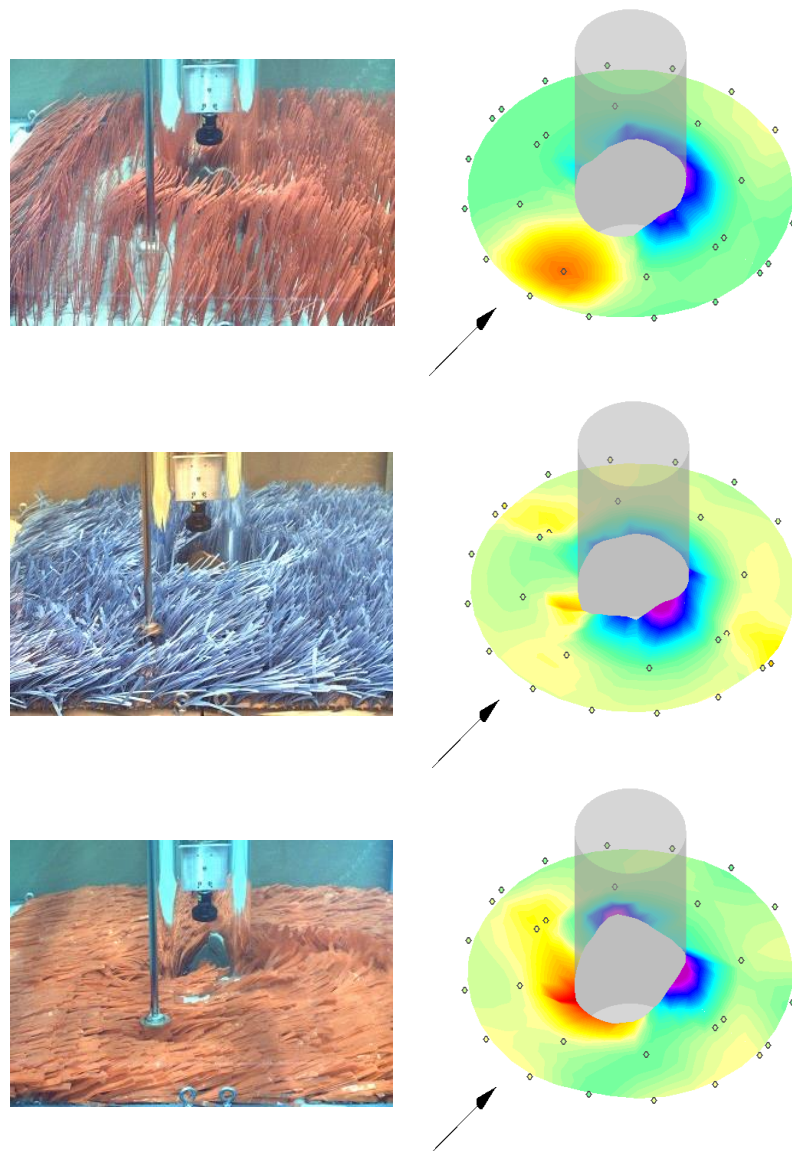


Figure 10.4 From top to bottom: stiff, medium and flexible fronds. Left figures show the bending of model scale fronds under  $U_c = 0.3$  m/s steady current (model scale, current-only tests), and right figures show the bathymetry around the pile after a series of current-only tests.

Concluding, the tests indicated that the most optimal frond type for the interface scour prevention is the medium flexibility of fronds with Ca in the range of 100-700. Ideally an artificial vegetation scour protection would consist of medium flexibility fronds near the pile face (with D/4 from the pile) and more flexible fronds further away.

**Frontal area** of the fronds and consequently the population density can be expressed through the dimensionless frontal area as:

$$a = l \cdot n \cdot b \quad (29)$$

where:	a	=	dimensionless frontal area	[-]
	l	=	frond length	[m]
	n	=	population density (number of fronds per m <sup>2</sup> )	[1/m <sup>2</sup> ]
	b	=	frond width	[m]

The dimensionless frontal area of an SSCS frond mat is equal to 40. In the scale model tests in JIP HaSPro flexible fronds with the same frontal area were also tested, yielding positive results. Also, medium stiff fronds with the dimensionless frontal area of 16 were tested, where no additional issues were encountered.

Concluding, it would be recommended to apply frond mats with the minimum dimensionless frontal area in the order of 20 - 40, however it is difficult to estimate the optimized minimum value for this parameter based on the limited data available.

The effect of different frond length to width ratios was not explicitly investigated in model tests. Both in the prototype fronds of SSCS and in the scale model tests this ratio remained equal to approximately 16. A similar value would be recommended for other frond mat designs.

#### Hydrodynamic conditions

Model tests were performed with artificial vegetation scour protection around a monopile in a wave-current basin with mobile bed to investigate the effectiveness of the scour protection under current-only, wave-only and storm conditions. These tests were performed on a scale of 1:30 and are described in a dedicated test report (Deltares, 2023i). A first estimate of the expected scour development in artificial vegetation can be made based on these test results, keeping in mind the relevant scale effects.

#### Physical model tests considerations

Scaling of artificial vegetation for physical model test purposes is complex. Full Froude (linear) scaling is often not possible due to material and manufacturing limitations. It is advised to apply linear scaling where possible (e.g. scaling of frond length, frond mat dimensions). For the scaling of frond population density, the dimensionless frontal area can be used as a scaling parameter. Correct scaling of vegetation flexibility is crucial for such model tests, and it can be done considering similarity based on Cauchy and buoyancy numbers.

As in all scale model tests with sediment, an important scale effect in scour tests with artificial vegetation is associated with the sediment mobility (grain size). The sediment size cannot be scaled in model tests simultaneously with the Froude scaling of hydrodynamic conditions because that would lead to very small grain diameters with cohesive erosion behaviour. This means that the sediment underneath the vegetation scour protection is less mobile in the model than in the field, with larger timescales of scour development in the model than the Froude-scaled timescales. This scale effect needs to be kept in mind when evaluating the quantitative test results.

### 10.5.3 Design considerations to prevent stability failure

In order to perform its scour protection function, the frond mat system needs to remain stable, i.e. to withstand the hydrodynamic loading acting on the vegetation without uplift or displacement of the frond mats. Stability failure of frond mats can be prevented by sufficient anchoring or ballasting. Stability is also increased by build-up of sediment within a frond mat which is expected to occur after the frond mat installation (how quickly the build-up occurs is dependent on the hydrodynamic conditions after the mat installation).

Frond mats are currently most commonly stabilised by ballasting. Ballast can be pre-attached to the frond mat before installing it using a deployment frame. A successful ballasting system for a frond mat needs to have adequate weight and needs to be flexible in order to be able to adapt to uneven seabed and edge scour. Flexible tubes filled with small rock or shingle, as used by SSCS, can satisfy both requirements provided that the ballast weight is selected correctly.

Current standard design of SSCS for the 5.0 x 2.5 m rectangular frond mat with filled weighted edge ballast tubes has a total weight of approximately 750 kg (source: SSCS). In this design, the ballast consists of six ballast tubes around the perimeter of the mat, each with a weight of approximately 115 kg. After installation progressive sediment build-up is expected to occur resulting in a fibre-reinforced sediment bank over the froned area, that provides additional stability.

The required ballast weight is dependent on the severity of the hydrodynamic conditions at the relevant location. On sandy seabed frond mats will become more stable over time after they capture sufficient sediment. The stability of the mats in the period between their installation and formation of the sediment banks inside the vegetation area still needs to be ensured by proper ballasting.

Since very little information is available on how to design the ballast weight for frond mats, it is recommended to perform extra model tests or field experiments to this end. Forces acting on the frond mats are associated with drag and lift forces acting on individual fronds, therefore a better understanding and scaling of these forces should be a priority in model tests.

When designing the ballast system for a frond mat, it is also important to ensure that the gaps between the mat and the ballast tubes, as well as between neighbouring mats with ballast at the edges, are very limited. Tests in the Delta Flume within JIP HaSPro (Deltares, 2023i) have shown that local scour can occur along the ballast tubes.

### 10.5.4 Design considerations to prevent edge scour

Edge scour around the frond mat scour protection and in between the individual frond mats may lead to failure of the scour protection if it negatively affects the scour at the foundation or if it causes sliding of the mats into the edge scour holes.

Parameters that have an influence on the development of edge scour are the extent of the scour protection, dimensions of the ballast tubes (especially their height above seabed), frond flexibility and length.

Edge scour around frond mat scour protections is especially a concern in strong-current-dominated conditions and is more pronounced around protections with less flexible fronds. The larger the bent height of the fronds in the flow, the larger the edge scour depth. Edge scour in current-only conditions is illustrated in Figure 10.5 around fronds of medium flexibility. At the sides of the protection the frond mats are visibly leaning in the edge scour hole, this situation in the field may make the frond mats less stable (in the model tests frond mats were anchored). At the same time, the frond mats with flexible edges are able to follow changes in bed level due to edge scour very well, without becoming severely undermined.

Notable is the significant accretion of sediment in the wake of the vegetation in current conditions (see Figure 10.5). This accretion is also observed in storm conditions with a following current. This effect may result in edge scour backfilling at locations where the direction of waves and currents are highly variable.

Insufficient extent of the scour protection around a monopile leads to increased edge scour due to velocity amplification around the structure. In physical model tests of JIP HaSPRO a diametral extent of 2.5D was applied (see Figure 10.5), which proved to be too small to limit the effect of the pile on the edge scour development. When edge scour is a concern, it is advisable to increase the diametral extent to 3D or larger.

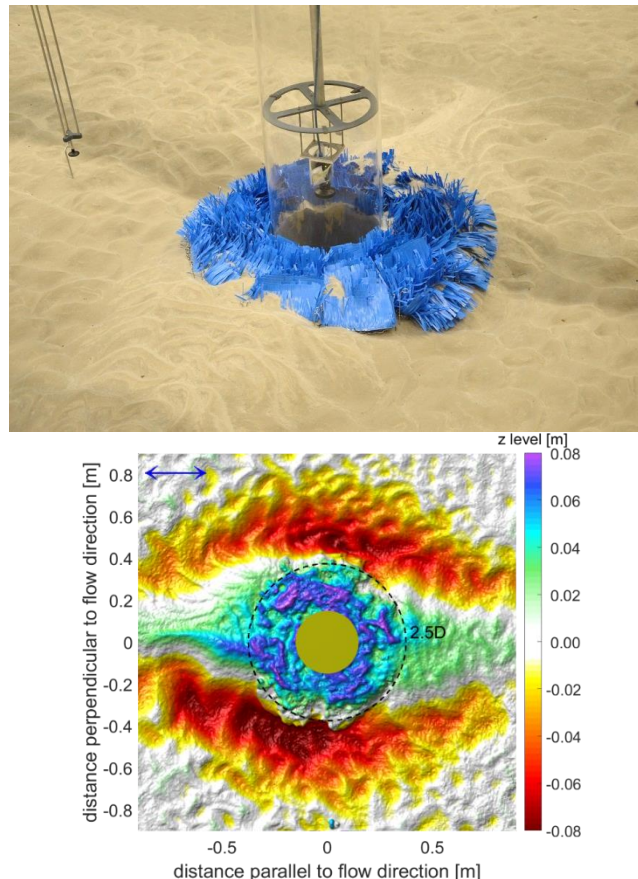


Figure 10.5 Edge scour around an artificial vegetation scour protection in current-only scale model tests. A photo (left) and a bathymetry plot derived from stereophotography (right).

### 10.5.5 Design considerations for different foundations

FronD mats can be applied at other types of foundations than monopiles, e.g. at suction bucket jackets (SBJ), gravity-base structures, piled jackets, cable crossings etc. Little information is available in the public domain regarding application of frond mats around these structures, (other than that obtained by SSCS completed projects). Below several examples of structures are considered.

#### Suction bucket jackets

A series of model tests were performed in JIP HaSPRO with artificial vegetation around a suction bucket jacket (SBJ). In the model tests trapezoidal frond mats were applied around the buckets of an SBJ structure with a diametral extent of 2.5D (see Figure 10.6). The length of the fronds was larger than (approximately double) the stick-up height of the buckets. A range of conditions were tested including current-only and wave-current conditions (following and opposing currents). Details regarding this programme can be found in the dedicated test report (Deltares, 2023i). During this

test programme no scour was observed within the areas protected by the fronds; on the contrary, only sediment accumulation was observed. This is likely due to the large frond length compared to the bucket stick-up height (frond length was double the stick-up height in the model tests). At the same time, edge scour was observed around the frond mats and especially at the unprotected centre of the structure footprint, which would be a point of attention for designing a frond mat scour protection for a jacket structure.

Model tests have shown that both very flexible and medium stiff vegetation were able to protect the suction buckets from scour, with the very flexible vegetation resulting in a more evenly distributed sediment build-up. Compared to monopile foundations, the downflow upstream of the structure is much less pronounced in case of the suction bucket jacket, due to the bucket tops acting as collars with small overall height. The absence of the strong downflow in front of the structure makes very flexible vegetation effective as a scour protection for such a structure.

Concluding, it would be recommended to apply flexible vegetation around the buckets of the suction bucket jacket. The layout must ensure minimal gaps between the mats and the structure, as well as between the neighbouring mats. The extent of the protection around each bucket needs to be selected based on the geotechnical requirements considering the potential for edge scour in the unprotected part of the SBJ footprint.

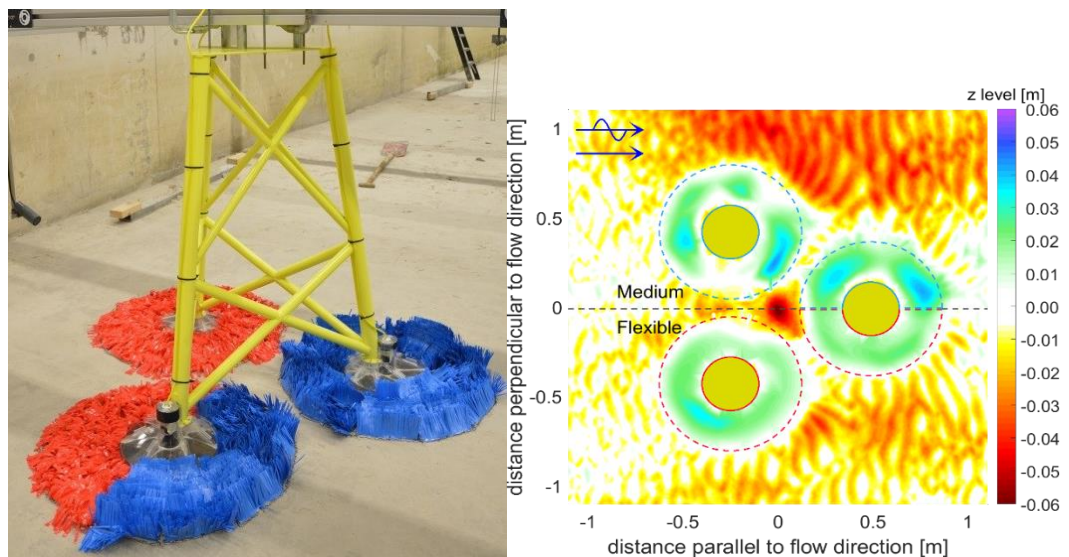


Figure 10.6 Scale model tests with artificial vegetation scour protection around a suction bucket jacket. Left: protection layout with two different frond types (medium and flexible). Right: bathymetry after a storm test (derived from stereo photography and scour pin measurements within the frond field).

For other foundations with suction piles, spud cans or geometrically similar foundations with collar-like footings artificial vegetation can also be considered and is likely to be effective. However, structure-specific assessment and model tests are always recommended.

#### Cable crossings

Frond mats can also be used to prevent scour at cable crossings. The layout of the frond mats and the extent of the protection would be dependent on current speed, sediment type, cable geometry and would therefore be determined on case-by-case basis. Figure 10.7 schematically shows how frond mats can be placed at a cable to mitigate scour. It is important that the mats are placed on a horizontal surface, which makes them more stable and promotes sediment build-up within the mats.



Figure 10.7 Schematic representation of frond mat placement around a cable / pipeline (Source: SSCS).

## 10.6 Installation

FronD mats are mostly installed after installation of a foundation (post-installation), but concepts involving self-installed frames are also being developed. Pre-installation of mats is not commonly considered; therefore it will not be described in this section. Below some specific aspects of frond mat installation are addressed.

### Post-installation of frond mats

The installation procedure, as commonly used by the supplier SSCS, is illustrated in Figure 10.8 and can be outlined as follows:

1. Manufacturing of frond mattresses;
2. Transport of the mats and the deployment frame by container to the installation vessel;
3. Manual filling of weighted edge tubes, final assembly of mat and attachment to deployment frame;
4. Lifting, overboarding and lowering by crane of deployment frame with frond mat attached;
5. Positioning on seabed using crane in conjunction with diver or ROV to ensure accurate placement;
6. Release frond mat and retrieve deployment frame by which also the protective net covering will be removed activating the fronds.

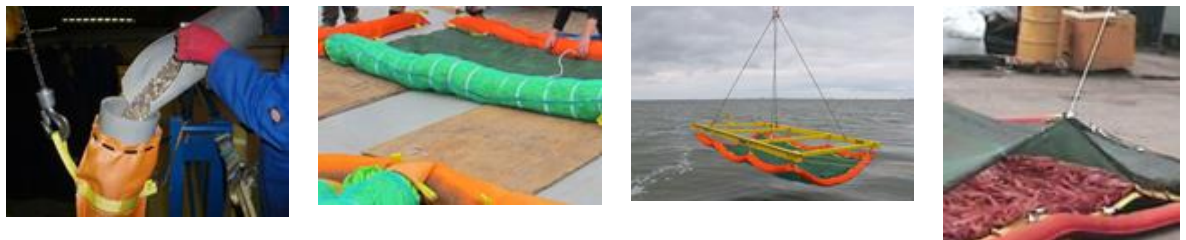


Figure 10.8 SSCS weighted frond mats installation procedure

When post-installing the frond mats, it is important to consider that some scour may have occurred in the time between the structure and the scour protection installation. In general, minor scour at the pile would not pose a problem for the frond mats, when the ballasting tubing around the mat is flexible enough to follow the outline of the scour hole, and when the stability of the mat is not threatened.

### Self-installable systems

Methods for installing frond mats simultaneously with the structure itself have been developed for application at suction pile foundations and pre-piled jackets. SPT Offshore has developed and applied in the field an umbrella-like self-deploying system with SSCS frond mats for use with suction piles, while a piling template placing frond mats could be used for pre-driven piles. Such systems benefit from enhanced control of quality and tolerances thanks to full onshore pre-assembly and furthermore provide immediate scour protection around the entire (suction) pile. The scour protection system and installation procedure designed by supplier SPT Offshore is illustrated in Figure 10.9 and can be outlined as follows:



1. Manufacturing of frond mats and of steel outriggers for deployment frame;
2. Transport of mats and deployment frame by container to assembly / mobilisation yard;
3. Filling of weighted edge tubes (or preparing other means of ballast), assembly of deployment frame with frond mats, connection to the suction piles;
4. Transport of suction pile jacket outfitted with scour protection system, lifting and lowering by heavy-lifting vessel;
5. Suction installation during which the scour protection system will automatically deploy.

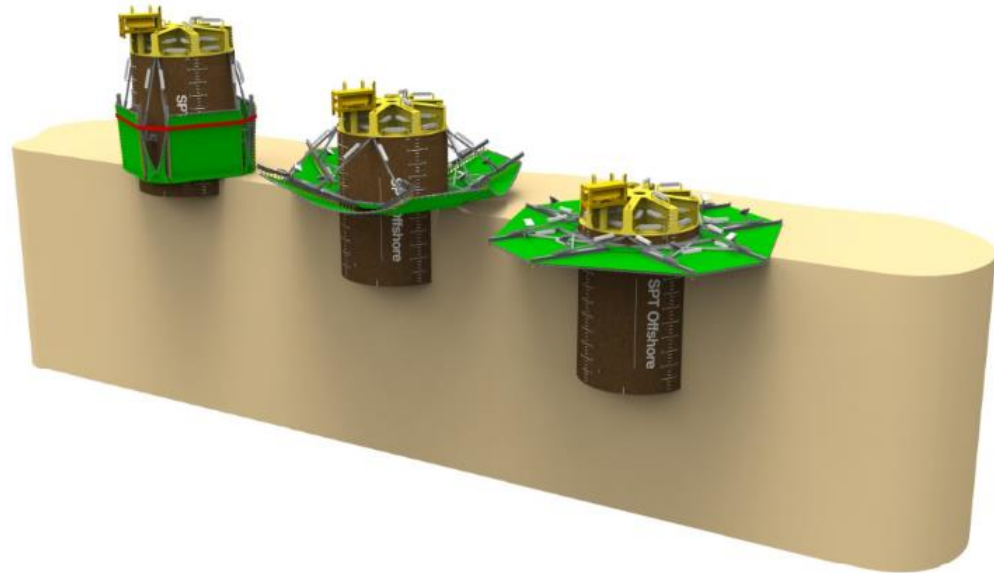


Figure 10.9 The self-deploying scour protection system installation for a single pile by SPT Offshore.

Model tests were performed at Deltares within JIP HaSPro to investigate the behaviour and failure mechanisms of a self-installable scour protection system using a lowering frame. In the Delta Flume the test set-up depicted in Figure 10.10 was used to study the two critical phases during installation: the lowering through the splash zone and the unfolding at the seabed. The tests were performed on a scale of 1:6 at hydrodynamic conditions representative for operational wave conditions (irregular waves up to  $H_s \approx 2.5$  m), in part combined with tidal current schematised by a long wave (Deltares, 2023a).

During the tests it was observed that installation can be successfully executed at operational wave conditions up to  $H_s = 2.5$  m (this value is specific to the test setup as it likely depends on the weight of ballasting). However, the presence of a background current can hamper the unfolding process. Therefore, the risk of uneven deployment should be assessed and mitigated if required, e.g. by planning installation during slack tide or by structural adjustments that allow deployment in higher currents (e.g. a push out rod in the SPT Offshore design).

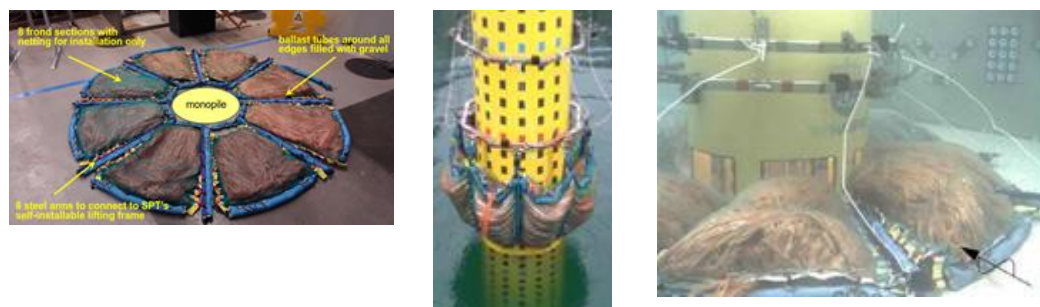


Figure 10.10 Self-installable system test set-up in Delta Flume

# 11 Block, gabion and ballast-filled mattresses

## 11.1 Introduction

Besides artificial vegetation, most alternative scour protection systems consist of weighted mattresses, which are placed on the seabed to prevent scour around subsea structures or protect vital infrastructure (pipelines, cables). In this chapter, three of these mattress systems are discussed: block mattresses, gabion mattresses and ballast-filled mattresses.

In general, the working principle of these mattresses, their failure mechanisms and design considerations are very similar. Therefore, this chapter will discuss all three mattresses combined. Where relevant, separate sections are dedicated to specific mattress types or additional comments are provided to highlight characteristics of specific mattresses.

Section 11.2 provides an overview of the working principles of the various kind of mattresses that are considered in this handbook. Generic protection characteristics are described in Section 11.3, followed by an overview of potential failure mechanisms in Section 11.4. Design considerations are discussed in Section 11.5, and guidance for installation is provided in Section 11.6.

## 11.2 Description and working principle

### 11.2.1 Block mattresses

A block mattress consists of a matrix of concrete blocks connected to each other (usually with a polypropylene rope or a geotextile). Block mattresses are very common in protection of hydraulic boundaries, such as river beds, embankments, flow outlets, etc. They are also widely used within the offshore industry to protect subsea structures, pipelines and cables. Some examples are given in Figure 11.1. Block mattresses are characterised by their flexibility (ability to follow different shapes), permeability (open to water) and relatively small height (compared to rock protections). A key feature of concrete block mattresses is their ability to withstand wave conditions in excess of the threshold for block uplift, because a single block cannot be moved without moving other nearby blocks.



Figure 11.1 Examples of block mattress functions: boat landing (left, [www.conteches.com](http://www.conteches.com)), embankment protection (middle, [www.acfenvironmental.com](http://www.acfenvironmental.com)) or pipeline protection (right, [www.geosynthetica.net](http://www.geosynthetica.net)).

Concrete block mattresses are available in various shapes and sizes, dependent on the manufacturer but also on the application. For offshore applications they are usually implemented without a geotextile, while a mattress with a geotextile is more common for inland waterway or revetment applications. The advantage of a mattress with geotextile is that there is no need for an additional filter layer to prevent erosion through the blocks (winnowing), which results in a very thin

protection layer. On the other hand, a geotextile could reduce the stability since the overall permeability of the mattress decreases.

On the current offshore market block mattresses are mainly used for stabilization of offshore cables. As a scour protection (either at a monopile or over cables) block mattresses have found very limited application yet. Besides the potential advantages mentioned in Section 9.2, block mattresses can offer the following possible advantages compared to a traditional rock protection:

- Relatively thin protection layer, which limits the edge scour and secondary scour development, which in turn is beneficial for the required extent of the protection and the cable burial depth;
- Enhanced stability, by virtue of connection between adjacent blocks
- Dependent on the situation, potentially easy to remove.

### 11.2.2 Gabion mattresses

A gabion mattress is a double-twisted wire mesh container uniformly partitioned into internal cells with relatively small height in relation to other dimensions. The base, diaphragms front, and end sides of the unit are usually manufactured from one continuous panel of mesh; the base is folded onto itself at regular intervals to form double diaphragms that are secured with spirals. The units are filled with stone to form flexible, permeable, monolithic structures. Gabion mattresses are very common as protection of hydraulic boundaries, especially in high flow velocity conditions or under wave attack. Main (hydraulic) applications are river banks, channel linings and flow outlets. Some examples are given in Figure 11.2. Gabion mattresses are characterised by their flexibility (ability to follow different shapes) and permeability (very open to water).



Figure 11.2 Examples of gabion mattress functions ([www.maccaferri.com](http://www.maccaferri.com)): stepped weir (left), river bank protection (middle) or scour protection at a bridge(right).

The working principle of gabions is very similar to loose rock scour protections: flow reduction within the rock layer to prevent erosion of the base particles. However, compared to a loose rock scour protection the rock layer is entrapped within the wire mesh, preventing loss of rock material or significant deformation to the rock layer itself. Gabion mattresses can furthermore be implemented with a geotextile, which can easily be attached to the wire mesh. The advantage of a mattress with geotextile is that the interface stability criterion is fulfilled by the geotextile rather than the rock layer in the mattress. This is expected to result in a very thin protection layer (mattress thickness), as the thickness now solely depends on the external stability of the mattress.

As an offshore scour protection (either at a monopile or over cables) gabion mattresses have found very limited application yet. Nevertheless, it could be a promising solution to prevent scour around offshore structures, as they are also applied as an erosion mitigating system in many land-based protections. Besides the potential advantages mentioned in Section 9.2, gabion mattresses can offer the following possible advantages compared to a traditional rock protection:

- Relatively thin protection layer, which limits the edge scour and secondary scour development, which in turn is beneficial for the required extent of the protection and the cable burial depth;
- Automatic rock stability due to entrapment within wire mesh, while maintaining permeability.

- Possibilities to add ecological elements within the gabion (see Chapter 0 for more information).

There is a lot of knowledge on the design of gabions retention structures at hydraulic boundaries. However, to the knowledge of the authors of this Handbook (at the moment of writing), there are no guidelines available for the application of a gabion mattress scour protection in offshore conditions. In order to investigate the feasibility of gabion mattresses as an offshore scour protection and to apply this system more widely around offshore wind monopile foundations and other structures, it is necessary to assess the performance of gabion mattresses in offshore conditions and what characteristics have a positive or negative effect on its scour prevention functionality.

### 11.2.3 Ballast-filled mattresses

A ballast-filled mattress is a new alternative scour protection method for monopile and cable protections. It consists of an impermeable (generally watertight) outer layer, with an empty compartment in between, which can be filled with a certain substance. The method is loosely based on conventional air mattresses but are filled with a heavier substance (for instance water, bentonite, slurry, etc.) to keep it on the seabed and protect the bed against scour during hydraulic loading. Alternatively, it can be filled with a granular material such as sediment. An impression of a ballast-filled impermeable mattress around a monopile is provided in Figure 11.3.

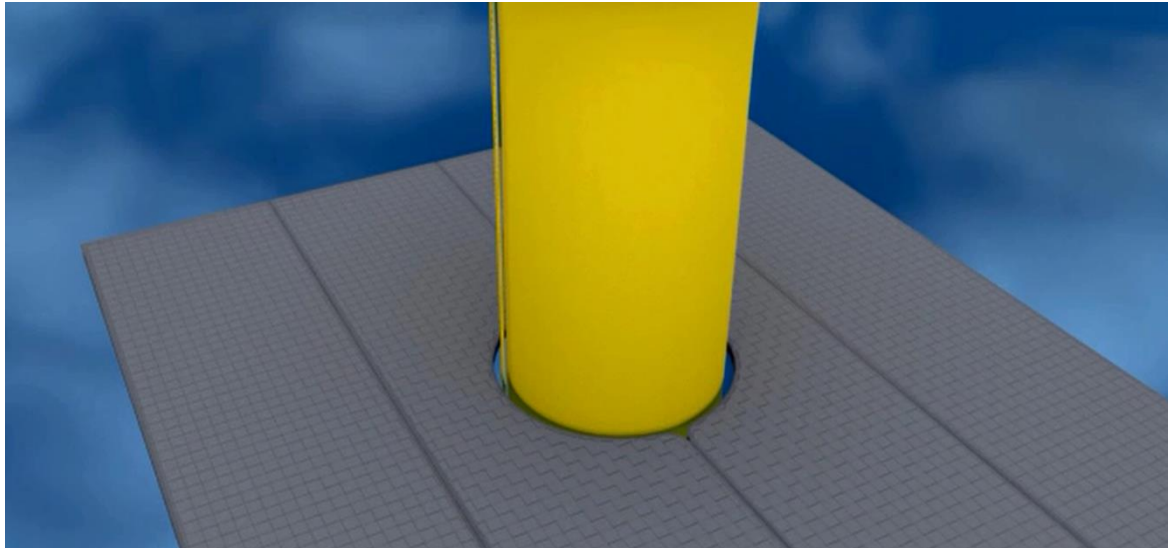


Figure 11.3 Impression of a ballast-filled mattress around a monopile.

This method is a concept, as it has not been applied in prototype conditions yet. Nevertheless, there is a lot of similarity with for instance sandbags or geo-tubes (material enclosed in a sand-tight material). With an impermeable shell, there is furthermore no need for a geotextile to ensure the interface stability.

Besides the potential advantages mentioned in Section 9.2, ballast-filled mattresses can offer the following possible advantages compared to a traditional rock protection:

- Relatively thin protection layer, which limits the edge scour and secondary scour development, which in turn is beneficial for the required extent of the protection and the cable burial depth;
- Potentially installable during or immediately after monopile installation;
- Dependent on the situation, potentially easy to remove.

## 11.3 Protection characteristics

### 11.3.1 Block mattresses

Concrete block mattresses can be split into two categories, both of them made by specific marine grade concrete to deliver consistent technical performance of the mattresses:

- Cable-connected blocks
- Geotextile-bonded blocks

#### Cable-connected blocks

Numerous cable-connected block systems are available, and the blocks can be made in a variety of shapes and thicknesses. Blocks to be cabled usually have pre-formed holes cast in them for placement of the cable, although some systems are manufactured with the blocks cast directly onto the cables; the holes should be smooth to prevent damage to the cable. The blocks may be open cell or closed cell; open-cell block systems provide an overall open area ranging from 17 to 23 percent for the system. The most widely used connections consist of polypropylene cable and stainless-steel cable.



Figure 11.4 Cable-connected block mattress (courtesy of Maccaferri).

#### Geotextile-bonded blocks

With such systems, the blocks are connected directly to a geotextile mat, usually by casting the blocks. The geotextile, preferably a woven polypropylene fabric, must be adequately strong as a connector and should also serve as a protective filter.



Figure 11.5 Geotextile-bonded block mattress (courtesy of Maccaferri).

Both categories (cable-connected and geotextile-bonded) of block mattresses are available in various shapes and sizes, dependent on the manufacturer but also on the application. Just for offshore purposes (currently mainly protection and stabilization of pipelines) there are already many different suppliers of block mattresses. Compared to non-offshore applications the offshore block mattresses are quite similar, except for their dimensions. Similar block shapes and connection types are applied in an offshore environment while non-offshore mattresses have more variety in shape (non-tapered, open cells, etc.) and connection type (steel cable, geotextile, etc.). This can be explained by the current main offshore application of block mattresses: pipeline stabilization. This requires a certain flexibility (flexible connections, large angle possibilities between the blocks) in the mattress to follow the pipeline shape, resulting in similar designs.

A number of proprietary and non-proprietary designs have been developed, typically utilizing square or rectangular blocks ranging from 0.3 to 0.6 m in horizontal dimensions (length and width) and 0.15 to 0.45 m in height. Blocks are often tapered, both for ease of construction and to improve stability. In keeping with the relatively modest design loads anticipated, the concrete blocks are generally not reinforced. Typically, the standard concrete density is 2400 kg/m<sup>3</sup>.

For cable-connected block mattresses typical unit sizes are: 3 to 6 m length, 2 to 3 m width, 0.15 to 0.45 m thickness. For geotextile-bonded block mattresses typical unit sizes are: 3 to 8 m length, 2 to 4 m width, 0.15 to 0.3 m thickness. For both types of mattresses generally larger units or different shapes (trapezoid mattresses or mattresses with a rounded edge) can be manufactured in case of project-specific needs. Furthermore, variations in design have been developed resulting in:

- concrete blocks with increased density to improve stability (up to 4800 kg/m<sup>3</sup>);
- tapered and wedge edges for stability and over-trawlability;
- introduction of synthetic fronds to encourage the build-up of seabed material in areas of known seabed mobility and scour (see Chapter 10).

For geotextile-bonded block mattresses the geotextile acts as a filter, preventing wash-out of sediment through the mattress. These mattresses can be constructed with an overlap band (i.e. an additional extension of the geotextile on the edge of the mattress). This can help realise a sand-tight transition when the edge blocks of the adjacent mattress are placed on top of the overlap.

### 11.3.2 Gabion mattresses

Gabion mattresses are available in various shapes and sizes, dependent on the manufacturer but also on the application. Here, two different types are distinguished: box gabions and gabion mattresses, also see Figure 11.6. Please note that in the remainder of this handbook the different types are interchangeable.

Like many other construction technologies, gabion mattresses require proper engineering, design, and installation to perform at their best and this is particularly so in high-energy hydraulic environments. The selection and placing of suitable stone fill and the specification of appropriate wire mesh size, wire diameter and corrosion protection are important steps in this process. Some of the important properties of hexagonal double-twist wire gabions and the hard, durable stone used to fill them are presented below.

#### Box gabions

Box gabions are double twisted steel wire mesh boxes made with a base panel and lateral sides, uniformly partitioned into internal cells and filled with durable stone. In order to reinforce the structure, all mesh panel edges are selvedged with a wire having a greater diameter than the mesh wire. Box gabions are filled with stones at the project site to form flexible, permeable, monolithic structures such as retaining walls, channel linings and weirs for erosion control projects; gabions

can be pre-filled and then placed at the final position using a crane. A typical box gabion would have dimensions of 2 m (length) × 1 m (width) × 1 m (height) and comprise of mesh type 8x10.

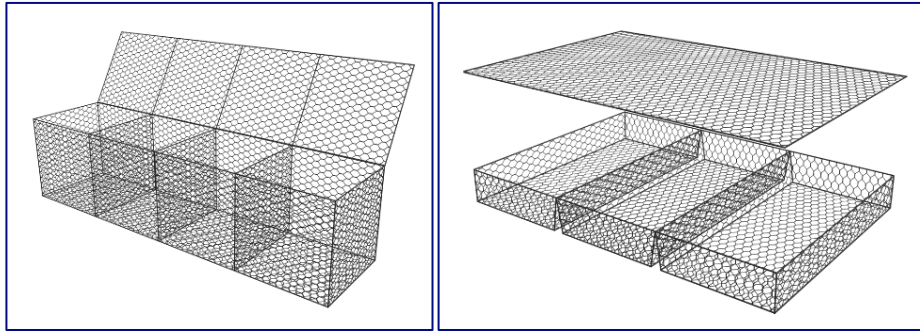


Figure 11.6 A typical box gabion (left) and gabion mattress (right).

### Gabion mattresses

Gabion mattresses are double twisted steel wire mesh units with large dimensions and small thickness, provided with internal diaphragms with a nominal spacing of 1.0 m and a separated lid which can also be supplied in rolls. Gabion mattresses are filled with stones at the project site to form flexible, permeable, monolithic structures such as river bank protection and channel linings for erosion control projects. The base, diaphragms, front, end and sides or gabion mattresses are manufactured from one continuous panel of mesh. The base is folded onto itself at 1.0 m intervals to form double diaphragms that are automatically secured with spirals, prior to folding up the sides and securing to the diaphragms. To reinforce the unit, all mesh panel edges are selvedged with a wire having a greater diameter than the mesh wire. A typical mattress would have dimensions of 6 m (length) × 2 m (width) × 0.30 m (height) and comprise of mesh type 6x8. Gabion mattresses specifically designed for underwater installations have pre-assembled geotextile coupled with an extra wire mesh panel with extend side bands on two sides below the mattress units and are manufactured to be pre-filled and then laid in their final position (see Figure 11.7 for a schematisation).

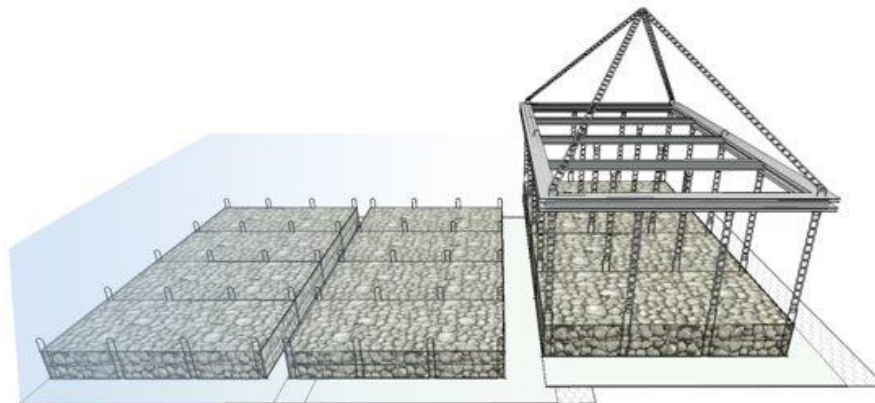


Figure 11.7 Schematisation of pre-assembled and pre-filled gabion mattresses with extended side bands.

Recent studies at Colorado State University (Di Pietro et al., 2021) have shown that the performance of gabion mattresses can be considerably increased by installing vertical bracings within the cells to firmly connect the lid to the base panel of the unit, thus limiting the stone movements.

Gabion mattresses are manufactured using double-twisted wire mesh, which enables the completed structures to deform significantly without failing and also prevents unravelling in the event that the mesh is cut. The double-twisted wire mesh and the lacing wire or C-rings used to construct the gabion mattresses should conform to the relevant standards. In Europe, the most relevant existing

standard for gabions is EN 10223-3, which refers to the mechanical and corrosion protection properties of the mesh wire. A summary of the relevant European standards and their scope is presented in Table 11.1; the most common mesh types and wire diameters are summarised in Table 11.2.

Table 11.1 European standards for double-twisted wire mesh.

Wire properties	European standard	Content
Steel wire composition	EN 10223-3	Steel composition, tensile strength, elongation
Steel mesh composition	EN 10223-3	Wire diameter $d$ (mm) depends on mesh type: Mesh type 6x8 => $d = 2.2$ or $2.4$ or $2.7$ mm Mesh type 8x10 => $d = 2.7$ or $3.0$ or $3.4$ mm
Corrosion protection (metallic coating)	EN 10244-1 EN 10244-2	Thickness of the coating conforms to class A, mass of coating, $m_c$ depends on wire diameter $d$ (mm)
Corrosion protection (polymer coating)	EN 10245-1 EN 10245-2 EN 10245-3 EN 10245-5	Requirements for organic coatings, PVC, PA6 or PE: thickness, composition, strength, durability, flexibility

Table 11.2 Common mesh-wire combinations.

Mesh Type	Wire Diameter (mm)
6x8	2.2
8x10	2.7
8x10	3.0
8x10	3.4

Corrosion protection for the mesh is provided in two ways: first by the process of galvanising the wire with a Zn/Al alloy coating (class A, EN 10244-1) and second by an additional polymer coating, manufactured in accordance with EN 10245-1, 2, 3 and 5. Conventional galvanised PVC-coated gabion mattresses have been in place and shown to be durable in chemically aggressive hydraulic environments for more than 50 years to date; today, more advanced organic coatings with a superior corrosion protection than PVC are available in order to improve the assumed working life.

Gabion stone should be strong and durable and typically it will be convenient to specify quality using EN 13383-1 & 2. Mudstones and other argillaceous weak rocks should be avoided if possible, primarily because they tend to degrade once placed. Suitable gradings are the EN 13383-1 standard coarse grading 90/180 mm specifically designed for gabion use and 90/130 for mattress use.

The void porosity of gabions varies depending upon the type of rock fill and the nature of the filling operation. Values can vary from 25% to 35%. Values of 25% would be appropriate when rock fill is carefully hand-placed, while 35% would be typical of gabions filled for the most part by mechanical means. A consequence of their high porosity is that gabions are highly permeable, even with a void porosity of 25% (hand-placed rock). A lower void porosity is generally preferable (as long as the mattress remains highly permeable), as the stability of the mattress will increase due to the increased weight.

Tests have been undertaken on gabions to assess their compression and shear strength characteristics. The compression strength of a gabion depends on the type of mesh, wire diameter and rock used to fill the baskets. The shear strength of gabions also depends on the type of mesh, wire diameter, and type of stone used to fill the baskets: experience has suggested that gabions have a shearing resistance very similar to an equivalent soil with a relatively high friction angle (35–45°) and an apparent cohesion (up to 40 kPa) provided by the confining effect of the wire basket.



### 11.3.3 Ballast-filled mattresses

The ballast-filled mattress consists of an impermeable (generally watertight) outer layer, with an empty compartment in between, which can be filled with a certain heavy substance (for instance water, bentonite, slurry, etc.) or granular material. As mentioned before, the ballast-filled mattress is still a concept; no prototype mattress exists at the moment. As a result, there are no detailed protection characteristics available and only a schematized prototype concept is therefore presented here. The schematization is provided in Figure 11.8, which contains all relevant parameters of a ballast-filled mattress.

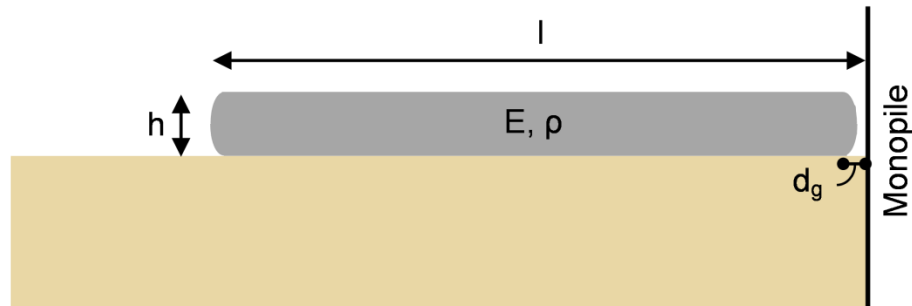


Figure 11.8 Schematization ballast-filled mattress.

The mattress is schematised as an impermeable (for sediment), homogeneous mattress with a certain bending stiffness (determined by elastic modulus  $E$ ) and an (overall) density  $\rho$ . Its dimensions are given by the height  $h$  and the extent from the monopile  $l$  (which may include the gap size). The space in between the monopile and the mattress is given by the gap size  $d_g$ .

In reality the mattress will not be homogeneous but consist of many different materials (i.e. outer layer, strengthening fibres, fill material, etc.), with different densities. However, as long as the mattress is equally distributed and completely filled up (and thus no redistribution of fill material will occur under hydraulic loading) this can be schematized with a single, overall density. The same holds for the bending stiffness of the mattress, as this depends amongst others on the mattress construction, distribution of fill material and filling degree.

A ballast-filled mattress scour protection can consist of single mattresses, but preferably consists of a single mattress which wraps around the monopile. This prevents movement or sliding of the mattress and can theoretically limit the gap size at the monopile. On the other hand, this will probably require filling of the mattress on site or even after placing the outer shell on the seabed.

#### Density

The mattress density determines the weight, and thus the resistance against uplift. Applying the mattress underwater requires a density higher than the density of the surrounding water. The fill material should be a granular material or a liquid to ensure complete filling possibilities and ability to apply overpressure (in case of liquid fill material).

#### Bending stiffness

The bending stiffness gives the mattress additional resistance against uplift of (part of) the mattress. A stiff mattress will have more additional resistance against uplift than a flexible mattress. On the other hand, the bending stiffness of the mattress also determines the ability of the mattress to follow edge scour or different bed shapes. The bending stiffness of the mattress is mainly dependent on the materials of the outer lining, the filling degree and whether or not overpressure is applied within the mattress (in case of a liquid fill material).

### Dimensions

Assuming a single mattress layout, the ballast-filled mattress dimensions are given only by the extent from the monopile ( $l$ ) and the height ( $h$ ) of the mattress, see Figure 11.8. The extent is determined by the area with increased bed load due to the presence of the monopile. The flow amplification around monopiles increases the bed load mainly up to one diameter ( $D$ ) from the pile wall. Therefore, the minimal extent of the mattress is  $1D$  (pile diameter) from the pile wall (or  $3D$  as a diameter, including the pile itself).

The height of the mattress, combined with the density of the mattress, determines the underwater weight of the mattress, and thus the stability. A thicker mattress generally improves the stability (although the drag on the mattress side will increase). However, the mattress should not be too thick, as this would contradict the thin protection layer advantage (see Section 11.3.3).

## 11.4 Potential failure mechanisms

To judge the behaviour of the weighted mattresses as a scour protection there should be insight in the potential failure mechanisms of these mattresses, i.e. the mechanisms in which a mattress scour protection doesn't function properly anymore. As for any scour protection, its function is to prevent excessive scour development beyond acceptable levels. Without a mattress on top of the bed significant scour can occur around the considered foundation, and therefore a mattress scour protection is considered to fail when (part of) the underlying bed is directly exposed to the hydrodynamic loads due to waves and currents.

A scour protection consisting of mattresses may fail if the protection is not sufficiently sand-tight, i.e. sediment can wash-out through the scour protection. This can for instance be relevant for mattresses without a geotextile, or at mattress transitions. Furthermore, stability-related failures need to be considered, i.e. when the mattress is lifted or displaced creating unprotected areas vulnerable to scour. A third type of failure has to do with the flexibility of the mattresses, as they should be flexible enough to follow changing bed topography (such as edge scour). If the mattresses are not flexible enough, undermining can occur.

The following (hydraulic) failure mechanisms of a mattress scour protection are expected:

1. Wash-out of sediment through the scour protection (winnowing)  
For a gabion or block mattress with a geotextile, or a ballast-filled mattress (which is generally impermeable), wash-out of sediment should in general not be an issue, except at the transitions (between mattresses and at the structure). An open space between two mattresses or between the mattress and the structure can lead to erosion of bed material. Minimal scour development at the structure may still be acceptable if it is successfully limited by the scour protection and does not exceed the acceptable scour levels. However, if deep scour develops this constitutes failure of the scour protection, as this will lead to undermining/sinking of the mattresses at the transition.
2. Undermining  
At the edge of the mattress, edge scour is expected due to the sudden transition from protection to bed. As long as the protection can follow this edge scour, this will not directly lead to failure. However, if the mattress is too stiff (resulting in a disability to follow edge scour), it can be undermined by on-going scour underneath the mattress, which will eventually lead to failure (either sinking or moving of the mattress). Please note that, as mentioned above, undermining can also be a consequence of winnowing.
3. Uplift of mattress  
Uplift of (part of) a mattress due to waves/current results in an exposed bed and is therefore regarded as failure. Uplift occurs due to a pressure difference between the top and bottom

of the mattress. Especially with impermeable mattresses or mattresses with a geotextile these pressure differences can build up, as the permeability is limited (permeability allows for penetration of pressure fluctuations). When the lift forces are greater than the gravity force, (part of) the mattress will be lifted.

4. Sliding/moving of the mattresses

Sliding or moving of the mattress will directly result in an exposed bed, which is considered failure. Sliding/moving can for instance occur due to deep edge scour holes or uplift of the entire mattress.

Figure 11.9 illustrates the different failure mechanisms for scour protections consisting of block mattresses, gabion mattresses or ballast-filled mattresses around a monopile.

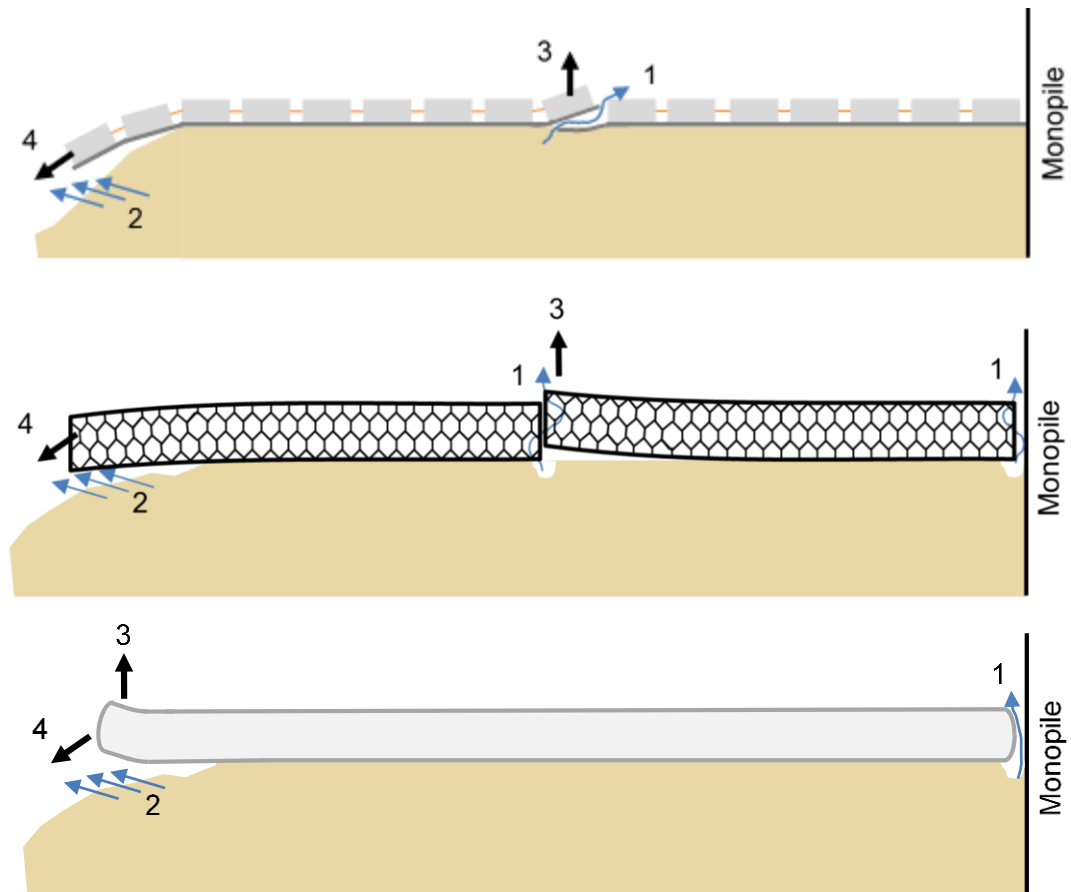


Figure 11.9 Schematic representation of failure mechanisms of a scour protection consisting of block mattresses (top), gabion mattresses (middle) or ballast-filled mattresses (bottom).

Please note that, especially for alternative systems, there are also failure mechanisms related to the material strength and durability of the scour protection in offshore conditions. This can for instance be tears in the geotextile, corrosion or breaks of the wire mesh (gabion mattress), dislocation of blocks from the geotextile (block mattress), leaks of the outer lining (ballast-filled mattress), etcetera. These failure mechanisms are not addressed in this Handbook but should also be considered in the design of a mattress scour protection.

## 11.5 Design considerations

### 11.5.1 Introduction

In general, there is limited experience in applying mattresses with different parameters around offshore structures. Moreover, there are no existing design guidelines to support the design choices of mattresses in offshore conditions (i.e. wave and current conditions). Please note that for current-only conditions, Section 5.2.3.1 of the Rock Manual (CUR/CIRIA/CETMEF, 2007) presents a relationship between the stability of block/gabion mattresses and the hydraulic and structural parameters.

Model tests performed within JIP HaSPro were therefore aimed at exploring the proof-of-concept of mattresses in offshore conditions, around both monopile foundations and as a cable protection. These tests are described in more detail in their respective test reports (block mattresses: Deltares (2023j), document ref.: 1230924-004-HYE-0010, gabion mattresses: Deltares (2023k), document ref.: 1230924-004-HYE-0006, ballast-filled mattress: Deltares (2023m), document ref.: 1230924-004-HYE-0008). The resulting considerations should not be viewed as all-conclusive and definitive, but as an indication for the design. Validation by physical model tests will still be needed where the available results of JIP HaSPro are not sufficiently conclusive.

Below the design considerations are discussed for three different aspects: preventing scour at the structure (sediment wash-out failure mechanism), preventing stability failure (uplift and sliding failure mechanisms) and how to deal with edge scour (undermining failure mechanism). The design considerations focus on monopile foundations and cable protections.

### 11.5.2 Design considerations to prevent scour at the structure

A functioning scour protection should prevent scour at the structure (e.g. at monopile face). In case of scour protection consisting of mattresses, this means that the mattresses should cover the sediment bed in the vicinity of the structure, such that no scour can occur.

In order to retain the bed underneath a scour protection with permeable mattresses (block/gabion mattress), it is generally necessary to equip these mattresses with a geotextile. The geotextile functions as the filter layer, preventing wash-out of sediment through the mattress. As a rule of thumb, the pore size ( $O_{90}$ ) of the geotextile should be smaller than the mean sediment diameter ( $d_{50}$ ) of the bed material. Without a geotextile, the fill material (gabion mattress) or the blocks (block mattress) should ensure the interface stability (i.e. prevent winnowing). It should be noted however, that the hydraulic stability of mattresses with a geotextile is generally lower than mattresses without a geotextile, as the geotextile reduces the dissipation of pressure differences and mattresses with a geotextile have a larger potential drag force during uplift. Therefore, it is suggested to choose a geotextile with a porosity suitable for the granulometry of the bed material and which allows for the dissipation of the uplifting forces. Please note that the ballast-filled mattress is expected to be sand-tight, and therefore wash-out of sediment through the mattress is not an issue.

Although dependent on the required area that needs to be protected around an offshore structure, a mattress scour protection generally consists of multiple mattresses (with the potential exception of the ballast-filled mattress). In this case, special attention should be given to the transition between the mattresses. Small openings or gaps between mattresses can already result in wash-out of sediment and should therefore be prevented. It is therefore strongly recommended to apply an overlap between the mattresses, for instance by extending the geotextile (for gabion mattresses preferably including mesh) at the underside of the mattress. This overlap should be placed such that the adjacent mattress is placed on top of the overlap, thereby ensuring a sand-tight mattress transition. Please note that this sand-tight transition should be maintained over the lifetime of the scour protection and can be affected by movement of individual mattresses. Attaching adjacent

mattresses to each other can help to prevent openings between mattresses due to individual mattress movement.

Special consideration should also be given to the interface with the structure, as a sand-tight transition between the structure and the mattresses should be guaranteed if no scour around the foundation is allowed. Similar to the transition between individual mattresses, small openings or gaps at this interface can result in wash-out of sediment at the structure. Generally, the risk of wash-out here is even larger than between mattresses due to the increased flow amplification close to the structure and there is (generally) no possibility to use an overlap. It is therefore highly recommended to apply tailor-made mattresses to ensure a tight transition between the structure and the mattresses. Nevertheless, even with tailor-made mattresses wash-out of sediment can occur near the structure if the transition is not sufficiently sand-tight.

Examples of the wash-out of sediment are given in Figure 11.10, which shows the winnowing at the transverse sides of a monopile during a test (left photo) and the resulting scour around the monopile (right photo) for both gabion mattresses and block mattresses. As visible, even with tailor-made mattresses (gabion mattresses) still there was significant wash-out of sediment around the monopile (mainly at the transition of the individual mattresses). For the ballast-filled mattress, and example of the effects of winnowing at the pile face is given in Figure 11.11.

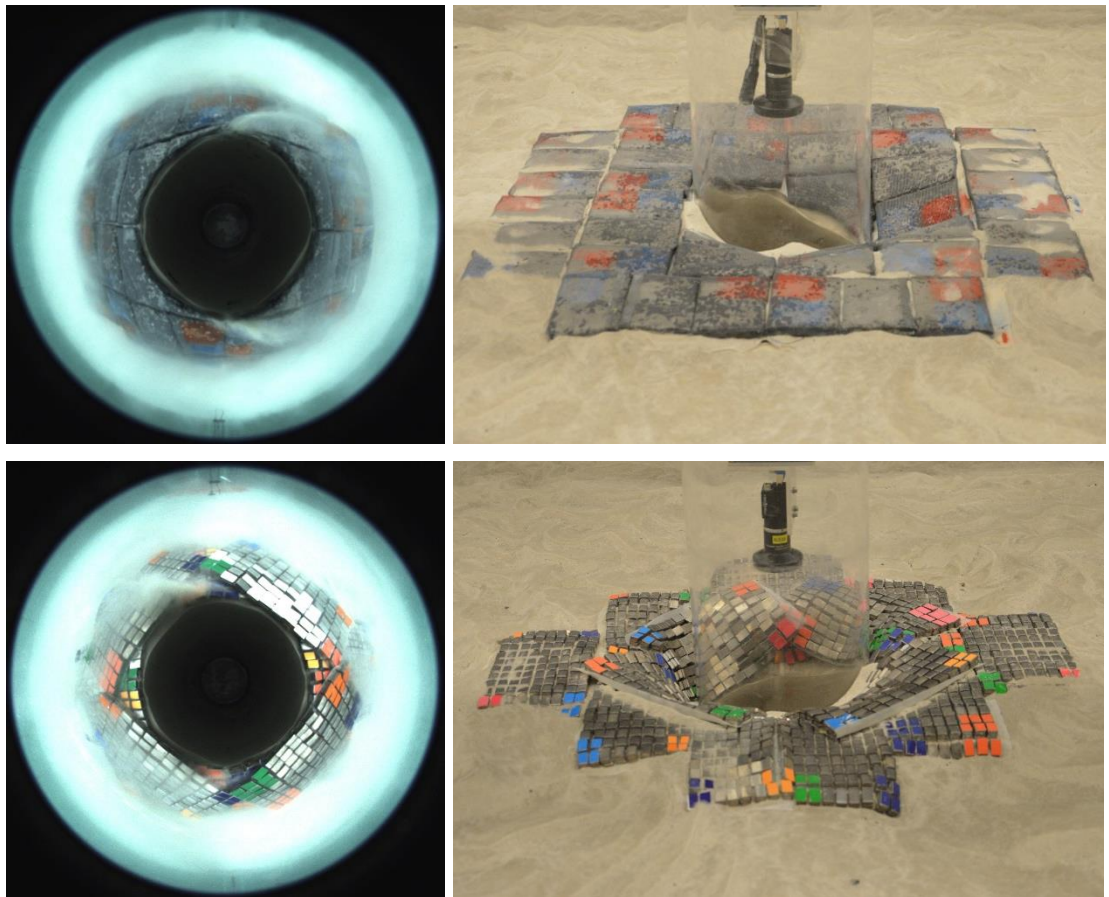


Figure 11.10 Examples of winnowing at pile face during JIP HaSPro tests (left) and resulting effect after the test (right). Top: gabion mattresses. Bottom: block mattresses.

To prevent winnowing close to the structure, either a hybrid solution (for instance with additional rocks dump around the structure) or a two-layered mattress solution might help to prevent or reduce winnowing at the structure interface. Alternatively, if possible, another option would be to attach the

mattresses to the structure. This requires specialist equipment (ROV) or a self-installing system (see Section 9.3.2).

For a hybrid solution, it should be kept in mind that the second protection method should be sufficiently stable as well under the design conditions, and that this protection method should also provide the necessary (additional) interface stability to prevent scour at the structure. Furthermore, please note that the second protection method should not damage the mattresses (for instance due to rock movement over the gabion wire mesh), which could compromise the overall scour protection integrity.

In some cases, a two-layered mattress solution might also help to prevent or reduce the wash-out of sediment (both at the structure and at mattress transitions). For this two-layered mattress layout it is advised to apply a different mattress placement in the secondary layer, such that most of the transitions of the first layer are covered by mattresses. At the structure, a secondary layer increases the overall layer thickness and is thereby expected to reduce the hydraulic load at the bed, which should reduce the wash-out through any openings/gaps. An example of a two-layered gabion mattress solution is given in Figure 11.12. Compared to the test with only one layer (Figure 11.10), no significant scour has occurred around the monopile. This is visible on both the photo (right) and the bathymetry measurement after the tests (left).

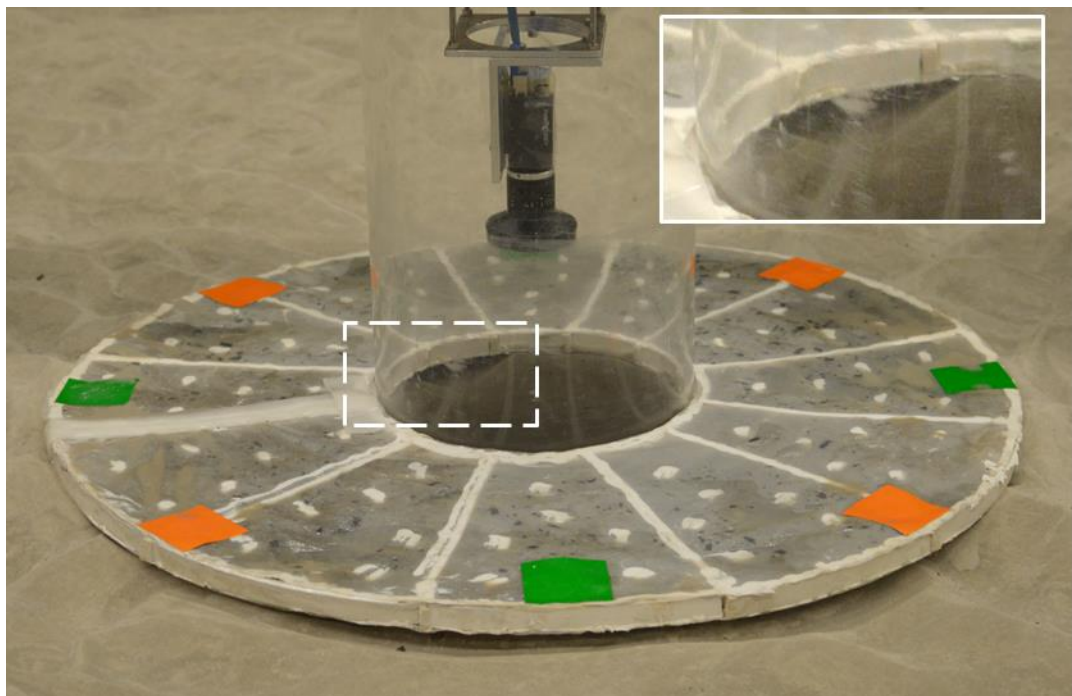


Figure 11.11 Example of winnowing at ballast-filled mattress, including magnification of winnowing scour hole adjacent to the pile.

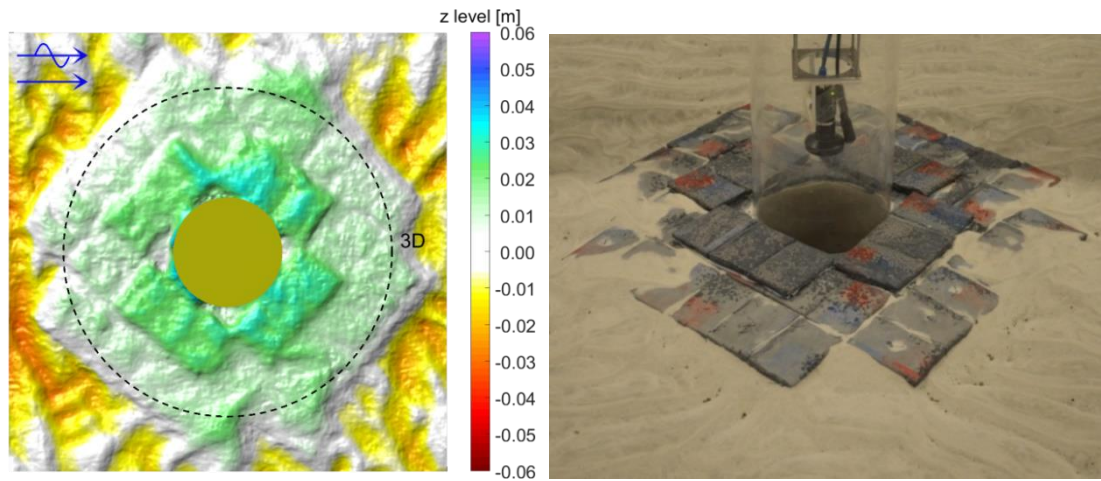


Figure 11.12 Two-layered gabion mattress protection layout after tests: bathymetry from stereophotography (left) and photo from downstream side (right).

Based on the performed physical model tests during JIP HaSPRO a two-layered layout is preferable over a one-layered layout to reduce the winnowing at the mattress transitions (including the interface at the structure), especially for gabion mattresses and block mattresses. In such a two-layered layout, a staggered layer layout is preferred. It should be kept in mind however, that the top layer mattresses are generally less stable, as the friction on top of another mattress is smaller compared to a sediment bed. This makes the top layer mattresses more susceptible to movement/sliding, which should be considered when designing a two-layered mattress layout.

As both the transition between individual mattresses and between the structure and the mattresses should be sand-tight, a very accurate placement of the mattresses is of utmost importance. Gaps between mattresses or mattresses on top of each other will expose the underlying seabed and therefore result in scour and undermining of the scour protection. The installation accuracy of the mattresses could therefore very well be a limiting factor in offshore conditions, especially at deeper foundations and/or in challenging conditions. In the design phase the installation accuracy should already be taken along, such that undesired installation effects are minimized.

Please keep in mind that the mattress scour protection tests performed during JIP HaSPRO were based on proof-of-concept. It is therefore strongly recommended to validate the scour prevention performance of a scour protection design consisting of mattresses by means of physical model tests. This is briefly discussed further in Section 11.5.5.

As not all aspects can be sufficiently validated in physical model tests (especially with regard to sand-tightness), additional visual monitoring of installed mattress scour protection is advised during the lifetime of the scour protection. This visual monitoring should ensure that no significant winnowing occurs through the scour protection during various conditions and serves as additional validation with regard to the sand-tightness of the scour protection. In the first years after installation of the scour protection this visual monitoring should be performed more frequently; the frequency can be relaxed if no significant wash-out is observed.

### 11.5.3 Design considerations to prevent stability failure

In order to perform its scour protection function, a mattress scour protection needs to remain stable, i.e. to withstand the hydrodynamic loading acting on the mattresses without uplift or displacement of the mattresses. As mentioned in Section 11.4, two different types of stability failure are recognized: uplift and sliding. Uplift generally occurs under wave crests or troughs (when the orbital bed velocity is largest), due to the lift force exerted on the mattress. Examples of mattress uplift during the JIP HaSPRO tests is given in Figure 11.13. Due to the orbital flow velocity at the bed the

edge of the mattress was lifted up slightly. This increased the drag force on the mattress, which increased the uplift even further. During the JIP HaSPro tests, uplift of mattresses was generally only observed at mattresses positioned at the edge of the protection (except when surrounding mattresses were already displaced), with uplift and/or movement starting at the exposed edge. Mattresses orientated parallel (i.e. with the longer edge) to the wave- and flow direction were more prone to uplift than perpendicular orientated mattresses.

Once uplift has occurred, the drag area of the mattress increases. Dependent on the wave and current conditions, this can cause sliding of the mattress (or increase the uplift even further). Based on the various observations, only minor uplift is required to cause displacement of mattresses. This is primarily dependent on the presence of a current, as movement is governed by the drag force on the mattress (which increases during uplift). This could also occur during severe wave events, in case uplift occurs well before the peak orbital velocity of that wave. Displacement of the mattress (from its original position) was observed in case uplift occurred before the peak bed orbital velocity (of that wave crest/trough) was achieved. Generally, mattresses became less stable (more prone to uplift and/or movement) once they shifted from their original place (i.e. no longer an integral part of the protection).

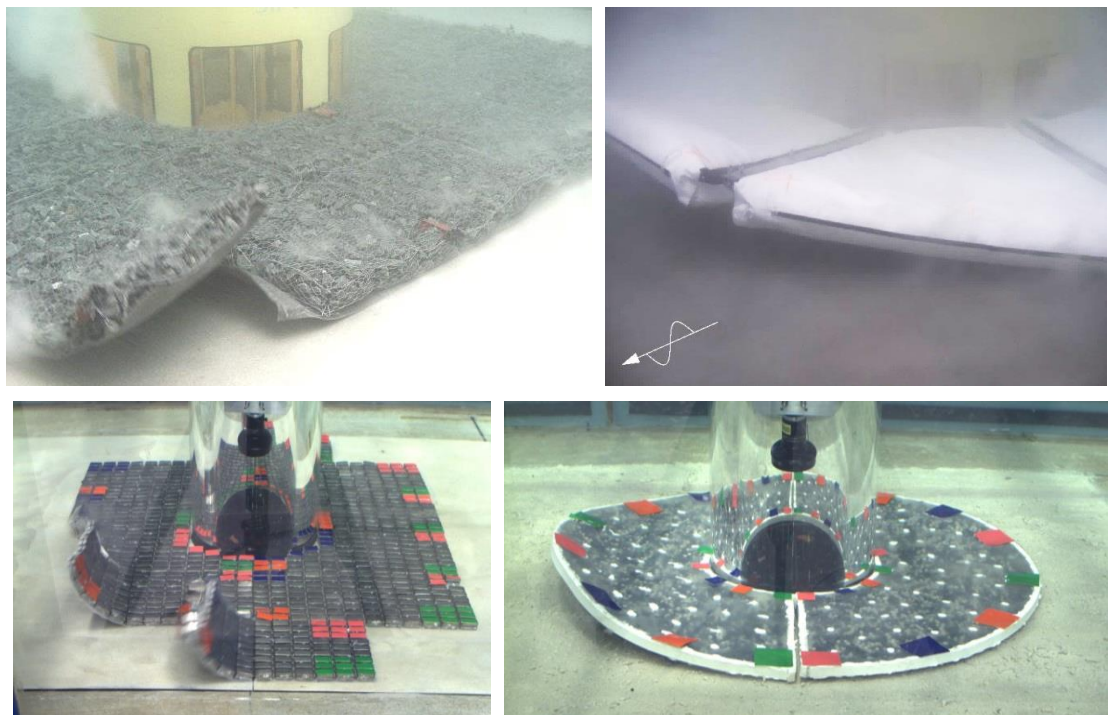


Figure 11.13 Example of uplift of mattresses during JIP HaSPro tests.

Uplift and sliding are, besides the weight of the mattress, also dependent on the bending stiffness of the mattress. With similar mattress weight and density, stiffer mattresses are generally more stable than flexible mattresses, due to their additional resistance against bending. Flexible mattresses are therefore expected to already show uplift under less severe conditions. Furthermore, flexible mattresses will lift up higher than stiffer mattresses. However, when stiffer mattresses lift up, the uplift area (area of mattress that lifts up) is similar or larger compared to flexible mattresses, as the additional resistance against bending causes a larger part of the mattress to be affected by uplift. The threshold against uplift is therefore generally higher for stiffer mattresses, but the threshold against sliding is relatively similar (for mattresses with similar mattress weight and density).

Stability failure of mattresses can be prevented by ensuring that the resistance against uplift/sliding is larger than the acting lift/drag forces on the mattress. This is generally achieved by ensuring the



mattress has sufficient weight. Stability of the entire mattress scour protection could be increased by attaching multiple individual mattresses to each other. Stability is also increased by build-up of sediment on top or within a mattress, which could occur dependent on the occurring hydrodynamic conditions and the type of mattress. Mattresses over a cable are more stable than mattresses around the monopile. This is as expected, as the monopile creates more flow amplification, and the 'hanging' behaviour of the mattress over the cable improve the stability as significant uplift is required before the drag force can cause movement of the mattresses.

It should be noted that uplift doesn't necessarily constitute failure. As long as the integrity of the entire scour protection is not affected, some limited uplift (for instance a single block row) of a mattress on the edge of the protection, without displacement of the mattress itself, can be allowed for. During these limited uplift events, the sediment underneath the edge will erode, causing the edge of the mattress to 'hang' in the developing scour hole. This will stabilize the mattress, as the drag force on the mattress now acts as additional resistance (i.e. 'pushes' the mattress down), which in time will prevent more uplift events. Please note however, that this only holds for limited uplift events (limited area of mattress that lifts up), as otherwise the risk of displacement increases significantly.

Based on the results of the JIP HaSPro tests, a first estimation of the mattress stability is given in the following sections. It should be noted that the provided formulation and graphs are only indicative and should not be used for detailed designs. For block mattresses and gabions, these estimations are based on mattresses with a geotextile (which have a lower hydraulic stability compared to mattresses without a geotextile). At this moment, the stability of any scour protection design consisting of block, gabion or ballast-filled mattresses should be validated by means of physical model tests. This is briefly discussed further in Section 11.5.5.

#### 11.5.3.1 Stability formulation: modified Pilarczyk method

At the moment, no guidelines or formulations exist to calculate the necessary dimensions of a mattress scour protection around a monopile or at cables in offshore conditions with combined waves and currents. To present an indicative stability graph of the mattresses tested in JIP HaSPro, the formulation by Pilarczyk, see for instance Pilarczyk & Klein Breteler (1998), is used as a starting point. This formulation is developed for revetment protections in current-dominated conditions and resembles the bed shear stress stability approach. To use this formulation for typical offshore hydraulic forcing with combined waves and currents, this formulation is further modified. The modified Pilarczyk formulation for combined wave and current forcing and accounting for mattress flexibility as a design parameter is presented below.

$$\frac{\Delta D_m}{f} = 0.035 \frac{\Phi}{\theta_{crit}} \frac{K_t}{K_s} \frac{u_{char}^2}{2g} \quad (30)$$

Where

$$u_{char} = u_{wa,max} + K_h \cdot U_c, \quad K_h = \frac{\sqrt{2}}{\log\left(\frac{12h_w}{k_s}\right)}$$

In which:

D	=	Thickness of mattress	[m]
$\Delta$	=	Relative density	[-]
f	=	Mattress flexibility coefficient	[-]
$\Phi$	=	Stability parameter	[-]
$\theta_{crit}$	=	Critical Shield's parameter	[-]

$K_s$	=	Slope factor	[-]
$K_t$	=	Turbulence factor	[-]
$U_{char}$	=	Characteristic velocity	[m/s]
$U_{wa,max}$	=	Maximum near bed orbital velocity	[m/s]
$U_c$	=	Depth-averaged current speed	[m/s]
$K_h$	=	Factor to translate current near the bed (fully-developed flow)	[m/s]
$h$	=	Water depth	[m]
$k_s$	=	Equivalent roughness height	[-]

Regarding the design parameters, the thickness of the mattress and the relative density can be determined in a straightforward manner. On the contrary, the flexibility coefficient can only be determined based on dedicated tests given a certain mattress design and depending on the connections between different mattresses, potential stiffeners etc.

The Critical Shields' parameter depends on the material of the mattress whereas the stability parameter depends on the application of the mattress. In general, to account for the presence of many edges and transitions in the application of mattress protections at offshore foundations, a stability parameter at the upper end of the Pilarczyk ranges accounting for the presence of weak locations (edges and transitions) is recommended. Furthermore, the equivalent roughness height can be assumed equal to the mattress thickness. Finally, in the modified stability formulation, the characteristic velocity is approximated as a linear summation of wave- and current-induced speeds near the bottom. More in specific, for the wave-induced stresses near the bed, the *maximum* near-bed wave orbital velocity is used which can be calculated based on linear wave theory. As opposed to loose rock protections, mattress protections are more prone to instantaneous failure, which motivates the use of the maximum wave parameter.

#### Measured data of mattress stability in JIP HaSPro

Indicative graphs regarding the stability of the different mattresses are given in the sections below, based on stability tests performed at two facilities characterized by a different applicable scale factor, namely the Scheldt Flume and the Delta Flume, in the framework of JIP HaSPro. The primary goal of the tests was to explore different alternatives and to provide a proof-of-concept concerning these mattresses. These physical model tests involved various mattress types (e.g., varying block height, gabion fill material, etc.) and different layouts (e.g. arrangement and connection between different mattresses) at both monopile and cable foundations. A pragmatically chosen collection of hydraulic conditions was applied including Current-only (CO), Regular waves-only (RWO), and finally Irregular Waves without and with Current (IWO/IWC). More information regarding the exact test conditions can be found in the individual factual reports of each mattress system. Following the completion of the tests, the mattress stability was assessed based on visual observation of the test videos, by applying the classification as presented in Table 11.3.

Table 11.3 Classification used for the assessment of mattress stability based on visual observation.

Stability classification	Description
1	No movement at all; all mattresses remained perfectly still during the test
2	Limited uplift; at least one mattress at any location for at least once during the test was flapping at its edge with uplift limited by approximately half its height
3	Significant uplift; at least one mattress at any location for at least once during the test was flapping at its edge with uplift larger than its height but without sliding from original position
4	Significant uplift and sliding; at least one mattress at any location for at least once during the test was flapping at its edge with uplift larger than its height and sliding away from original position
5	Complete failure; at least one mattress has completely moved away from its initial footprint or all the mattresses

Given the large variability in control parameters applied in these proof-of-concept tests, the amount of available measured data (per tested mattress application) is insufficient for the purpose of deriving reliable design formulations. This would require testing with a larger range of hydraulic conditions. Here, the model test results are treated and presented jointly for all different mattresses and hydraulic conditions and separately only for the two different foundation types (monopile and cable). Subsequently, the stability graphs presented here are only meant to provide a first indication regarding the stability of the different mattresses and should not be used in detailed design. These stability graphs can be used as a starting point for developing conceptual scour protections with mattresses. The conceptual designs can then be validated with dedicated physical model tests.

#### 11.5.3.2 Stability of block mattresses

Based on the JIP HaSPro test results, the parameter values in the modified Pilarczyk formulation were estimated for block mattresses. These values are presented in Table 11.4, for block mattresses on top of a nearly flat seabed.

Table 11.4 Values of parameters in modified Pilarczyk equation for block mattresses.

Parameter	Value	Explanation
$\phi$	1.0	According to Pilarczyk for block mattress (edges and transitions)
$\psi$	0.07	According to Pilarczyk for block mattress
$K_s$	1.0	No slope
$K_{t,monopiles}$	1.5	Increased turbulence at edge of protection due to monopile presence
$K_{t,cables}$	1.0	No increased turbulence in case of cable protection
$f$	2.0	Very flexible mattresses (note: may vary dependent on mattress)

#### Stability graph monopile protection

Block mattress stability tests around monopiles were performed in the Scheldt Flume. Overall, four different mattress types were tested using the same test layout. All block mattresses have a density of 2700 kg/m<sup>3</sup> and based on the test results a flexibility coefficient of 2.0 is determined (for the mattresses applied in the physical model tests). A short summary of those tests is presented in Table 11.5. Examples of tested layouts are presented in the photographs taken during the execution of tests in Figure 11.14.

Table 11.5 Short overview of tests with block mattresses around monopiles.

Facility	Scale factor	Mattress scale model	Test conditions (No. of tests)	No. of layout variations
Scheldt Flume	30	Type B: block height 4mm	CO (7)	1
		Type C: block height 6mm	RWO (14), IWO (4)	
		Type D: block height 8mm	RWO (19), IWO (3), IWC (3)	
		Type E: block height 10mm	RWO (10), IWO (5), IWC (3)	

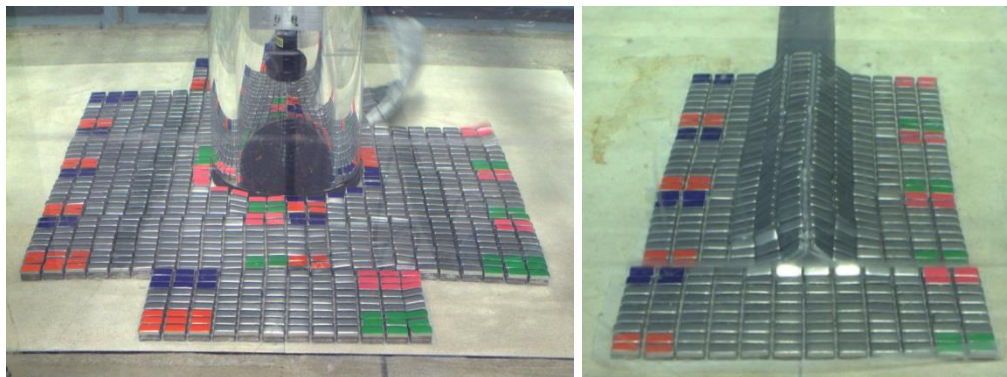


Figure 11.14 Left: Block mattress scour protection around a monopile in Scheldt Flume. Right: Block mattress scour protection at a cable in Scheldt Flume.

Figure 11.15 presents an indicative stability graph with a (fitted) modified Pilarczyk stability line plotted through data points corresponding to individual tests performed in JIP HaSPRO per mattress type tested around a monopile. The data points are colored based on the classification presented in Table 11.3, expressing the stability of the block mattress(es). The design parameters ( $\Delta \cdot D/f$ ) are on the vertical axis, and the hydraulic forcing parameter on the horizontal axis (expressed by  $u_{char}$ ). Within the tested range of design and hydraulic forcing parameter, the black solid line is presented based on the fitted parameters summarized in Table 11.4. Essentially, at the area to the left from this line, block mattresses can be assumed to be (nearly) stable, and vice versa. In this plot, all tested hydraulic conditions are plotted together, and hence given the large variability of control parameters, an increase in  $u_{char}$  is not necessarily accompanied by a degrading performance of block mattress in terms of stability. Overall, the fitted Pilarczyk formulation appears to be representative for the stability of block mattresses at monopile locations.

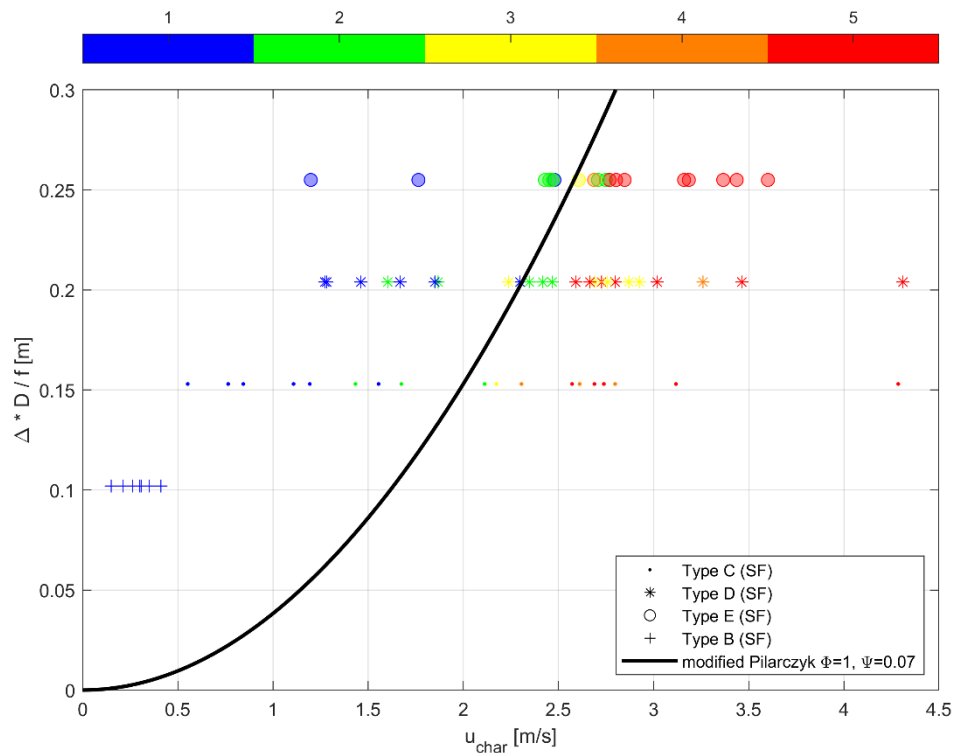


Figure 11.15 Indicative stability graph (not for detailed design) based on modified Pilarczyk formulation for block mattresses monopile scour protections. Colored data points present the classification of mattress stability according to Table 11.3 for all individual tests performed in JIP HaSPro. Solid black line presents the theoretical modified Pilarczyk formulation (parameters according to Table 11.4) within the tested ranges of  $\Delta D/f$  and  $u_{char}$ .

**Stability graph cable protection**

Block mattress stability tests at cables were also performed in the Scheldt Flume. Overall, four different mattress types with density of 2700 kg/m<sup>3</sup> were tested in Scheldt flume using with the same layout. For all block mattresses tested in JIP HaSPro a flexibility coefficient (f) of 2 is determined based on the test results. A short summary of those tests is presented in Table 11.6.

Table 11.6 Short overview of tests with block mattresses as a cable protection.

Facility	Scale factor	Mattress scale model	Test conditions (No. of tests)	No. of layout variations
Scheldt Flume	30	Type A: block height 2mm	CO (5)	1
		Type B: block height 4mm	CO (8), RWO (14), IWO (4)	
		Type C: block height 6mm	RWO (26), IWO (5), IWC (3)	
		Type D: block height 8mm	RWO (23), IWO (11), IWC (3)	

Figure 11.16 presents an indicative stability graph with a (fitted) modified Pilarczyk stability line plotted through data points corresponding to individual tests performed in JIP HaSPro per mattress type tested around a cable. Essentially, at the area to the left from this line, block mattresses can be assumed to be (nearly) stable, and vice versa. In this plot, all tested hydraulic conditions are plotted together, and hence given the large variability of control parameters, an increase in  $u_{char}$  is not always accompanied by a degrading performance of block mattress in terms of stability. In general, the fitted Pilarczyk line is deemed somewhat representative although, outliers are detected (e.g., Type A mattress stability in current-only conditions).

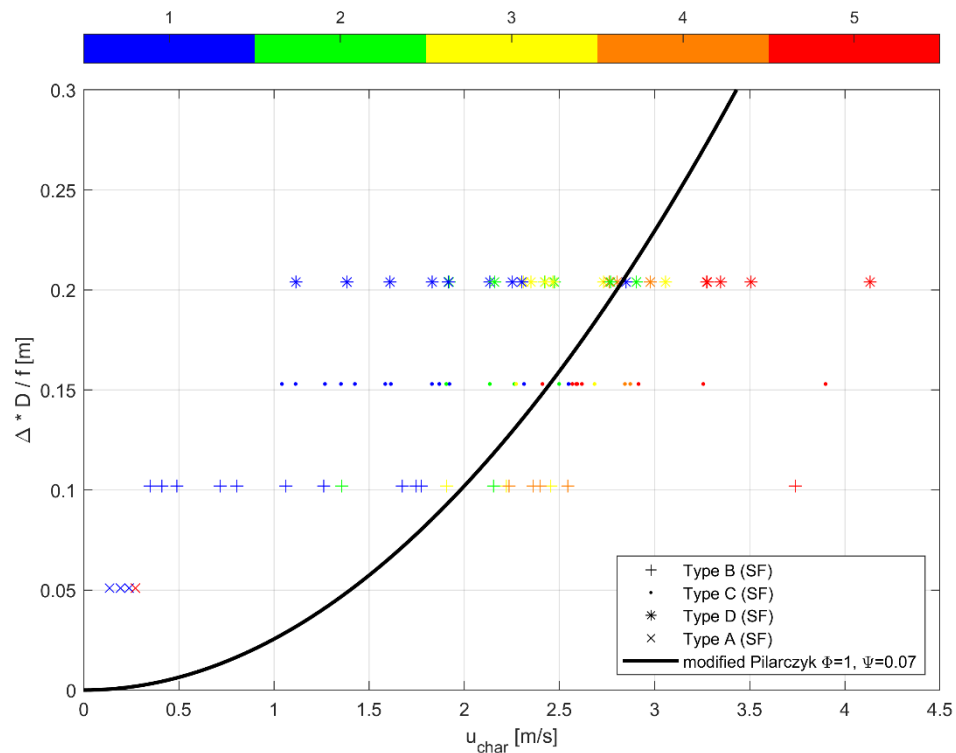


Figure 11.16 Indicative stability graph (not for detailed design) based on modified Pilarczyk formulation for block mattresses cable scour protections. Colored data points present the classification of mattress stability according to Table 11.3 for all individual tests performed in JIP HaSPro. Solid black line presents the theoretical modified Pilarczyk formulation (parameters according to Table 11.4) within the tested ranges of  $\Delta D/f$  and  $u_{char}$ .

### 11.5.3.3 Stability of gabion mattresses

Based on the JIP HaSPro test results, the parameter values in the modified Pilarczyk formulation were estimated for gabion mattresses. These values are presented in Table 11.7, for gabion mattresses on top of a nearly flat seabed.

Table 11.7 Values of parameters in modified Pilarczyk equation for gabion mattresses.

Parameter	Value	Explanation
$\phi$	1.0	According to Pilarczyk for gabions (edges and transition)
$\psi$	0.07	According to Pilarczyk for gabion mattress
$K_s$	1.0	No slope
$K_{t,monopiles}$	1.5	Increased turbulence at edge of protection due to monopile presence
$K_{t,cables}$	1.0	No increased turbulence in case of cable protection
$f$	1.0	Relatively flexible mattresses (note: may vary dependent on mattress)

#### Stability graph monopile protection

Gabion mattress stability tests around monopiles were performed in both the Scheldt Flume and Delta Flume. Overall, three different mattress types were tested using the same test layout in the Scheldt flume, whereas in the Delta Flume only one mattress type was tested in two different layouts. All gabion mattresses are considered to have a flexibility coefficient ( $f$ ) of 1, based on the test results (for the mattresses applied in the physical model tests). A short summary of those tests is presented in Table 11.8. Examples of tested layouts are presented in the photographs taken during the execution of tests in Figure 11.17.

Table 11.8 Short overview of tests with gabion mattresses around monopiles.

Facility	Scale factor	Mattress scale model	Test conditions (No. of tests)	No. of layout variations
Scheldt Flume	30	Type A: density $\sim 1838 \text{ kg/m}^3$	CO (6), RWO (41), IWO (11), IWC (20)	1
		Type B: density $\sim 2150 \text{ kg/m}^3$		
		Type C: density $\sim 2650 \text{ kg/m}^3$		
Delta Flume	6	Rock: density $\sim 2650 \text{ kg/m}^3$	FWO (16), IWO (6)	2

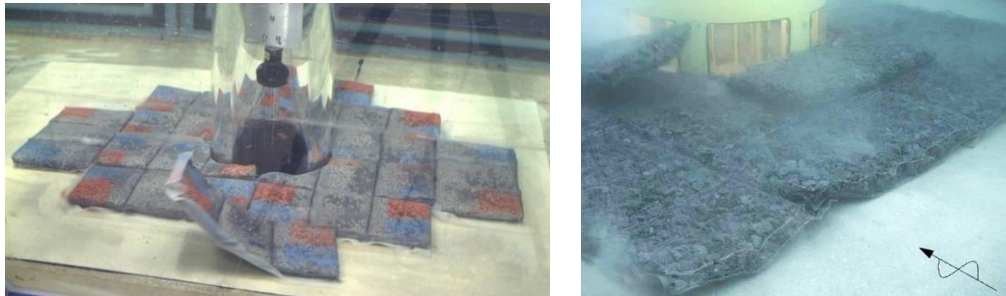


Figure 11.17 Left: single layer of gabion mattresses around a monopile in Scheldt Flume. Right: double layer of gabion mattresses around a monopile in Delta Flume.

Figure 11.18 presents an indicative stability graph with a (fitted) modified Pilarczyk stability line plotted through data points corresponding to individual tests performed in JIP HaSPro per mattress type tested around a monopile. The data points are colored based on the classification presented in Table 11.3, expressing the stability of the gabion mattress(es). The design parameters ( $\Delta^*D$ ) are on the vertical axis, and the hydraulic forcing parameter on the horizontal axis (expressed by  $u_{char}$ ). Within the tested range of design and hydraulic forcing parameter, the black solid line is presented based on the fitted parameters summarized in Table 11.7. Essentially, at the area to the left from this line, gabion mattresses can be assumed to be (nearly) stable, and vice versa. In this plot, all tested hydraulic conditions and layouts are plotted together, and hence given the large variability of control parameters, an increase in  $u_{char}$  is not necessarily accompanied by a degrading performance of gabion mattress in terms of stability.

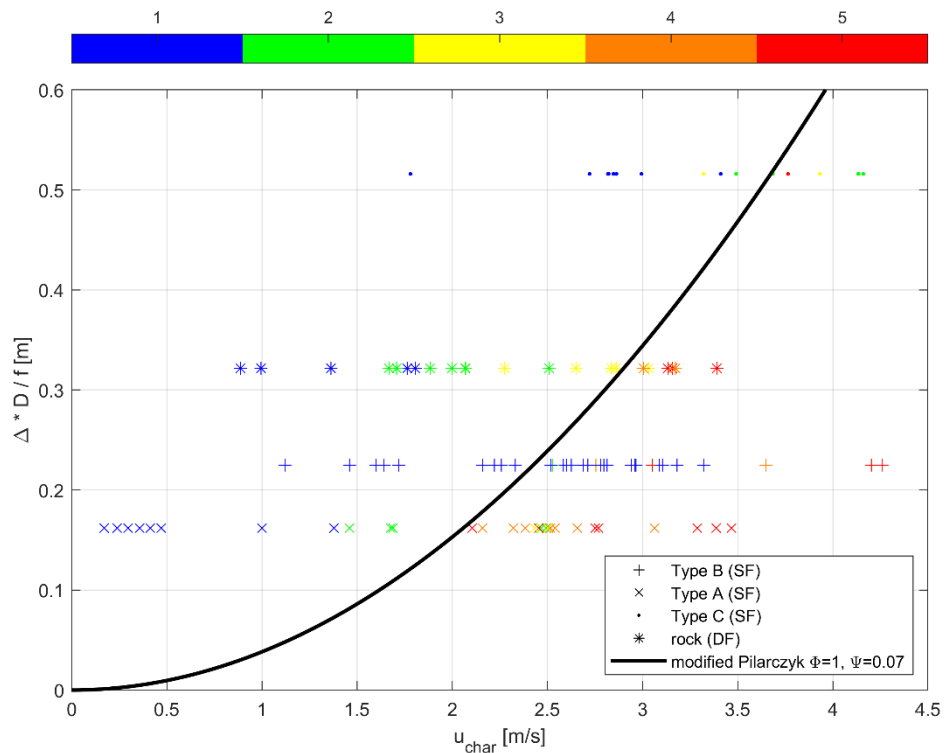


Figure 11.18 Indicative stability graph (not for detailed design) based on modified Pilarczyk formulation for gabion mattresses monopile scour protections. Colored data points present the classification of mattress stability according to Table 11.3 for all individual tests performed in JIP HaSPro. Solid black line presents the theoretical modified Pilarczyk formulation (parameters according to Table 11.7) within the tested ranges of  $\Delta D/f$  and  $u_{char}$ .

Stability graph cable protection

Gabion mattress stability tests at cables were also performed in both the Scheldt Flume and Delta Flume. Overall, three different mattress types and 5 different test layouts were tested in the Scheldt flume, whereas in the Delta Flume two mattress types were tested with the same layout. All gabion mattresses are considered to have a flexibility coefficient ( $f$ ) of 1, based on the test results. A short summary of those tests is presented in Table 11.9.

Table 11.9 Short overview of tests with gabion mattresses as a cable protection.

Facility	Scale factor	Mattress scale model	Test conditions (No. of tests)	No. of layout variations
Scheldt Flume	30	Type A: density ~1838 kg/m <sup>3</sup>	CO (6), RWO (41), IWO (11), IWC (20)	4
		Type B: density ~2150 kg/m <sup>3</sup>		3
		Type C: density ~2650 kg/m <sup>3</sup>		1
Delta Flume	6	Rock: density ~2650 kg/m <sup>3</sup>	FWO (16), IWO (3)	1
		Rock: density ~2650 kg/m <sup>3</sup> (with geotextile)		1

Figure 11.19 presents an indicative stability graph with a (fitted) modified Pilarczyk stability line plotted through data points corresponding to individual tests performed in JIP HaSPro per mattress type tested around a cable. Essentially, at the area to the left from this line, gabion mattresses can be assumed to be (nearly) stable, and vice versa. In this plot, all tested hydraulic conditions and layouts are plotted together, and hence given the large variability of control parameters, an increase



in  $u_{char}$  is not always accompanied by a degrading performance of gabion mattress in terms of stability. In general, the fitted Pilarczyk line is deemed representative although, tests with stability failure were not reported for certain mattress types.

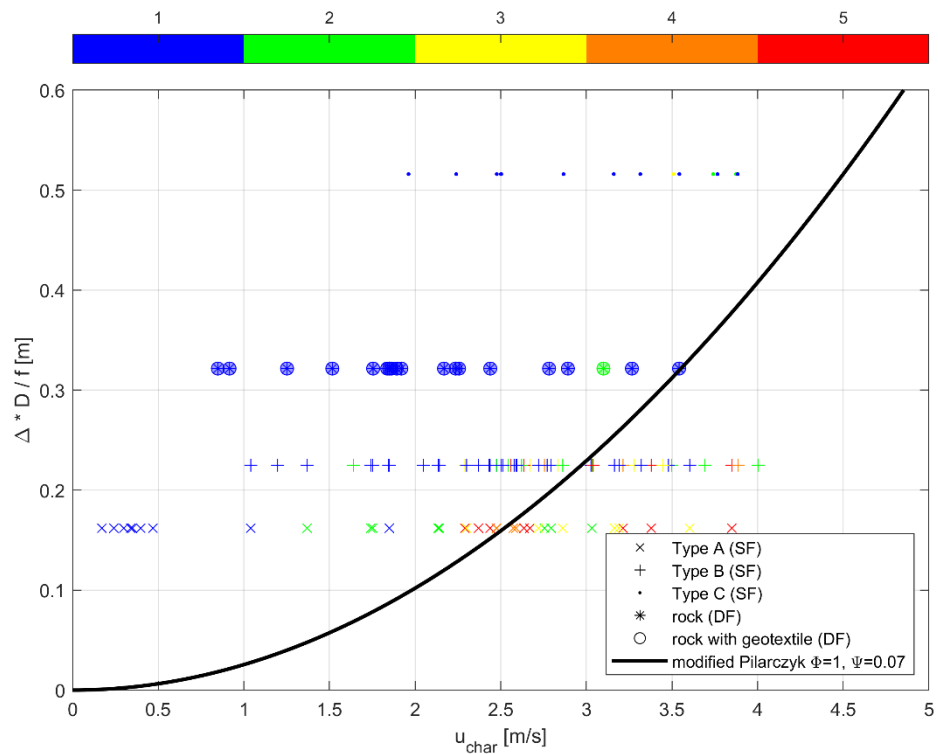


Figure 11.19 Indicative stability graph (not for detailed design) based on modified Pilarczyk formulation for gabion mattresses cable scour protections. Colored data points present the classification of mattress stability according to Table 11.3 for individual tests performed in JIP HaSPro. Solid black line presents the theoretical modified Pilarczyk formulation (parameters according to Table 11.7) within the tested ranges of  $\Delta D/f$  and  $u_{char}$ .

#### 11.5.3.4 Stability of ballast-filled mattresses

Based on the JIP HaSPro test results, the parameter values in the modified Pilarczyk formulation were estimated for ballast-filled mattresses. These values are presented in Table 11.10, for ballast-filled mattresses on top of a nearly flat seabed.

Table 11.10 Values of parameters in modified Pilarczyk equation for ballast-filled mattresses.

Parameter	Value	Explanation
$\phi$	1.0	According to Pilarczyk for ballast-filled mattress
$\psi$	0.07	According to Pilarczyk for ballast-filled mattress
$K_s$	1.0	No slope
$K_{t;monopiles}$	1.5	Increased turbulence at edge of protection due to monopile presence
$K_{t;cables}$	1.0	No increased turbulence in case of cable protection
f	-	Dependent on flexibility of mattress

#### Stability graph monopile protection

Ballast-filled mattress stability tests around monopiles were performed in both the Scheldt Flume and Delta Flume. Overall, six different mattress types were tested using the same test layout in the Scheldt Flume, whereas in the Delta Flume two mattress types were assessed with an identical layout as well. A short summary of those tests is presented in Table 11.11. The flexibility coefficient is determined per mattress type based on the test results. Examples of tested layouts are presented in the photographs taken during the execution of tests in Figure 11.20.

Table 11.11 Short overview of tests with ballast-filled mattresses around monopiles.

Facility	Scale factor	Mattress scale model	f (-)	Test conditions (No. of tests)	No. of layout variations
Scheldt Flume	30	A1: flexible, 10 mm	2	CO (6), RWO (18), IWO (3)	1
		A2: flexible, 12 mm		CO (7), RWO (16), IWO (3)	
		B1: medium flexible, 10 mm	1	RWO (23), IWO (3), IWC (2)	
		B2: medium flexible, 12 mm		RWO (17), IWO (5)	
		C1: stiff, 10 mm	0.8	RWO (11), IWO (2), IWC (3)	
		C2: stiff, 12 mm		RWO (13), IWO (4), IWC (2)	
Delta Flume	6	D1: 39% 2-5mm ND rock, 61% rubber, unconnected	2	IWO (6)	1
		D2: 39% 2-5mm ND rock, 61% rubber, connected with aluminium bars	0.8	IWO (5)	

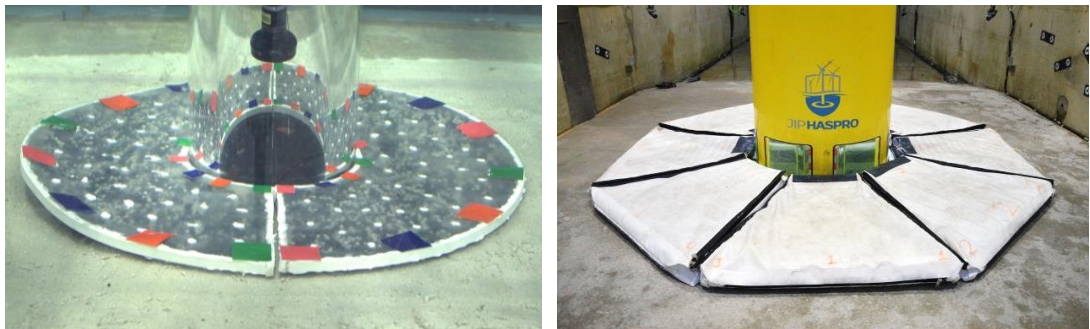


Figure 11.20 Left: single layer of ballast-filled mattresses around a monopile in Scheldt Flume. Right: single layer of unconnected ballast-filled mattresses around a monopile in Delta Flume.

Figure 11.21 presents an indicative stability graph with a (fitted) modified Pilarczyk stability line plotted through data points corresponding to individual tests performed in JIP HaSPro per mattress type tested around a monopile. The data points are colored based on the classification presented in Table 11.3, expressing the stability of the ballast-filled mattress(es). The design parameters ( $\Delta \cdot D/f$ ) are on the vertical axis, and the hydraulic forcing parameter on the horizontal axis (expressed by  $u_{char}$ ). Within the tested range of design and hydraulic forcing parameter, the black solid line is presented based on the fitted parameters summarized in Table 11.10. Essentially, at the area to the left from this line, ballast-filled mattresses can be assumed to be (nearly) stable, and vice versa. In this plot, all tested hydraulic conditions are plotted together, and hence given the large variability of control parameters, an increase in  $u_{char}$  is not necessarily accompanied by a degrading performance of ballast-filled mattress in terms of stability. Overall, the fitted Pilarczyk line is deemed representative for a first estimate of ballast-filled mattress stability.

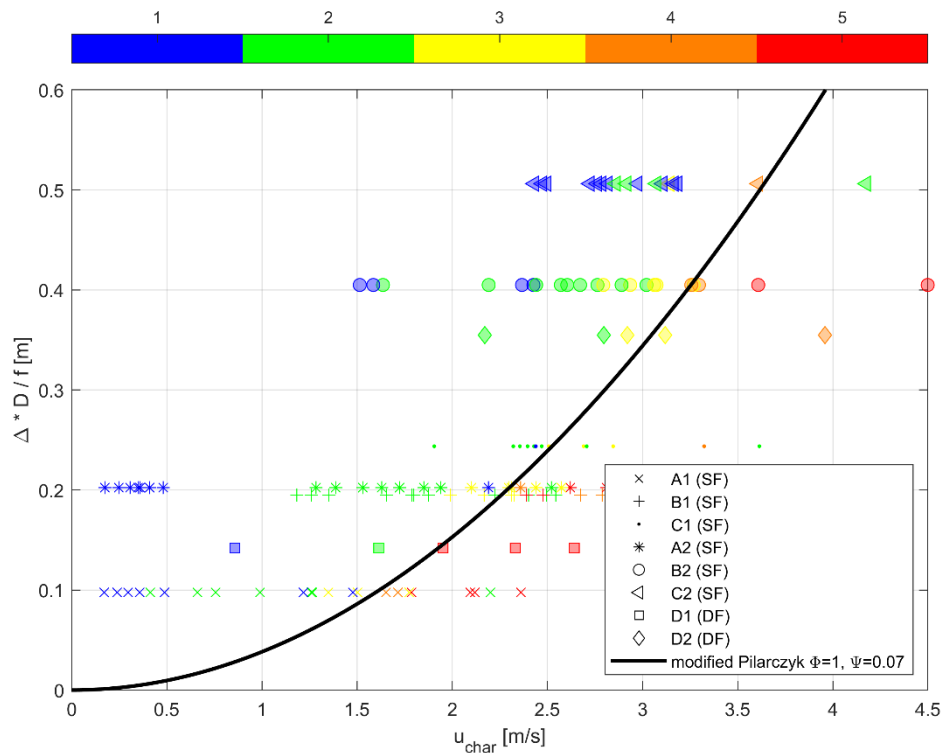


Figure 11.21 Indicative stability graph (not for detailed design) based on modified Pilarczyk formulation for ballast-filled mattresses monopile scour protections. Colored data points present the classification of mattress stability according to Table 11.3 for all individual tests performed in JIP HaSPro. Solid black line presents the theoretical modified Pilarczyk formulation (parameters according to Table 11.10) within the tested ranges of  $\Delta D/f$  and  $u_{char}$ .

Stability graph cable protection

Ballast-filled mattress stability tests at cables were also performed in both the Scheldt Flume and the Delta Flume. Overall, two different mattress types were tested in the Scheldt flume with the same layout, whereas in the Delta Flume two mattress types were tested with two layout variations. A short summary of those tests is presented in Table 11.12. Examples of tested layouts are presented in the photographs taken during the execution of tests in Figure 11.22.

Table 11.12 Short overview of tests with ballast-filled mattresses as a cable protection.

Facility	Scale factor	Mattress scale model	f (-)	Test conditions (No. of tests)	No. of layout variations
Scheldt Flume	30	A1: flexible, 10 mm	2	CO (6), RWO (18), IWO (3)	1
		A2: flexible, 12 mm		CO (7), RWO (16), IWO (3)	
Delta Flume	6	D3: 31% 2-5 mm ND rock, 61% rubber, unconnected	2	IWO (11)	2
		D4: 23% 2-5 mm ND rock, 77% rubber, unconnected		IWO (11)	

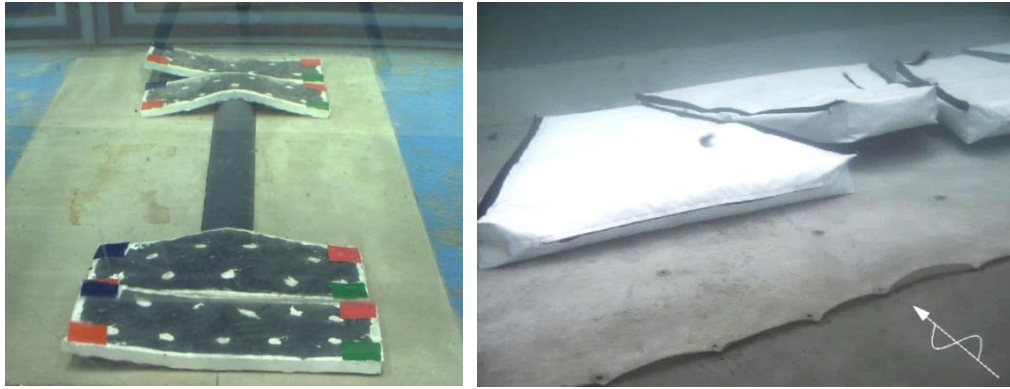


Figure 11.22 Left: ballast-filled mattresses at a crossing in Scheldt Flume. Right: ballast-filled mattresses at a cable in Delta Flume.

Figure 11.23 presents an indicative stability graph with a (fitted) modified Pilarczyk line plotted through data points corresponding to individual tests performed in JIP HaSPro per mattress type tested around a cable. At the area to the left from this line, ballast-filled mattresses can be assumed to be (nearly) stable, and vice versa. In this plot, all tested hydraulic conditions and layouts are plotted together, and hence given the large variability of control parameters, an increase in  $u_{char}$  is not always accompanied by a degrading performance of ballast-filled mattress in terms of stability. In general, the fitted Pilarczyk line is deemed representative.

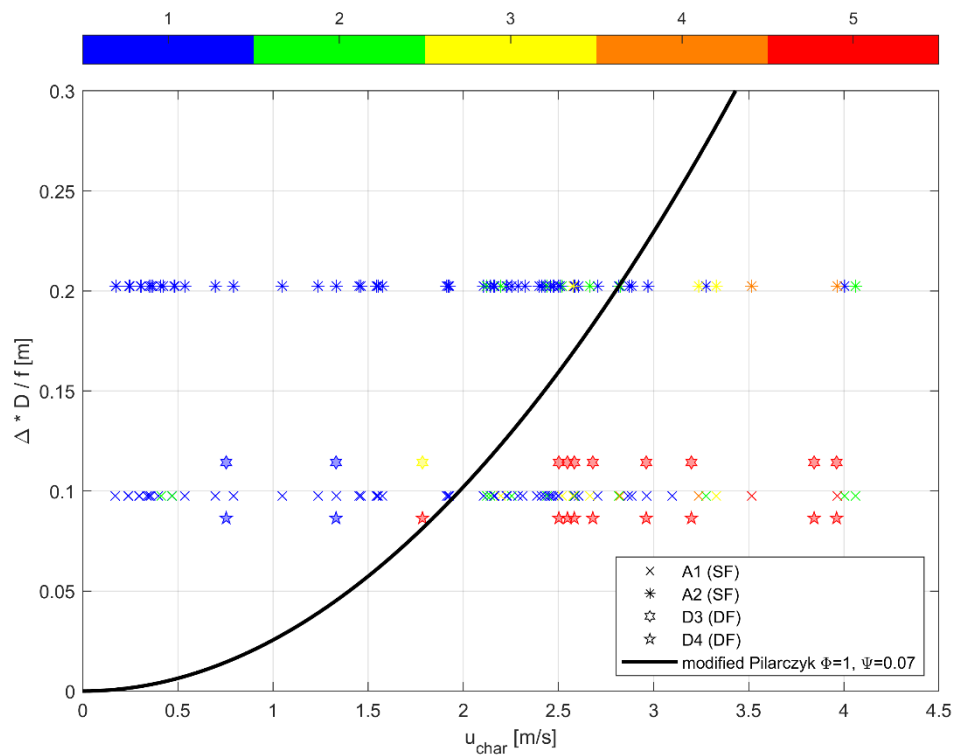


Figure 11.23 Indicative stability graph (not for detailed design) based on modified Pilarczyk formulation for ballast-filled mattresses cable scour protections. Colored data points present the classification of mattress stability according to Table 11.3 for individual tests performed in JIP HaSPro. Solid black line presents the theoretical modified Pilarczyk formulation (parameters according to Table 11.10) within the tested ranges of  $\Delta D/f$  and  $u_{char}$ .

#### 11.5.4 Design considerations to deal with edge scour

Edge scour around a mattress scour protection can lead to failure of the entire scour protection if it causes undermining of the mattresses (possible when the mattresses are not flexible enough) or if it causes sliding of the mattresses into the edge scour holes. The edge scour that occurs around a protection is mainly dependent on the hydrodynamic conditions at the site, the composition of the seabed and the dimensions of the structure and scour protection. In this, the scour protection characteristics that influence the development of edge scour are the extent of the protection (from the structure) and the height of the protection itself. Insufficient extent of the scour protection around a monopile leads to increased edge scour due to the flow amplification around the structure.

For the mattresses in the physical model tests of JIP HaSPRO a diametral extent of approximately  $3.0D$  was applied (see Figure 11.24), which in general should be sufficient to limit the effect of the pile on the edge scour development. When a smaller extent is applied, more edge scour is expected due to the increased flow amplification close to the monopile. Similarly, a larger scour protection thickness generally leads to an increase in edge scour due to the increased flow disturbance over the scour protection itself. This disturbance (and thus the edge scour development) can generally be reduced by decreasing the scour protection thickness (although this can be contradictory to the external or scour prevention requirement) or by ensuring a smoother transition to the bed (tapered/sloping edge of the protection).

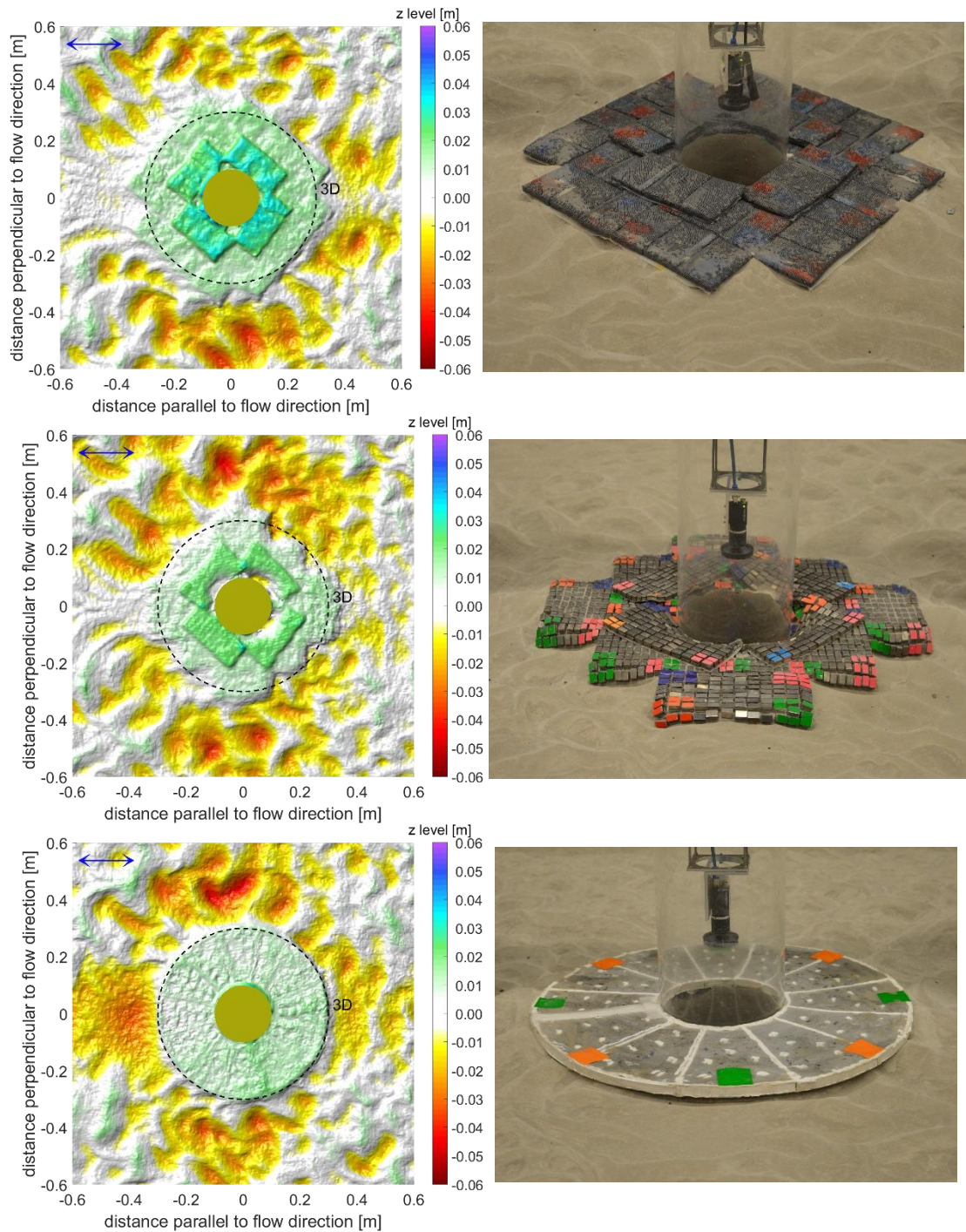


Figure 11.24 Edge scour around a gabion mattress scour protection (top), block mattress scour protection (middle) and ballast-filled scour protection (bottom) in current-only scale model tests, with a bathymetry plot derived from stereophotography (left) and a photo after the current-only tests (right).

### Gabion mattresses

For the gabion mattress (top row of Figure 11.24), some limited undermining occurred underneath the corners of the edge mattresses. However, in time (with increased undermining) this undermining was covered by the lowering of the mattress edges. Consequently, the flexibility of the mattresses covered the slopes of developing scour holes, thereby protecting the bed underneath the mattresses. During the model tests the gabion mattresses were therefore flexible enough to follow bed level changes (edge scour or winnowing at the pile face). However, it should be mentioned that it was very difficult to properly scale the stiffness of the gabion mattress. For field scale applications

the flexibility of the mattresses should therefore be determined on a larger scale, based on previous experiences or by means of a monitoring campaign. Flexibility tests of gabion mattresses in river training works show that generally undermining of the mattresses occurs in case of limited scour, and that only with increasing scour (i.e. further undermining) the mattress starts to follow the changing bed shapes. Based on the test data, it is recommended to extend the mattresses by at least 1.5 to 2.0 times the expected scour depth. This will ensure there is sufficient extent to allow for some undermining before the mattresses will be able to follow the scour hole.

During the physical model tests, no sliding of the edge mattresses (into the edge scour hole) was observed. There generally is sufficient friction between the mattresses and the seabed to prevent sliding. It should be noted here that this is the case for mattresses with a geotextile. Furthermore, sediment build-up within the gabion mattresses themselves helps to prevent the sliding here.

#### Block mattresses

The block mattresses (middle row of Figure 11.24), by its nature, are very flexible. During the JIP HaSPro physical model tests they were able to follow any bed level changes at the edge of the scour protection. The ability of the blocks to move individually immediately stabilizes the side slopes of the developing edge scour holes. The mattress flexibility therewith prevents undermining of the mattresses and protects the bed underneath the mattresses from ongoing edge scour.

It should be noted that ongoing edge scour or morphological development can in time lead to some small gaps between individual mattresses, either through sliding of the mattresses or uplift events. This was also observed during the JIP HaSPro model tests, where mattresses lowering/sliding into a scour hole led to small gaps between mattresses. This should be considered during the design phase, as such gaps can lead to increased winnowing between the mattresses, which compromises the integrity of the entire scour protection. Interconnecting individual mattresses should prevent these gaps, as the mattresses can no longer move on their own.

#### Ballast-filled mattresses

The ability of ballast-filled mattresses (bottom row of Figure 11.24) to follow bed level changes (edge scour and/or morphological development) is dependent on the flexibility of the ballast-filled mattress. During the JIP HaSPro tests, both flexible and more stiff ballast-filled mattresses were tested. In general, the flexible mattresses were able to follow these changing bed levels and cover the bed. However, stiffer mattresses were not able to follow the developing edge scour hole, which resulted in undermining underneath the mattress. This also holds for rigid parts of the protection, such as steel bars/arms of self-installable systems. Flexible mattresses are therefore preferred with regard to following changing bed shapes.

It should be mentioned that mattresses which follow the edge scour, and thereby are slightly hanging into the edge scour hole, are more stable than horizontal mattresses. Mattresses where the edge is acting as a falling apron experience less lift and more (resisting) drag, and therefore have improved external stability. Based on the JIP HaSPro tests, it is therefore recommended to increase the weight on the edge of the mattresses (for instance by incorporating a steel chain). This will improve the external stability (as uplift starts at the edge) and improves the flexibility of the mattress (the edge should start with following changes of bed shapes).

#### General considerations

It should be noted that there were no dedicated edge scour tests with alternative systems during the JIP HaSPro tests. Therefore, the observed edge scour holes were relatively shallow and with mild slopes. If a mattress scour protection is considered at locations with large edge scour potential (for instance with high tidal currents) or morphological development (migrating sand waves), the flexibility of the mattresses will need to be rechecked in dedicated physical model tests. In such conditions, it is expected that a larger extent (from the structure) is necessary to prevent ongoing undermining of the scour protection. This might result in entire mattresses being positioned on the

side slope of the edge scour. The stability of those mattresses (and their resistance against sliding) should be determined in advance (i.e. in dedicated physical model tests). Interconnecting the individual mattresses might help to increase the resistance against sliding of the edge mattresses.

As mentioned above, flexible mattresses are generally required to follow changing bed shapes such as edge scour and morphological development. However, flexible mattresses are generally more prone to uplift (less resistance against bending) and are thus less stable than mattresses which have a higher bending stiffness. These requirements are contradicting, and therefore often a balance needs to be struck in the design of mattress scour protection: not too flexible mattresses (to prevent frequent uplift) but flexible enough to follow bed shapes (to prevent mattress undermining). Another option would be to over-dimension a flexible mattress, to counteract the limited resistance against bending.

### 11.5.5 Physical model test considerations

As mentioned in Section 11.5.1, the tests within JIP HaSPro were aimed at exploring the proof-of-concept of weighted mattresses in offshore conditions and the resulting considerations should not be viewed as all-conclusive and definitive, but as an indication for the design. Therefore, it is highly recommended to perform dedicated physical model tests to validate the performance of any scour protection design with weighted mattresses. This section provides some considerations with regard to such model tests, based on the experience of the JIP HaSPro physical model tests.

#### Scour prevention

An important scale effect in scour tests with mattresses is associated with the sediment mobility (grain size). Sediment size cannot be scaled in model tests simultaneously with the Froude scaling of hydrodynamic conditions because that would lead to very small grain diameters with cohesive erosion behaviour. This means that the sediment underneath the mattress scour protection is less mobile in the model than in the field, with larger timescales of scour development in the model than the Froude-scaled timescales. This scale effect needs to be kept in mind when evaluating the quantitative test results.

With regard to preventing scour, physical model tests with a mattress scour protection should be performed on a sediment bed. It is advised to perform both current (tidal) tests and storm tests to investigate the scour prevention of the design in both hydrodynamic conditions. Furthermore, it is highly advised to take potential installation accuracies into account, to investigate the effect of mattress placement in the field on the scour prevention performance. It is advised to perform these scour tests on an as large as possible scale, to minimize the scale effects mentioned in the previous paragraph.

#### Mattress stability

The stability formulation and graphs provided in Section 11.5.3 only provide a first indication of the stability of mattresses, but this is of course also dependent on the specific mattress dimensions and protection layout. Therefore, it is important to validate the stability of a mattress scour protection with dedicated physical model tests. In these model tests, the stability of the entire scour protection under design storm conditions should be investigated. With regard to mattress stability, it is important that a conservative test setup is chosen to ensure the model test results are representative for the field situation.

This for instance means that the stability of the mattresses is preferably tested on a fixed bed rather than a sediment bed to prevent sediment infill inside or on top of the mattresses, which would increase the stability on model scale but might not occur on field scale. To ensure a similar friction between the mattresses and the bed, artificial roughness can be applied on the fixed bed. Furthermore, it is advised to construct scale model mattresses with a flexibility in the same order as the field scale mattresses to ensure relatively similar bending/sliding behaviour under uplift events.



Please note that already small stability failures (i.e. limited mattress movement) can lead to gaps in the protection that cause scour underneath the protection. Therefore, the results of mattress stability tests should not just focus on the stability of the mattresses but also on the consequences with regard to the scour prevention performance of the protection.

#### Edge scour and flexibility

The expected edge scour development around a mattress scour protection should be investigated as well. Therefore, physical model tests should be performed on a sediment bed to assess the edge scour potential and the response of the scour protection to the edge scour. These tests should contain the conditions that are dominating the edge scour development (generally tidal conditions). Based on the measured amount of edge scour around the scour protection, the extent of the scour protection might need to be adjusted to ensure sufficient bed level fixation around the structure.

Furthermore, the mattress scour protection should be sufficiently flexible to follow these bed level changes, as to prevent undermining of the scour protection. Therefore, it is advised to construct model scale mattresses with similar flexibility as the field scale mattresses and simultaneously test the flexibility of the scour protection. However, for larger scale factors (smaller scale models) similar flexibility might be difficult to achieve, as this is dependent on the available mesh material. In those cases, it is advised to test the flexibility of full-scale mattresses in the field and compare this to the required flexibility based on the edge scour tests. Please note that the stability of mattresses on the edge scour side slopes (risk of sliding) should still be investigated in this case, for instance by applying artificial edge scour and installing mattresses on the side slopes (i.e. artificially installing the situation after edge scour development).

## 11.6 Installation

Weighted mattresses are generally installed pre- or post-foundation installation by means of lifting frames. The general installation approach for these mattresses has been described in more detail in Section 9.3. This section specifies additional mattress-specific installation requirements and/or considerations.

### 11.6.1 Block mattresses

The deployment of concrete mattresses is a fairly moderate marine operation, but a comprehensive lifting and rigging study must be carried out. The installation beam or frame must be capable of a safe, accurate and time effective handling of the mattress under dynamic sea conditions.

Before installation commences it is important to have agreed installation accuracy criteria. For offshore foundations, generally a very high installation accuracy is required to prevent exposed seabed in between the mattresses, as gaps in the mattress protection will lead to scour of the seabed near the foundation. Similarly, overlapping mattresses (one mattress partly on top of another mattress) should be prevented as much as possible, because these mattresses are less stable as they are exposed to higher drag loads. Before installation there should be a detailed plan on remedial measures in case either of these installation issues occur.

To prevent exposed seabed in between different mattresses, the geotextile underneath the mattress can be extended (outside of the concrete blocks). It should be kept in mind however, that most geotextiles are lighter than seawater and will tend to be buoyant. This will complicate placing a neighbouring mattress on top of the geotextile overlap band. Measures should be taken to prevent the overlap bands from floating upward, for instance with small bars or a mesh.

Concrete mattresses are mainly installed one-by-one by transferring a single mattress to the seabed at a time. The deployment tools should be ROV friendly (or use for instance a GPS frame), easily controlled by the crane operator and have an as much as possible automated releasement system.

The equipment utilized during installation are lifting frames and beams, ROVs and rigging equipment (shackles, slings etc.) and is described in more detail in Section 9.3.1.

### 11.6.2 Gabion mattresses

After being delivered in flat packs, gabions are pre-filled and placed by a crane equipped with lifting hooks and a placement frame (see Figure 11.25 for an example with installation from a pontoon). For offshore applications it can be chosen to pre-fill the gabion mattresses on shore (might require more deck space dependent on the number of gabions) or fill them at sea (requires additional equipment and time). Generally, a DP2 vessel is sufficient to install gabion mattresses. The maximum size of the mattresses is determined by the capacity of the crane and the deformations of the mattresses. With sufficient crane capacity, multiple mattresses can be installed simultaneously, which might also help in achieving the required installation accuracy. Similar to block mattresses, gaps between mattresses and overlapping mattresses should be avoided and a detailed plan should be in place (before installation) on remedial measures in case this does happen.

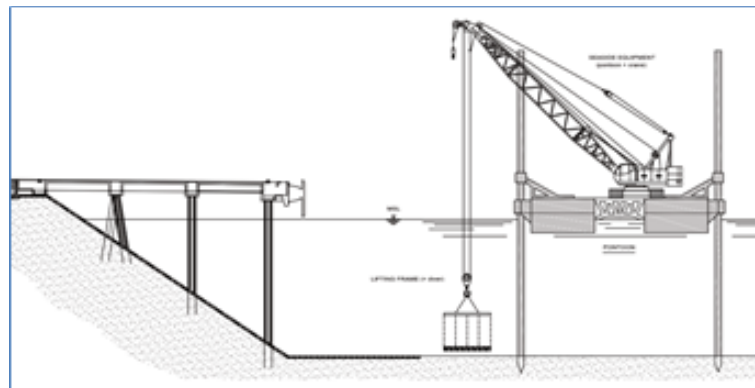


Figure 11.25 Placing of mattress with a crane from pontoon.

The recommended lifting accessories are:

- Lifting re-bars;
- Shackles and hooks;
- Lifting straps, chain ropes, or cable slings.

The use of  $\Omega$ -shaped lifting bars placed at bottom of the empty unit is recommended. The  $\Omega$ -shaped lifting bars should be placed so that the upper side of the  $\Omega$  sticks out above the unit (see Figure 11.26). The use of prefabricated units, with the lifting accessories assembled at the factory, should be preferred to guarantee higher product quality.



Figure 11.26  $\Omega$ -shaped lifting re-bars for gabions and gabion mattresses.

In most hydraulic applications of gabions and mattresses, a geotextile is required at the interface between the unit and soil for separation and filtration purposes. To prevent erosion at the gaps between the units (whose installation accuracy depends on the local conditions: visibility, currents, etc.), large sized prefabricated gabions and gabion mattresses can be equipped with side bands, to avoid that any portion of bottom soil might remain unprotected (Figure 11.27). The side bands can be 0.3-0.5 m wide and made from a geotextile coupled to the wire mesh, stiffened by extended re-bars from the main unit.

For the laying of gabions, ROV operated frames equipped with a specific mechanical device in order to have a contemporary unhooking of the lifting loops are usually adopted; for further details on installation procedures and equipment reference is made to Section 9.3.



Figure 11.27 Installation of a gabion mattress with side bands using an automatic frame.

Considering the relative stiffness of the gabion mattress, a very uneven bed at the project site can result in (partial) free-spanning of the mattresses. Before installation of the mattresses it should therefore be determined whether they are flexible enough to follow the bed forms present at the project site. Any mattress free-spanning will severely reduce the stability of the gabions. Therefore, it is recommended to remove any significant unevenness (i.e. which can lead to mattress free-spanning) before installation of the gabions.

### 11.6.3 Ballast-filled mattresses

As mentioned before, the ballast-filled mattress is still a concept and hence no guidelines or best practices exist for installing this system. Similar to block and gabion mattresses, ballast-filled mattresses can be installed by a conventional method (placing individual mattresses on the seabed).

Potentially this system can be installed during or immediately after monopile installation by means of an automatic frame (similar to the artificial vegetation, see Sections 9.3.2 and 10.6). With an automatic frame, empty ballast-filled mattresses (i.e. only the shell) can be lowered along the monopile. An example of an automatic frame with mattresses is shown in Figure 11.28, which were performed on scale 1:6 during JIP HaSPro.



Figure 11.28 Frame with ballast-filled mattresses during model tests.

Upon reaching the seabed, the protection can be slowly folded out, see Figure 11.29. After unfolding, the bed is protected against immediate scour. For more information on the tests with the automatic frame, reference is made to Deltares (2023I).

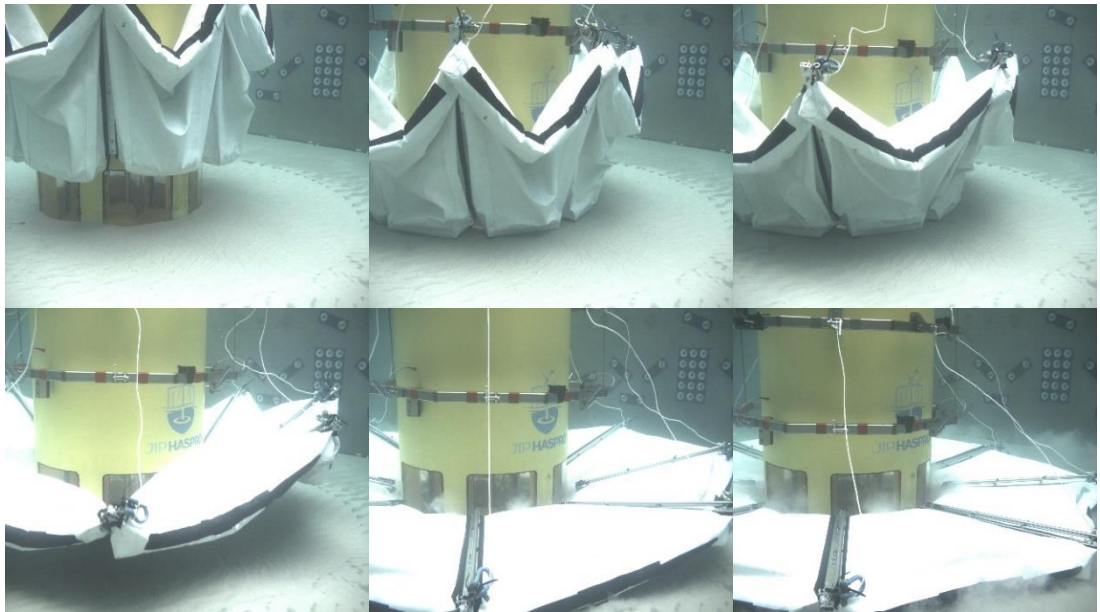


Figure 11.29 Unfolding of the frame with ballast-filled mattresses at the bottom of the flume.

After unfolding, the mattresses still need to be ballasted to ensure stability under more severe wave and current conditions. The ballast (for example bentonite or slurry) needs to be pumped into the shells, which requires an additional connection to the installation vessel and equipment to pump the ballast into the mattresses.

Please note that with an automatic frame, consideration must be given to any protuberances or holes along the monopile. Furthermore, please note that in the figures above the scour protection consists of multiple mattresses. To prevent wash-out as mattress transitions, it is recommended to

apply a single mattress, covering the entire scour protection (see for example Figure 11.11). This prevents any mattress transitions and might simplify the filling process.

During JIP HaSPro, filling tests were performed with a type of ballast-filled mattress on model scale. In general, these small-scale mattresses could be filled relatively quickly without clogging of the mattresses. For more information on these tests, reference is made to Deltares (2023m). Before application in the field, it is recommended to perform similar tests on field scale to ensure the filling process also works with larger mattresses.

# Part IV

## Ecological Impact

# 12 Nature Inclusive Design

## 12.1 Introduction

Offshore wind projects are usually accompanied by extensive environmental impact assessments. These are mainly focused on potential negative effects on the environment such as noise impacts on mammals and fish especially during the installation phase, collision threat to seabirds and cumulative effects from changing habitats e.g. Hiscock et al. (2002) and OSPAR (2008). Recently, growing interest is also shown in possible positive environmental impacts of wind farms. These are especially related with scour protections around offshore infrastructure foundations.

The steel structures of foundations together with the scour protections that usually consist of loose rock, introduce a hard substrate to the sandy seabed areas, in which wind farms are commonly built for practical reasons. Consequently, a new habitat is formed which can affect the composition of marine species occupying this area (Hammar et al., 2010). In addition, a wind farm acts as a marine protected area, due to limitation of pressure activities e.g. Ashley et al. (2014) and Langhamer (2012). Scour protections have thus the potential to become successful artificial reefs. Artificial reefs in a sandy environment are known to result in an increase in local biodiversity (Coolen, 2017). The growth of organisms on the offshore wind infrastructure leads to development of hard substrate communities, that can in turn provide a source of food for many mobile species Andersson & Öhman (2010). In fact, monitoring of Offshore Windpark Egmond aan Zee (OWEZ) and Prinses Amalia Wind Park (PAWP) in the Netherlands, where conventional loose rock scour protections were installed, has proven the presence of many species and a large biodiversity e.g. Reubens et al. (2014) and Bouma & Lengkeek (2012).

Moreover, in some areas, human activities have led to degradation of historical hard substrate habitats. For example, in the North Sea, due to overexploitation and bottom trawling, oyster grounds and rocky substrate habitats have largely disappeared (Van Duren et al., 2016). The loss of the previously present areas of hard substrate has led to a loss of habitat and a loss of biodiversity on an ecosystem scale, as well as a reduction of keystone species that were iconic for the North Sea. The growth of offshore wind and the associated introduction of hard substrates in sandy seabed areas could, in some cases, lead to an opportunity of partial restoration of lost habitats.

This chapter discusses Nature-Inclusive Design principles (Section 12.2) and provides an overview of various concepts (Section 12.3). For each of these concepts, a table is provided which discusses primary objectives, ecological benefits, target species and technical considerations.

## 12.2 Nature-inclusive design principles

Despite the inherent complexity of predicting ecosystem functioning and the relatively short time scale of available data from ongoing field studies, when it comes to ecofriendly scour protections, there are many concepts to choose from. The most suitable strategy relates to the target species under consideration. For example, when artificial structures are supposed to be colonized by species similar to the species that were originally present in an area of interest, it is important that the new structure closely resembles the original natural reef structure (Coolen, 2017). However, potential negative effects on the original local often sandy habitat species are also possible. Furthermore, invasive species can potentially use the new artificial habitat as well. Therefore, an informed decision is important when constructing scour protections with ecological improvements in mind.

The extent of colonization of the scour protection by various species depends on the protection design and on the environmental factors (e.g. salinity, turbidity and temperature) (Langhamer, 2012). Offshore structures such as scour protection can be optimized for ecological purposes

through the “nature-inclusive design” approach, aiming to increase biodiversity by closely resembling a natural situation in terms of substrate and creating structural complexity in the habitat (Lengkeek et al. (2017) and Van Duren et al. (2016)). It is suggested that a wider spectrum of niche sizes is thought to suit a larger number of different organisms at various stages of development Langhamer (2012). Crevices found in the scour protections can attract mobile species by providing feeding grounds or shelter from predators and water movement. Moreover, some species are more likely to grow where materials that have specific favourable chemical properties exist (e.g. chalk-rich substrates for flat oysters, see Lengkeek et al. (2017)). Finally, complex surface texture of introduced elements in the marine environment is also proven by field studies to promote the colonization by marine fauna and flora (Perkol-Finkel & Sella, 2014).

Based on the considered prevalent ecological parameters relating to specific umbrella species, there are several concepts that are aimed at optimizing the ecological functioning of wind farms. These concern either adjustments to conventional scour protections consisting of loose rock (e.g. by integrating the so-called “ecological units” in their vicinity), or alternative eco-friendly scour protection concepts. To start with adjustments of conventional scour protection, the grading of loose rock can be designed such that the optimum pore sizes are present at the surface of the scour protection. These pores provide the required crevices to attract various types of species. Also, part of the rock material can consist of limestone. This is favourable settlement material for oysters (Vasquez et al., 2014) because it consists of calcium carbonate. Similar to this approach is the integration of shells in the loose rock scour protections that are also chalk-rich. Another approach is to integrate in the scour protection, artificial reef elements such as tubes and reef balls of various sizes to provide shelter for target species. Furthermore, alternative scour protections are considered to loose rock, amongst which gabions with packed shells and rock, and concrete block mattresses consisting of favourable material composition and surface texture. Finally, a concept with growing attention is to deploy small populations of living organisms as part of the scour protection, in locations with scarce naturally occurring species of interest (e.g. living oyster material, see Lengkeek et al. (2017)). It is expected that through monitoring of field studies and iterations in the design, significant advancements will be made in the near future, such that for many different target species the optimum characteristics of a scour protection will be known.

### 12.3 Overview of nature-inclusive design concepts

More detailed information for the well-known eco-friendly scour protection concepts is given in this section. Per nature-inclusive design an elaboration is provided for the concept objectives, the related ecological benefit (e.g. increase of biomass, biodiversity etc.), reference target species that the concept could preferably favor. Moreover, some technical specifications related to installation phase and/or the design requirements are provided, as well as possible limitations and risks. Finally, the current status of implementation or assessment of the performance of these concepts in terms of both ecological functioning and hydraulic stability is shown.

Note that several target species are presented in the tables below. These include *Homarus gammarus* (European lobster), *Cancer pagurus* (Crab), *Gadus morhua* (Atlantic cod), *Ostrea edulis* (European flat oyster), sea anemones and *Jassa marmorata* (amphipods). These target species concern parts of potential Dutch offshore wind farm general region, for which studies are available with regards to optimizing environmental impacts of scour protections. These are intended to serve as reference species only, in the sense that the same environmental conditions may not apply in other sites.

The concepts that are presented in the remainder of this chapter are presented in Table 12.1 below, and it is also noted whether they were assessed in JIP HaSPro. In the following Table 12.2 until Table 12.10 further details are provided.



Table 12.1 Nature-inclusive design concepts, some of which tested in JIP HaSPro.

Nature-inclusive design concept	Tested in JIP HaSPro	Detailed information
Optimized grading of conventional scour protection	yes	Table 12.2
Optimized material of conventional scour protection	no	Table 12.3
Integration of large rock clusters in a scour protection	yes	Table 12.4
Integration of concrete tubes in a scour protection	yes	Table 12.5
Placement of concrete reef elements	yes	Table 12.6
Sprinkle layer of loose shells on the top layer of a scour protection	yes	Table 12.7
Deployment of living oysters in the vicinity of a scour protection	no	Table 12.8
Oyster shell gabions	yes	Table 12.9
Block mattresses with “econcrete”	no	Table 12.10

Table 12.2 Characteristics of nature-inclusive design option “optimized rock grading”.


<b>Optimized grading of conventional scour protection</b>	
	
<b>Objective</b>	<b>Technical specifications</b>
<p>Creation of pores (of various sizes) at the top layer of scour protection.</p>	<p>There are two options when it comes to the adjustment of rock grading of a scour protection. At one hand, a double-layer scour protection with a distinct armour layer consisting of large, relatively uniform rocks in size is expected to create large crevices near the surface, which can be beneficial for large mobile species.</p> <p>On the other hand, single-layer scour protections, characterized by a wide grain size distribution, are generally beneficial for creating pores with a variability in sizes, which may benefit small species of various types and sizes in various stages of their lives.</p> <p>No additional installation considerations arise from using this eco-friendly concept.</p>
<b>Ecological benefit</b>	<b>Limitations and risks</b>
<p>Creation of crevices where several species can find shelter.</p> <p>Subsequent increase of biomass and biodiversity.</p>	<p>A dynamically stable scour protection which is often used in offshore wind farms generally allows for significant redistribution of rock. This in turn leads to some mixing of rocks that are originally installed at the surface, deeper in the scour protection and vice versa. Therefore, significant storm events might disrupt spatially and/or temporarily the growth of an artificial reef and hence threaten habitat stability and durability that consist two of the main ecological principles for habitat optimization.</p>
<b>Reference target species</b>	<b>Current assessment status</b>
<p>Target species include European lobster, crab, juvenile and adult Atlantic cod, European flat oyster, sea anemones and amphipods.</p>	<p>Ecological monitoring in windfarms Horns Rev 1 (Denmark), Egmond aan Zee and Prinses Amaliawindpark (Netherlands) proved that double-layer scour protections allowed for significant benthos recruitment and biodiversity. Hydraulic stability of all loose rock scour protections is well researched and understood.</p>

Table 12.3 Characteristics of nature-inclusive design option “optimized material”.


<b>Optimized material of conventional scour protection</b>	
	
<b>Objective</b>	<b>Technical specifications</b>
Inclusion of calcareous limestone as part of the rock mixture (usually consisting of granite) used in the scour protection.	It is important that the part of the mixture consisting of limestone is exposed as much as possible at the top layer of the scour protection. This could be accounted for during the installation phase of the scour protection.
<b>Ecological benefit</b>	<b>Limitations and risks</b>
Provision of material with favorable chemical properties for colonization by specific species. Subsequent increase of biomass due to settlement substrate. Restoration of oyster reefs. Increase of biodiversity.	Limestone rock is generally known to be prone to deterioration over a time scale of several years especially in acidic (fresh water) environments. This should be taken into account, in the design of scour protections.
<b>Reference target species</b>	<b>Current assessment status</b>
The target species is the European flat oyster.	No testing focused on the ecological functioning of this concept, either in laboratory or field conditions has taken place so far.

Table 12.4 Characteristics of nature-inclusive design option “integration of large rock clusters”


<b>Integration of large rock clusters in a scour protection</b>	
	
<b>Objective</b>	<b>Technical specifications</b>
Creation of large-sized pores at the top layer of scour protection.	The large rock clusters should be installed after the completion of the scour protection layer. Thorough placement of very large rocks to create the needed large pore sizes is required with crane operation.
<b>Ecological benefit</b>	<b>Limitations and risks</b>
Creation of crevices where large mobile species can find shelter. Provision of additional adhesion surface. Subsequent increase of biomass and biodiversity.	Hydraulic stability of the cluster as whole is dependent on the initial placement and interlocking of the rocks. However, these individual heavy rocks are characterized from very low mobility. Therefore, any displacement is expected to be such, that large pores are still present even after some rock movement has occurred.
<b>Reference target species</b>	<b>Current assessment status</b>
Target species include European lobster and adult Atlantic cod.	No testing focused on the ecological functioning of this concept, either in laboratory or field conditions has taken place so far. Conclusions can be drawn from monitoring of Egmond aan Zee and Prinses Amaliawindpark in the Netherlands that regards growth on double-layer scour protection rock. Regarding hydraulic stability, this concept is tested in laboratory conditions for JIP HaSPro and was deemed to have potential for success.

Table 12.5 Characteristics of nature-inclusive design option “integration of concrete tubes”


<b>Integration of concrete tubes in a scour protection</b>	
	
<b>Objective</b>	<b>Technical specifications</b>
<p>Creation of sheltered space and of horizontal surface in the top layer of the scour protection.</p>	<p>Concrete tubes should be large enough to accommodate target species accounting for the potential of sand or rock infill. Openings should be included at the surface of the tube to allow for water renewal. The diameter of the openings should be optimized to prevent predators but also to account for marine growth that could lead to clogging.</p> <p>Because it is needed to embed the pipes in the scour protection rock, the installation of the scour protection should be adjusted accordingly. For example, cranes may be used to place the pipes on top of the filter layer before starting the installation of the armour layer, in the case of a double-layer scour protection.</p>
<b>Ecological benefit</b>	<b>Limitations and risks</b>
<p>Provision of shelter to (large) mobile species. Surface for adhesion of many different species leading to reef function. Subsequent increase of biomass and biodiversity.</p>	<p>Embedment depth inside the scour protection and permeability to flow (related to orientation with main current and wave propagation direction) are governing the hydraulic stability of these elements.</p> <p>Sand from ambient sediment transport or rock from scour protection may lead to unwanted clogging of the entrance openings.</p> <p>While generally the orientation of the tubes should be such that some shelter from flow is provided to the target species, in relatively calm areas it may also be important to ensure enough water movement in the tubes. This is to prevent water from becoming stagnant and the associated low-oxygen conditions.</p> <p>During installation of the armour rock, there may be a risk of crushing of the ecological elements. Integrity of the elements in relation to rock impact should therefore be considered.</p> <p>Finally, tube stability might suffer from edge scour when the elements are placed at the edge of the scour protection.</p>
<b>Reference target species</b>	<b>Current assessment status</b>
<p>Target species include European lobster, Crab, and juvenile and adult Atlantic cod.</p>	<p>Regarding hydraulic stability, this concept is tested in laboratory conditions for JIP HaSPRO and was deemed to have potential for success, when pipes have sufficient embedment in the scour protection rock as well as sufficient diameter.</p>

Table 12.6 Characteristics of nature-inclusive design option “placement of concrete reef elements”.

<b>Placement of concrete reef elements</b>	
<b>Objective</b>	<b>Technical specifications</b>
<p>Creation of sheltered space and of horizontal surface in the top layer of the scour protection.</p>	<p>Reef elements are either 3d printed or molded and hence can consist of many natural shape with variable sizes. Rough surface texture and the use of concrete material with chemical properties that promote colonization by specific target species is recommended. The most common reef elements are the so called “reef balls” that are hollow spheres with many openings. A similar concept concerns solid concrete spheres with large openings. This provides less opportunities for predators and hence an ideal nursery and shelter. Reef elements are preferably installed at a distance from the monopile such that flow amplification effects are minimized. Dimensions are related to the target species. Installation on top of cable protections is also possible.</p>
<b>Ecological benefit</b>	<b>Limitations and risks</b>
<p>Provision of shelter to (large) mobile species. Surface for adhesion of many different species leading to reef function. Increase of prey. Subsequent increase of biomass and biodiversity.</p>	<p>It was observed in tests with specific layouts in laboratory conditions that under extreme conditions reef balls can become unstable. In this case, provided that they are placed at a sufficient distance from the monopile face, it was concluded from the experiments that reef balls will get displaced by flow further away from the monopile face. Therefore, the risk for the monopile coating is likely to be low, yet movement of reef balls under specific conditions may threaten other infrastructure at the scour protection (e.g. free spanning cables).</p> <p>Furthermore, the ecological functioning of a reef ball will not be at risk from possible movement, as long as the element remains exposed to the seabed surface or on top of the scour protection.</p> <p>The risk of clogging is reduced compared to tube elements because of increased protrusion in the water column leading to significant flow amplification.</p>
<b>Reference target species</b>	<b>Current assessment status</b>
<p>Target species include European lobster, adult Atlantic cod and other epifauna.</p>	<p>This is a widely applied concept all over the world with most applications of specifically reef balls in the USA and South East Asia. Nevertheless, reef balls have not been placed yet on top of a scour protection at any existing windfarm. They were placed directly on the seabed inside OWF Luchterduinen as well as in Belwind and C-Power windfarms. Hydraulic stability of reef elements was largely researched in the JIP HaSPro and the concept was deemed to have potential for success for specific design conditions.</p>

Table 12.7 Characteristics of nature-inclusive design option “sprinkle layer of loose shells”


<b>Sprinkle layer of loose shells on the top layer of a scour protection</b>	
	
<b>Objective</b>	<b>Technical specifications</b>
<p>Introduction of loose shells at the top layer of scour protection to create settlement substrate for specific species.</p>	<p>All seashells are composed of calcium carbonate which has favourable chemical properties for settlement of oysters. Therefore, any shell material available may be used as a sprinkle layer.</p> <p>It is important that shells are present at the uppermost layer of the scour protection so the deployment of shells is preferably performed after the completion of the scour protection.</p>
<b>Ecological benefit</b>	<b>Limitations and risks</b>
<p>Provision of material with favorable chemical properties for colonization by specific species. Subsequent increase of biomass due to settlement substrate and oyster reef restoration.</p>	<p>Shells are generally lightweight, and this may lead to a wash out of the sprinkle layer even during relatively mild events that occur with high frequency.</p> <p>From tests performed in laboratory conditions, it was concluded that shells gain their hydraulic stability from hiding behind the protruding rocks of the scour protection. This means that the size of the deployed shells should be related to the size of the installed rock to allow for this effect to take place, which given the uniformity of the various shell sizes is limited mainly from the design rock grading.</p> <p>At the same time, shells should not be too small compared to rock, as they can vanish from the top layer by moving through the pores deeper in the scour protection.</p> <p>Finally, scour holes that usually develop in the vicinity of a scour protection, may prevent oysters to colonize the soft (sandy) substrate that surrounds the scour protection, hence limiting further expansion of oyster beds.</p>
<b>Reference target species</b>	<b>Current assessment status</b>
<p>The target species is European flat oysters.</p>	<p>There is extensive research conducted so far related to the support of the oyster life cycle for restoration purposes. The focus has been on both settlement of larvae on substrate material as well as on the transport of settled larvae to another area. Nevertheless, this is not yet incorporated in wind farm scour protections.</p> <p>For hydraulic stability, this concept is tested in laboratory conditions for JIP HaSPro and was deemed to have potential for success.</p>

Table 12.8 Characteristics of nature-inclusive design options “deployment of living oysters”

<b>Deployment of living oysters in the vicinity of a scour protection</b>	
<b>Objective</b>	<b>Technical specifications</b>
<p>Introduction of adult oysters or oyster larvae in the vicinity of scour protections to promote growth of oyster reefs.</p>	<p>To facilitate deployment of living oysters in the vicinity of scour protections their availability at certain amounts should be guaranteed through a supply chain. A recommended method is to grow oysters in dedicated hatcheries as opposed to sourcing them from commercial hatcheries that can be expensive, built in controlled laboratory conditions and to deploy them offshore with the use of installation vessels.</p> <p>Note that if restoration is aimed for oyster species that have become extremely rare, and has limited dispersal potential through larval stages that float in the water column for elongated periods of time before they settle, it is necessary to actively (re-)introduce an adult source population.</p>
<b>Ecological benefit</b>	<b>Limitations and risks</b>
<p>Direct increase of biomass and oyster reef restoration. Support for oyster life cycle.</p>	<p>Large living oysters may suffer from sedimentation, and hence their deployment would be preferable in areas with relatively low ambient sediment transport.</p> <p>To increase the chances that oyster reef restoration, through deployment of oyster larvae, is successful, hard substrates (preferably consisting of calcareous material) should be considered as settlement areas.</p> <p>Furthermore, low ambient current velocities contribute to increasing the successful settlement potential.</p> <p>Finally, scour holes that usually develop in the vicinity of a scour protection, may prevent oysters to colonize the soft (sandy) substrate that surrounds the scour protection, hence limiting further expansion of oyster beds.</p>
<b>Reference target species</b>	<b>Current assessment status</b>
<p>The target species is European flat oysters.</p>	<p>A lot of research in field conditions is being conducted in the Netherlands at the moment regarding this concept. In Luchterduinen OWF the survival and growth of adult flat oyster and the settlement rates of oyster larvae on different types of substrate is researched. In OWF Borselle 3&amp;4 the settlement of oyster larvae and the biodiversity development on scour protection are researched. Finally, for Borselle V wind farm research is focused on methods for oyster displacement and on the supply chain.</p>



Table 12.9 Characteristics of nature-inclusive design option “oyster shell gabions”.

<b>Oyster shell gabions</b>	
	
<b>Objective</b>	<b>Technical specifications</b>
<p>Introduction of loose shells at the top layer of scour protection to create settlement substrate for specific species.</p>	<p>Oyster shell gabions can be successful in the offshore environment when they have enough ballasting. Therefore, the gabions cannot consist exclusively of oyster shells but also rock and hence crevices may have an additional positive effect in creating habitat. Gabion mattresses can then be used directly as scour protection for monopiles or cables. The layering inside the gabion mattress should be such that the shells are exposed at the top of the scour protection. Also, the mesh net size is deemed to be comparable to the shell size such that the latter do not fall out of the gabion. Installation of the oyster shell gabions is possible with lowering at the area of interest with the use of a crane.</p>
<b>Ecological benefit</b>	<b>Limitations and risks</b>
<p>Provision of material with favorable chemical properties for colonization by specific species. Subsequent increase of biomass and restoration of oyster reefs.</p>	<p>The main risks associated with the use of eco-friendly gabions concern the corrosion of the mesh and sedimentation. If the wire mesh corrodes or is broken due to rock movement too quickly, then the shells are more prone to get washed away compared to their rock counterpart. This is especially the case if larvae did not have yet enough time to settle and reinforce the loose shell material by gluing it together.</p>
<b>Reference target species</b>	<b>Current assessment status</b>
<p>oyster, <i>Ostrea edulis</i></p>	<p>Offshore pilots have been executed by WNF and “De Rijke Noordzee” on sandy substrates that have not been successful in terms of the desired ecological function, due to high sedimentation. Another pilot aimed at dissipating wave energy, with Pacific oysters is conducted by Stichting Ecoshape in the Eastern Scheldt with promising results regarding oyster larvae colonization.</p> <p>Hydraulic stability of oyster shell gabions was assessed in the framework of JIP HaSPro and was deemed successful for a range of hydrodynamic conditions. It was seen that it is governed by the underwater weight of the whole unit.</p>

Table 12.10 Characteristics of nature-inclusive design options “block mattresses with econcrete”.

<b>Block mattresses with “econcrete”</b>	
<b>Objective</b>	<b>Technical specifications</b>
<p>Application of an alternative scour protection concept that additionally focuses on providing a more suitable settlement surface for various type of species.</p>	<p>These structures are focused on providing a more suitable settlement surface for various species by adjusting accordingly the surface texture and hence roughness of the blocks, and by working with concrete enriched with chalk-rich mixtures at various compositions. The installation of such a mattress requires lowering with the use of a crane and connection of the different mattresses with the provided wire mesh.</p>
<b>Ecological benefit</b>	<b>Limitations and risks</b>
<p>Provision of favorable adhesion surface for various types of species. Subsequent increase of biomass and biodiversity.</p>	<p>Because of the thin layer of a single mattress, its surface might be prone to sedimentation that might reduce the potential of adhesion by various species.</p>
<b>Reference target species</b>	<b>Current assessment status</b>
<p>Target species is European flat oyster and other epifauna.</p>	<p>Several field trials are ongoing to measure the performance in attracting certain, pre-defined target species based predominantly on the provided texture and material composition. Hydraulic stability of these mattresses has not yet been tested either in the field or in laboratory conditions.</p>

# 13 Bibliography

## 13.1 Scientific literature

- Andersson, M. H., & Öhman, M. C. (2010). Fish and sessile assemblages associated with wind-turbine constructions in the Baltic Sea. *Marine and Freshwater Research*, 61(6), 642-650.
- Angus, N. M., & Moore, R. L. (1982). *Scour repair methods in the Southern North Sea*. Paper presented at the Offshore Technology Conference.
- Ashley, M., Mangi, S., & Rodwell, L. (2014). The potential of offshore windfarms to act as marine protected areas—a systematic review of current evidence. *Marine Policy*, 45, 301-309.
- Beemsterboer, T. (2013). *Modelling the immediate penetration of rock particles in soft clay during subsea rock installation, using a flexible fallpipe vessel*. (Master Thesis), Delft University of Technology,
- Bouma, S., & Lengkeek, W. (2012). *Benthic communities on hard substrates of the offshore wind farm Egmond aan Zee (OWEZ), including results of samples collected in scour holes* (11-205). Bureau Waardenburg
- Breusers, H., Nicollet, G., & Shen, H. (1977). Local scour around cylindrical piers. *Journal of Hydraulic Research*, 15(3), 211-252.
- Broekema, Y., Labeur, R., & Uijttewaai, W. (2018). Observations and analysis of the horizontal structure of a tidal jet at deep scour holes. *Journal of Geophysical Research: Earth Surface*, 123(12), 3162-3189.
- Coolen, J. P. W. (2017). *North Sea reefs: benthic biodiversity of artificial and rocky reefs in the southern North Sea*. (Ph.D. Thesis), Wageningen University,
- De Sonnevile, B., Joustra, R., & Verheij, H. (2014). *Winnowing at circular piers under currents*. Paper presented at the Scour and Erosion: Proceedings of the 7th International Conference on Scour and Erosion, Perth, Australia, 2-4 December 2014.
- De Sonnevile, B., Van Velzen, G., Verheij, H., & Dorst, K. (2012). *Falling aprons at circular piers under currents*: Société Hydrotechnique de France (SHF).
- De Wit, L., Plenker, D., & Broekema, Y. (2023). *3D CFD LES process-based scour simulations with morphological acceleration*. Paper presented at the 11th International Conference on Scour and Erosion (ICSE-11), Copenhagen, Denmark.
- Di Pietro, P., Lelli, M., Rahman, A., & Serkandi. (2021). Hydraulic Tests and Interpretation of Test Data for Reno Mattresses in Open Channel Flow. *IOP Conference Series: Earth and Environmental Science*, 930(1), 012025. doi:10.1088/1755-1315/930/1/012025
- Dixen, M., Hatipoglu, F., Sumer, B. M., & Fredsøe, J. (2008). Wave boundary layer over a stone-covered bed. *Coastal Engineering*, 55(1), 1-20.
- Fredsøe, J., & Deigaard, R. (1992). *Mechanics Of Coastal Sediment Transport*: World Scientific Publishing Company.
- Guan, D.-w., Xie, Y.-x., Yao, Z.-s., Chiew, Y.-M., Zhang, J.-s., & Zheng, J.-h. (2022). Local scour at offshore windfarm monopile foundations: A review. *Water Science and Engineering*, 15(1), 29-39. doi:<https://doi.org/10.1016/j.wse.2021.12.006>

- Hammar, L., Andersson, S., & Rosenberg, R. (2010). Adapting offshore wind power foundations to local environment. *Swedish Environ. Prot. Agency*, 87.
- Hiscock, K., Tyler-Walters, H., & Jones, H. (2002). High level environmental screening study for offshore wind farm developments—marine habitats and species project.
- Hoffmans, G. J., & Verheij, H. J. (1997). *Scour manual* (Vol. 96): CRC press.
- Hoffmans, G. J. C. M. (2012). *The influence of turbulence on soil erosion* (Vol. 10): Eburon Uitgeverij BV.
- Jacobsen, N. G., Bakker, W., Uijttewaal, W. S. J., & Uittenbogaard, R. (2019). Experimental investigation of the wave-induced motion of and force distribution along a flexible stem. *Journal of Fluid Mechanics*, 880, 1036-1069. doi:10.1017/jfm.2019.739
- Klein Breteler, M., Den Adel, H., & Koenders, M. A. (1992). *Placed (pitched) stone revetments: filter design rules* (M1795/H195, XXI). Delft Hydraulics & Geo Delft
- Langhamer, O. (2012). Artificial reef effect in relation to offshore renewable energy conversion: state of the art. *The Scientific World Journal*.
- Larsen, B. E., & Fuhrman, D. R. (2023). Re-parameterization of equilibrium scour depths and time scales for monopiles. *Coastal Engineering*, 185, 104356. doi:<https://doi.org/10.1016/j.coastaleng.2023.104356>
- Lengkeek, W., Dideren, K., Teunis, M., Driessen, F., Coolen, J., Bos, O., . . . Van Koningsveld, M. (2017). *Eco-friendly design of scour protection: potential enhancement of ecological functioning in offshore wind farms: Towards an implementation guide and experimental set-up*. Bureau Waardenburg
- Luhar, M., & Nepf, H. (2016). Wave-induced dynamics of flexible blades. *Journal of Fluids and Structures*, 61, 20-41.
- Luhar, M., & Nepf, H. M. (2011). Flow - induced reconfiguration of buoyant and flexible aquatic vegetation. *Limnology and Oceanography*, 56(6), 2003-2017.
- Melville, B. (2008). *The physics of local scour at bridge piers*. Paper presented at the 4th International Conference on scour and erosion, Tokyo, Japan.
- Nagakawa, H., & Suzuki, K. (1976). Local scour around bridge pier in tidal current. *Coastal Engineering in Japan*, 19, 89-100.
- Nielsen, A. W. (2011). *Scour protection of offshore wind farms*. (Ph.D. Thesis), Technical University of Denmark,
- Nielsen, A. W., Liu, X., Sumer, B. M., & Fredsøe, J. J. C. E. (2013). Flow and bed shear stresses in scour protections around a pile in a current. 72, 20-38.
- Nielsen, A. W., & Petersen, T. U. (2018). Onset of motion of sediment underneath scour protection around a monopile. *Journal of Marine Science and Engineering*, 6(3), 100.
- Nielsen, A. W., Probst, T., Petersen, T. U., & Sumer, B. M. (2015). Sinking of armour layer around a vertical cylinder exposed to waves and current. *Coastal Engineering*, 100, 58-66. doi:<http://dx.doi.org/10.1016/j.coastaleng.2015.03.010>
- OSPAR. (2008). Assessment of the environmental impact of offshore windfarms. *OSPAR Commission Biodiversity Series*, 14-15.
- Perkol-Finkel, S., & Sella, I. (2014). *Ecologically active concrete for coastal and marine infrastructure: innovative matrices and designs*. Paper presented at the From Sea to Shore—Meeting the Challenges of the Sea.

- Petersen, T. U., Mutlu Sumer, B., Fredsøe, J., Raaijmakers, T. C., & Schouten, J.-J. (2015). Edge scour at scour protections around piles in the marine environment — Laboratory and field investigation. *Coastal Engineering*, 106, 42-72. doi:<http://dx.doi.org/10.1016/j.coastaleng.2015.08.007>
- Pilarczyk, K., & Klein Breteler, M. (1998). Design alternative revetments + gabions. In *Dikes and Revetments*
- Pilarczyk, K., & Zeidler, R. (1996). *Offshore breakwaters and shore evolution control*. Rotterdam: Balkema.
- Raaijmakers, T. C., & Rudolph, D. (2008). *Time-dependent scour development under combined current and waves conditions-laboratory experiments with online monitoring technique*. Paper presented at the Proceedings 4th International Conference on Scour and Erosion (ICSE-4), November 5-7, 2008, Tokyo, Japan.
- Reubens, J. T., Degraer, S., & Vincx, M. (2014). The ecology of benthopelagic fishes at offshore wind farms: A synthesis of 4 years of research., 727, 121-136.
- Riezebos, H., Raaijmakers, T., Tönnies-Lohmann, A., Waßmuth, S., & van Steijn, P. (2016). *Scour protection design in highly morphodynamic environments*. Paper presented at the Scour and Erosion: Proceedings of the 8th International Conference on Scour and Erosion (Oxford, UK, 12-15 September 2016).
- Roulund, A., Jensen, P., Marten, K., & Whitehouse, R. (2018a). *Scour and seabed changes at cable protection rock berms - field observations*. Paper presented at the 9th International Conference on Scour and Erosion (ICSE 2018), Taipei, Taiwan.
- Roulund, A., Larsen, S., Sutherland, J., & Whitehouse, R. (2018b). *Scour at cable protection rock berms - model test observations*. Paper presented at the 9th International Conference on Scour and Erosion (ICSE 2018), Taipei, Taiwan.
- Roulund, A., Larsen, S., Whitehouse, R., & Crossouard, N. (2017). *Hydraulic stability of cable crossing rock berms in combined waves and current*. Paper presented at the Offshore Site Investigation Geotechnics 8th International Conference Proceeding.
- Roulund, A., Sumer, B. M., Fredsøe, J., & Michelsen, J. (2005). Numerical and experimental investigation of flow and scour around a circular pile. *Journal of Fluid Mechanics*, 534, 351-401.
- Roulund, A., Sutherland, J., Todd, D., & Sterner, J. (2016). *Parametric equations for Shields parameter and wave orbital velocity in combined current and irregular waves*. Paper presented at the 8th International Conference on Scour and Erosion (ICSE 2016), Oxford, UK.
- Sheppard, D. M., & Miller, W. (2006). Live-bed local pier scour experiments. *Journal of Hydraulic Engineering*, 132(7), 635-642.
- Soulsby, R. (1997). *Dynamics of marine sands: a manual for practical applications*: Thomas Telford.
- Soulsby, R. L. (2006). *Simplified calculation of wave orbital velocities* (TR 155). HRWallingford
- Sumer, B. M. (2014). Flow–structure–seabed interactions in coastal and marine environments. *Journal of Hydraulic Research*, 52(1), 1-13.
- Sumer, B. M., & Fredsøe, J. (2002). *The mechanics of scour in the marine environment*. Singapore: World Scientific.
- Van de Sande, S. A. H., Uijtewaal, W., & Verheij, H. (2014). *Validation and optimization of a design formula for stable geometrically open filter structures*. Paper presented at the 34th International Conference on Coastal Engineering, ICCE2014, Seoul, Korea.

- Van Duren, L., Gittenberger, A., Smaal, A., Van Koningsveld, M., Osinga, R., van der Lelij, J. C., & De Vries, M. (2016). *Rijke riffen in de Noordzee: verkenning naar het stimuleren van natuurlijke riffen en gebruik van kunstmatig hard substraat*. Deltares
- Van Velzen, G. (2012). *Flexible scour protection around cylindrical piles*. (M.Sc. Thesis), Delft University of Technology,
- Vasquez, H. E., K., H., H., K., & Satuito, C. J. (2014). Wheat Germ Agglutinin-Binding Glycoprotein Extract from Shells of Conspicifics Induces Settlement of Larvae of the Pacific Oyster *Crassostrea gigas* (Thunberg). (33(2)), 415-423.
- Verheij, H., Hoffmans, G., Dorst, K., & Van de Sande, S. (2012). *Interface stability of granular filter structures under currents*. Paper presented at the ICSE 6: Proceedings of the 6th International Conference on Scour and Erosion, Paris, France, 27-31 August 2012.
- Wörman, A. (1989). Riprap protection without filter layers. *Journal of Hydraulic Engineering*, 115(12), 1615-1630.

## 13.2 Standards & Guidelines

- EN 1097-1:2011 (2011), "Tests for mechanical and physical properties of aggregates – Part 1: Determination of resistance to wear (micro-Deval)", Edition January 2011.
- EN 1926:2006 (2006), "Natural stone test methods – Determination of uniaxial compressive strength", Edition December 2006.
- EN 10223-3:1997 (2008), "Steel wire and wire products for fences – Part 3: Hexagonal steel wire netting for engineering purposes", Edition December 2008.
- EN 10244-1:2001 (2009), "Steel wire and wire products – Non-ferrous metallic coatings on steel wire – Part 1: General principles", Edition April 2009.
- EN 10244-2:2001 (2022), "Steel wire and wire products – Non-ferrous metallic coatings on steel wire – Part 2: Zinc or zinc alloy coatings", Edition March 2022.
- EN 10244-1:2001 (2020), "Steel wire and wire products – Non-ferrous metallic coatings on steel wire – Part 3: Aluminium coatings", Edition March 2020.
- EN 10245-1:2011 (2011), "Steel wire and wire products – Organic coatings on steel wire – Part 1: General rules", Edition November 2011.
- EN 10245-2:2011 (2022), "Steel wire and wire products – Organic coatings on steel wire – Part 2: PVC finished wire", Edition June 2022.
- EN 10245-3:2011 (2012), "Steel wire and wire products – Organic coatings on steel wire – Part 3: PE coated wire", Edition April 2012.
- EN 10245-5:2011 (2021), "Steel wire and wire products – Organic coatings on steel wire – Part 5: Polyamide coated wire", Edition December 2021.
- EN 13383-1 (2013), "Armourstone – Part 1: Specification", Edition May 2013
- EN 13383-2 (2019), "Armourstone – Part 2: Test Methods", Edition June 2019.

CIGRE TB 623 (2015), "Recommendations for mechanical testing of submarine cables", WG B1.43, Edition June 2015, ISBN: 978-2-85873-326-2

CUR/CIRIA/CETMEF (2007), "The Rock Manual, the use of rock in hydraulic engineering", 2<sup>nd</sup> edition, C683.

DNV-RP-F107 (2019), "Recommended practice Risk assessment of pipeline protection", Edition September 2019.

DNV-RP-0618 (2022), "Recommended practice Rock scour protection monopiles", Edition September 2022.

OSPAR Commission (2008), "List of Threatened and/or declining species and habitats", June 2008, OSPAR Agreement 2008-06.

### 13.3 JIP HaSPro reports and documentation

**Deltares (2023a)**, *JIP HaSPro - Innovative scour protection installation tests using self-installable frame*, ref. nr. 1230924-004-HYE-0011, final, dated August 2023.

**Deltares (2023b)**, *JIP HaSPro – WP2 External stability of loose rock scour protection*, ref. nr. 1230924-003-HYE-0001, final, dated August 2023.

**Deltares (2023c)**, *JIP HaSPro – WP2 Flexibility of Loose rock scour protection*, ref. nr. 1230924-003-HYE-0002, final, dated August 2023.

**Deltares (2023d)**, *JIP-HaSPro – WP5 Loose rock cable protection Delta Flume*, ref. nr. 1230924-033-HYE-0001, final, dated August 2023.

**Deltares (2023e)**, *JIP HaSPro – WP5 Loose rock cable protection Atlantic Basin*, ref. nr. 1230924-033-HYE-0002, final, dated August 2023.

**Deltares (2023f)**, *JIP HaSPro – WP6 Ecological aspects – Delta Flume*, ref. nr. 1230924-037-HYE-0002, final, dated August 2023.

**Deltares (2023g)**, *JIP HaSPro – WP6 Ecological aspects – Atlantic Basin*, ref. nr. 1230924-037-HYE-0003, final, dated August 2023.

**Deltares (2023h)**, *JIP HaSPro – WP2 Interface stability of loose rock scour protections*, ref. nr. 1230924-003-HYE-0003, final, dated August 2023.

**Deltares (2023i)**, *JIP HaSPro – WP2 Artificial vegetation*, ref. nr. 1230924-004-HYE-0007, final, August 2023.

**Deltares (2023j)**, *JIP HaSPro – WP2 Block mattress*, ref. nr. 1230924-004-HYE-0010, final, dated August 2023.

**Deltares (2023k)**, *JIP HaSPro – WP2 Gabion mattress*, ref. nr. 1230924-004-HYE-0006, final, dated August 2023.

**Deltares (2023l)**, *JIP HaSPro – WP2 Filling tests of ballast-filled mattress*, ref. nr. 1230924-004-HYE-0009, final, dated August 2023.

**Deltares (2023m)**, *JIP HaSPro – WP2 Ballast-filled mattress*, ref. nr. 1230924-004-HYE-0008, final, dated August 2023.

**Deltares (2023n)**, *JIP HaSPro Analysis of scour protection deformation tests*, ref. nr. 1230924-002-HYE-0003 (v0.1).



# Appendices

# A Appendix I– Calculation of mobility number

## A.1 Introduction

The mobility number (MOB) is given by the ratio between the Shields number,  $\theta$ , and the critical Shields number,  $\theta_{cr}$ , of a certain rock grading, see equation (A.1).

$$\text{MOB} = \frac{\theta}{\theta_{cr}} \quad (\text{A.1})$$

This appendix presents the formulae used to calculate the undisturbed relative mobility value of rock under hydrodynamic loading of combined waves and currents. The input parameters for the calculations are based on the relevant boundary conditions:

- Hydrodynamic conditions (e.g.  $H_s$ ,  $T_p$ ,  $U_c$ ,  $h_w$ )
- Rock grading characteristics (e.g.  $D_{50}$ ,  $\rho$ )

The following sections first provide general parameters (Section A.2) and parameters related to rock characteristics (Section A.3). Next the current-related parameters are introduced, as is the current-related mobility calculation, in Section A.4. Subsequently the wave-related parameters and wave-related mobility calculation are presented in Section A.5. Finally, Section A.6 presents the methodology assessing the wave-current related mobility.

It is explicitly noted here that the calculation methodology of the wave- and current-related mobility follows the method presented in the DNV Recommended Practice (DNV-RP-0618). However, one important and major difference is that in the present calculation method the mobility on top of the scour protection is calculated, whereas the calculation in the DNV Recommended Practice calculates the mobility on the seabed. It was found that scour protection deformation correlates significantly better with mobility on top of the scour protection, hence this parameter was selected as the primary driving force.

## A.2 General parameters

General parameters of importance for the mobility calculation are the kinematic viscosity of the water, which determines the shear exerted by the flow on the particles, and the gravitational acceleration, which determines for a part the resistance the particles offer.

### Kinematic viscosity

For a volumetric concentration of particles smaller than 0.1:

$$\nu = \left(1.14 - 0.031 \cdot (T - 15) + 0.00068 \cdot (T - 15)^2\right) \cdot 10^{-6} \quad (\text{A.2})$$

In which:  $\nu$  = kinematic viscosity [m<sup>2</sup>/s]  
 $T$  = temperature [°C]

Note that for very high sediment concentrations the viscosity may be affected. This situation is generally not applicable for loose rock scour protections.

### Gravitational acceleration

$$g = 9.81 \text{ m/s}^2 \quad (\text{A.3})$$

### A.3 Parameters related to rock characteristics

Here, several parameters related to the rock characteristics are presented. The underwater weight of the rocks follows from the specific density of the rocks. The threshold of motion of the rocks follows from the Shields curve, which is expressed in a parameterized form needing a dimensionless particle diameter as input. The way the size of the rocks influences the roughness is given by the equivalent roughness height.

#### Specific density

$$\Delta_s = \frac{\rho_s - \rho_w}{\rho_w} \quad (\text{A.4})$$

In which:  $\Delta_s$  = specific density [-]  
 $\rho_w$  = density of water [kg/m<sup>3</sup>]  
 $\rho_s$  = density of rock grading [kg/m<sup>3</sup>]

#### Dimensionless particle diameter

$$d_* = D_{50} \cdot \left( \frac{\Delta_s \cdot g}{\nu^2} \right)^{\frac{1}{3}} \quad (\text{A.5})$$

In which:  $d_*$  = dimensionless particle diameter [-]  
 $d_{50}$  = particle diameter for which 50% by weight is smaller [m]  
 $g$  = gravitational constant (9.81) [m/s<sup>2</sup>]

#### Critical Shields parameter

The critical Shields parameter follows from a parameterization of the Shields curve by Soulsby (1997).

$$\theta_{cr} = \frac{0.3}{(1 + 1.2d_*)} + 0.055 \left( 1 - e^{(-0.02d_*)} \right) \quad (\text{A.6})$$

In which:  $\theta_{cr}$  = critical Shields parameter [-]  
 $d_*$  = dimensionless particle diameter [-]

#### Equivalent roughness height

$$k_s = n \cdot d_{50} \quad (\text{A.7})$$

In which:  $k_s$  = equivalent roughness height [m]  
 $n$  = ratio between roughness height and particle diameter. [-]

A value of  $n = 2.5$  is considered for the mobility calculation.

## A.4 Current-related mobility calculation

The current-related relative mobility value follows from a parameterization of the vertical profile of the steady depth-averaged current. The equivalent roughness height,  $k_s$ , is used to determine a representative bed roughness length. The flow exerts drag over the bed dependent on this roughness; using a drag coefficient the drag force is then translated to a shear stress, which in non-dimensional form can be related to the critical Shields parameter to determine the current-related mobility value,  $MOB_c$ .

### Bed roughness length

$$z_0 = k_s / 30 \quad (A.8)$$

In which:  $z_0$  = bed roughness length [m]

### Drag coefficient

$$C_D = \left( \frac{0.4}{\ln\left(\frac{h_w}{z_0}\right) - 1} \right)^2 \quad (A.9)$$

In which:  $C_D$  = drag coefficient [-]  
 $h_w$  = still water depth [m]

### Current-related shear velocity

$$u_{*c} = \sqrt{C_D} \cdot U_c \quad (A.10)$$

In which:  $u_{*c}$  = current-related shear velocity [m/s]  
 $U_c$  = depth-averaged current velocity [m/s]

### Current-related bed shear stress

$$\tau_c = \rho_w \cdot u_{*c}^2 \quad (A.11)$$

In which:  $\tau_c$  = current-related bed shear stress [N/m<sup>2</sup>]

### Current-related Shields parameter

$$\theta_c = \frac{\tau_c}{(\rho_s - \rho_w) g d_{50}} \quad (A.12)$$

In which:  $\theta_c$  = current-related Shields parameter [-]

### Current-related relative mobility

$$MOB_c = \frac{\theta_c}{\theta_{cr}} \quad (A.13)$$

In which:  $MOB_c$  = current-related relative mobility [-]

## A.5 Wave-related mobility calculation

This section provides the calculation methodology to determine the wave-related relative mobility. The contents of this section are split into two distinct parts: firstly, the determination of the near-bed (i.e., on top of the scour protection) wave orbital velocity is discussed, followed by how the orbital motion translates into a shear stress at the bed. To determine the wave orbital motion on top of the scour protection linear wave theory is used. In general, this method follows the methodology outlined in the DNV Recommended Practice, with a difference in how the motion on top of the scour protection is determined. For this, it is assumed that the size of the scour protection is relatively small with respect to the wave length and thus that the wave is not influence by the presence of the scour protection. Therefore, all wave-related properties are calculated assuming the water depth at the ambient seabed level. Then, these wave characteristics are used to determine the near-bed wave orbital motion on top of the scour protection. Following this methodology leads to the best correlation with the observed scour protection deformation and mobility number.

### A.5.1 Near bed wave orbital velocity

#### Definitions

The orbital wave motion induces horizontal flow velocity at the seabed or on top of the scour protection (Figure A.1), leading to a periodic bed shear stress. A general expression of the wave orbital velocity is made by

$$u_{w,a} = \begin{cases} u_{m,bed} & \text{at seabed} \\ u_{m,top} & \text{on top of scour protection} \end{cases} \quad (\text{A.14})$$

In which:

$u_{w,a}$	= orbital wave motion velocity	[m/s]
$u_{m,bed}$	= orbital wave motion velocity at seabed	[m/s]
$u_{m,top}$	= orbital wave motion velocity on top of scour protection	[m/s]

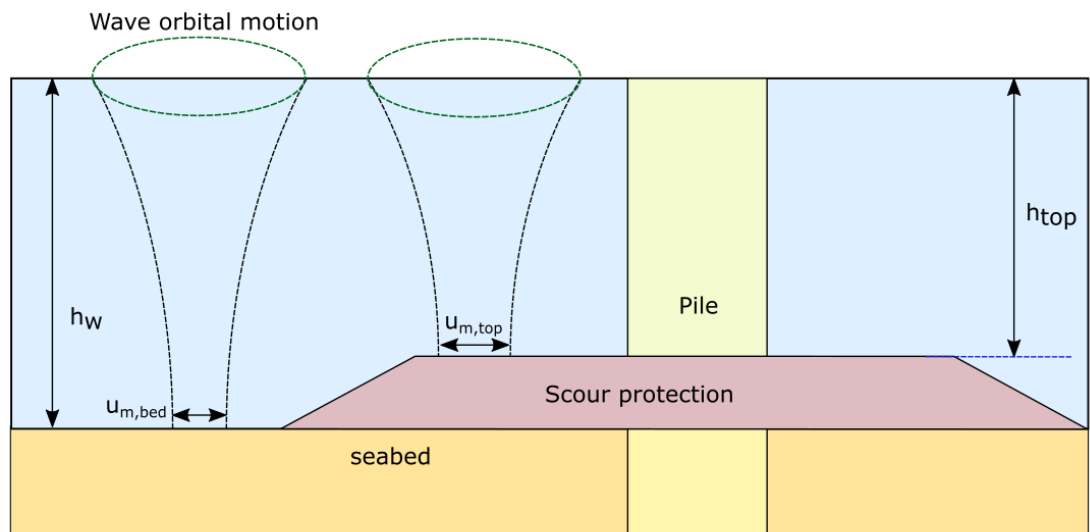


Figure A.1 Wave velocity at seabed and on top of scour protection.

In Figure A.1:

$h_{top}$	= depth from still water surface to top of scour protection	[m]
$h_w$	= still water depth	[m]

### Orbital wave motion at the bed ( $U_{m,bed}$ )

The near-bed motion is determined from the wave velocity spectrum using linear wave theory. For irregular wave conditions, the orbital wave velocity spectrum is calculated by the spectral analysis method.

$$S_{u,bed}(f) = S(f) \left( \frac{2\pi f}{\sinh\left(\frac{2\pi}{L(f)} h_w\right)} \right)^2 \quad (\text{A.15})$$

In which:  $S(f)$  = ocean wave spectrum [m<sup>2</sup>s]  
 $S_{u,bed}(f)$  = wave orbital velocity spectrum at seabed [m<sup>2</sup>s<sup>-1</sup>]  
 $f$  = component wave frequency [Hz]  
 $L(f)$  = wave length as a function of  $f$  [m]

The wave length  $L(f)$  satisfies

$$L(f) = \frac{g(1/f)^2}{2\pi} \tanh\left(\frac{2\pi h_w}{L(f)}\right) \quad (\text{A.16})$$

The orbital velocity at seabed,  $U_{m,bed}$  can be obtained by

$$u_{m,bed} = \sqrt{2} \sqrt{\int_0^\infty S_{u,bed}(f) df} \quad (\text{A.17})$$

It was shown that for a JONSWAP spectrum, the orbital wave motion at the seabed can be calculated using the Soulsby's approximation as below (Soulsby, 2006):

$$u_{m,bed} = \sqrt{2} \left( \frac{H_s}{4} \right) \sqrt{\frac{g}{h_w}} \exp \left[ - \left( \frac{3.65}{T_z} \sqrt{\frac{h_w}{g}} \right)^{2.1} \right] \quad (\text{A.18})$$

In which:  $T_z$  = zero-upcrossing period [s]  
 $H_s$  = significant wave height [m]

And

$$T_z = \frac{T_p}{1.3} \quad (\text{A.19})$$

In which:  $T_p$  = peak period [s]

### Orbital wave motion on top of scour protection ( $U_{m,top}$ )

For the wave orbital velocity on top of the scour protection, the orbital velocity spectrum can be written as,

$$S_{u,top}(f) = S(f) \left( \frac{2\pi f}{\sinh\left(\frac{2\pi}{L(f)} h_{top}\right)} \right)^2 \quad (\text{A.20})$$

In this expression, the wave length is based on the ambient water depth, thus following Equation (A.16). The wave velocity on top of the scour protection is then:

$$u_{m,top} = \sqrt{2} \sqrt{\int_0^{\infty} S_{u,top}(f) df} \quad (A.21)$$

In which:  $S_{u,top}(f)$  = wave orbital velocity spectrum on top of scour protection [m<sup>2</sup>s<sup>-1</sup>]

In the case of an irregular sea with JONSWAP spectrum,  $U_{m,bed}$  can be calculated by the Soulsby's approximation Eq. (A.18). For the case on top of the scour protection, a similar approximation can be made with the addition of a correction factor. The results fit well with the spectral analysis presented in Equations (A.20) and (A.21) since the correction factor performs the same operation that is else performed within the spectral analysis.

$$u_{m,top} = K_{top} u_{m,bed} \quad (A.22)$$

$$K_{top} = \frac{\sinh\left(\frac{2\pi h_w}{L}\right)}{\sinh\left(\frac{2\pi h_{top}}{L}\right)} \quad (A.23)$$

$$L = \frac{g \cdot T_p^2}{2\pi} \tanh\left(\frac{2\pi \cdot h_w}{L}\right) \quad (A.24)$$

In which:  $L$  = wave length based on peak period [m]  
 $K_{top}$  = correction factor for orbital velocity on top of scour protection [-]

#### Orbital wave motion amplitude (linear wave theory)

The orbital wave motion amplitude (or wave excursion) at seabed or scour protection is expressed by,

$$A_{w,a} = \begin{cases} A_{w,bed} = \frac{u_{m,bed} T_p}{2\pi} & \text{at sea bed} \\ A_{w,top} = \frac{u_{m,top} T_p}{2\pi} & \text{on top of scour protection} \end{cases} \quad (A.25)$$

In which:  $A_{w,bed}$  = wave orbital motion amplitude at seabed [m]  
 $A_{w,top}$  = wave orbital motion amplitude on top of scour protection [m]

### A.5.2 Wave related shear stress

The wave related shear stress follows from a wave friction factor, which similarly to the current-related drag force relates the bed roughness and stroke of the wave motion to an exerted drag force on the bed. This is translated into a shear stress, which in a non-dimensional form is related to the value of the critical Shields parameter, leading to the wave-related mobility number.

#### Wave friction factor

For the conditions of a rough bed and a turbulent regime, Roulund et al. (2016) proposed a piecewise function to better fit a wide range of the wave stroke to bed roughness ratio of  $A/k_s$ , which combines the methods from Dixen et al. (2008), Soulsby (1997) and Fredsoe & Deigaard (1992).



Typically, it is stated that the methodology by Dixen et al. (2008) is more valid for larger rocks whereas the Soulsby method (Soulsby, 1997) is more applied for smaller particle ranges. The combination presented by Roulund et al. (2016) provides a smooth fit to capture all these ranges. The expression is written as:

$$f_w = \begin{cases} 0.32 \left( \frac{A_{w,a}}{k_s} \right)^{-0.8} & 0.2 < \frac{A_{w,a}}{k_s} < 2.92 \\ 0.237 \left( \frac{A_{w,a}}{k_s} \right)^{-0.52} & 2.92 \leq \frac{A_{w,a}}{k_s} < 727 \\ 0.04 \left( \frac{A_{w,a}}{k_s} \right)^{-0.25} & \frac{A_{w,a}}{k_s} \geq 727 \end{cases} \quad (\text{A.26})$$

Wave-related shear velocity

$$u_{*w} = \sqrt{\frac{f_w}{2}} \cdot u_{w,a} \quad (\text{A.27})$$

In which:  $u_{*w}$  = wave-related shear velocity [m/s]  
 $f_w$  = wave friction factor [-]

Wave-related bed shear stress

$$\tau_w = \rho_w \cdot u_{*w}^2 \quad (\text{A.28})$$

In which:  $\tau_w$  = wave-related bed shear stress [N/m<sup>2</sup>]

Wave-related Shields parameter

$$\theta_w = \frac{\tau_w}{(\rho_s - \rho_w) \cdot g \cdot d_{50}} \quad (\text{A.29})$$

In which:  $\theta_w$  = wave-related Shields parameter [-]

Wave-related relative mobility

$$\text{MOB}_w = \frac{\theta_w}{\theta_{cr}} \quad (\text{A.30})$$

In which:  $\text{MOB}_w$  = wave-related relative mobility [-]

## A.6 Combined current- and wave-related mobility calculation

The total relative mobility number associated with combined wave-current forcing is calculated following a vector addition of the current- and wave-related bed shear stresses.

### Mean combined current- and wave-related bed shear stress

$$\tau_m = \tau_c + 1.2 \cdot \tau_c \cdot \left( \frac{\tau_w}{\tau_c + \tau_w} \right)^{3.2} \quad (\text{A.31})$$

In which:  $\tau_m$  = mean combined current- and wave-related bed shear stress [N/m<sup>2</sup>]

### Maximum combined current- and wave-related bed shear stress

$$\tau_{\max} = \sqrt{\tau_m^2 + \tau_w^2 + 2 \cdot \tau_w \cdot \tau_m \cdot \left| \cos \left( \frac{\alpha \cdot \pi}{180} \right) \right|} \quad (\text{A.32})$$

In which:  $\tau_{\max}$  = max. combined current- and wave-related bed shear stress [N/m<sup>2</sup>]  
 $\alpha$  = angle between waves and current [°]

### Combined current- and wave-related Shields parameter

$$\theta = \frac{\tau_{\max}}{(\rho_s - \rho_w) \cdot g \cdot d_{50}} \quad (\text{A.33})$$

In which:  $\theta$  = combined current- and wave-related Shields parameter [-]

### Combined current- and wave-related relative mobility

$$MOB = \frac{\theta}{\theta_{cr}} \quad (\text{A.34})$$

In which: MOB = combined current- and wave-related relative mobility [-]

## A.7 Mobility on a slope

To calculate the mobility on a slope, a slope factor may be used on the calculated value of the mobility on a flat bed. The value of this correction factor depends on the orientation of the slope relative to the currents. In the worst-case scenario this is flow down a slope. The correction factor is then defined as follows:

$$K_s = \frac{\sin(\varphi - \alpha)}{\sin(\varphi)} \quad (35)$$

In which:  $\varphi$  = the angle of repose of rocks (typically 40 degrees)  
 $\alpha$  = the external slope angle of the scour protection.

The mobility on a slope then follows from multiplying the critical Shields number with the reduction factor  $K_s$ . In other words, the mobility on a slope follows from dividing the mobility on a flat bed by the slope factor  $K_s$ .

## B Appendix II– Calculating total KC number

The Keulegan-Carpenter (KC) number characterizes the vortex structures of oscillating flow passing the pile. Due to the interaction between current and waves, the oscillation (direction and amplitude) of the flow shows an asymmetrical behavior. The relative velocity ratio is defined as,

$$u_{rel} = \frac{|u_c|}{|u_c| + u_{w,a}} \quad (B.1)$$

In which:  $u_{rel}$  = relative velocity ratio. [-]

$u_{rel}=0$  indicates pure wave flow;  $0 < u_{rel} < 1$  indicates wave combined with current;  $u_{rel}=1$  indicates pure current flow.

Figure B.1 shows the asymmetrical behaviors of three different scenarios. In a wave only condition, the asymmetry of flow oscillation is weak and is only due to wave nonlinearity. When current is imposed on top of waves, significant asymmetry emerges and increases as the current velocity increases. In a current-alone condition or when the current velocity is much larger than the wave velocity, the oscillatory behavior disappears.

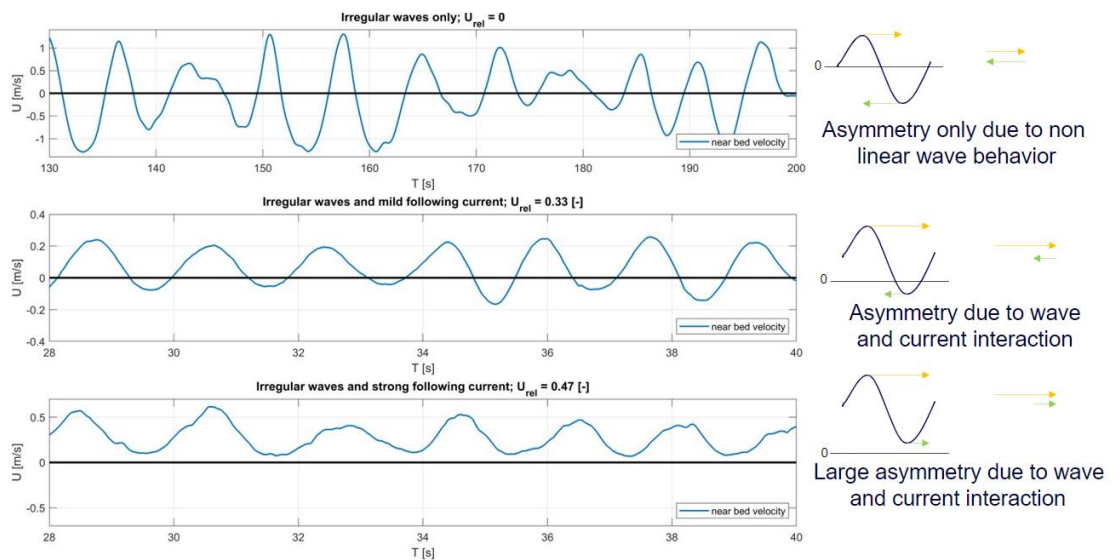


Figure B.1 Asymmetrical oscillatory flow around pile, in which  $u_{rel} = |u_c| / (|u_c| + u_{w,a})$ . Top figure : pure wave flow  $u_{rel}=0$ ; middle figure: low current combined with waves,  $u_{rel}=0.33$ ; Bottom figure: high current combined with waves,  $u_{rel}=0.47$ .

The wave related KC number is defined as

$$KC_w = \frac{u_{w,a} T_p}{D_p} \quad (B.2)$$

In which:  $D_p$  = pile diameter. [m]  
 $KC_w$  = wave related Keulegan-Carpenter number [-]

The current related KC number is defined as

$$KC_c = \frac{|u_c|T_p}{D_p} \quad (B.3)$$

In which:  $KC_c$  = current related Keulegan-Carpenter number. [-]

The asymmetry of flow oscillation can be expressed by a total KC number,  $KC_{tot}$ . In wave following current conditions,  $KC_{tot}$  is a summation of the  $KC_c$  and  $KC_w$ . In wave opposing current conditions,  $KC_{tot}$  is a summation of the  $KC_w$  and 2 times  $KC_c$ . Opposing currents typically lead to larger scour protection deformation than following currents. To be able to separate these datapoints, they are weighed more heavily in the formulation of the KC number.

$$KC_{tot} = \begin{cases} KC_w + KC_c, & u_c \geq 0 \text{ (wave following current)} \\ KC_w + 2KC_c, & u_c < 0 \text{ (wave opposing current)} \end{cases} \quad (B.4)$$

In which:  $KC_{tot}$  = total KC number. [-]

## C Appendix III– Calculation example

### C.1 Example 1: Calculating hydrodynamic parameters

A monopile with a diameter of  $D_p = 8.4$  m is applied in this example. Given a design wave condition of  $H_s = 8$  m,  $T_p = 14$  s and a depth-averaged current condition of  $u_c = 0.5$  m/s. The wave and current are in the same direction. The high density armour stone is applied ( $\rho_s = 3200$  kg/m<sup>3</sup>), the armour stone grading is 20-200kg, which corresponds to  $D_{15} = 18$  cm,  $D_{50} = 27$  cm,  $D_{85} = 40$  cm. The design thickness of the armour layer is 91 cm (4 times  $D_{n50}$ ). The water depth at the site is  $h_w = 30$  m.

The wave velocity near the bed is calculated using Eq. (A.19) and Eq. (A.18):

$$T_Z = \frac{T_p}{1.3} = \frac{14.0\text{s}}{1.3} = 10.770\text{ s}$$
$$u_{m,bed} = \sqrt{2} \left( \frac{H_s}{4} \right) \sqrt{\frac{g}{h_w}} \exp \left[ - \left( \frac{3.65}{T_Z} \sqrt{\frac{h_w}{g}} \right)^{2.1} \right]$$
$$= \sqrt{2} \left( \frac{8.0}{4} \right) \sqrt{\frac{9.81}{30.0}} \exp \left[ - \left( \frac{3.65}{10.77} \sqrt{\frac{30.0}{9.81}} \right)^{2.1} \right] = 1.159\text{ m/s}$$

The wave length is solved using the implicit formula Eq (A.24). The result is,

$$L = \frac{g \cdot T_p^2}{2\pi} \tanh \left( \frac{2\pi \cdot h_w}{L} \right) = 215.4\text{ m}$$

The correction factor is calculated by Eq. (A.23):

$$K_{top} = \frac{\sinh \left( \frac{2\pi h_w}{L} \right)}{\sinh \left( \frac{2\pi h_{top}}{L} \right)} = \frac{\sinh \left( \frac{2\pi \times 30}{215.4} \right)}{\sinh \left( \frac{2\pi \times (30 - 0.91)}{215.4} \right)} = 1.039$$

The wave velocity on top of scour protection is then obtained by Eq. (A.22),

$$u_{m,top} = K_{top} u_{m,bed} = 1.039 \times 1.159 = 1.204\text{ m/s}$$

The wave orbital motion amplitude on top of scour protection is calculated by Eq. (A.25),

$$A_{w,a} = A_{w,top} = \frac{u_{m,top} T_p}{2\pi} = \frac{1.204 \times 14}{2\pi} = 2.683\text{ m}$$

The KC numbers are calculated by Eq. B.2 and Eq.B.3

$$KC_c = \frac{|u_c| T_p}{D_p} = \frac{0.5 \times 14.0}{8.4} = 0.833$$

The total KC number should be calculated under wave following current condition (Eq.B.4), which gives:

$$KC_{tot} = KC_w + KC_c = 1.932 + 0.833 = 2.765$$

## C.2 Example 2: Calculating bed shear stresses

The roughness of the bed is calculated by Eq. (A.7), where  $n=2.5$ .

$$k_s = n \cdot d_{50} = 2.5 D_{50} = 2.5 \times 0.27 = 0.675$$

The ratio between wave motion amplitude and bed roughness becomes,

$$\frac{A_{w,a}}{k_s} = \frac{2.683}{0.675} = 3.975$$

Using Roulund's roughness formulation in Equation (A.26) can be applied to calculate the wave friction coefficient. The Soulsby's part is used for  $2.92 < A_{w,a}/k_s < 7.27$

$$f_w = 0.237 \cdot \left( \frac{A_{w,a}}{k_s} \right)^{-0.52} = 0.237 \times 3.975^{-0.52} = 0.116$$

The wave shear velocity on top of the scour protection is obtained by Eq. (A.27).

$$u_{*w} = \sqrt{\frac{f_w}{2}} \cdot u_{w,a} = \sqrt{\frac{0.116}{2}} \times 1.204 = 0.290 \text{ m/s}$$

The wave bed shear stress is estimated using Eq. (A.28),

$$\tau_w = \rho_w \cdot u_{*w}^2 = 1025 \times (0.290)^2 = 86.203 \text{ N/m}^2$$

Then we compute the current induced bed shear stress. The bed roughness length is,

$$z_0 = \frac{k_s}{30} = \frac{0.675}{30} = 0.023 \text{ m}$$

The drag coefficient is computed via Eq. (A.9),

$$C_D = \left( \frac{0.4}{\ln\left(\frac{h_w}{z_0}\right) - 1} \right)^2 = \left( \frac{0.4}{\ln\left(\frac{30}{0.023}\right) - 1} \right)^2 = 4.198 \times 10^{-3}$$

Hence, the current shear velocity is:

$$u_{*c} = \sqrt{C_D} \cdot u_c = \sqrt{4.198 \times 10^{-3}} \times 0.5 = 0.032 \text{ m/s}$$

We can compute the current shear stress by Eq. (A.11),

$$\tau_c = \rho_w \cdot u_{*c}^2 = 1025 \times (0.032)^2 = 1.050 \text{ N/m}^2$$

The mean combined current and wave related bed shear stress is obtained by Eq. (A.32),

$$\tau_m = \tau_c + 1.2 \cdot \tau_c \cdot \left( \frac{\tau_w}{\tau_c + \tau_w} \right)^{3.2} = 1.050 + 1.2 \times 1.050 \times \left( \frac{86.203}{1.050 + 86.203} \right)^{3.2} = 2.262 \text{ N/m}^2$$

The maximum combined current and wave related bed shear stress is obtained by Eq. (A.32), with the angle between current and wave  $\alpha=0^\circ$ .

$$\tau_{\max} = \sqrt{\tau_m^2 + \tau_w^2 + 2 \cdot \tau_w \cdot \tau_m \cdot \left| \cos\left(\frac{\alpha \cdot \pi}{180}\right) \right|} = \tau_m + \tau_w = 2.262 + 86.203 = 88.465 \text{ N/m}^2$$

### C.3 Example 3: Calculating mobility number

The dimensionless particle diameter is:

$$d_* = d_{50} \cdot \left( \frac{\Delta_s \cdot g}{\nu^2} \right)^{\frac{1}{3}} = 0.27 \times \left( \frac{\left( \frac{3200 - 1025}{1025} \right) \cdot 9.81}{(1.14 \times 10^{-6})^2} \right)^{\frac{1}{3}} = 6806$$

The critical Shields parameter can be calculated by Eq. (A.6),

$$\theta_{cr} = \frac{0.3}{(1 + 1.2d_*)} + 0.055 \left( 1 - e^{(-0.02d_*)} \right) = \frac{0.3}{(1 + 1.2 \times 6806)} + 0.055 \left( 1 - e^{(-0.02 \times 6806)} \right) = 0.055$$

The combined waves and current Shields parameter is calculated by Eq. (A.33),

$$\theta = \frac{\tau_{\max}}{(\rho_s - \rho_w) \cdot g \cdot d_{50}} = \frac{88.465}{(3200 - 1025) \times 9.81 \times 0.27} = 0.015$$

The mobility parameter (MOB) on top of scour protection is obtained by Eq. (A.34)

$$MOB = \frac{\theta}{\theta_{cr}} = 0.015 / 0.055 = 0.279$$

#### C.4 Example 4: Estimating depth of deformation

Using the calculated values for the mobility number  $MOB_{top}$ ,  $KC_{tot}$  and the given water depth and pile diameter, calculating the resulting deformation is straightforwardly done using Eq. (4):

$$f(KC_{tot}) = 1 + \frac{3.9274}{1 + \exp[-0.7401 \times KC_{tot} + 4.7518]} = 1.2461$$

$$S_{50\%} = D_{pile} \times 1.2461 \times 0.0707 MOB_{top}^{1.6492} = 0.09 \text{ m}$$

$$S_{90\%} = D_{pile} \times 1.2461 \times 0.1134 MOB_{top}^{1.6492} = 0.14 \text{ m}$$

Alternatively, we can look at the mobility limits as provided in Section 4.4.1.4 to estimate the expected deformation. The monopile diameter of 8.4 m means we can use both Table 4.9 (valid for 8.0 m monopile diameters) and Table 4.10 (valid for 10.0 m monopile diameters). The mobility limits presented in those tables show for the  $S_{90\%}$  prediction that for an 8.0 m pile “very limited deformation” (up to 0.25 m) is expected for mobilities up to 0.36. For a 10.0 m pile, the same classification is valid for mobilities up to 0.32. The calculated mobility for the present case-study is 0.28, which according to the deformation model leads to deformation that is less than 0.25 m.

#### C.5 Example 5: Rock berm characteristics

The same conditions as prescribed in Section C.1 are applied, thus: a design wave condition of  $H_s = 8 \text{ m}$ ,  $T_p = 14 \text{ s}$  and a depth-averaged current condition of  $u_c = 0.5 \text{ m/s}$ . The wave and current are in the same direction. The high density armour stone is applied ( $\rho_s = 3200 \text{ kg/m}^3$ ), the armour stone grading is 20-200kg, which corresponds to  $D_{15} = 18 \text{ cm}$ ,  $D_{50} = 27 \text{ cm}$ ,  $D_{85} = 40 \text{ cm}$ . The water depth at the site is  $h_w = 30 \text{ m}$ . In addition to these parameters, a Minimum Top of Cable Cover (MTOC) of 2.0 m is required. A cable diameter of 0.4 m is assumed. Installed rock berm side-slope steepness of 1:2 is assumed, so  $\alpha = 2$ .

As shown in Section C.3, the total Shields parameter for these conditions is 0.014. The reshaped rock berm profile  $B_{berm}/h_{berm}$ , also defined as  $f(\theta)$  following Equation 26, is then:

$$f(\theta) = 6000\theta^2 + 50\theta + 2.4 = 6000 \times 0.014^2 + 50 \times 0.014 + 2.4 = 4.28$$

Using the first line of Equation 26 then provides a simple estimate for the required  $TOPC$ :

$$TOPC = 0.5 \left[ \sqrt{\left(\frac{W_{top}}{\alpha}\right)^2 + \frac{4}{\alpha} \frac{2}{3} f(\theta) (MTOC + \Delta)^2} - \frac{W_{TOP}}{\alpha} \right]$$

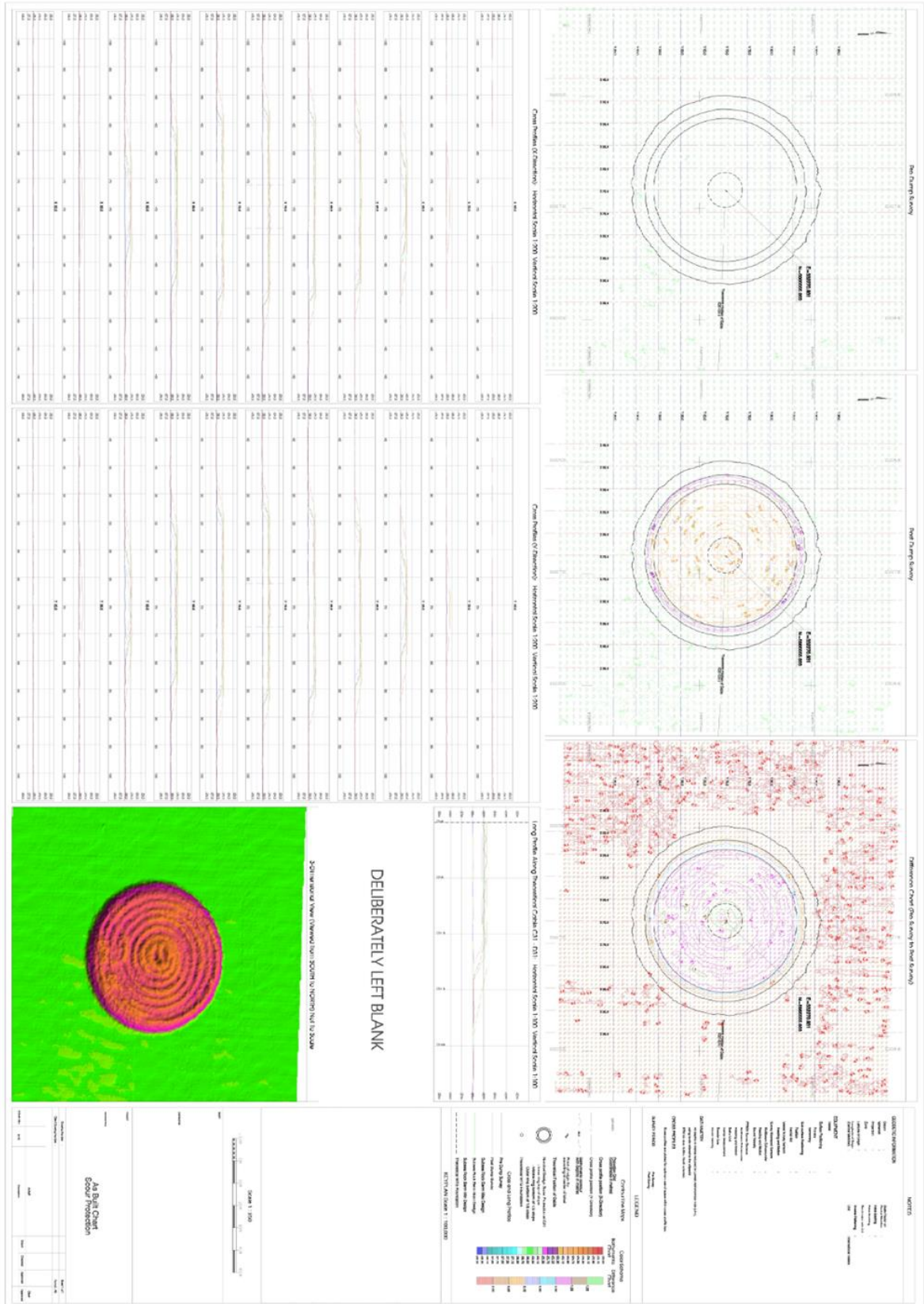
$$TOPC = 0.5 \left[ \sqrt{\left(\frac{1}{2}\right)^2 + \frac{4}{2} \frac{2}{3} \times 4.5 \times 2.4^2} - \frac{1}{2} \right] - 0.4 = 2.23 \text{ m}$$



For a minimum cable coverage of 2.0 m, the installed Top of Product Cover (*TOPC*) should be 2.2 m. This translates to a berm height ( $h_{berm}$ ) of 2.6 m following Equation 21.

Given the low Shields number, an additional check is performed with the RoBeD model. The mobility on top of the protection is 0.31, which is (significantly) lower than the threshold of 0.95. Taking into account the slope steepness of 1:2 leads to a mobility value of 0.86 on top of the slope and of 0.73 at the bottom of the slope (Deformation class 1). This implies that no reshaping will occur over the entire length of the slope, and no lowering at the top is expected, thus leaving room to lower the top-height of the berm.

# D As-built survey chart scour protection



# E Survey examples seabed changes at scour protection

The presented surveys in this appendix were made available by Ørsted.

## E.6 Inline edge scour at featureless seabed

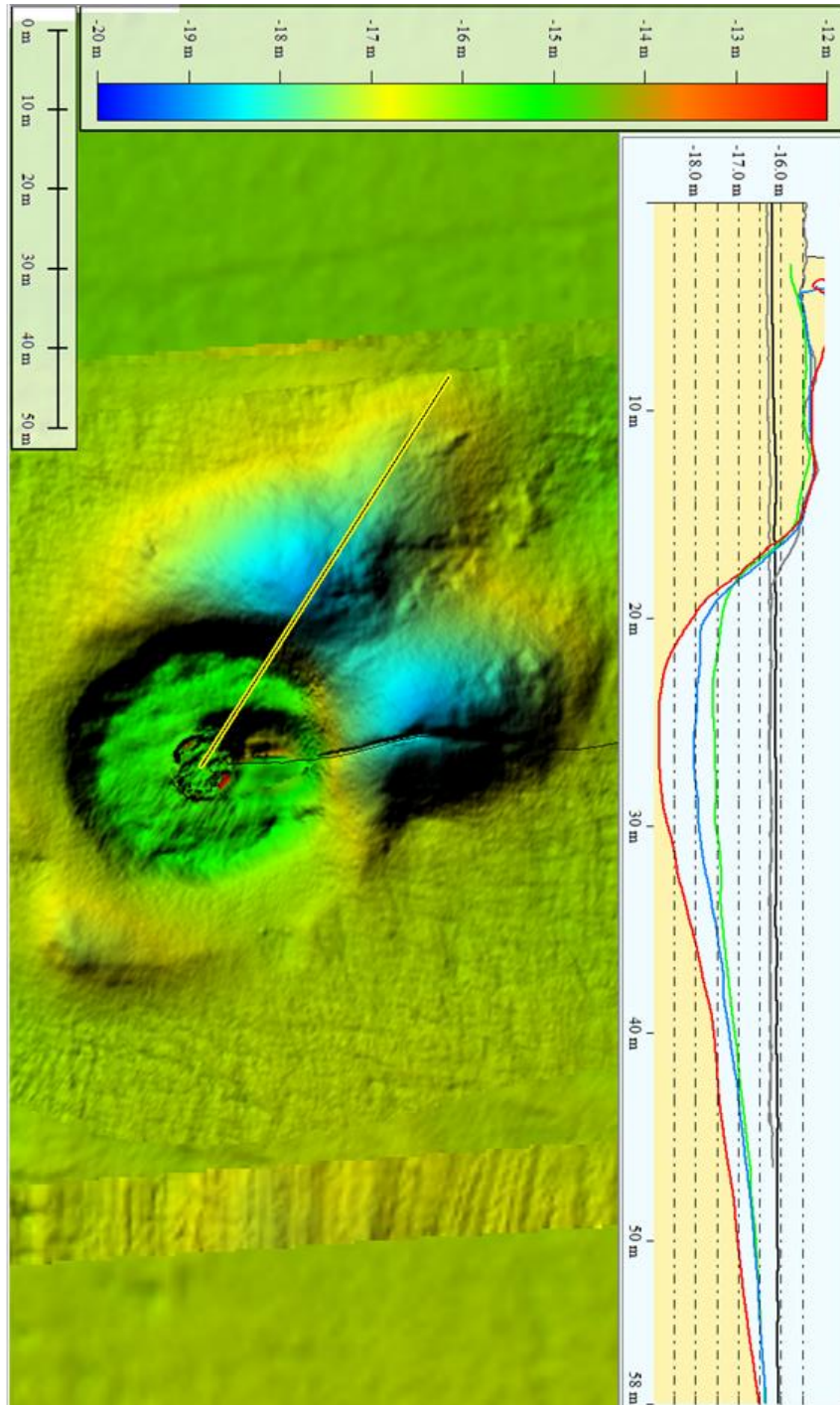


Figure E.1 Example of seabed surveys around scour protection. Surveys taken in 2014 (black), 2016 (as-built, grey), 2018 (green), 2021 (blue) and 2023 (red). Levels are in mLAT.

## E.7 Sand wave migration past a monopile and scour protection

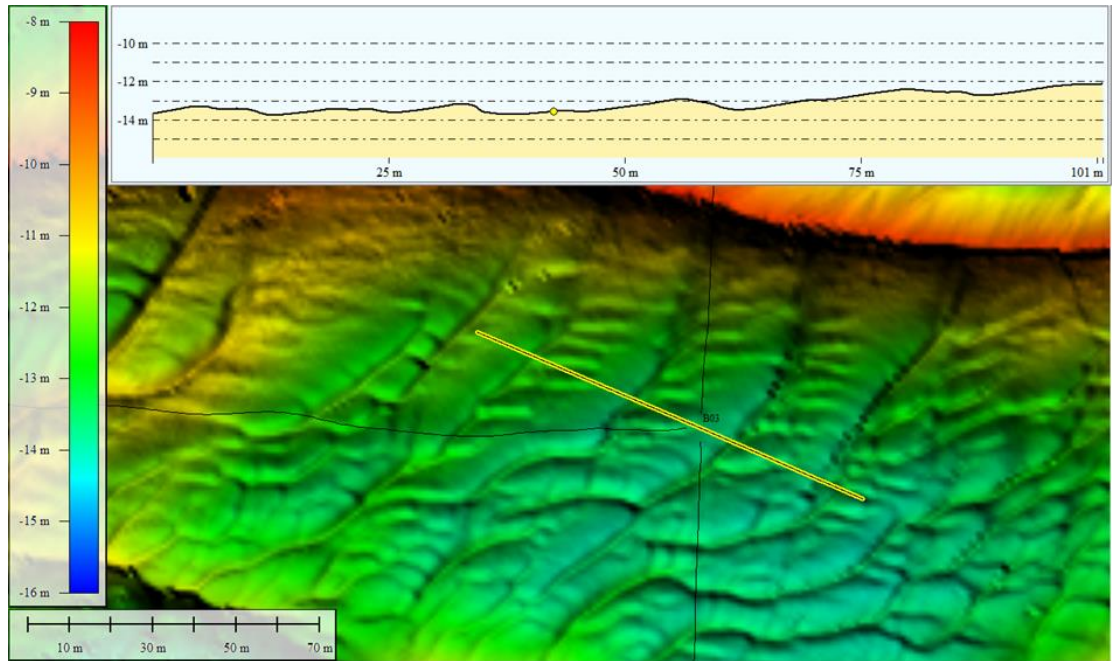


Figure E.2 Sand wave migration past monopile and scour protection, survey 1. Bed level measured in 2014 (black) in mLAT.

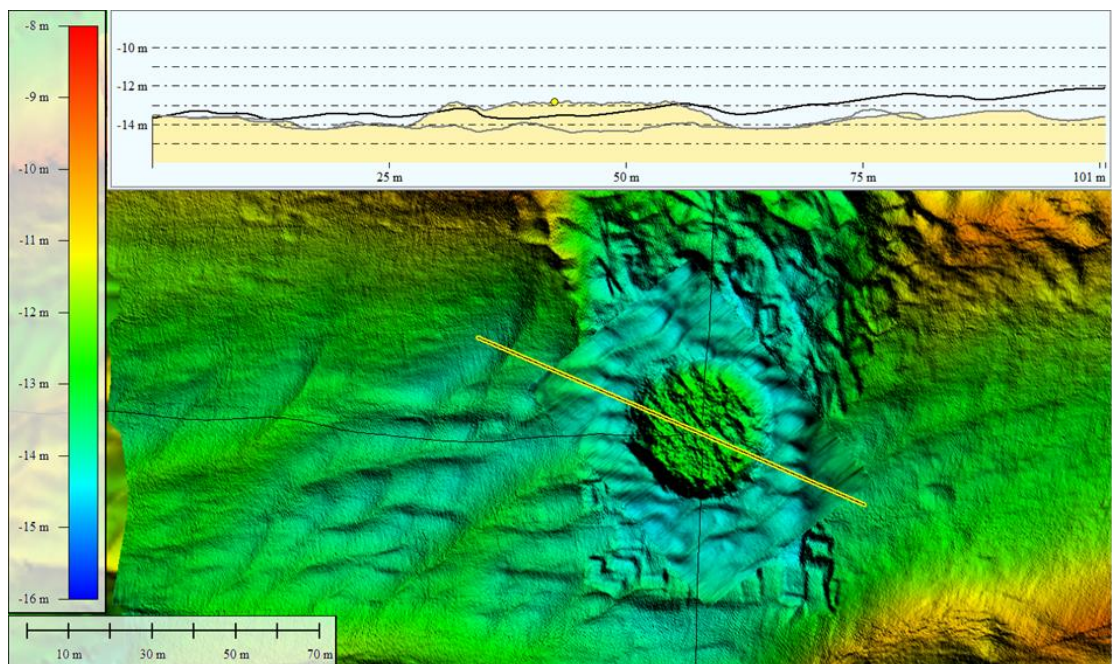


Figure E.3 Sand wave migration past monopile and scour protection, survey 2. Bed level measured in 2014 (black), as-built dredging and scour protection in 2016 (grey) in mLAT.

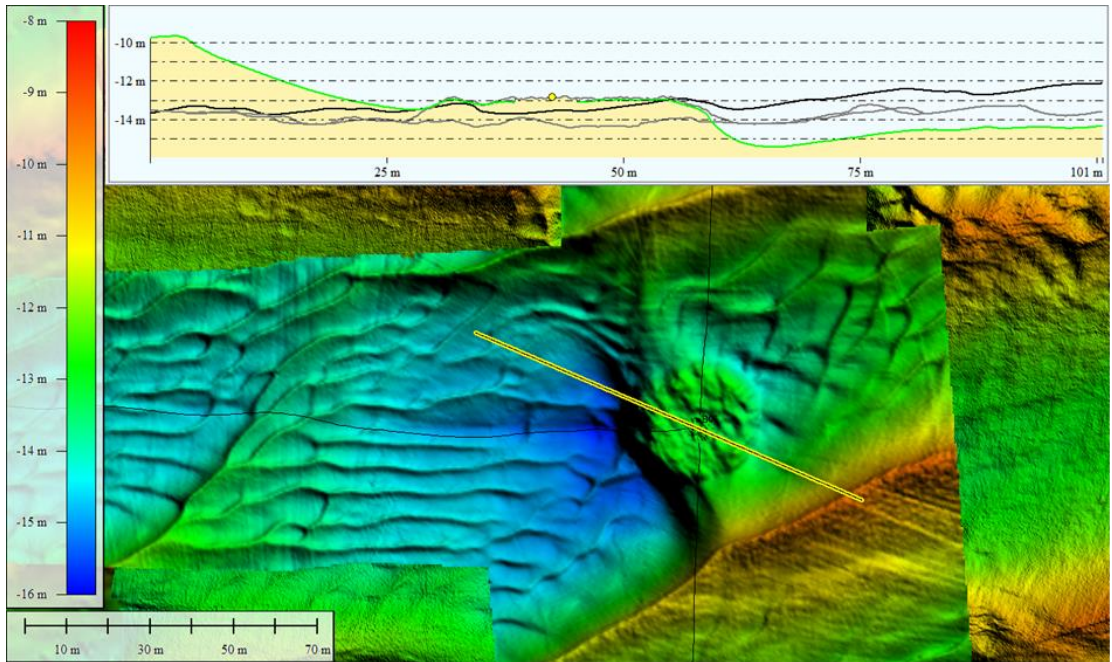


Figure E.4 Sand wave migration past monopile and scour protection, survey 3. Bed level measured in 2014 (black), as-built 2016 (grey) and in 2018 (green) in mLAT.

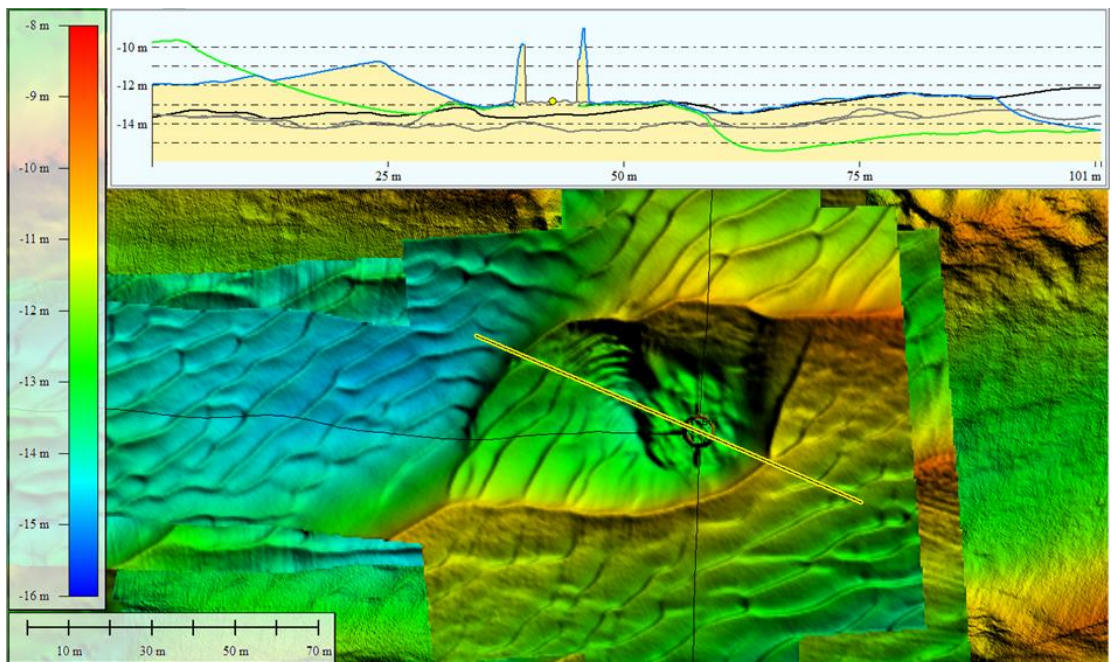


Figure E.5 Sand wave migration past monopile and scour protection, survey 4. Bed level measured in 2014 (black), as-built (2016), in 2018 (green) and in 2021 (blue) in mLAT.

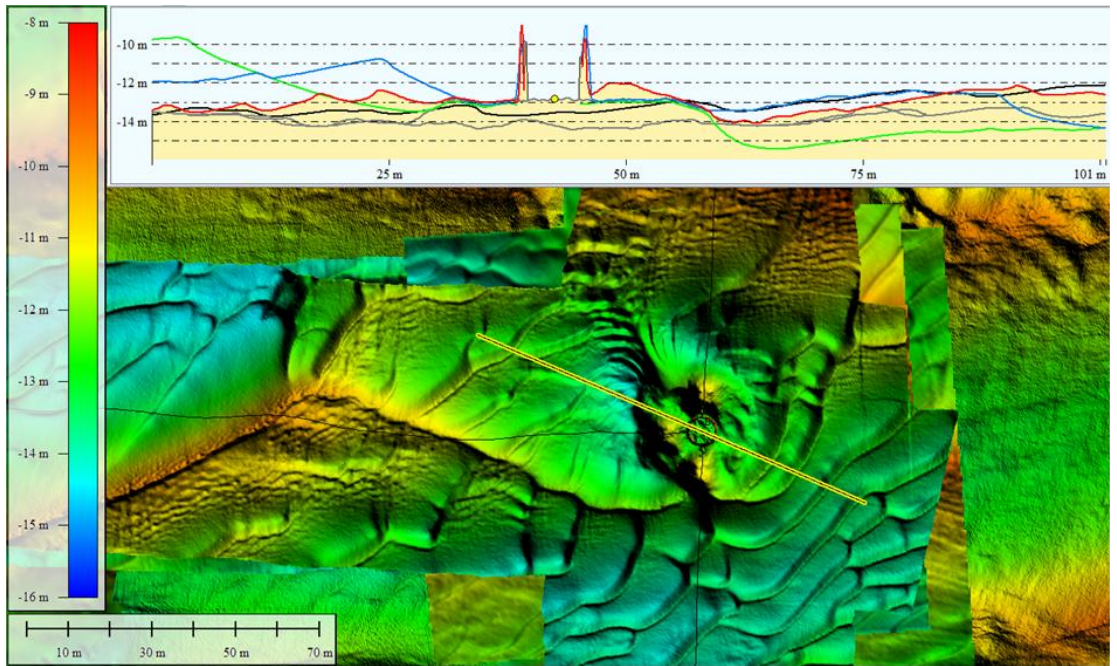


Figure E.6 Sand wave migration past monopile and scour protection, survey 5. Bed level measured in 2014 (black), as-built 2016 (grey), in 2018 (green), in 2021 (blue) and in 2023 (red) in mLAT.

## E.8 Sand wave migration past a monopile and scour protection

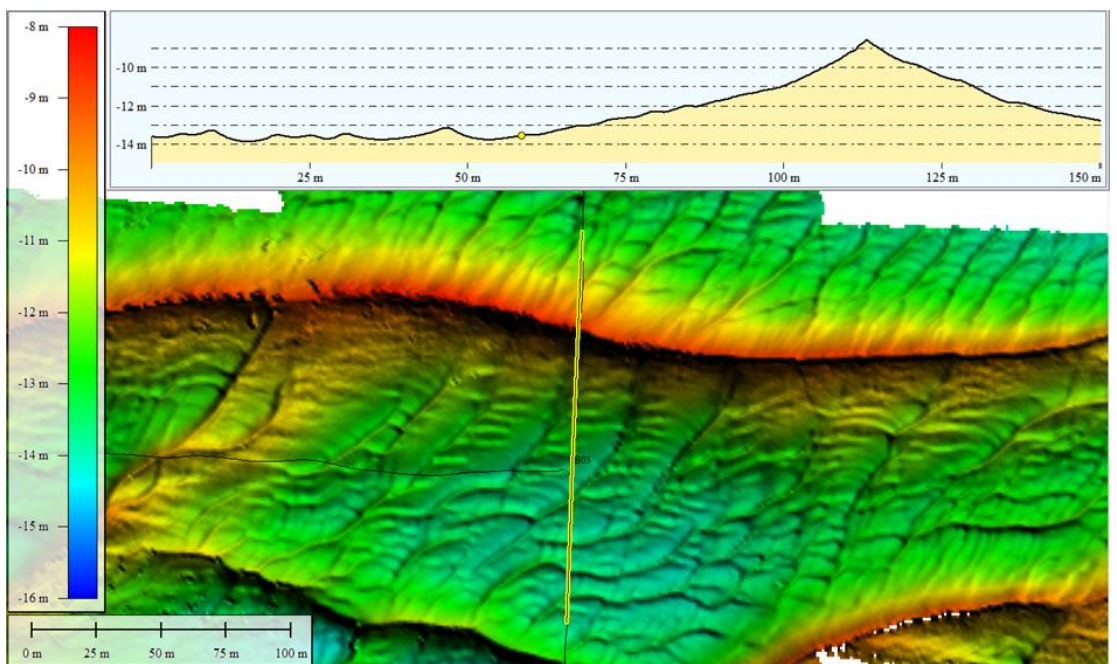


Figure E.7 Sand wave migration past monopile and scour protection, survey 1. Bed level measured in 2014 (black) in mLAT.

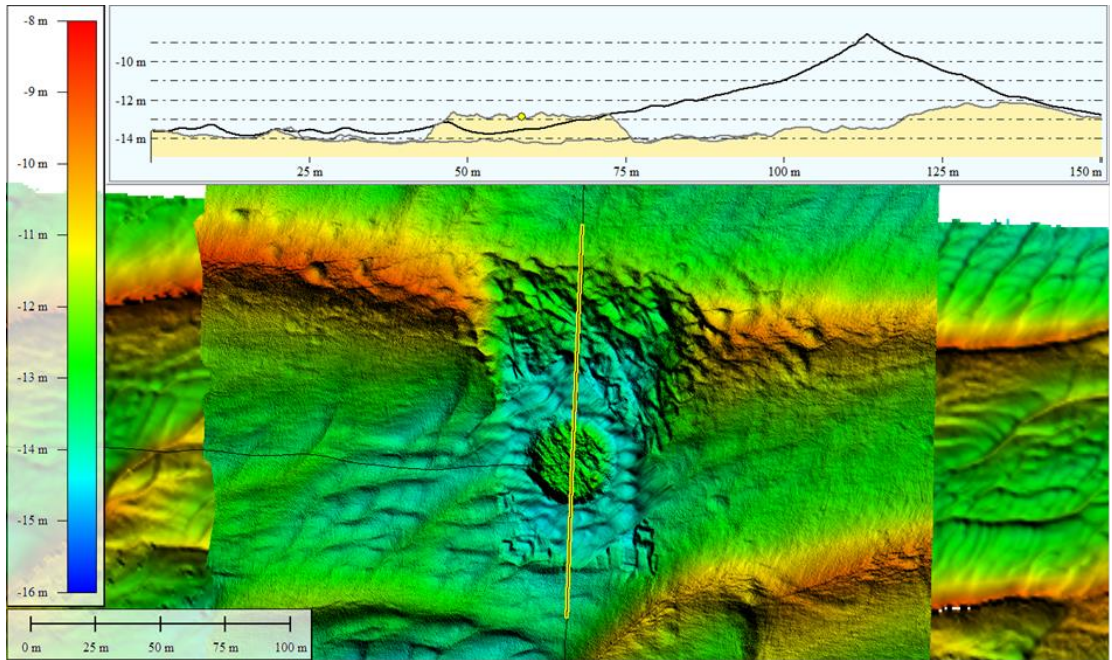


Figure E.8 Sand wave migration past monopile and scour protection, survey 2. Bed level measured in 2014 (black), as-built dredging and scour protection in 2016 (grey) in mLAT.

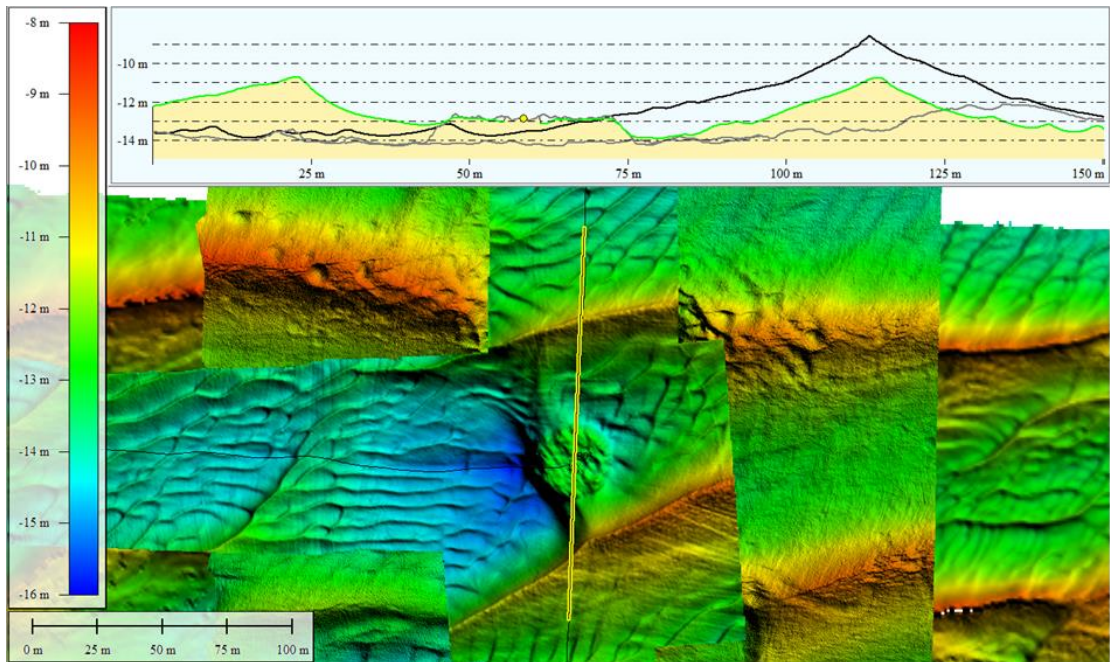


Figure E.9 Sand wave migration past monopile and scour protection, survey 3. Bed level measured in 2014 (black), as-built 2016 (grey) and in 2018 (green) in mLAT.

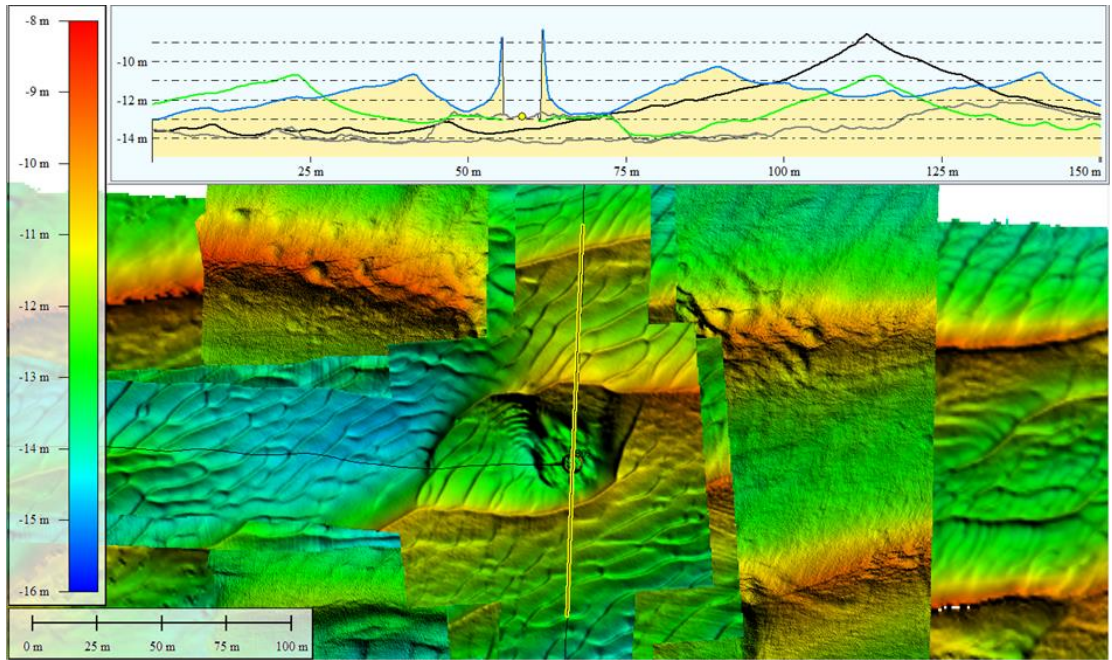


Figure E.10 Sand wave migration past monopile and scour protection, survey 4. Bed level measured in 2014 (black), as-built (2016), in 2018 (green) and in 2021 (blue) in mLAT.

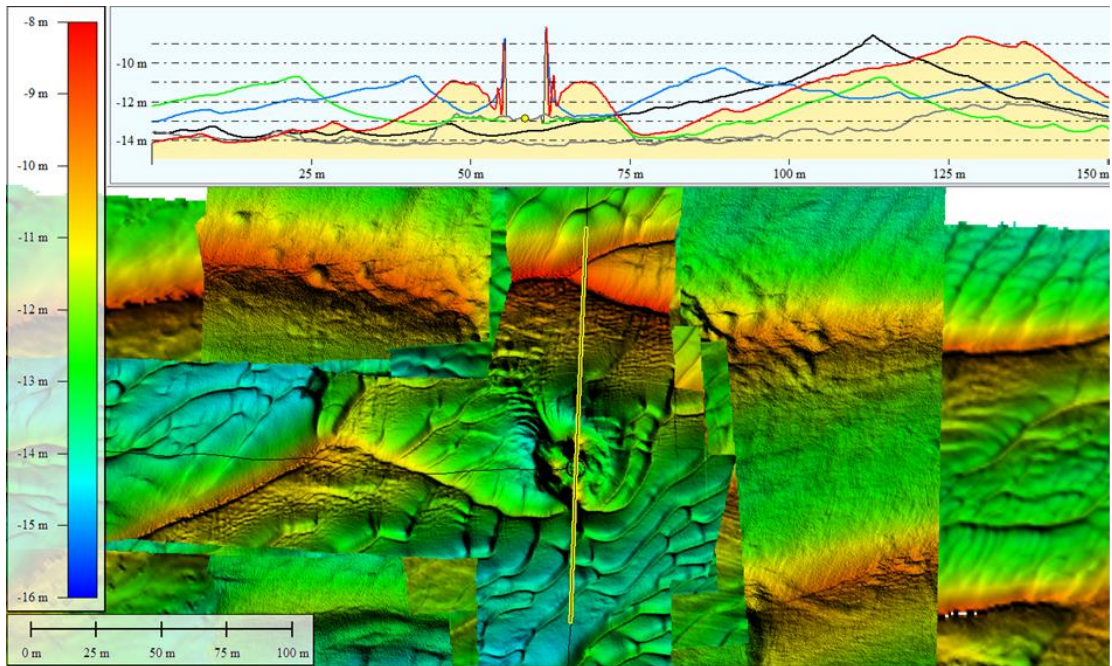


Figure E.11 Sand wave migration past monopile and scour protection, survey 5. Bed level measured in 2014 (black), as-built 2016 (grey), in 2018 (green), in 2021 (blue) and in 2023 (red) in mLAT.